

***Environmental Degradation Study of FRP Composites
Through Evaluation of Mechanical Properties***

Sanghamitra Sethi



***Department of Metallurgical and Materials Engineering
National Institute of Technology
Rourkela -769008, odisha
INDIA***

Environmental Degradation Study of FRP Composites Through Evaluation of Mechanical Properties

*A Thesis submitted in partial fulfilment of the
requirements for the degree of*

DOCTOR OF PHILOSOPHY

by

Sanghamitra Sethi
(Roll No-510MM101)



***Department of Metallurgical and Materials Engineering
National Institute of Technology
Rourkela -769008, odisha
INDIA***

December 2014

Supervisor

Prof. Bankim Chandra Ray



“Dedicated to my family and nation”



Department of Metallurgical and Materials Engineering
National Institute of Technology
Rourkela-769008
INDIA

CERTIFICATE

This to certify that the thesis entitled “**Environmental degradation study of FRP composites through evaluation of mechanical properties**” being submitted by Sanghamitra Sethi for the award of the degree of Doctor of Philosophy in Metallurgical and Materials Engineering of NIT Rourkela, is a record of bonafide research work carried out by her under my supervision and guidance. The candidate has fulfilled all prescribed requirements for the thesis, which is based on candidate’s own work and has not been submitted elsewhere for a degree or diploma.

Place: Rourkela
Date:

Prof. Bankim Chandra Ray
Supervisor
NIT-Rourkela

Acknowledgement

Though only my name appears on the cover of this dissertation, a great many people have contributed to its production. I owe my gratitude to all those people who have made this dissertation possible and because of whom my research experience has been one that I will cherish forever.

My deepest gratitude is to my supervisor, Prof. Bankim Chandra Ray. I have been amazingly fortunate to have an advisor who gave me the freedom to explore on my own, and at the same time the guidance to recover when my steps faltered. He taught me how to question thoughts and express ideas. I am deeply grateful to him for the long discussions that helped me sort out the technical details of my work. I am also thankful to him for encouraging the use of correct grammar and consistent notation in my writings and for carefully reading and commenting on countless revisions of this manuscript. I am grateful to him for holding me to a high research standard and enforcing strict validations for each research result, and thus teaching me how to do research. His patience and support helped me overcome many difficult situations and finish this dissertation. I hope that one day I would become as good an advisor to my students as Prof. Ray has been to me.

I would like to acknowledge Prof. B.B. Verma, Prof. M.Kumar, Prof. S.Jayanthu my Doctoral scrutiny committee members for fulfilling their duties of assessing my Ph.D work without fail.

I am also indebted to our director Prof. Sunil Kumar Sarangi, for all the facilities provided during the course of my tenure. I would like to thank Head of the Department of Metallurgical and Materials Engineering department and all the faculty for all their support through out my research work.

I am greatful to Prof.Addis Kidane, University of South Carolina,USA for all cooperation during my testing and analyseing the data.

I am like to acknowledge Mr. Rajesh Pattnaik, Subrat Pradhan for their cooperation during my testing.

Special thanks to all my ex and present lab mates Dinesh, Kishore, Rajesh, Meet, Santosh, Rajkishore, Pravash for their encouragement and help during my Ph.D work.

I am also thanks to my dear friends Meena, Beauty, Achala, Aparajita and subhashree for their moral and friendly atomosphere in Rourkela.

Finally I would like to give a big thanks to my beloved husband Managobinda for his kind support and understanding my each and every problem. His words of suggestion always show me the right path when I feel disturbed. Thanks to My parents and all my family members for their mental support and wishes. Lastly I offered my regards and gratitude to almighty god for kind shower of blessings and support through out my Ph.D work.

22nd December 2014

National Institute of Technology, Rourkela

Sanghamitra Sethi

Abstract

The performance of fibre-reinforced composites is, to a large extent, controlled by the properties of fibre-matrix interfaces. The interface chemistry and character is vital to a composite material. Good interfacial properties are essential to ensure efficient load transfer from matrix to reinforcement, which helps to reduce stress concentrations and improves overall sustainability of mechanical properties. The strength of composite materials depends not only on the substrate but also on the interface strength. The interface here does not have unique fracture energy unlike homogeneous materials. Consequently, there is a great interest in developing new concepts for tailoring the strength of fibre-matrix interface. Some of researchers have been reported the mechanisms responsible for improved fibre-matrix interface adhesion is removing weak boundary layer, and thereby improving wettability. However, a high performance composite functions because a weaker interface or matrix stops a crack running continuously between the strong brittle reinforcements. Fibre reinforced composite materials do, however, suffer some serious environmental limitations. Environmental exposures include temperature, moisture, radiations, UV and other different alkali treatments, which cause deterioration in the mechanical and/or physical behaviour, adhesion between fibre/matrix interface regions of the composite material over a period of time. The aim of the current investigation is to present the variation of mechanical properties of glass fiber/epoxy composite under the synergistic effect of temperature and rate of loading. In case of temperature we performed 2 types of cases as above and below glass transition temperature (T_g) and in second case above and below-ambient temperature. Glass fibre reinforced polymer composites (GFRP), carbon fibre reinforced polymer composites (CFRP) and Kevlar fibre reinforced polymer composites were fabricated by hand-lay up method followed by compression molding press. The composite specimens were subjected to elevated and high temperatures as +60°C, +100°C, +150°C and +200°C temperatures. 3-Point short beam shear test and 4-point short beam shear test were conducted in order to characterize the mechanical behavior of laminated composite and to determine the influence of loading rate on interlaminar shear strength. To understand the interactions between various failure mechanisms in the fiber, matrix and fiber/matrix interface, microscopic analyses were conducted.

In second case we performed in-depth analysis of interlaminar shear test and failure mechanisms of glass fibre/epoxy, carbon fibre/epoxy and Kevlar fibre/epoxy composites under $+50^{\circ}\text{C}$, -50°C , $+100^{\circ}\text{C}$ and -100°C temperatures and different crosshead velocity. Different high and low temperature conditioning were performed using Instron with environmental chamber providing additional information regarding in-situ failure of laminated composites. Following the test, the fracture surfaces of the samples were scanned under SEM to understand the dominating failure modes. Microstructural assessments can also reveal the response of each constituent viz. fibre, matrix resin and the interface/interphase; under temperature and mechanical loading. This section comprehensively presents the mechanical behaviour and structural changes in fibrous polymeric composite systems during the mechanical loading under high and low temperature service environment. We specifically tailored this potential to describe the contradiction and confusion at polymer composite interface which may not be underestimated by material scientists. Fibre/matrix adhesion involves very complex physical and chemical mechanisms. One of the most important physical aspects is the geometry of reinforcing fibres, which influences adhesion between fibre and matrix, stress transfer and local mechanisms of failure. In addition to chemical bonding, the fibre/matrix bond strength in shear is largely dependent on the roughness of the fibre surface and the fibre/matrix contact area.

At cryogenic temperatures, due to difference in coefficient of thermal expansion between the fibre and the matrix phase, microcracks initiate and propagate through the laminated composites. Therefore, knowledge of the resistance to different failure modes of woven fabric composites laminates at cryogenic temperatures is essential to the materials scientist and design analyst. The aim of this investigation was to study deformation and mechanical behaviour of glass fibre/epoxy composites subjected to 3-point short beam shear test at low and ultra-low temperature with different loading speeds. The laminates were tested at ambient ($+27^{\circ}\text{C}$) temperature and at (-20°C , -40°C , -60°C) temperatures using liquid nitrogen in an environmental chamber installed on an Instron testing machine. Testing was carried out in different loading covering low to high medium speeds. Following the test the fracture surfaces were scanned under SEM microscope. A need probably exists for an assessment of mechanical performance of such potentially promising materials under the influence of changing environment and loading speed. Using fractography study to characterize the onset and growth of failure modes has become generally accepted method.

During thermal cycling differential coefficient of thermal expansions and residual stresses is a prime cause in fibre reinforced polymer composites (FRP) material. The behavior of the interfacial contact between fibre and matrix is strongly influenced by the presence and nature of residual stresses. GFRP and CFRP composite laminates are used to analyze the thermal cycle effect on the mechanical behavior with different loading rates. 3-point short beam shear test was performed for the analyze the mechanical behavior. To study the failure modes which have great impact on mechanical behavior, Scanning electron microscope (SEM) was used.

The ensuing research revealed a number of key challenges regarding interface issues in producing polymer nanocomposites that exhibit a desired behavior. The greatest stumbling block to the large-scale production and commercialization of nanocomposites is the dearth of cost effective methods for controlling the dispersion of the nanoparticles in polymeric matrix. Current interest in alumina/epoxy nanocomposites, Cu nano particle and Multi walled carbon nanotube (MWCNT) has been generated and maintained because nanoparticles filled polymers exhibit unique combinations of properties not achievable with conventional composites. In the present study, glass fiber reinforced composites filled with nanoparticle have been prepared. 3-point short beam shear test was conducted to analyze the Interlaminar shear strength (ILSS) variation with different loading rate. Alumina nanoparticle was well dispersed in epoxy polymer matrix to achieved high mechanical performance. The results show that it is possible to improve the interlaminar shear strength with the loading rate variations. Clearly, no follow-up work in this area will be commendation for better understanding of effect of nanoparticle in FRP composites in assessment of loading rate sensitivity. Under these conditions, fibre reinforced polymer nanocomposites have been shown to exhibit two glass-transition temperatures, T_g : one associated with polymer chains far from the nanoparticles, and a second, larger T_g , associated with chains in the vicinity of the particles. To analyze different failure modes SEM analyses was conducted. Good interfacial properties are essential to ensure efficient load transfer from matrix to fillers, which helps to reduce stress concentrations and improves overall mechanical properties. Consequently, there is great interest in developing new concepts for improving the strength of fibre–matrix interface.

Key Words: Fibre reinforced polymer composites, environmental degradation, fibre/matrix interface, mechanical behavior, fractography, glass transition temperature, spectroscopy analysis, Al_2O_3 nano-filler.

Contents

Certificate	i
Acknowledgement	ii
Abstract	iv
List of Figures	xii
List of tables	xviii
Abbreviations	xix

Chapter-1: Introduction

1.1 Fibre reinforcements and polymer matrices	2
1.2 Recent advances of PMCs	3
1.3 Nano-fillers reinforcement	5
1.4 Motivation and relevant case studies	6
1.5 Scope of the investigation	6
1.6 Organisation of thesis	7
References	8

Chapter -2: Literature link

2.1 Introduction	16
2.2 Environmental degradation	
2.2.1 Thermal environment	16
2.2.2 Hygrothermal environment	19
2.2.3 Effect of temperature on mechanical behavior	21
2.2.4 Other environmental exposures	22
2.2.5 Effects of loading speed	24
2.3 Nano filler in polymer composites	26
2.4 Mechanical behavior of polymer composites	
2.4.1 Tensile Failure	27
2.4.2 Stress-strain curve	29
2.5 Microstructural and micro- interfacial characterization	
2.5.1 Micro-characterization of interface	31
References	35

Chapter-3: Materials and Methods

3.1 Materials	43
3.2 Experimental Methods	46
3.3 Instrument used	47

Chapter 4 Results and Discussion

4.1. Effect of high temperature on mechanical response of materials: Assisted with viscoelastic nature

Theories and Thoughts

4.1.1. Introduction	50
4.1.2 Materials and experimental set-up	
4.1.2.1 Materials and fabrication technique	51
4.1.2.2 In-situ conditioning and characterization	52
4.1.3 Results and Discussion	
4.1.3.1 In-situ testing	53
4.1.3.2 Fractography study	60
4.1.3.3 Interfacial chemistry study	72
4.1.3.4 Glass transition study	74
4.1.4 Summary	75
References	76

4.1.1a AFM study of thermally conditioned samples

Theories and Thoughts

4.1.1a. 1 Introduction	78
4.1.1a.2 Materials and experimental set-up	
4.1.1a.2.1 Materials	79
4.1.1a.2.2 Fabrications and experimental technique	79
4.1.1a.3 Results and Discussion	
4.1.1a.3.1 In-situ testing	80
4.1.1a.3.2 Fractography analysis	82
4.1.1a.4 Conclusion	83
References	83

4.1.1b Effect of above-ambient and below-ambient of FRP composite materials with different loading rates

Theories and Thoughts

4.1.1b.1 Introduction	84
4.1.1b.2 Experimental work	
4.1.1b.2.1 Materials	86
4.1.1b.2.2 Temperature conditioning and characterization	86
4.1.1b.3 Results and Discussion	
4.1.1b.3.1 Mechanical testing	88
4.1.1b.3.2 Fractography study	93
4.1.1b.3.3 Thermal analysis	103
4.1.1b.4 Summary	104
References	104

4.2 Effect of low temperature on mechanical response of FRP composite materials with different loading rates

Theories and Thoughts

4.2.1 Introduction	106
4.2.2 Experimental work	
4.2.2.1 Materials	107
4.2.2.2 Low temperature conditioning and characterization	107
4.2.3 Results and Discussion	
4.2.3.1 Mechanical testing	110
4.2.3.2 Fractography study	113
4.2.4 Summary	114
References	114

4.3 An assessment of high and low temperature on prepreg glass fibre/epoxy composites

Theories and Thoughts

4.3.1 Introduction	116
4.3.2 Experimental section	
4.3.2.1 Materials and instrument	118
4.3.2.2 Processing of laminates	118

4.3.3 Results and Discussions	
4.3.3.1 Short beam shear test	120
4.3.3.2 Fractography study	122
4.3.4 Summary	123
References	127
4.4 An effect of thermal cycle on interlaminar shear strength of FRP composites	
<i>Theories and Thoughts</i>	
4.4.1 Introduction	129
4.4.2 Experimental section	
4.4.2.1 Materials and instrument	130
4.4.2.2 Procedure and materials characterization	130
4.4.3 Results and Discussions	
4.4.3.1 Short beam shear test	132
4.4.3.2 Fractography study	133
4.4.4 Summary	136
References	136
4.5 Effect of UV treatment on loading rate sensitivity	
<i>Theories and Thoughts</i>	
4.5.1 Introduction	137
4.5.2 Experimental work	
4.5.2.1 Materials	138
4.5.2.2 Conditioning and characterization	138
4.5.3 Results and Discussion	139
4.5.3.1 Mechanical testing	140
4.5.3.2 Fractography analysis by SEM	141
4.5.4 Summary	142
References	142

4.6 Effect of nanoparticle addition to evaluate FRP composites under different environmental conditioning

Theories and Thoughts

4.5.1 Introduction	143
4.5.2 Experimental work	
4.5.2.1 Materials	144
4.5.2.2 Materials characterization	144
4.5.2.3 Environmental conditioning	145
4.5.3 Results and Discussion	
4.5.3.1 mechanical testing by Instron	146
4.5.3.2 Failure modes study by SEM	148
4.5.4 Summary	149
References	150

4.7 Effect of strain rate and environment on the dynamic flexural behavior of GFRP and CFRP composites

Theories and Thoughts

4.7.1 Introduction	151
4.7.2 Experimental work	
4.7.2.1 Materials and fabrication	153
4.7.2.3 Environmental conditioning	153
4.7.3 Results and Discussion	
4.7.3.1 Mechanical testing	156
4.7.3.2 Failure modes study by SEM	158
4.7.4 Summary	163
References	164
5. Summary and Conclusions	165
Critical comments and future scope of work	168

List of Figures

Figure No.	Figure Description	Page No.
Fig.1	Flexural stress–strain curves of control and conditioned neat/nano epoxy specimens.	18
Fig.2	Absorption curves in SFC specimen and iso concentration lines at 10%, 25%, 50%, 75%, 90% moisture	20
Fig.3	Short and long term moduli in terms of water concentration	20
Fig.4	Change in snap-through load with exposure to 20°C and 65%RH	22
Fig.5	Load-displacement traces for bistable plate over several days exposure to 20°C and 65%RH	22
Fig.6	(a) Example of the damage in the treated fiber carbon composites: (a) XY plane, (b) YZ plane, (c) XZ plane and (d) 3D view, One of the delaminations in the treated E-glass resin composites: (a) XY plane, (b) YZ plane, (c) XZ plane and (d) 3D view	24
Fig.7	ILSS with loading rate of glass fibre/epoxy composites at -50°C temperature	25
Fig.8	Bond strength distributions for Kevlar 49/polyethylene microcomposites and their counterparts aged in water at 88°C for 24 h	26
Fig.9	(a) Interfacial regions as a function of filler particle size. The filler is shown in red, the interfacial region in dark blue and the bulk polymer in pale blue. (b) Large particles produce a low radius of curvature, and relatively less polymer in the ‘interfacial region, (c) the same volume filler broken into smaller particles creates a higher radius of curvature and more polymers in the interfacial region	27
Fig.10	Geometry and dimensions of composite specimens under tensile loading (b) untested specimen	28
Fig.11	(a) Stress-strain curve at different strain rate (b) Absorbed energy under stress-strain curve	29
Fig.12	Different regions of a typical strain softening curve. The displacement, rather than strain, is used, to avoid implications of violating basic principles	30
Fig.13	FTIR spectra of different sizing agents/epoxy resin before and after boiling water aging	32
Fig.14	AFM topography images of the same cross-section area of AS4/VRM34 using Tapping Mode (a) and contact mode (b). The scan size was 30*30 μm	33
Fig.15	AFM micrograph shows plastic deformation results in the formation of permanent indentation on the surface of the sample	33

Fig.16	(A)Variation of ILSS with loading rates of glass fibre/epoxy composites with 3-point short beam shear test at different temperatures (a) Load-displacement curve of glass fibre/epoxy composites at +60°C temperature (b) load-displacement curve of glass fibre/epoxy composites at +100°C temperature (c) load-displacement curve of glass fibre/epoxy composites at +150°C temperature (d) load-displacement curve of glass fibre/epoxy composites at +200°C temperature (e) load-displacement curve of glass fibre/epoxy composites at +250°C temperature.	54
Fig.17	(a,a') Scanning electron microscopy images of 3-point bend tested glass fibre/epoxy composites at 200mm/min and flexural stress with flexural strain curve at ambient temperature, (b,b') at +60°C temperature, (c,c') at +100°C temperature, (d,d') at +150°C temperature, (e,e') at +200°C temperature, (f,f ') at +250°C temperature	58
Fig.18	Interlaminar shear strength with loading rate of carbon fibre/epoxy composites at +27°C, +60°C, +100°C,+150°C and +200°C.	59
Fig.19	Load-displacement curve of carbon fibre/epoxy composites above and below glass transition temperatures as +60°C,+100°C,+150°C,+200°C.	60
Fig.20	Represents the different failure modes observed at different temperatures and the stress-strain behavior of corresponding temperatures at 200mm/min loading speed (a) at ambient (+27°C) temperature (b) at +60°C temperature (c) +100°C temperature (d) +150°C temperature (e) +200°C temperature	62
Fig.21	(a)Interlaminar shear strength (ILSS) values with loadin rate curve at different temperature of Kevlar fibre/epoxy composites (a') load-displacement curve of without conditioning samples (+27°C) at different loading rates	64
Fig.22	Load-displacement curves (a) at +60°C temperature(b) at +100°C temperature (c) at+150°C temperature (e) +200°C temperature	64
Fig.23	Different failure modes observed in Kevlar fibre/epoxy composites at high temperature	66
Fig.24	Variation of ILSS with loading rate of glass fibre/epoxy composites tested with 4-point bend test at different temperatures. (a) Load-displacement curve of glass fibre/epoxy composites at +60°C temperature (b) load-displacement curve of glass fibre/epoxy composites at +100°C temperature (c) load-displacement curve of glass fibre/epoxy composites at +150°C temperature (d) load-displacement curve of glass fibre/epoxy composites at +200°C temperature (e) load-displacement curve of glass fibre/epoxy composites at +250°C temperature.	68

Fig.25	(A,A') Scanning electron microscopy images of glass fibre/epoxy composites tested at 4-point short beam shear test at 200mm/min and flexural stress with flexural strain curve at ambient temperature, (B,B') at +60°C temperature, (C,C') at +100°C temperature, (D,D') at +150°C temperature, (E,E') at +200°C temperature, (F,F') at +250°C temperature.	68
Fig.26	FTIR-ATR spectroscopy analysis of glass fibre/epoxy and carbon fibre/epoxy composites	73
Fig.27	Curing reaction of epoxy matrix resin.	74
Fig.28	Glass transition temperatures values of glass fibre,carbon fibre and Kevlar fibre epoxy composite materials.	74
Fig.29	AFM topography images of untreated GFRP composites (a) line analysis of image (b) 3D image analysis	79
Fig.30	AFM topography image of treated GFRP interphase failure after treatment	81
Fig.31	SEM micrograph matrix failure of GFRP composite after treatment	81
Fig.32	AFM topography image of treated GFRP adhesion failure after thermal conditioning treatment.	82
Fig.33	(a) Schematic representation of 3-point short beam shear test. (b) Experimental set up for 3-point short beam shear test (c) Instron machine used for the test	88
Fig.34	Variation of ILSS with loading rate for glass/epoxy composite system at different temperatures.	90
Fig.35	Interlaminar shear strength of glass/epoxy composite at 1 mm/min for different temperature	91
Fig.36	Scanning electron microscopy (SEM) images of the glass fibre/epoxy composites: (A, A') at -100°C temperature (B, B') at -50°C temperature (C,C') at ambient temperature (D,D') at +50°C temperature (E,E') at +100°C temperature	93
Fig.37	Variation of interlaminar shear strength with different loading rates at different temperatures for carbon fibre/epoxy composite system.	94
Fig.38	Interlaminar shear strength of Carbon/epoxy composite at 1 mm/min for different temperature.	96
Fig.39	Scanning electron microscopy (SEM) images of the carbon fibre/epoxy composites: (A, A') at -100°C temperature; (B, B') at -50°C temperature; (C,C') at ambient temperature; (D,D') at +50°C temperature; (E,E') at +100°C temperature. Variation of ILSS with loading rate for Kevlar/epoxy composite system at various temperatures and loading rates.	97
Fig.40	Interlaminar shear strength of Carbon/epoxy composite at 1 mm/min for different temperature.	98
Fig.41	Scanning electron microscopy (SEM) images of the Kevlar	100

	fibre/epoxy composites: (A, A') at -100°C temperature (B, B') at -50°C temperature (C,C') at ambient temperature (D,D') at +50°C temperature (E,E') at +100°C temperature	
Fig. 42	Comparison of glass transition temperatures of glass fibre/epoxy composites at different conditioning temperature. (a) Glass fibre/epoxy composites (b) Carbon fibre/epoxy composites (c) Kevlar fibre/epoxy composites	101
Fig. 43	(a) Interlaminar shear strength with different loading rates of glass fibre/epoxy composites at 25°C, -20°C, -40°C and -60°C temperature (b) Flexural stress vs Flexural strain at 1mm/min loading speed.	103
Fig. 44	Fractography analysis of glass fibre/epoxy composites at ambient (27°C) temperature	111
Fig. 45	Fractography analysis of glass fibre/epoxy composites at ambient (-20°C) temperature	112
Fig. 46	Fractography analysis of glass fibre/epoxy composites at -40°C temperature	113
Fig. 47	Fractography analysis of glass fibre/epoxy composites at -60° temperature	113
Fig. 48	Curing cycle for glass/epoxy composite followed within autoclave	114
Fig. 49	Instron 5967 with environmental chamber used during the in-situ testing of sample.	119
Fig. 50	(a) Loading rate with ILSS of GFRP samples at different temperature	120
Fig. 51	(b) Loading speed with ILSS curves of glass/epoxy composite at different temperature	121
Fig. 52	Matrix micro cracking and brittle fracture of fiber at -50 degree at 1mm/min and 800mm/min	123
Fig. 53	Cleavage marking and fiber/matrix debonding at -50 degree 1000mm/min	125
Fig. 54	Scanning electron micrograph at ambient 1mm/min and 800mm/min shows steps and welts as well as matrix cracking respectively.	126
Fig. 55	Thermal conditioning sample at 1mm/min and 800mm/min showing fiber/matrix debonding and macromatrix cracking.	126
Fig. 56	Interlaminar shear strength with loading rate at different thermal cycle of glass fibre/epoxy composites	132
Fig. 57	Interlaminar shear strength with loading rate at different thermal cycle of carbon fibre/epoxy composites.	133
Fig. 58	. Different failure modes were observed in glass fibre/epoxy composites (a) fibre imprint at 0.5 cycle treatment (b) riverline marking at 1 cycle treatment (c) fibre/matrix debonding at 1.5 cycles.	134
Fig. 59	Different failure modes are observed in carbon fibre/epoxy composites (a) fibre fracture at 0.5 cycle treatment (b) toughened matrix at 1 cycle treatment (c) fibre/matrix debonding at 1.5 cycle treatment.	135

Fig. 60	Interlaminar shear strength with loading rate at different time exposure of UV treatment (a) carbon fibre/epoxy composites (b) glass fibre/epoxy composites.	139
Fig. 61	(a) Bunch of fibre fracture (b) resin tearing (c) fibre fracture sliding failure modes observed in glass fibre/epoxy composites at 30 days, 60 days and 90 days UV treatment of samples.	140
Fig. 62	(a) steps formation on the matrix resin (b) deep riverline marking (c) small cusps formation failure modes are observed in carbon fibre/epoxy composites at 30 days, 60 days and 90 days UV treatment of the samples.	141
Fig. 63	(a)Average stress-strain curves for the woven GFRP composite with nanoparticles	146
Fig. 64	(b)Average stress-strain curves for the woven GFRP composite without nanoparticles	146
Fig. 65	(a),(b) Scanning electron micrograph of epoxy resin and fiber of alumina/epoxy glass fiber reinforced composites. Tilted 20°.	149
Fig. 65	(c),(d) Scanning electron micrograph of epoxy glass fiber reinforced composites. Tilted 20°.	149
Fig. 66	Configuration of Experimental Apparatus	154
Fig. 67	Loading Fixture, Specimen, and Incident Bar	154
Fig. 68	Loading arrangement and field of the camera system	155
Fig. 69	Typical mid-point deflection a) CFRPAMB at 300/s b) GFRP5_250 at 500 /s	156
Fig. 70	Typical Strain-time plot for GFRP_AMBat different strain rate	158
Fig. 71	Typical Strain-time plot for CFRP_60s at different strain rate	159
Fig. 72	Typical load- time plot for CFRP_AMB at 276 /s	160
Fig. 73	(a) Angles cusps formation on the matrix surface at 5 psi (b) Cusps formation between the fibres spacing at 10 psi (c) Cusps in very small size at 15 psi.	161
Fig. 74	(a) Tension failure of glass fibre/epoxy at 5psi (b) deadhesion between fibre and matrix at 10psi (c) bunch of fibre failure at 15psi	162
Fig. 75	Topography change of AS4/VRM34 exposed to 100% RH for different periods of time. The vertical distance between the two selected points decreased from 130.7 nm before treatment to 83.7 nm after 1495 h of hygroscopic treatment at 100% RH.	168
Fig. 76	Unit cell FE model of glass fibre hybrid composites(a)aligned (b)misaligned fibres	168

List of Tables

Table No.	Description	Page No.
1	Physical and mechanical properties of glass fibre	42
2	Mechanical Properties of high-modulus carbon fibre	42
3	Mechanical properties of Kevlar-49 fibre.	43
4	Mechanical properties of epoxy resin.	43
5	Temperatures Effect	49
6	UV radiation treatment	49
7	Fibre reinforced epoxy composites with nano-fillers	50
8	Percentage change in ILSS with temperatures at 1 mm/min.	92
9	Percentage change in ILSS with temperatures at 1 mm/min loading speed	96
10	Percentage change in ILSS with temperatures at 1 mm/min.	100

Abbreviation

GFRP	Glass fibre reinforced polymer composites
CFRP	Carbon fibre reinforced polymer composites
KFRP	Kevlar fibre reinforced polymer composites
FRP	Fibre reinforced polymer composites
ILSS	Interlaminar Shear Strength
DSC	Differential Scanning Calorimeter
FTIR-ATR	Fourier Transform Infrared Spectroscope
SEM	Scanning Electron Microscope
AFM	Atomic Force Microscope
ASTM	Americal Society for Testing of Material
PNC	Polymer Matrix Nanocomposites

Chapter 1

Introduction

1. Introduction

Polymer composites demonstrate remarkable electrical, thermal, and mechanical properties, which allow a number of exciting potential applications. Polymer composites have wide range of applications in various sectors due to many features including low weight, low cost, ease of processing and fabrication, environmental stability and corrosion resistance. Fibres are typically added to enhance chemical and/or physical, mechanical properties of polymer matrix. Of these properties, optimizing the mechanical properties has always been the most desired objective. Inorganic fibres (glass and carbon fibres) and aromatic organic fibres (Aramid) are the traditional fillers used to boost the mechanical properties of polymers. With hundreds of available fibres and thousands of unique polymers, it is costly to determine an ideal combination for a given application [1]. Further complications arise from the many additives and fillers which contribute to the final mechanical properties of a given fiber – matrix system [2]. The dispersion of inorganic additives (at nanometric size and/or micrometer size) in polymers significantly improves their electrical, mechanical and thermal properties [3]. These properties involve spatial and orientational distribution of fibres, and requires information from the nano to the macroscale, which is over 6 orders of magnitude in length scale [4]. One of the most enduring problems in the evolution of science and technology using nanoscale materials is the characterization of their morphology in macroscopic systems [5-7]. In a polymer composite, the properties of the polymer region near the reinforcing agent i.e. interface/interphase, are different from those of the bulk [4]. The strength of composite materials depends not only on the substrate strength but also on the interface strength. The interface here does not have unique fracture energy unlike homogeneous materials [8]. The adhesive fibres elongate in a stepwise manner as folded domains are pulled open. The elongation events occur for forces of a few hundred piconewton. These are smaller than the forces of over a nanonewton, which are required to break the polymer backbone. When the force rises to a significant fraction of the force required to break a strong bond and threatens to break the backbone of the molecule, a domain unfolds. Thus, it could avoid the breaking of a strong bond in the backbone [9]. The interface between the fibre/polymer plays a defining role in the overall material properties such as glass transition temperature [10-13], relaxation dynamics [14-16], thermal aging [17], dielectric behavior (i.e., breakdown strength, voltage endurance, and dielectric permittivity) [18], mechanical properties (i.e., stiffness, debonding, fracture,

internal stress distribution, and toughness) [19,20,21]. The measurement of the interface volume fraction is, therefore, pivotal for structure property-processing investigation and modelling of polymer nanocomposites. Tuning the interfaces between fillers and polymer matrix potentially plays a critical role in composites to enhance their adaptive responses.

1.1 Fibre reinforcement and polymer matrices

Durability of composites depends on the integrity of the interface and the region known as the interphase between the matrix and the reinforcing material. The fibre/matrix interface has always been considered as a crucial aspect of polymer composites. It is at the interface where stress concentration develops because of differences between the reinforcement and matrix phase thermal expansion coefficients. The interface may also serve as a locus of chemical reaction [22]. Environmental exposure results in reduced interfacial stress transmissibility due to matrix plasticization, chemical degradation and mechanical degradation. Matrix plasticization reduces matrix modulus. Chemical degradation is the result of hydrolysis of the bonds at the interface [23, 24]. The influence of environmental effects on mechanical properties of FRP composites and interfacial degradation is well documented in literatures [25-30]. Although thousands of polymer matrix composite components are currently in service in many applications as well as civil infrastructure repair and rehabilitation, barrier are still there to further implementation in a more structurally critical and complex temperature applications. The level of adhesion between matrix and fibre affects the mechanical behavior in the off-axis and also parallel to the fibre [31].

The fibre and matrix interactions are likely to be greater in woven fabric composites as compared to composite made up of unidirectional fibres. Localized strains in the matrix may increase as the fibres straighten under tensile loading or buckle under compression [32]. Differential coefficients of thermal contraction may modify the local stress threshold required for interfacial debonding. This eventually leads to nucleation of delamination [33]. The different reinforcements as glass fiber, carbon fibre and Kevlar fibre, which has high elastic constants, gave a significant increase in stiffness of composites over the well-established performance, hence made possible a wide range of applications for composites. Steel cord reinforced polymer (SCRCP) is a new material that can be used as external reinforcement. SCRCP combines the advantages of steel and CFRP. The Young's modulus is high, as well as the strength which is comparable to CFRP. The material cost is low and the

laminate remains quite flexible. Another advantage is the ductile behaviour of the steel composite. Therefore, lower material safety factors can be applied in design [34].

In particular, the fibre/matrix interface is highly prone to in-service degradation. In general, the influence of in-service degradation is reflected in its mechanical performance and fracture morphology, but analyzing and identifying the reason behind the particular degradation is problematic. The most common types of environmental conditions to which composite material was exposed during loading as moisture [35-37], temperature [38-41], hygrothermal effects [42-50], UV, low earth orbit environment [51-54] and sea water [55-57].

The response of fibre/matrix interface within the composite plays an important role in determining the gross mechanical performance, because it transmits the load from the matrix to the fibres, which contribute the greater portion of the composite strength. Better the interfacial bond better will be the ILSS, de-lamination resistance, fatigue and corrosion resistance [58]. An interfacial reaction may induce various morphological modifications to the interphase at the fibre/polymer interface [59, 60]. A need probably exists for an assessment of mechanical performance of such potentially promising materials under the influence of changing environment and loading speed. A strong interface displays an exemplary strength and stiffness, but is very brittle in nature with easy crack propagation through the interface. A weaker interface reduces the stress transmissibility and consequently decreased strength and stiffness. A crack here is more likely to deviate and grow at the weak interface. It results in debonding and/or fiber pull-out and contributes to improved fracture toughness [61,62].

1.2 Recent advances of PMCs

The Delamination failure mode is known to be the major life-limiting failure process in a composite laminate. Delamination can induce stiffness loss, local stress concentration and local instability that can cause buckling failure under compressive loading. The matrix in a fibre reinforced composites serves to transfer the load between fibres and to integrate the whole structure to form useful shape. If the incident impact energy exceeds a critical value (E_c), then the fibre-resin composite will suffer damage in the form of delamination. The delamination in composites is caused by the interlaminar stresses produced by out-of-plane loading, eccentricities in load paths, or discontinuities in the structure [63]. Prediction of initiation and growth of delamination is, however, complicated and the success of the predictions relies on accurate interlaminar toughness data for the material under both static and fatigue loading and at different environmental conditions. The strain energy release rate

threshold values for delamination growth were significantly affected by fatigue loading, and the fatigue threshold values at 100°C were only about 10% of the critical static values for all three mode conditions tested [64,65]. For review of the problem and various approaches suggested for the determination of mode mixity in delamination tests has been reported [66-68].

Z-pinning is an effective reinforcement method for increasing the delamination resistance of fibre-polymer composites. Z-pins are thin metallic or fibrous rods inserted in the through - thickness direction of composite materials to increase the interlaminar fracture toughness properties [69]. Z-pinning has proven a highly effective method for increasing the modes I and II interlaminar fracture toughness [70-74] and impact damage resistance [75, 76] of composites. Z-pins also increase the delamination resistance and structural properties of bonded composite joints [77-80]. These improvements to the toughness properties are reliant on the z-pins generating bridging traction loads along the delamination crack [81–83]. The traction loads resist crack opening (under mode I) and crack sliding (under mode II), which increases the delamination fracture resistance.

1.3 Nano-filler reinforcement

The field of polymer nanocomposites has attracted considerable attention as a method of enhancing polymer properties and extending their utility, by using molecular or nanoscale reinforcements rather than conventional particulate filled microcomposites. Nanocomposites are a combination of two or more phases containing different compositions or structures, where at least one of the phases is in the nanoscale regime [84]. Polymer nanocomposites exhibit greater resistance to breakdown mechanisms than pure polymers due to their improved properties. The mechanisms that can lead to polymer nanocomposites failure are the same as those that lead to pure polymer failure. In recent years, polymer-nanoparticle composite materials have attracted the interest of a number of researchers, due to their synergistic and hybrid properties derived from several components. Whether in solution or in bulk, these materials offer unique mechanical, electrical, optical and thermal properties. Such enhancements are induced by the physical presence of the nanoparticle and by the interaction of the polymer with the particle and the state of dispersion [85-88]. It is logical to anticipate that the dispersion of fillers with dimensions in the nanometer level having very large aspect ratio and stiffness in a polymer matrix could lead to even higher mechanical performances. Polymer nanocomposites can attain a substantially greater stiffness, strength,

and thermal stability and barrier properties at very low filler content compared to plastics filled with traditional micrometer-sized particles [89].

However, despite the large volume of literature published on the relationships between the nano-scale structural variables and macroscale physical and mechanical properties of polymer nanocomposites over the last 15 years, the understanding of the basic physical origin of these large property changes remains in its infancy [90-92]. This is partly due to the complexity of polymer nanocomposites, requiring re-considering the meaning of some basic polymer physics terms and principles, and partly by the lack of reliable experimental data. In addition to detailed knowledge of molecular structure of the polymer matrix, the theory also requires a sufficient description of particle dispersion, self-assembly phenomena, particle chain interactions and nanocomposites preparation processes [93, 94].

1.4 Motivation and relevant case studies

The main motivation of this research work comes from the large applications of the fibre reinforced polymer matrix composites. The wide structural applications of fibre reinforced polymer and polymer nanocomposites are extremely important for the past few decades in aerospace, spacecraft, marine, sports equipments and many other research fields. During their service period, the materials are exposed to different environmental conditions. For long period of exposure, materials leads to ageing of the polymer matrix resin, this tends to quick degradation of its overall mechanical and thermo-mechanical properties.

1.5 Scope of the investigation

This research is of general interest to study the mechanical and fracture behavior of fibre reinforced polymer and fibre reinforced polymer nanocomposites in different environmental conditions at different loading rates. This study will give an idea about the loading rate sensitivity of FRP's under different environments. Fractography study reveals different characteristics of fracture surfaces, failure modes and crack growth behavior. This research also provides information on changes in glass transition temperature(T_g) of the material. T_g is an important aspect in obtaining, maintaining mechanical behavior of the composites. Attenuated total reflection fourier transform infrared spectroscopy is used to obtain information on the change in chemistry occurring in epoxy resin at different environmental conditions. Here an attempt is made to correlate the mechanical behavior of the materials with change in chemistry and change in its glass transition temperature.

This research intends to pivot the development of different aspects of fibre/polymer composites. These are (i) mechanical behavior with environmental instability (ii) response of stress-strain curve (iii) isolated unprecedented failure (iv) nano filler in polymer composites. The majority of previous efforts were concentrated on the mechanical and chemical aspects of fibre/polymer composites. However, from last few decades different research groups have synthesized and studied the properties and applications of nanofillers on fiber/polymer nanocomposites.

To date some researchers have also published some reviews as well as book and book chapters [95,96], mainly highlighting some specific areas and materials as fibre/epoxy properties and processing [97], mechanics of composites [98], environmental degradation [99-101], damage modelling [102], mechanical behavior [103,104], failure criteria [105-107], nanofillers to polymer matrix [108-110] and some applications in different fields. Utilizing the full potential of this amazing material in different engineering and structural applications, there is still need of extensive research work with current literature and research perspective of fibre/epoxy polymer composites.

1.6 Organisation of the thesis

The thesis has been divided in four chapters. Chapter-1, is an introductory section in fibre reinforced polymer matrix and fibre reinforced polymer nanocomposites. Chapter-2, contains the present literature survey covering different environmental exposures of these materials, role of nano-filler in polymer composites, mechanical behavior study, microstructural and micro-interfacial characterization. Chapter-3 represents the materials used, fabrication techniques, environmental conditions, experimental methods used during this research work. Chapter-4 consists of all the results and discussion part which is further divided into seven sections. Chapter 4.1 related to prior thermal conditioning on FRP composites where an observation of failure modes with different loading rates has been correlated. Chapter 4.2 study the effect of post curing hardening treatment on failure and fracture of FRP composites at different temperature and loading rates. Chapter-4.3 effect of high temperature on mechanical response of materials has been studied. Thermal and fractographic analysis are correlated to the mechanical behavior of these materials. Chapter-4.4 in this section low temperature effect on mechanical response of materials with different loading rates has been plotted. Chapter-4.5 is about the effect of thermal cycling on interlaminar shear strength of FRP composites. In this section different failure modes are observed which are responsible

for the degradation of these material. Chapter-4.6 this section dedicated to study the effect of UV treatment on loading rate sensitivity. Chapter-4.7 presents the effects of nanoparticle addition to fibre reinforced polymer composites under different environmental conditions and also at different loading rates. Finally, Chapter-5, represents the summary of the work and some key point for further study.

Overall, this thesis dedicated to visualize the different environmental conditions subjected to these materials in different sections, however, the selection of these materials are on the basis of their huge applications.

References

1. Jacob, G.C., Energy absorption in polymer composites for automotive crashworthiness, *Journal of Composite Material* 2002; 36:813–50.
2. Yeung P., Broutman L.J., The effect of glass-resin interface strength on the impact strength of fiber reinforced plastics. *Polymer Engineering Science* 1978; 18:62–72.
3. Despoina P., Michael G.D., Interfaces Features in polymer nanocomposites: a review of proposed models, *NANO: Brief Reports and Reviews*, 2011; 6:497–508
4. Mauro Zammarano, Paul H. Maupin, Li-Piin Sung, Jeffrey W. Gilman, Edward D. McCarthy, Yeon S. Kim, Douglas M. Fox, Revealing the Interface in Polymer Nanocomposites, 2011; 4: 3391–3399 ' 2011.
5. Krishnamoorti, R., Strategies for Dispersing Nanoparticles in Polymers. *MRS Bull.* 2007, 32, 341–346.
6. Dzenis, Y., Structural Nanocomposites. *Science* 2008; 319: 419–420.
7. Schandler, L., Model Interfaces. *Nature Material.* 2007; 6:257–258.
8. Ray B.C., Effects of Changing Environment and Loading Speed on Mechanical Behavior of FRP Composites, *Journal of Reinforced Plastics and Composites.* 2006; 25: 1227–1240.
9. Smith, B.L., Schaffer, T.E., Viani, M., Thompson, J.B., Frederrick, N.A., Kindt, J., Belchers, A., Strucky, G.D., Morse, D.E. and Hansma, P.K., Molecular Mechanistic Origin of the Toughness of Natural Adhesive, Fibres and Composites, *Nature*, 1999; 399:761–763.
10. Sudharsan P., Priya V. Parandekar, Om Prakash, Thomas K. Tsotsis, Nisanth N. Nair, Basu S., Controlling the sub-molecular motions to increase the glass transition temperature of polymers, *Chemical Physics Letter.* 2014; 593:24–27.
11. Awalendra K. Thakur, S.A. Hashmi, Polymer matrix–filler interaction mechanism for modified ion transport and glass transition temperature in the polymer electrolyte composites, *Solid State Ionics* 2010; 181:1270–1278.
12. Yang, B., Huang, W.M., Li, C., Chor, J. H., Effects of moisture on the glass transition temperature of polyurethane shape memory polymer filled with nano -carbon powder, *European Polymer Journal.* 2005; 41:1123–1128.
13. Cecen, V., Ismail H. Tavman, Kok, M., Aydogdu, Y., Epoxy- and Polyester-Based Composites Reinforced With Glass, Carbon and Aramid Fabrics: Measurement of Heat Capacity and

- Thermal Conductivity of Composites by Differential Scanning Calorimetry, *Polymer Composite*.2009; 12: 34-37.
14. Christos J. Tsenoglou, Pavlidou,S., Constantine D. Papaspyrides, Evaluation of interfacial relaxation due to water absorption fiber –polymer composites, *Composite Science and Technology*,2006; 66: 2855–2864.
 15. Jiang,X., Kolstein,H.,Bijlaard, F., Qiang,X., Effects of hygrothermal aging on glass-fibre reinforced polymer laminates and adhesive of FRP composite bridge: Moisture diffusion characteristics, *Composites Part A* 2014; 57:49–58.
 16. Al-Haik,M., Vaghar,M.R., Garmestani,H.,Shahawy, M. Viscoplastic analysis of structural polymer composites using stress relaxation and creep data, *Composites Part B* 2001; 32 ;165–170
 17. Rittigstein, P., Torkelson, J.M., Polymer Nanoparticle Interfacial Interactions in Polymer Nanocomposites: Confinement Effects on Glass Transition Temperature and Suppression of Physical Aging, *Journal of Polymer Science, Part B: Polymer. Physics*. 2006; 44:2935–2943.
 18. Roy, M., Nelson, J.K., MacCrone, R.K., Schadler, L.S., Polymer Nanocomposite Dielectrics: The Role of the Interface. *IEEE Trans. Dielectric Electronic. Insulation*. 2005, 12, 629–643.Kim JK, Mai YW. Engineered interfaces in fiber reinforced composites. New York: Elsevier; 1998
 19. Zhandarov S., Mäder E., Characterization of fiber/matrix interface strength: applicability of different tests, approaches and parameters. *Composite Science and Technology* 2005; 65:149–60.
 20. Selzer, R., Friedrich,K., Mechanical properties and failure behaviour of carbon fibre-reinforced polymer composites under the influence of moisture, *Composite Part-A* 1997; 28:595-604.
 21. Guedes,R.M., Durability of polymer matrix composites: Viscoelastic effect on static and fatigue loading, *Composite. Science and Technology*.2007; 67: 2574–2583.
 22. Ray B.C., Effect of Thermal Shock on Interlaminar Strength of Thermally Aged Glass Fiber Reinforced Epoxy Composites, *Journal of Applied polymer science*.2006; 100: 2062-2066.
 23. Ray B.C.,Loading Rate Effects on Mechanical Properties of Polymer Composites at Ultra-low Temperatures, *Journal of Applied polymer science*.2006;100: 2289-2292.
 24. Parvatareddy, H., Wang, J.Z.,Dillard,D.A.,Ward,T.C., Environmental aging of high-performance polymeric composites: effects on durability, *Composite Science and Technology*, 1995; 53:399-409.
 25. Jiang,X.,Kolstein,H.,Bijlaard,F.,Qiang, X., Effects of hygrothermal aging on glass-fibre reinforced polymer laminates and adhesive of FRP composite bridge: Moisture diffusion characteristics, *Composites Part A* 2014; 57:49–58.
 26. Jiang,X.,Kolstein,H.,Bijlaard, F.S.K., Moisture diffusion in glass–fiber-reinforced polymer composite bridge under hot/wet environment, *Composites Part B* 2013; 45: 407–416.
 27. Awaja F., Moon J.B., Gilbert M., Zhang S. , Kim C.G., Paul J. Pigram P.J. Surface molecular degradation of selected high performance polymer composites under low earth orbit environmental conditions, *Polymer Degradation and Stability* 2011;96: 1301-1309.
 28. Arun,K.V.,Basavarajappa,S.,Sherigara,B.S., Damage characterisation of glass/textile fabric polymer hybrid composites in sea water environment, *Materials and Design* 2010; 31:930–939.

29. Jiang,X.,Kolstein,H.,Bijlaard, F.S.K., Moisture diffusion and hygrothermal aging in pultruded fibre reinforced polymer composites of bridge decks, *Materials and Design* 2012; 12; 304–312.
30. Ray B.C., Temperature effect during humid ageing on interfaces of glass and carbon fibers reinforced epoxy composites, *Colloid and Interface Science*, 2006; 298:111-117.
31. P. J. Herrena-Franco and L. T. Drzal, *Composites* 1994;23; 2.
32. J. Harding, L. M. Weish, *J. Mater. Sci.* 1983;18;1810.
33. Ray B.C., Effects of Thermal and Cryogenic Conditionings on Mechanical Behavior of Thermally Shocked Glass Fiber/Epoxy Composites,*Journal of Reinforced Plastics & Composites*, 2005.
34. Figeys,W., Schueremans,L., Van Gemert,D.,Brosens,K., A new composite for external reinforcement: Steel cord reinforced polymer, *Construction and Building Materials* 2008;22:1929–1938
35. Daly, H.B., Brahim, H.B., Hfaied, N., Harchay, M., Boukhili, R., Investigation of water absorption in pultruded composites containing fillers and low profile additives. *Polymer Composite* 2007; 28:355–64.
36. Shao, Y.X., Kouadi, S., Durability of fiberglass composite sheet piles in water. *J Composite Construction* 2002; 6:280–7.
37. Muliana, A., Nair, A., Khan, K.A., Wagner, S., Characterization of thermo-mechanical and long-term behaviors of multi-layered composite materials, *Composite Science and Technology* 2006; 66:2907–24.
38. Zhang,Y.C.,Wang,X., Thermal effects on interfacial stress transfer characteristics of carbon nanotubes/polymer composites, *International Journal of Solids and Structures* 2005; 42:5399–5412.
39. Adams,R.D., Singh,M.M., Low temperature transition in fiber reinforced polymers, *Composites Part A* 2001; 32:797–814.
40. Rupnowski,P.,Gentz,M.,Kumosa,M., Mechanical response of a unidirectional graphite fiber/polyimide composite as a function of temperature, *Composites Science and Technology* 2006; 66:1045–1055.
41. Bai, Yu.,Valle´e,T.,Keller,T.,Modeling of thermal responses for FRP composites under elevated and high temperatures, *Composites Science and Technology* 2008; 68:47–56
42. Phifer S.P., Hygrothermal evaluation of pultruded polymer composite laminates experimentation, analysis, and prediction. Blacksburg, VA: Virginia Tech; 2003.
43. Shao, Y.X., Kouadi, S., Durability of fiberglass composite sheet piles in water. *J Composite Construction* 2002; 6:280–7.
44. Robert, M., Roy, R., Benmokrane, B., Environmental effects on glass fiber reinforced polypropylene thermoplastic composite laminate for structural applications. *Polymer Composite* 2010; 31:604–11.
45. Shen, C.H., Springer, G.S., Moisture absorption and desorption of composite materials, environmental effects on composite materials. Westport, CT: Technomic Publishing Company; 1981.
46. Doxsee L.E., Janssens, W., Verpoest, I., Demeester, P., Strength of aramid–epoxy composites during moisture absorption. *J Reinforced Plastic and Composite* 1991; 10:645–55.

47. Arun, K.V., Basavarajappa, S., Sherigara, B.S., Damage characterisation of glass/ textile fabric polymer hybrid composites in sea water environment. *Materials and Design* 2010; 31:930–9.
48. Hu, R.H., Sun, M.Y., Lim, J.K., Moisture absorption, tensile strength and microstructure evolution of short jute fiber/polylactide composite in hygrothermal environment. *MaterialandDesign* 2010; 31:3167–73.
49. Ray, B.C., Hygrothermal Effects on the Mechanical Behaviour of Fiber Reinforced Polymeric Composites, *J Metals Materials and Process*,1991;3:99-108
50. Ray, B.C., Assessment of mechanical behavior of Kevlar/polyester composites after thermal shock conditioning *J. of Material Science*. 1992;21;1391-1392
51. Fong, H., Vaia, R.A., Sanders, J.H., Lincoln, D., Vreugdenhil, A.J., Liu, W., et al. Self-passivation of polymer-layered silicate nanocomposites. *Chemistry of Material* 2001; 13:4123-9.
52. Wang, X., Zhao, X., Wang, M., Shen, Z., An experimental study on improving the atomic oxygen resistance of epoxy resin/silica nanocomposites. *Polymer Engineering Science* 2007; 47:1156-62.
53. Deev, I.S., Nikishin, E.F., Effect of long-term exposure in the space environment on the microstructure of fibre-reinforced polymers. *Compos Sci Technol* 1997; 57:1391-401.
54. Golub, M.A., Cormia, R.D., ESCA study of poly (vinylidene fluoride),tetra fluoroethylene - ethylene copolymer and polyethylene exposed to atomic oxygen *Polymer* 1989; 30:1576-81.
55. Abdel-Hamid, I., Mourad, Beckry Mohamed Abdel-Magid, Tamer El-Maaddawy ,Maryam E. Grami, Effect of Seawater and Warm Environment on Glass/Epoxy and Glass/Polyurethane Composites, *Appl Compos Mater* ,2010,17:557–573.
56. Deniz M.E., Karakuzu R., Seawater effect on impact behavior of glass–epoxy composite pipes, *Composites: Part B* 2012; 43; 1130–1138.
57. Strait, L.H., Karasek, M.L., Amateau, M.F., Effects of seawater immersion on the impact resistance of glass fiber reinforced epoxy composites. *Journal of Composite Material* 1992; 26:2118–33.
58. Sethi, S., Ray, B.C., Mechanical behavior of polymer composites at cryogenic temperatures. In: ShusheelKalia, Fu Shao-Yun, editors. *Polymers at Cryogenic Temperature*. Germany: Springer BerlinHeidelberg; 2013.Springer book.
59. Ray, B.C., Thermal Shock on Interfacial Adhesion of Thermally Conditioned Glass Fiber/epoxy Composites, *Materials Letters*, 2004;58:2175-2177.
60. Ray, B.C., Effects of Crosshead Velocity and Sub-zero Temperature on Mechanical Behavior of Hygrothermally Conditioned Glass Fiber Reinforced Epoxy Composites, *Materials Science and Engineering, A*; 2004; 379:39-44.
61. Zafeiropoulos, N.E., Baillie, C.A., Hodgkinson, J.M., Engineering and Characterisation of the Interface in Flax Fiber/Polypropylene Composite Materials. Part II. The Effect of Surface Treatments on the Interface, *Composite: Part A*, 2002; 33:1185-1190.
62. Ray, B.C., Effects of Thermal and Cryogenic Conditionings on Mechanical Behavior of Thermally Shocked Glass Fiber/Epoxy Composites. *Journal of Reinforced Plastics and composites*.2005;24;12-14
63. Jang, B.Z., Interfaces and interphases in composites, *Advanced Polymer Composites*, 1994, ASM International, Materials Park, OH.

64. Sjogren, A., Asp, L.E.; Effects of temperature on delamination growth in a carbon/epoxy composite under fatigue loading, *International Journal of Fatigue* 2002; 24: 179–184
65. Asp, L.E.; The effects of moisture and temperature on the interlaminar delamination toughness of a carbon/epoxy composite. *Composite Science Technology* 1998; 58: 967–77.
66. Pagano, N.J., Schoeppner, G.A., Delamination of polymer matrix composites: problems and assessment. In: Kelly A, Zweben C, editors-in-chief. *Comprehensive composite materials*, vol. 2. New York: Pergamon; 2000.
67. Tay, T.E., Characterization and analysis of delamination fracture in composites: an overview of developments from 1990 to 2001. *Applied Mechanical Review* 2003; 56:1–32.
68. Davidson, B.D., Gharibian, S.J., Yu, L., Evaluation of energy release rate-based approaches for predicting delamination growth in laminated composites. *International Journal of Fracture* 2000; 105:343–65.
69. Mouritz, A.P., Review of z-pinned composite laminates. *Composite Part A Application Science Manufacturing* 2007; 38A:2383–97.
70. Cartié, D.D.R., Troulis, M., Partridge, I.K., Delamination of z-pinned carbon fibre reinforced laminates. *Composite Science Technology* 2006; 66:855–61.
71. Grassi, M., Zhang, X., Finite element analyses of mode I interlaminar delamination in z-fibre reinforced composite laminates. *Compos Sci Technol* 2003; 63:1815–32.
72. Mouritz, A.P., Chang, P., Isa, M.D., Z-pin composites: aerospace structural design considerations. *J Aeronautics Engineering* 2011; 24:425–32.
73. Rugg, K.L., Cox, B.N., Massabò, R., Mixed mode delamination of polymer composite laminates reinforced through the thickness by z-fibres. *Composite Part A Applied Science and Manufacturing* 2002; 33:177–90.
74. Yan, W., Liu, H.Y., Mai, Y.W., Mode II delamination toughness of z-pinned laminates. *Compos Sci Technol* 2004; 64:1937–45.
75. Rezai, A., Cartié, D., Partridge, I., Irving, P., Aston, T., Negre, P., et al. Interlaminar damage resistance of z-fibre TM reinforced structural CFRP. In: *Proceedings of the 13th international conference on composite materials*, 25–29 June, Beijing; 2001.
76. Isa, M.D., Feih, S., Mouritz, A.P., Compression fatigue properties of z-pinned quasi isotropic carbon/epoxy laminate with barely visible impact damage. *Composite Structure* 2011; 93:2222–30.
77. Cartié, D.D.R., Dell'Anno G., Poulin, E., Partridge, I.K., 3D reinforcement of stiffener to-skin T-joints by z-pinning and tufting, *Engineering Fracture Mechanics* 2006; 73:2532–40
78. Koh, T.M., Feih, S., Mouritz, A.P., Experimental determination of the structural properties and strengthening mechanisms of z-pinned composite T-joints. *Composite Structure* 2011; 93:2269–76.
79. Toral Vazquez J., Castanie, B., Barrau, J.J., Swiergiel, N., Multi-level analysis of low-cost z-pinned composite joints, Part 2: Joint behaviour. *Composites: Part A* 2011; 42:2082–92.
80. Chang, P., Mouritz, A.P., Cox, B.N., Tensile properties and failure mechanisms of z-pinned composite lap joints. *Composite Science and Technology* 2006; 66:2163–76.
81. Cartié, D.D.R., Cox, B.N., Fleck, B.N., Mechanisms of crack bridging by composite and metallic rods. *Composite Part A: Applied Science and Technology* 2004; 35:1325–36.
82. Dai, S.C., Yan, W., Liu, H.Y., Mai, Y.W., Experimental study on z-pin bridging law by pullout test. *Composite Science and Technology* 2004; 64:2451–7.

83. Zhang, A.Y., Liu, H.Y., Mouritz, A.P., Mai, Y.W., Experimental study and computer simulation of z-pin reinforcement under cycle fatigue. *Composite PartA Applied Science and Technology* 2008; 39A:406–14.
84. Schmidt,G.,Malwitz,M.M., Properties of polymer–nanoparticle composites, *Current Opinion in Colloid and Interface Science*,2003; 8; 103–108
85. Kim, J.K., et al. Interfacial debonding and fiber pull -out stresses: Part I. A critical comparison of existing theories with experiments. *J Material Science* 1992; 27:3143–54.
86. Zhou, L.M., et al., Interfacial debonding and fiber pull -out stresses: Part II. A new model based on the fracture mechanics approach. *J Material Science* 1992; 27:3155–66.
87. Gupta, V., et al., Calculation, measurement and control of interface strength in composites. *J America Ceramic Society* 1993; 76:305–15.
88. Kelly, A., Tyson, W.R., Tensile properties of fiber-reinforced metals: copper/ tungsten and copper/molybdenum, *Journal of Mechanical Physics Solids* 1965; 13:329–50.
89. Hsueh, C.H., Interfacial debonding and fiber pull-out stresses of fiber-reinforced composites. *Material Science and Engineering A* 1990; 123:1–11.
90. Chua, P.S., Piggott, M.R., The glassfiber -polymer interface. II-work of fracture and shear stresses. *Composite Science and Technology* 1985; 22:107–19.
91. Sitterle, V.B., A modified lap test to more accurately estimate interfacial shear strength of bonded tissues. *J Biomechanical* 2008; 41:3260–4.
92. Tsai, M.Y., Morton,J., An experimental investigation of non-linear deformations in single-lap joints. *Mechanical Material* 1995; 20:183–94.
93. Kafkaldis, M.S., Thouless, M.D., The effects of geometry and material properties on the fracture of single lap-shear joints. *International J Solids Structure* 2002; 39:4367–83.
94. Ferreira, J.M., et al., Stress analysis of lap joints involving natural fibre reinforced interface layers. *Journal Composite Part B* 2005; 36:1–7.
95. Yu,A.,Gupta,V., Measurement of in situ fiber/matrix interface strength in graphite/epoxy composites, *Composites Science and Technology*, 1998;58; 1827–1837.
96. Weitsman, Y., Moisture in composites: sorption and damage. In: Reifsnider KL, editor. *Fatigue of Composite Materials* 1991; 385.
97. Xie,Y.,Hill,C.A.S.,Xiao,Z.,Militz,H.,Mai,C., Silane coupling agents used for natural fiber/polymer composites: A review, *Composites: Part A* 2010; 41; 806–819.
98. Mouritzas, A.P., Leongb,K.H.,Herszberg C, A review of the effect of stitching on the in-plane mechanical properties of fibre-reinforced polymer composites, *Composites Part A* 1997;28A; 979-99.
99. Böer,P., Holliday,L.,Kang,T.H.K., Interaction of environmental factors of fiber -reinforced polymer composites and their inspection and maintenance: A review, *Construction and Building Materials*, 2014; 50; 209–218.
100. Jiang,X.,Kolstein,H.,Bijlaard,F.,Qiang, X., Effects of hygrothermal aging on glass-fibre reinforced polymer laminates and adhesive of FRP composite bridge: Moisture diffusion characteristics.
101. Azwa, Z.N., Yousif, B.F., Manalo, A.C., Karunasena, W.,A review on the degradability of polymeric composites based on natural fibres, *Materials and Design*; 2013; 47; 424–442.

102. Hany El Kadi, Modeling the mechanical behavior of fiber-reinforced polymeric composite materials using artificial neural networks—A review.
103. Mouritz, A.P., Feih, S., Kandare, E., Mathys, Z., Gibson, A.G., P.E. Des Jardin S.W. Case, B.Y. Lattimer, Review of fire structural modelling of polymer composites, *Composites: Part A*, 2009; 40; 1800–1814.
104. Mohammed H. Al-Saleh, Sundararaj, U., Review of the mechanical properties of carbon nanofiber/polymer composites, *Composites: Part A*, 2011; 42; 2126–2142.
105. Bárány, T., Czigán, T., Karger-Kocsis, J., Application of the essential work of fracture (EWF) concept for polymers, related blends and composites: A review, *Progress in Polymer Science*; 2010; 35; 1257–1287.
106. Mouritz, A.P., Review of z-pinned composite laminates, *Composites: Part A*; 2007; 38; 2383–2397.
107. Echaabi, J., Troche, F., Gauvin, R., Review of Failure Criteria of Fibrous Composite Materials, *Polymer Composites*, 2009; 17; 32-37.
108. Lau, K., Gu, C., Hui, D., A critical review on nanotube and nanotube/nanoclay related polymer composite materials, *Composites: Part B* 2006; 37; 425–436.
109. Breuer, O., Sundararaj, U., Big Returns From Small Fibers: A Review of Polymer/Carbon Nanotube Composites, *Polymer Composites*, December 2004; 25, 7-82.
110. Bokobza, L., Multiwall carbon nanotube elastomeric composites: A review, *Polymer*; 2007; 48; 4907-4920.

Chapter 2

Literature Link

2.Literature Link

2.1 Introduction

Fibre reinforced polymer (FRP) composites are the most promising and elegant materials of present century. Their durability and integrity in various service environments can be altered by the response of its constituents i.e. fibre, polymer matrix, and the existing interface/interphase between the fibre and polymer matrix, in that particular environment. Their susceptibilities to degradation are dependent on the nature of environment and the different and unique response of each of the constituents. All these structures and components are exposed to some environment during their service life. The environmental conditions can be high and low temperatures, high humidity, UV light exposure, alkaline environment and may be more severe if there is cyclic variation of temperature, hygrothermal environment and low earth orbit space environment [1]. Widespread application spectrum of FRP's covers almost every type of advanced engineering structures. Their usage includes various components in aircraft, helicopters, spacecraft, boats, ships, offshore platforms and also in automobiles, chemical processing equipment, sports goods, and civil infrastructure such as buildings and bridges [2]. The behaviour and performance of advanced structural FRP composites cannot be explained only in terms of specific properties of its constituent fibre and matrix but the existing interface/interphase between fibre and matrix has great significance as well [3, 4]. The presence of moisture at the interface can modify the interfacial adhesion thereby affecting the mechanical performance of the FRP composites. The energy associated with the UV radiation is capable of dissociating the molecule bonds in polymer matrix and may lead to the degradation of the materials. The border surface between the fiber and the matrix is a result of the linking of constituents; it has its own morphology and chemistry and represents the critical area in fiber-reinforced composites [3].

2.2 Environmental Degradation

2.2.1 Thermal environment

Fibre reinforced polymer composites are now very popular to structural applications, aerospace spacecraft and other military fields. Due to its high strength to weight ratio, corrosion and damping vibration resistance these material are very well-known. During its service period they are very sensitive to different environmental conditions mostly moisture

and temperature. However, these materials are anisotropic and heterogeneous in nature which results in the formation of hygrothermoelastic stresses within their mesostructure [5]. The strength and integrity of the materials totally depends upon the strength of the interface/interphase and/or matrix especially at high temperature and moisture concentration [6-11]. The structural and physical changes in the matrix resin occurred during hygrothermal treatment and temperature effect which ultimately have a great significance effects on mechanical behavior of fibre reinforced polymer composite materials. During moisture ingress a new-phase formed between fibre and matrix region, at low temperature this phase has its own glass transition temperature different from its bulk matrix phase [12-14]. Epoxy polymer matrix usually behaves in ductile manner below its glass transition temperature whereas shows viscoelastic in nature above glass transition temperature. Below glass transition temperature the mobility of the polymer chain becomes restricted. Last few decades fibre reinforced polymer composites have numerous applications in low and cryogenic temperature. At cryogenic temperature the molecules are rearranged due to its relaxation behavior [15].

Residual stresses have great impact on the fibre matrix interface region of fibre reinforced polymer composites [16]. Because of these crack initiation and propagation occurs and some other failure modes are formed [17]. Thermal stresses present in the laminates and differential coefficients of thermal expansion at interface region may be the reason for creation of residual stresses in the laminates. Some disadvantages also observed as it weakens the interface and the interfacial region in the laminates, which leads to debonding. At this situation different types of failure modes are observed as micro and macro cracks, osmotic cracks, fibre/matrix debonding, and strain in matrix which lower the glass transition temperature of the laminates [20]. Wang et al. investigated environmental ageing on carbon fibre with cyanate ester resin and thermoplastic resin composites where 40-60% decrease in ultimate failure strain were observed. However, modulus values increases up-to 20% during 6 month of ageing [17]. Sookay et al. studied environmental effect on two different epoxy resins with woven glass reinforcement [18]. Hosur et al. investigated durability of montmorillonite clay filled epoxy composites under different environmental conditions. They considered 2 different conditions as hot environment (elevated temperature: dry, wet at 60 and 80°C) and cold (sub-zero: dry, wet, - 18°C) conditions for different durations. In cold conditions epoxy matrix shows environmental sensitivity. Fig. 1 represents the stress-strain curve of cold conditioned samples where discolorations of the materials are observed [19].

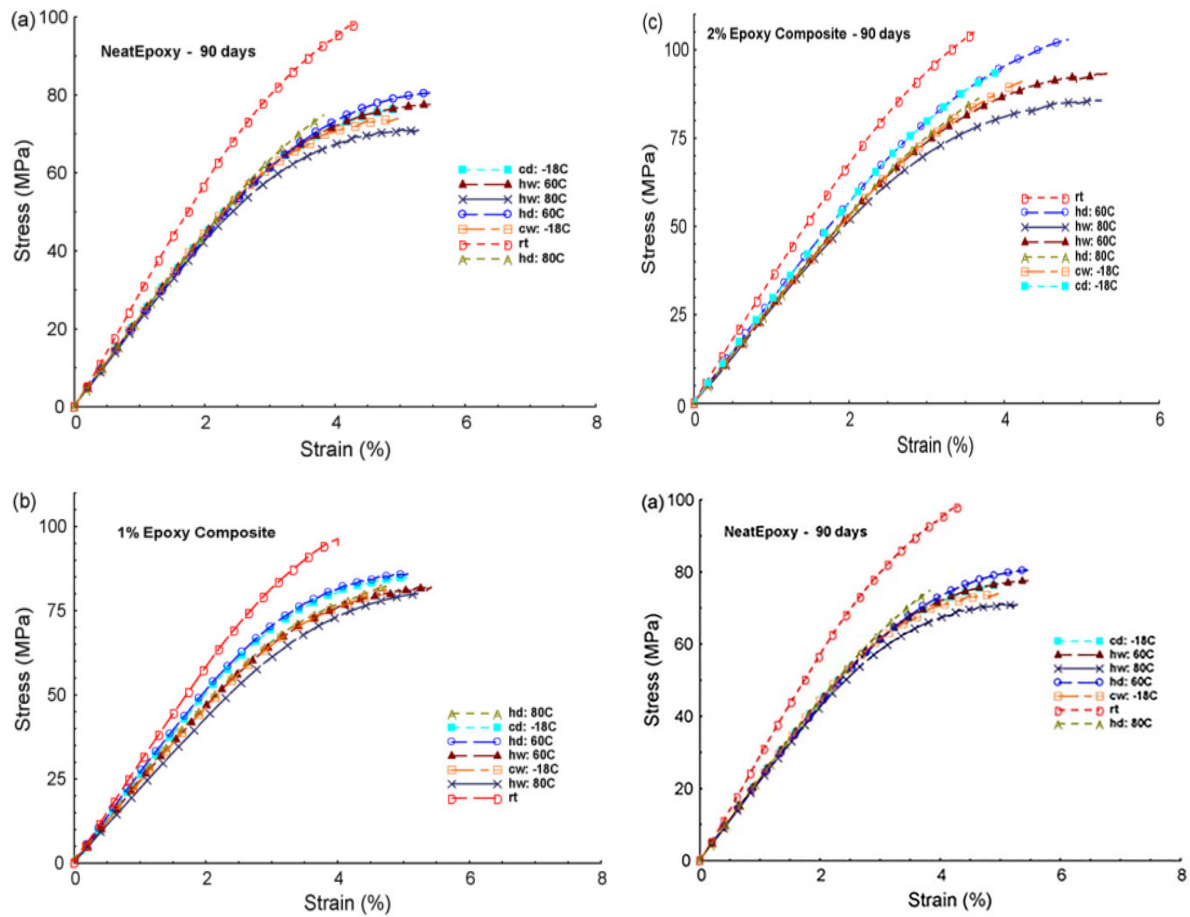


Fig 1. (A-C) Flexural stress-strain curves of control and conditioned neat/nano epoxy specimens [19].

Temperature is likely to influence moisture pick-up kinetics in polymer composites in a complex manner [20]. The equilibrium moisture content in fiber-reinforced polymer (FRP) composites is observed to be either independent of temperature [21] or dependent on temperature [22]. Absorbed water is rarely distributed uniformly and thus a distribution of internal stress associated with water uptake is noticed. Hygrothermal conditioned glass/epoxy composites, subjected to three point bend test at 1mm/min and 10mm/min crosshead speed, show that at higher strain rate the mechanical degradation is less pronounced for the same level of absorbed moisture [23]. Ray et al. have studied the effect of prior thermal conditioning on glass/epoxy composite in form of thermal shock and thermal spike. It is reported that the changes in the mechanical properties undergoes in two ways, either it may be in form of thermal stresses developed in matrix which cause matrix damage through crack formation or this conditioning can accelerate the moisture absorption by creating active sites which results in differential hygroscopic stresses in composites [24]. The

deterioration effect of hygrothermal shock on interfacial bonding of varied weight fraction constituents in the composite is also reported in some literatures. When glass/polyester matrix is treated in 50°C temperature water bath for 30 minutes and then immediately immersed in 100°C temperature water bath for the same duration, various failure modes are observed. Matrix as well as interface damages possibly contribute to the weakening phenomena of glass/polyester composite by the hygrothermal shock cycles [25].

2.2.2 Hygrothermal environment

The environmental actions, such as high moisture and high temperature can limit the usefulness of polymer composites by deteriorating their mechanical properties during service. One of the key features of this material class is their damage initiation and propagation behaviour which is spatially distributed in nature and comprises of a variety of mutually interacting damage modes. The most common damage modes are matrix cracking, delamination growth and fibre fracture. There has been a pressing need to quantify the degree of environmental degradation on the deviation of mechanical properties of fibre/polymer composites. Humid ageing is recognized as one of the main causes of long-term failure of organic matrix composite. There are several modes of humid ageing, such as, plasticization of matrix, differential swelling, embrittlement of macromolecular skeleton by hydrolysis, osmotic cracking, hygrothermal shock, and localized damage at the fibre/matrix interface [26] etc. Thermal expansion coefficients of polymers are considerably greater, thus failure of the bond between fibre and resin may occur under extreme temperature [15]. Moisture diffusion in the laminates is now very critical to justify the moisture ingress kinetic and degradation of mechanical properties during hygrothermal treatment as it predicts the life cycle of fibre reinforced polymer composites materials.

Differential coefficients of thermal expansion between fiber and polymer further develop residual stresses at the interface. These different natures of stresses may weaken the brittle thermoset epoxy resin and/or the interfacial region of the laminate. Moisture is introduced into the composite via diffusion flow along the fiber/matrix interface or transport via microcracks and voids, which leads to diffusion in to the surrounding matrix [27,28]. The effects of moisture on the matrix include reversible processes, such as hygroelasticity and swelling that can relieve tensile residual stresses which develop in the resin after cure and, thus enhance its performance.

A large number of literature is available regarding different direction of moisture ingress and absorption considering swelling hygrothermal stresses and absorption kinetics because here water acts as a plasticiser. NMR is a also a useful instrument to investigate the mobility of water inside the matrix resin which was studied by Zhou and Lucas [27] for fibre reinforced polymer composites. Depending upon the activation energy of the matrix and the bond formation they observed two types of bonding mechanism occurred. Van der Waals link formed having low activation energy consider as Type I bonding whereas multiple hydrogen or double hydrogen bond formed with the matrix resin considered as Type II bonding mechanism.

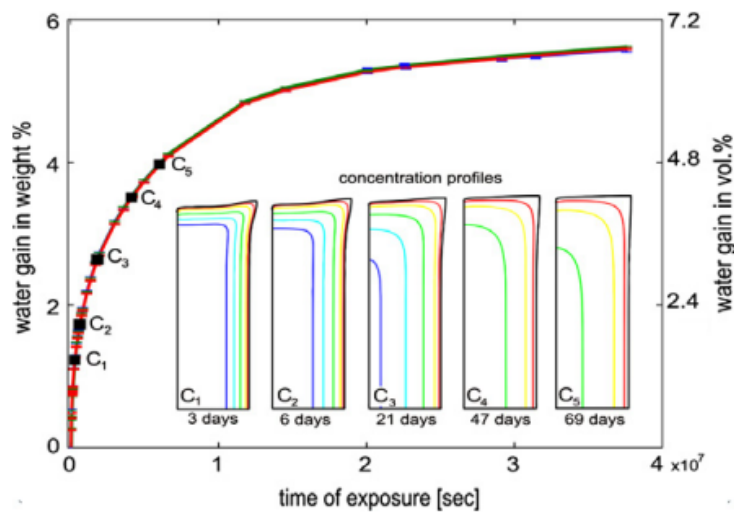


Fig 2. Absorption curves in SFC specimen and iso concentration lines at 10%, 25%, 50%, 75%, 90% moisture [27].

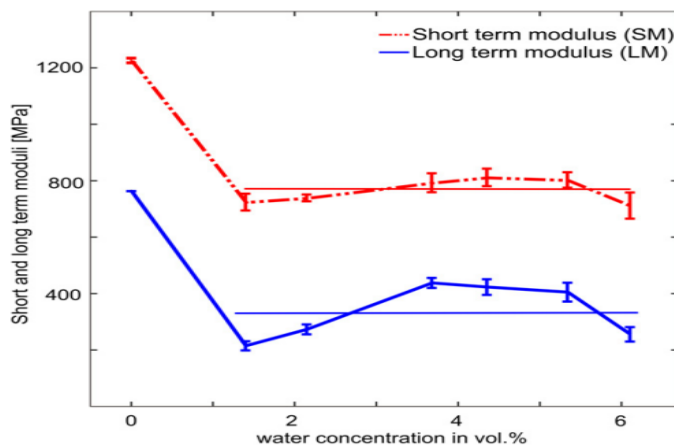


Fig 3: Short and long term moduli in terms of water concentration [27].

Fig 2 represents the absorption curve between weight and volume vs. immersion time and Fig 3 represents the short and long term moduli in terms of water concentration. The qualitative explanation of these curves shows hydrogen bond formation among polymer chain of resin matrix which are responsible for crosslinking. During this process the modulus values varies in large scale where resin matrix considered as viscoelastic in nature [28]. Temperature has a dominating effect in changing the nature of absorption kinetic curve at higher temperature conditioning. Water pick-up kinetics and mechanical tests such as interlaminar shear strength (ILSS) are supposed to be indicative of the adhesion chemistry at fiber/matrix interfaces and integrity of composites.

Environmental exposure results in reduced interfacial stress transmissibility due to matrix plasticization (reduces the matrix modulus), chemical changes and mechanical degradation. Chemical degradation causes hydrolysis of bond. Mechanical degradation is the outcome of matrix swelling strain. An interfacial reaction may induce various morphological modifications to the interphase at the fiber/polymer interface [29,30].

2.2.3 Effect of temperature on mechanical properties

FRP composites are sensitive to temperature variations as a result of induced thermal stresses between the fibres and polymer matrix [31] which arises due to their distinct thermal expansion coefficients. At elevated temperature, differential thermal expansion of fibre and matrix may lead to the formation of microcracks at the fibre/polymer interface [32]. The fibre matrix interface also becomes susceptible to aggressive reactions under the exposure of high temperature environment, which can leads to degradation of both the fibres and the matrix [33]. This in turn affects the integrity of the composites, since it is the interface through which the thermal and mechanical loads are transferred from the matrix to the fibres. Composite material may contain randomly spaced micro voids, incipient damage sites and microcracks with statistically distributed sizes and directions. Therefore, the local strength in the material varies in a random fashion. The failure location as well as degree of damage induced in the material also varies in an unpredictable manner. The mechanical and fracture behaviour can be strongly influenced by the loading rate and temperature [15]. The predominant failure mechanisms in a composite laminate are a very complex combination of energy absorption principle [5]. J. Etches [30] studied thermally multi-stability of composite materials at different environmental conditions.

Fig.4 represents the height changes occurred during the testing of load required to moisture absorption of the materials.

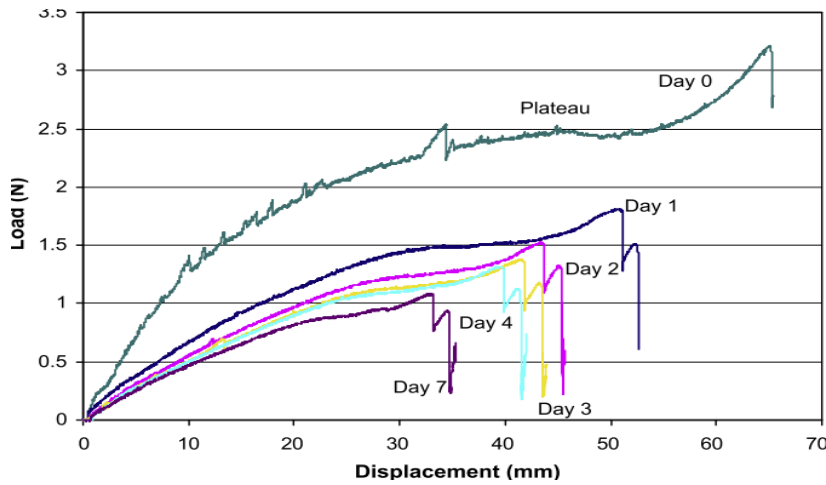


Fig 4. Change in snap-through load with exposure to 20°C and 65%RH [30]

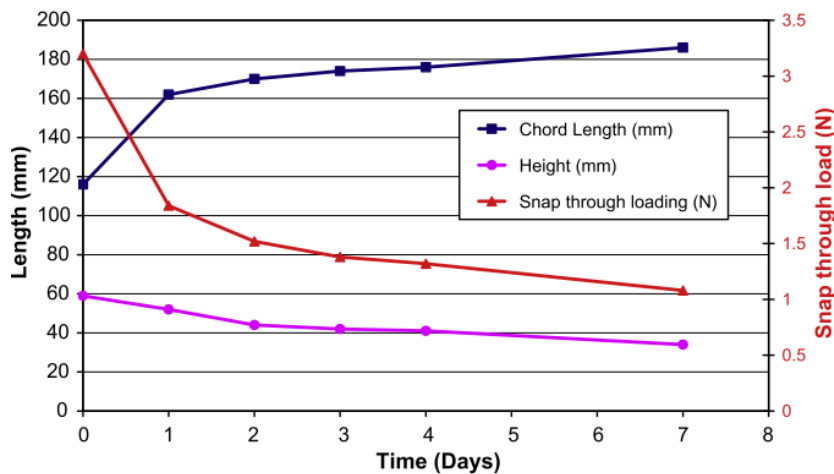


Fig 5. Load-displacement traces for bistable plate over several days exposure to 20°C and 65%RH [30].

The load–displacement of bistable plate can be seen in Fig. 5 and it is observed that the load value increases after the plateau region and before the bifurcation of the plate. In this case presence of moisture in the surrounding also considered which are responsible for thermal stresses of the material.

2.2.4 Effect of radiations and other external environments on FRPs

Fibre-reinforced composite materials such as glass, carbon and Kevlar fibre-reinforced plastics are finding numerous applications in structural engineering, because of its higher specific stiffness and strength, fatigue and corrosion resistance than the conventional engineering materials. Composite materials do, however, suffer from some serious environmental limitations. Environmental exposures include temperature, moisture,

radiations, UV and other different alkali treatments, which cause deteriorating the mechanical and/or physical behaviour, adhesion between fibre/matrix interface regions of the composite material over a period of time. In the previous section as 2.2.2, 2.2.3 we focused mostly on temperature and moisture conditioning environment. The main focus of this section was other environmental conditionings as radiations, space environments and alkali treatments. A large number of research work have been published on the topic of environmental exposure effects related to determining accelerated test methods for the prediction of long-term performance of FRP composite material.

Till now the durability and integrity of these magnificent materials are under question mark. How can we use the full potential of these materials under different harsh environmental conditions? Considering harsh environment point of view the organic polymers are very sensitive to the moisture, acid rain, UV radiation thermal cycling because presence of unexpected elements [31,32]. UV radiation with atmospheric oxygen induces chemical changes in the epoxy polymer matrix which is truly a very complex process. This is sometimes referred as photo-oxidation process which ultimately changes the mechanical behavior of the composite materials. The covalent bond present in the polymer dissociated and formed free radical by the effect of UV radiation light as it is absorbed the chromophoric group of polymer. These whole things followed by molecular cross linking and chain scission [33]. Visually surface yellowing discoloration occurred during UV radiation effect where light photons are reacting with polymer chain leads to instability in mechanical properties. As UV radiation have short wavelength and long wavelength in nature, where short wavelength have higher photon energies which are very sensitive to polymer matrix resin, thus there is chances of breaking of chemical bonds between molecular compounds [32]. There is decrease of 15% in average failure strain and 18% decrease in tensile modulus was observed by Shokrieh et al for polyester resin composites exposure to UV radiation for 100 h. It was reported that the strength retention of a 0.13 mm (1p ply) uni-directional DuPont Kevlar-49 epoxy laminate after 1000 h UV-exposure on both surfaces was -60% [34]. Chevali investigated flexural creep behavior of thermoplastic (LFT) composites as a function of ultraviolet irradiation and moisture absorption. Creep values increases with increasing UV conditioning duration whereas in some cases there is significant changes in creep value was observed [40]. Some authors investigate the inner structure of the materials after exposure of accelerated UV radiation. [41].

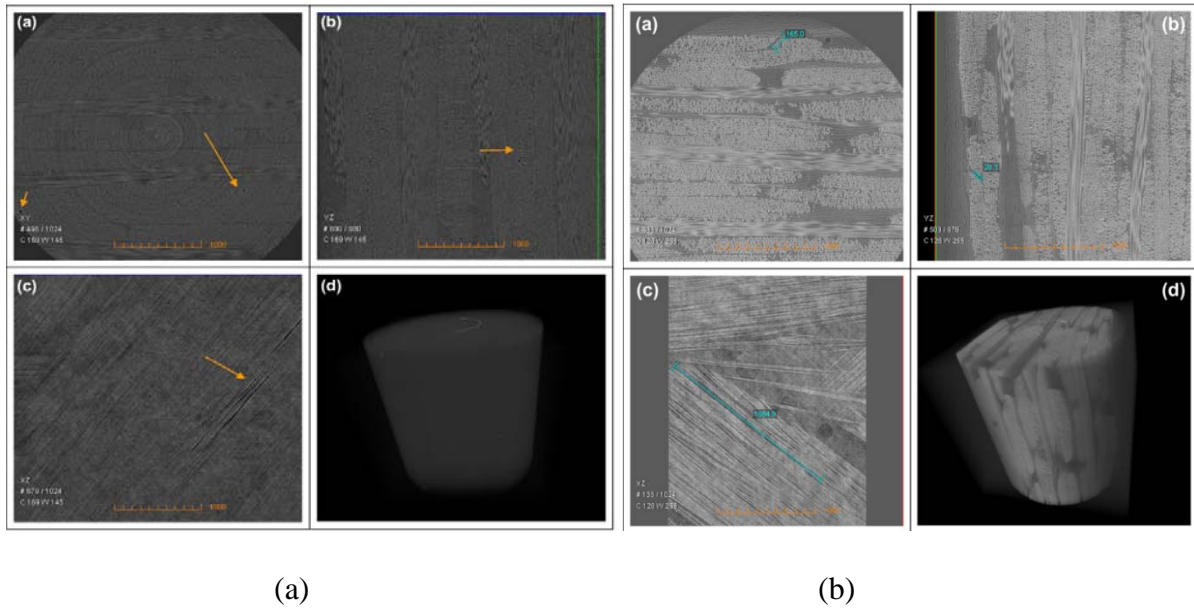


Fig6: (a) Example of the damage in the treated carbon fibre composites: (a) XY plane, (b) YZ plane, (c) XZ plane and (d) 3D view, One of the delaminations in the treated E-glass resin composites: (a) XY plane, (b) YZ plane, (c) XZ plane and (d) 3D view[41].

They reported the carbon fibre composite are less prone to damage than E-glass/resin composites after exposure to both UV irradiation and high temperature which shown in Fig. 6. Delamination failure modes are very natural failure modes observed in case of carbon fibre/epoxy composites. Various literatures are reported on damage and degradation effects of carbon fibre/epoxy composites under UV radiation [42,43]. In case of nano-filler addition some polymeric composites shows increase in flexural strength [44].

2.2.5 Effects of loading speed on conditioned composites

Sethi et.al studied the failure of glass fibre/epoxy composites in thermal and cryogenic environments. They observed the percentage of ILSS value decreases during above-ambient temperature testing in every mode of loading rate ranges because of thermal conditioning effect which leads to spreading of process zone in the matrix resin which impart high fiber/matrix debonding which shown in Fig.7. [45].

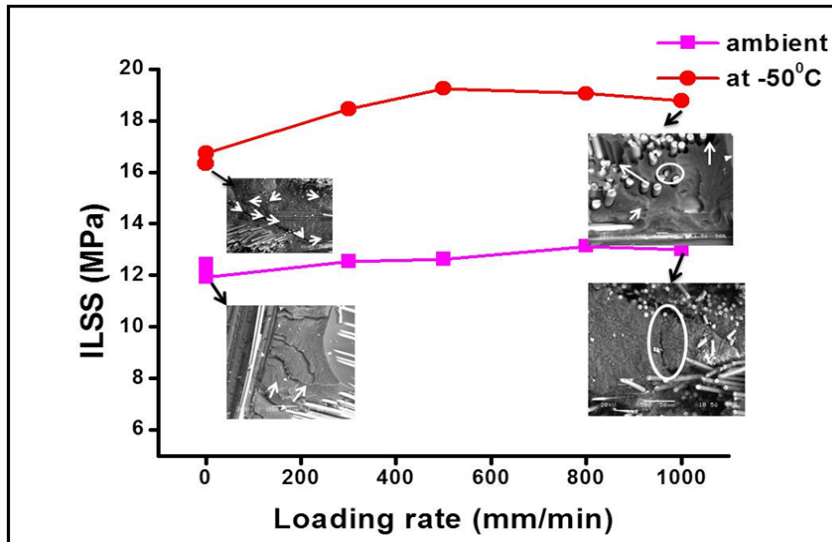


Fig.7: ILSS with loading rate of glass fibre/epoxy composites at -50°C temperature [45].

The rapid advancement of these materials has outstripped the understanding of appropriate failure analysis techniques [46]. The effects of strain rate on most polymers may be explained by the Eyring theory of viscosity, which assumes that the deformation of a polymer involves the motion of a chain molecule over potential energy barriers. Here, the yield stress varies linearly with the logarithm of strain rate. The polymer matrix has less time to localize at higher loading rates.

The mechanical properties behavior as interlaminar shear, flexural, compression and tensile in presence of moisture of FRP composites have been reported by many researchers. Joshi et al. [47] studied effect of moisture on the interlaminar shear strength in unidirectional laminates and tensile strength in ($\pm 45^\circ$) laminated carbon fibre-reinforced epoxy resin laminates. Slight increase in ILSS values was observed in early moisture ingress (0.1% weight) of the materials but it decreases around 25% of ILSS after 2% of weight gain. In case of tensile strength they observed 35% loss in value at 130°C. Fig.8 shows interfacial shear strength value with percentage change in moisture absorption. From the result we can understand the fibre/matrix bond strength changes in the presence of hygrothermal ageing [48].

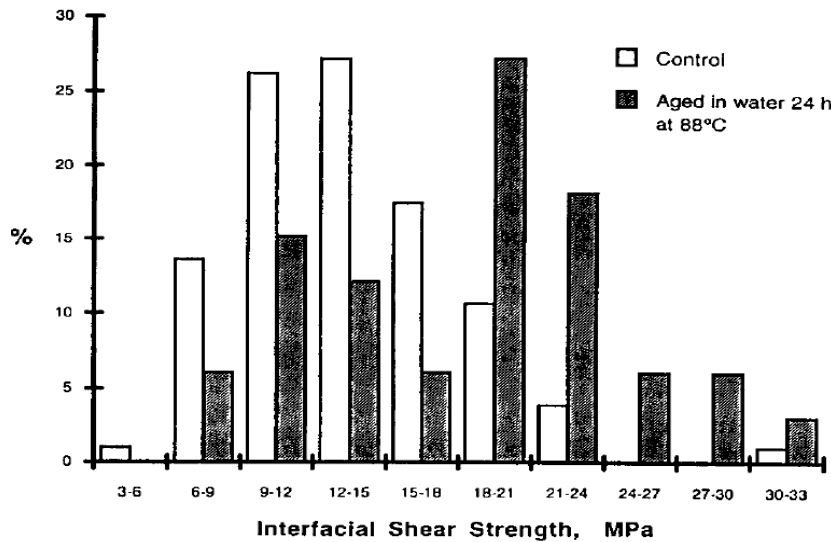


Fig 8. Bond strength distributions for Kevlar 49/polyethylene microcomposites and their counterparts aged in water at 88°C for 24 h [48].

Birger et al [49] studied the failure mechanisms of graphite fabric reinforced epoxy composites loaded in flexure followed ageing in dry, wet and hot environments. They observed composites are more tends to degrade in case of boiling water treatment whereas in case of wet environment there is no significant effect was found. Akay M. [50] investigated on unidirectional and woven fabric carbon fibre/epoxy composites under both the static and dynamic loading conditions in presence of hygrothermal environment. Here, strength at failure initiation under static loading is found to have greater significance, particularly in relation to fatigue behaviour.

2.3 Nanofiller in FRP system

Interface issues are more critical point of discussion in the field of polymer nanocomposites as it signifies excellent mechanical properties. During dispersion of nanoparticles in polymer matrix an interface region was formed which have specific behavior in comparison to bulk materials [51]. Various dispersion methods were obtained for the fabrication of these polymer matrix nanocomposites. In some cases nanoparticles are agglomerated in the matrix resin which leads to decrease in mechanical properties [52,53]. Polymer chain gets swell during dispersion of nanoparticles forming radius of gyration. If the volume fraction of nano-filler was increased the radius of gyration also increases. This entropically unfavourable process is offset by an enthalpy gain due to an increase in molecular contacts at dispersed nanoparticle surface as compared with the surfaces of phase-separated nanoparticles [53]. Now a day's materials scientists are facing big challenges for the fabrication of polymer composites

keeping in mind for the proper interfacial behavior [54]. In nanocomposites this interfacial polymer constitutes a significant volume fraction of the composite even at low filler concentrations as shown in Fig 9. The degree of interaction between polymer and the nano-filler can decide the size of the interfacial region (250nm) [55].

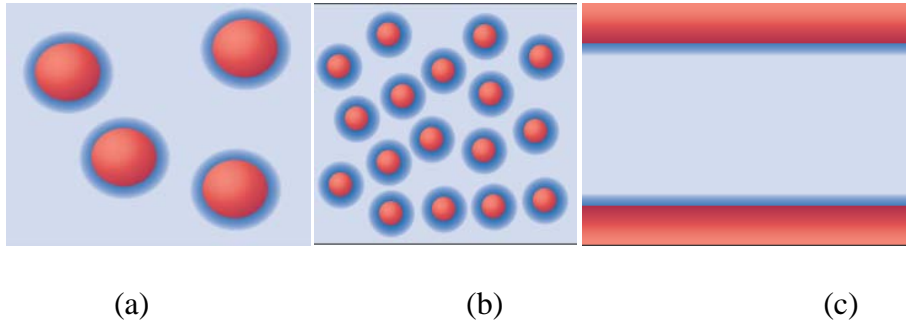


Fig 9: (a) Interfacial regions as a function of filler particle size. The filler is shown in red, the interfacial region in dark blue and the bulk polymer in pale blue. (b) Large particles produce a low radius of curvature, and relatively less polymer in the ‘interfacial region, (c) the same volume of filler broken into smaller particles creates a higher radius of curvature and more polymers in the interfacial region [55].

Thus the size of interfacial region profoundly influences the glass transition temperature of the polymer and the relaxation behavior of the materials. If the enthalpy reaction was high enough then there is a sign of permanent sign of good adhesion between nano-filler and polymer chain. Considering this stage, polymer nanocomposites exhibits low and high glass transition temperature on the basis of distance of nano-filler to the polymer chain. [56,57].

2.4 Mechanical behaviour of polymer composites

2.4.1 Tensile failure

The mechanical behavior of fibre-reinforced polymeric composites is sensitive to the environmental conditioning and the loading fixture [61]. Very few literatures are dedicated for the fibre reinforced polymer composites on the basis of strain rate and environmental conditioning compared to conventional materials. Some literatures are performed on tensile and compression behavior of these materials. Proper understanding was needed for these materials for its long life performance and durability.

Shokrieh et al [62] studied on tensile behavior of glass/epoxy composites at different strain rate shown in Fig.10. They found strain to failure, tensile modulus, tensile strength increases with increasing strain rate.

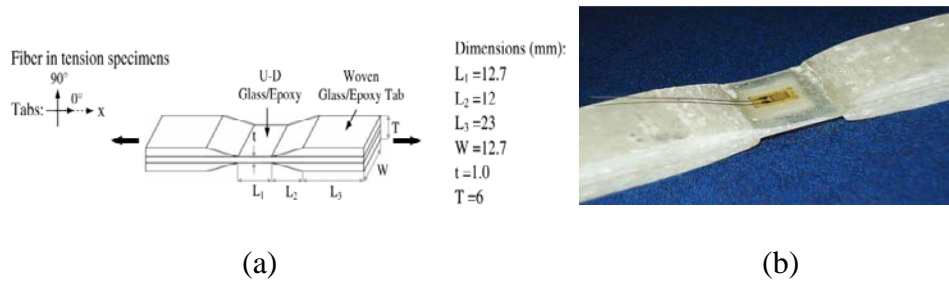


Fig 10: Geometry and dimensions of composite specimens under tensile loading (b) untested specimen [62].

In fibre reinforced polymer matrix composites both fibre and matrix are known to be strain rate sensitive. Compared to quasi-static test at high strain rate, tensile strength shows significant increase in load value. Harding and Welsh validated a dynamic tensile technique by performing tests (over the range 10^4 to 1000 s^{-1}) on carbon/epoxy, glass/epoxy, glass/polyester, carbon/polyester, and Kevlar/polyester composites [63,64]. They observed mechanical behaviors of carbon fibre/epoxy composites are more sensitive to loading rate. The dynamic modulus and strength for the glass/epoxy composite were about twice the static value. Barre et.al investigates the strain rate effect on fibre reinforced polymer composites, they observed strength and elastic modulus increases with increasing strain rate [65]. Similarly Peterson et al. [66] found 50–70% increase in the elastic modulus and strength with increase in strain rate. Split Hopkinson pressure bar also used during tensile test for the high strain rate analysis of fibre reinforced polymer composites [67].

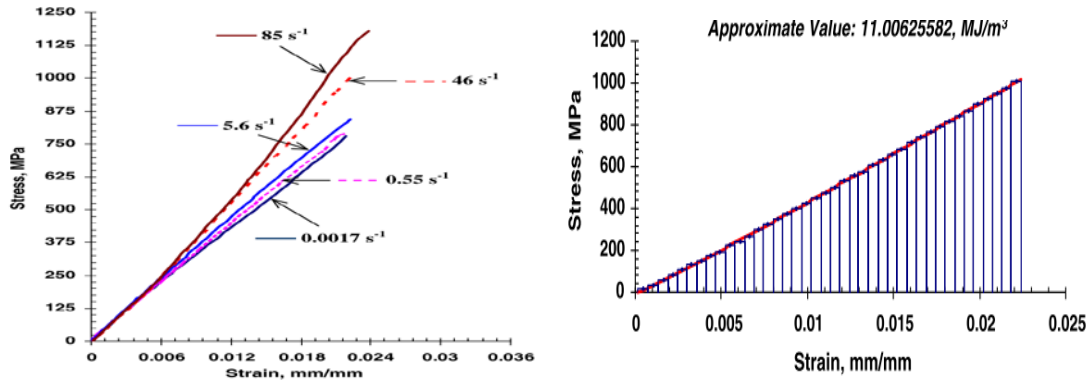


Fig: 11 (a) Stress-strain curve at different strain rate (b) Absorbed energy under stress-strain curve [67]

The stress–strain curves of the tested composites under different strain rates are presented in Fig.11 (a), the material shows a load rate dependency. Nonlinearities behavior was observed from the stress–strain curves with increased strain rate.

2.4.2 Responses of stress-strain behavior to environments

Stress-strain curve can analysed on the basis of materials behavior and its deformation. Now it's a big challenge for these materials to improve the resistance under different environmental conditions as temperature, moisture, alkali treatment and the loading conditions. Under different loading conditions as tensile, compression, flexural and interlaminar shear test the materials exhibit different failure mechanism. Theory of elasticity can be used for the analysis of tensile strength to calculate the elastic modulus and strength. Different models have been demonstrated on the basis of theory of elasticity for brittle and ductile materials. Fig.12 represents one stress-strain curve where the compression values were not affected by any types of materials defects [73]. The importance of polymer composites arises largely from the fact that such low density materials can have unusually high elastic moduli and tensile strength [68-72].

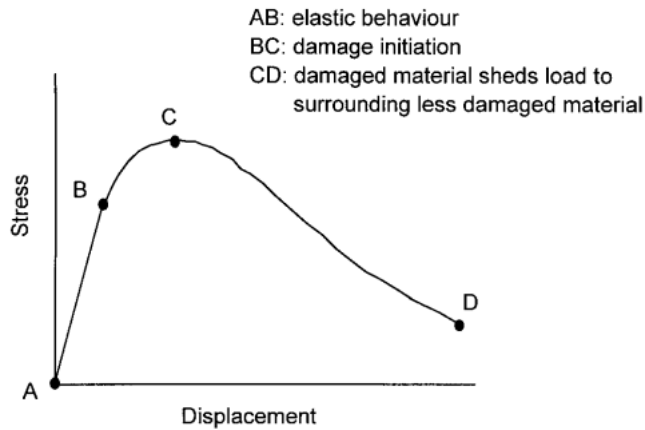


Fig 12: Different regions of a typical strain softening curve. The displacement, rather than strain, is used, to avoid implications of violating basic principles [73].

The curve reveals that stress increases during the loading condition and it starts damage in the process zone leads to large displacement and called as strain softening zone. Elastic zone also observed when materials under undamaged conditions [74].

Large difference between elastic modulus of reinforcement fibre and the matrix resin in fibre reinforced polymer composites results in interfacial shear yielding on the sides of fibre axis [75-79]. Thermosetting resins are usually used in applications for critical components of aerospace structure due to its good glass transition temperature, yield strength and modulus properties. The bulk matrix has high yield strength than the vicinity of the interfacial matrix region where a plastic zone was developed. In this case materials behave in brittle in manner under tensile loading. For microstructural understanding an extensive research have confirmed that yield region was present in the surrounding of the breaking point of fibre [80]. Johnson et al. [81] have demonstrated using photoelasticity that the sequence of events involves fibre fracture, which propagates into the matrix and delays the stress transfer back to the fibre through shear which shown in Fig.13. The shear stress can then initiate debonding which can propagate back towards the fibre -break and away from it. Kettle et al. [82] have demonstrated that all of these micromechanisms from debonding to transverse matrix cracking are function of the strength of the interfacial bond.

2.5 Microstructural and micro-interfacial characterization

The absorbed water particles in polymer matrix composites are known to have major effects on their final performance of composite structures especially in their long-term utilization. The combination of developing hygrothermal forces and residual stresses

with each other may be sufficiently large enough to influence the failure of laminated composite and thus, should not be neglected in modern design analysis and lifetime estimation. Fiber reinforced polymer composite structures are expected to experience a range of hygrothermal environmental conditions during service life. Since absorbed moisture can change the stress state and deteriorate the interface, understanding of hygrothermal behavior is critical for predicting structural performance.

It is necessary to obtain a stable interface region in glass fibre/epoxy composites to optimised its specific valuable properties under different environmental conditions.. Other reinforcements are also subjected to different sizing treatment during its working periods. To understand the basic principle behind this various characterization processes are employed now a days [84]. These instruments are very sensitive in nature which are included as near-infrared fourier transform infrared spectroscopy (NIR-FTIR), attenuated total reflection fourier transform infrared spectroscopy (ATR-FTIR), ultraviolet (UV) reflection, solid-state nuclear magnetic resonance (NMR), dielectric relaxation measurements, positron annihilation lifetime spectroscopy (PALS), electrochemical impedance spectroscopy (EIS), fluorescence, and molecular simulations [85] etc. Fourier transform infrared spectrometry (FTIR) and atomic force microscopy are particularly useful methods for the study of silane coupling agents adsorbed or bounded to glass surfaces [86]. However, very small amount of coupling agent is normally applied to the glass surface and the presence of strong bands from the substrate often makes the IR detection of the silane characteristic bands difficult.

2.5.1 Micro-characterization of interfaces

As it's a difficult task for obtaining the clear picture of interfacial characterization in the fibre reinforced polymer composites various macroscopic approaches are reported. These includes flexural test, fibre pull-out test, fragmentation test, transverse tensile test which are the main focusing study on fibre /matrix interface region. During environmental exposures it's very difficult to identify the clear reasons for failure of these materials. Matrix properties are very sensitive to environmental conditions which control the overall mechanical response. Characterizations of the laminates are influenced by matrix properties and fibre/matrix interfacial bonding. As fibre reinforced undergoes various sizing treatment on the surface, the bonding between fibre and matrix plays crucial role. The FTIR measurement is employed to the sample.

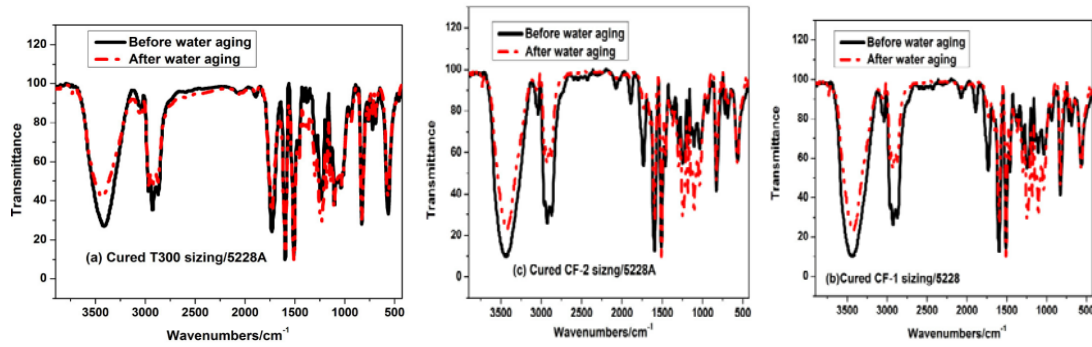


Fig 13. FTIR spectra of different sizing agents/epoxy resin before and after boiling water aging [87].

Fig 13 represents the FTIR spectra of T300 sizing/5228, CF-1 sizing/5228 and CF-2 sizing/5228 undergoing boiling water. There is no chemical transformation observed in the composite in the FTIR spectra under these conditions. It can only be reveals that chemical reaction does not have any effect on these samples during boiling water treatment [87].

The mechanical behavior of composites depends on the ability of interface to transfer stress from the matrix to the reinforcement fiber. The physical properties of polymer materials depend decisively on frequencies of molecular excitation through the relaxation time that depends on temperature [88]. The durability and integrity of these materials are totally depends upon the several failure modes observed during fractography testing. Scanning electron microscopy is very useful technique to understand the failure modes and the reason behind the materials failure. Hahn et. al [89] conducted a study to describe CFRP composites to study their interfacial properties and the effect of hygrothermal analysis using Atomic Force Microscope (AFM). Hygroscopic treatment is found to progressively reduce the height variation in between fiber and matrix showing the swelling of matrix by absorption of moisture. The fiber/matrix interface is susceptible to mechanical strength and thermal behaviour as revealed by the debonding. This debonding can be easily detected by AFM which is shown in Fig 14.

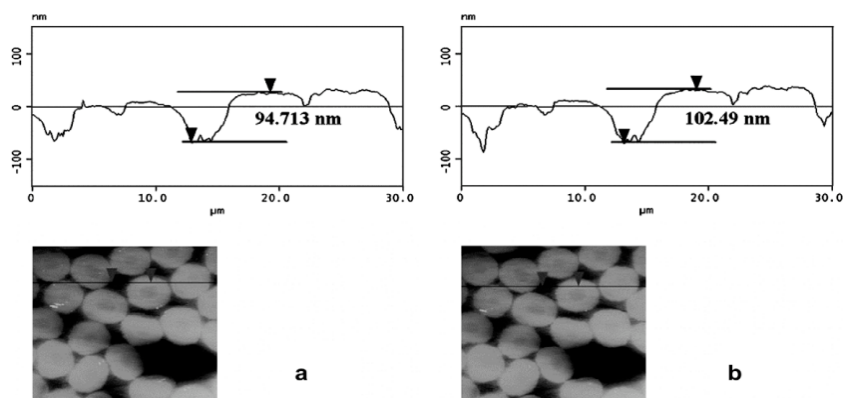


Fig 14. AFM topography images of the same cross-section area of AS4/VRM34 using Tapping Mode (a) and contact mode (b). The scan size was 30*30 μm [89].

It is seen that the Tapping Mode and contact mode AFM images in Fig. 14 exhibit nearly similar surface profiles. The height profile along the section analysis lines for the two images also looks equivalent to each other, signifying the consistency of the topography images of composite cross-section obtained by Tapping Mode.

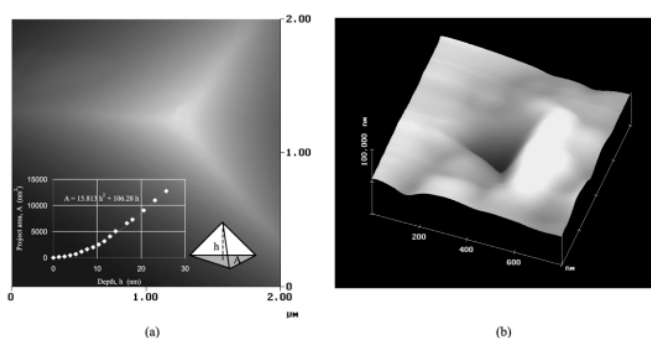


Fig 15: AFM micrograph reveals plastic deformation results in the formation of permanent indentation on the surface of the sample [90].

The leading characterization methods are compared with each other with relating to the information that can be gained, and also with reference to applicability to polymer surface and interface study. Exact T_g calculations require steady baselines before and after the transition as the curing exotherm interferes with the upper base line. The suitable alternatives for the measurement of T_g , is temperature modulated DSC (TMDSC). TMDSC utilizes a modulated temperature ramp. The origin for the modulation signals and evaluation, including the phase lag, is derived from electrical signal modulation in the electronics and telecommunications field. TMDSC mathematically de-convolutes the response into two kinds of signals, an in-phase and an out-of-phase response to the modulations, as well as producing an average heat flow. The advantages of TMDSC include improved resolution

and sensitivity and the ability to separate overlapping phenomena. With thermal analysis methods, average macroscopic properties of the multiphase materials can be determined as a function of time and temperature. Raman spectroscopy is one of the important method for the study of composite micromechanics, since it allows the point-to-point determination of stress and strain along the fibre/matrix interface in a range of systems. Moreover, the stresses and strains in the fibres and interface can be mapped at all levels of strain prior to overall catastrophic failure. The Raman method allows the determination of the variation of the interfacial shear stress along the fibre/matrix interface, whereas the micromechanical test technique gives a single-point value obtained only through failure of the fibre/matrix interface.

References

1. Ray B.C., Rathore D., Durability and integrity studies of environmentally conditioned interfaces in fibrous polymeric composites: Critical concepts and comments, *Advances in Colloid and Interface Science*, 2014; 209;68
2. Hollaway L.C, Application of Composite material in civil infrastructure, *Construction and Building Material*, 2010; 24; 2419.
3. Guigon M, Klinklin E, The interface and interphase in carbon fibre-reinforced composites. *Composites*, 1994; 25: 534-9.
4. Kuttner C, Hanisch A, Schmalz H, Eder M, Schlaad H, Burgert I, Fery A, Influence of the polymeric interphase design on the interfacial properties of fiber-reinforced composites. *Applied Material and Interfaces*, 2013; 5; 2469.
5. Bonniau I, Bunsell A. R., A comparative study of water absorption theories applied to glass epoxy composites. *Journal of Composite Material*, 1981; 15; 272.
6. Wright, W. W., The effect of diffusion of water into epoxy resins and their carbon-fibre reinforced composites. *Composites*, 1981; 12; 201.
7. Pritchard G. Speake S., The use of water absorption kinetic data to predict laminar property changes. *Composites*, 1987; 18; 227
8. Bao L.R, Yee A.F. Moisture diffusion and hygrothermal aging in bismaleimide matrix carbon fiber composites: part II woven and hybrid composites. *Composite Science and Technology*, 2002; 62; 2111
9. Aronhime M.T, Neumann S, Marom G. The anisotropic diffusion of water in Kevlar epoxy composites. *J Material Science*, 1987; 2; 2435

10. Benkhedda A. Tounsi E.A, Addabedia, Effect of temperature and humidity on transient hygrothermal stresses during moisture desorption in laminated composite plates, *Composite Structures*, 2008; 82; 629
11. Sereir Z, Addabedia E, Tounsi A. Effect of temperature on the hygrothermal behaviour of unidirectional laminated plates with asymmetrical environmental conditions. *Composite Structure*, 2006;72:383
12. Sereir Z, Addabedia E, Tounsi A. Effect of the accelerated moisture diffusivity on the hygrothermal behaviour of laminated plate with symmetrical environmental conditions. *Journal of Thermal Stresses*, 2005;28;889
13. Tounsi A, Amara K. Stiffness degradation in hygrothermal aged cross-ply laminates with transverse cracks. *AIAA Journal* 2005;43;1836
14. Tounsi A, Amara K.H, Adda-Bedia E. Analysis of transverse cracking and stiffness loss in cross-ply laminates with hygrothermal conditions. *Computational Material Science* 2005;32;167.
15. Tounsi A, Amara K.H, Megueni A, Benzair A. On the transverse cracking and stiffness degradation of aged angle-ply laminates. *Material Letter* 2006;60;2561.
16. Springer G.S. *Environmental effects on composite materials*, 4th Ed. Dayton, OH, 1988.
17. Wang J.Z, Parvatareddy H, Dillard D.A., Ward T.C., *Composites Science and Technology* 1995; 53; 399
18. Sookay N.K., Klemperer, C.J, Verijenko, V.E., *Environmental testing of advanced epoxy composites*, *Composite Structures* 2003; 62;429
19. M.V. Hosur, S. Zainuddina, Y. Zhoua, Ashok Kumar, S. Jeelani, *Durability studies of montmorillonite clay filled epoxy composites under different environmental conditions*, *Materials Science and Engineering A*, 2009;507;117
20. Ray B.C., Rathore, D., *Environmental damage and degradation of FRP composites: A review report*, *Polymer Composites*, 2014, DOI- 10.1002/PC.22967
21. Ray B.C, Biswas A., Sinha P.K., *Hygrothermal effects on mechanical behaviour of FRP composites*, *Metals Materials and Processes* 1991;3;99
22. Ray B. C., Mula S., Bera T, Ray P. K., *Prior Thermal Spikes and Thermal Shocks on Mechanical Behavior of Glass Fiber-epoxy Composites*, *Journal of Reinforced Plastics and Composites* 2006;2;216

23. Ray, B. C. Hydrothermal Shock Cycles on Shear Strength of Glass Fiber-Polyester Composites. *Journal of Reinforced Plastics and composites* 2005;24;12
24. Ray B.C, Freeze-thaw Response of Glass-polyester Composites at Different Loading Rates , *Journal of Reinforced Plastics and Composites* 2005;11;321
25. Ray. B.C, Thermal Shock and Thermal Fatigue on Delamination of Glass Fiber Reinforced Polymeric Composites. *Journal of Reinforced Plastics and Composites* 2005;24;461
26. Ray B.C, Effects of Thermal and Cryogenic Conditionings on Mechanical Behavior of Thermally Shocked Glass Fiber/Epoxy Composites. *Journal of Reinforced Plastics and composites* 2005;24;432
27. Zhou J, Lucas J.P. Hygrothermal effects of epoxy resin. Part I: the nature of water in epoxy. *Polymer* 1999; 40; 5505.
28. Herrera-Franco P.J., Drzal L.T., Comparison of Methods for the Measurement of Fiber/Matrix Adhesion in Composites, *Composites* 1992; 23;3
29. Lai M, Botsis J, Cugnoni J.,Coric D., An experimental–numerical study of moisture absorption in an epoxy, *Composites Part A:Applied Science and Manufacturing* 2012;43;1053
30. Etches J., Potter K., Paul Weaver, Ian Bond, Environmental effects on thermally induced multi stability in unsymmetric composite laminates, *Composites Part A : Applied Science and Manufacturing* 2009;40;1240
31. Drzal, L.T., Rich, M.J., Lloyd, P.F. Adhesion of Graphite fiber to epoxy Matrices. I. The Role of Fiber Surface Treatment, *Adhesion* 1982;16;1
32. Bockenheimer C., Fata D. Possart W. New Aspects of aging in Epoxy Networks. II. Hydrothermal Aging, *Journal of Applied Polymer Science* 2004;91;369
33. Yano O. Yamaoka H. Cryogenic Properties of Polymers, *Progresses in Polymer Science* 1995; 20;585
34. Shokrieh, M.M.,A. Bayat, Effects of ultraviolet radiation on mechanical properties of glass/polyester composites. *Journal of composite Materials*, 2007;41;2443
35. Andradý, A., et al., Effects of increased solar ultraviolet radiation on materials. *Journal of Photochemistry and Photobiology B: Biology*, 1998;46; 96
36. Feldman, D., Polymer weathering: photo-oxidation. *Journal of Polymers and the Environment*, 2002;10;163.

37. Awaja, F., et al., The investigation of inner structural damage of UV and heat degraded polymer composites using X-ray micro CT. *Composites Part A: Applied Science and Manufacturing*, 2011;42;408
38. Jacques, L.F.E., Accelerated and outdoor/natural exposure testing of coatings. *Progress in Polymer Science*, 2000;25;1337
39. Liao, W. and F. Tseng, The effect of long-term ultraviolet light irradiation on polymer matrix composites. *Polymer composites*, 1998;19;440
40. Chevali, V.S., D.R. Dean, and G.M. Janowski, Effect of environmental weathering on flexural creep behavior of long fiber-reinforced thermoplastic composites. *Polymer Degradation and Stability*, 2010;95;2628
41. Lixiang, J., A study of damage effects of CF/EP under vacuum ultraviolet radiation. *Applied laser-shanghai-*, 2002;22;409
42. Jiang, L. and L. Sheng, Research on effects of electronic irradiation of epoxy resin 648 and TDE-85. *Journal of Space Environment*, 2004;21;49
43. Liu, Y., G.-h. Li, and L.-x. Jiang, A study on the resistance performance of epoxy nano-composites under the vacuum ultraviolet irradiation. *Acta Astronautica*, 2008;63;1343
44. Paillous, A. and C. Pailler, Degradation of multiply polymer-matrix composites induced by space environment. *Composites*, 1994;25;287
45. Sethi, S., Ray B.C., An assessment of mechanical behavior and fractography study of glass/epoxy composites at different temperatures and loading speeds, *Materials and Design*, 2014;64;160
46. Hull D, Clyne T.W, *An introduction to composite materials*, Cambridge University Press, Cambridge, 1996.
47. Om.K. Joshi, The effect of moisture on the shear properties of carbon fiber, *Composites* 1983; 14; 196.
48. Gaur U, Chou C.T., Miller B., Effects of hygrothermal ageing on bond strength, *Composites* 1993; 25; 609.
49. Birger S., Moshonov A., Keing S., The effects of thermal and hygrothermal ageing on the failure mechanisms of graphite-fabric epoxy composites subjected to flexural loading. *Composites* 1989; 20;4

50. Akay M, Mun S.K.A, Stanley Afluenine of moisture on the thermal and mechanical properties of autoclaved and oven-cured Kevlar-49/epoxy laminates. *Composite Science and Technology* 1997; 57; 565.
51. Fischer H., Polymer nanocomposites: from fundamental research to specific applications, *Materials Science and Engineering C* 2003; 23;763
52. Ajayan P.M., Schadler L.S., Braun P.V, *Nanocomposite Science and Technology* Wiley VCH, Weinheim, 2003
53. Balazs A.C., Emrick T., Russell T.P., Nanoparticle Polymer Composites: Where Two Small Worlds Meet, *Science* 2006;314; 1107
54. Michael E. Mackay, Anish Tuteja1, Phillip M. Duxbury, Craig J. Hawker, Brooke Van Horn, Zhibin Guan, Guanghui Chen, R. S. Krishnan, General strategies for nanoparticle dispersion, *Science*; 2006;311;1740
55. Rittigstein P. Priestley R.D, Broadbelt L.J., Torkelson J.M, Model polymer nanocomposites provide an understanding of fundamental effects in real nanocomposites, *Nature Materials*, 2007; 6;278
56. Schadler L., Model interfaces, *Nature Materials*,2007;6;257
57. Tsagaropoulos, G.Eisenburg, A. Direct observation of two glass transitions in silica-filled polymers. Implications to the morphology of random ionomers. *Macromolecules* 1995;28;396
58. Reis J.M.L., Coelho J.L.V., Monteiro A.H, Costa Mattos H.S, Tensile behavior of glass/epoxy laminates at varying strain rates and temperatures, *Composites: Part B*, 2012;43:2041-2046
59. Mahmood M. S., Omid M.J., Tension behavior of unidirectional glass/epoxy composites under different strain rates, *Composite Structures*, 2009;88 :595–601
60. Harding J, Welsh LM. A tensile testing technique for fibre-reinforced composites at impact rates of strain. *J Material Science* 1983; 18:1810–26.
61. Welsh LM, Harding J. Effect of strain rate on the tensile failure of woven reinforced polyester resin composites. *J Physics* 1985; 46:405–14.
62. Barré S, Chotard T, Benzeggagh ML. Comparative study of strain rate effects on mechanical properties of glass-reinforced thermoset matrix composites. *Composites Part A* 1996; 27:1169–81.
63. Peterson B.L, Pangborn R.N, Pantano C.G. Static and high strain rate response of a glass fiber reinforced thermoplastic. *J of Composite Material* 1991; 25:887–906.

64. Gilat A, Goldberg R.K, Roberts G.D. Experimental study of strain-rate-dependent behavior of carbon/epoxy composite. *Composite Science and Technology* 2002; 62:1469–76.
65. Chow T.S., Prediction of stress-strain relationships in polymer composites, *Polymer*, 1991; 32: 12-15
66. Kongshavn I., Poursartip A., Experimental investigation of a strain-softening approach to predicting failure in notched fibre-reinforced composite laminates, *Composites Science and Technology*, 1999; 59:29–40
67. Zweiben C. Failure analysis of unidirectional fibre composites under combined axial tension and shear. *J Mechanical Physics Solids* 1974; 22:193–215.
68. Iremonger MJ, Wood WG. Effects of geometry on stresses in discontinuous composite materials. *J Strain Analysis*. 1969; 4:121–6.
69. Agarwal B.D, Bansal R.K. Plastic analysis of fibre interactions in discontinuous fibre composites. *Fibre Science and Technology*. 1977; 10: 281–97.
70. De Morais A.B. Stress distribution along broken fibres in polymer-matrix composites. *Composite Science and Technology*. 2001; 61:1571–80.
71. Gulino R, Schwartz P, Phoenix SL. Experiments on shear deformation, debonding and local transfer in a model graphite/glass/epoxy microcomposite. *J of Material Science*, 1991; 26: 6655–72.
72. Nath R.B, Fenner D.N, Galiotis C. Finite element modelling of interfacial failure in model carbon fibre-epoxy composites. *J Material Science* 1996; 31:2879–83.
73. Tripathi D, Chen F, Jones FR. The effect of matrix plasticity on the stress fields in a single filament composite and the value of interfacial shear strength obtained from the fragmentation test. *Proceedings Royal Society London A* 1996; 452:621–53.
74. Heuvel PWJ, Peijs T, Young R.J. Failure phenomena in two-dimensional multifibre microcomposites: 2. A Raman spectroscopic study of the influence of inter-fibre spacing on stress concentrations. *Composite Science and Technol* 1997; 57:899–911.
75. DiBenedetto AT, Jones K.D. The role of interphase debonding on cumulative fibre fractures in a continuous fibre-reinforced composite. *Composite Part A* 1996; 27A:869–79.
76. Accorsi M.L, Pegoretti A, DiBenedetto A.T. Dynamic analysis of fibre breakage in single- and multiple-fibre composites. *J of Material Science*. 1996; 31:4181–7.

77. Jacobs E, Verpoest I. Finite element modelling of damage development during longitudinal tensile loading of coated fibre composites. *Composite Part A* 1998; 29A:1007–12.
78. Johnson AC, Zhao FM, Hayes SA, Jones FR. Influence of a matrix crack on stress transfer to an alumina fibre in epoxy resin using FEA and photoelasticity. *Composite Science and Technol* 2006; 66:2023–9.
79. Kettle A.P, Beck A.J, OToole L, Jones F.R, Short R.D. Plasma polymerisation for molecular engineering of carbon-fibre surfaces for optimised composites. *Composite Science and Technol* 1997; 57; 1023–32.
80. Totry E. , Jon M. Molina-Aldareguía , González C. , LLorca J., Effect of fiber, matrix and interface properties on the in-plane shear deformation of carbon-fiber reinforced composites, *Composites Science and Technology*, 2010; 70; 970–980
81. Omiya, M., Kishimoto, K, Yang, W. Interface Debonding Model and its Application to the Mixed Mode Interface Fracture Toughness, *International Journal of Damage Mechanics* 2002;11;263
82. Asp L.E., The effects of moisture and temperature on the interlaminar delamination toughness of a carbon/epoxy composite. *Composite Science and Technology* 1998; 58;967

Chapter 3

Materials and Method

3.1 Materials

Fibres: In this research work three types of fibres reinforcement were used for the fabrication of laminate for fibre reinforced polymer matrix composites. These fibre reinforcements are E-Glass fibre, high-modulus Carbon fibre and Kevlar-49 fibres and they were selected for their potential use in structural engineering application. E-Glass fibres with nominal diameter of 14 μ m were supplied by Saint Gobain Bangalore, India. High modulus carbon fibres with nominal diameter of 7 μ m were supplied by Nikunj Bangalore, India. Kevlar-49 fibres, the nominal diameter of 5 μ m were supplied from Shah-Tool Limited Mumbai, India were used. Different mechanical properties of these reinforcements are given in the tables.

Table-1 Physical and mechanical properties of glass fibre

Property	E-glass
Diameter (μ m)	5-25
Density (g/cc)	2.54
Elastic modulus at 25°, kg/mm ²	7700
Tensile strength (GPa)	2.4
Young's modulus (GPa)	72.4
Coefficient of thermal expansion 10 ⁻⁶ °C	5

Table-2 Mechanical Properties of high-modulus carbon fibre

Property	High strength	Intermediate modulus	High modulus
Tensile strength, MPa	2300	2600	1420
Tensile modulus, GPa	145	180	210-250
Compression strength, MPa	1600	1800	900
Compression modulus, GPa	135	150	190-230
Short beam shear stress, MPa	120	120	80

Table-3 Mechanical properties of Kevlar-49 fibre.

Tensile strength (MPa)	3024
Tensile elongation (%)	2.48
Tensile modulus (GPa)	121.9
Tensile strain, %	2.5
Coefficient of thermal expansion (10^{-6}°C)	-2.0 (Kevlar 29)

Matrix: The epoxy resin used is diglycidyl ether of Bisphenol A (DGEBA) and the hardener is Triethylene tetra amine (TETA) supplied by Atul Industries Ltd, Gujarat, India under the trade name Lapox, L-12 and K-6 respectively. Some properties of the epoxy resin used in the study are provided in the table-4. The volume fraction of fibres is 60%. The ratio of epoxy and hardener is taken as 10:1.

Table-4 Mechanical properties of epoxy resin.

Property	Epoxy
Tensile strength (GPa)	0.11
Tensile Modulus (GPa)	4.1
Strain at failure %	4.6
Poisson's ratio	0.3
Density g/cm^3	1.162

Nano-fillers- In the present investigation Al_2O_3 nano-fillers are used for the fabrication of fibre reinforced polymer nanocomposites. Al_2O_3 nano nano-fillers used with a diameter of 30nm.

Fabrication Technique:

The laminated composites has been prepared by hand lay-up method with 16 layers of woven fabric cloth of reinforcement and then placed in a hot press. Then the curing of the laminate has been carried out at 60°C temperature and 20 kg/cm² pressure for 20 minutes. The laminates were then removed from the press and kept at room temperature for 24 hours. The test specimens have been cut from the laminates using diamond tipped cutter as per required standard.

Environmental Conditions: Fibre reinforced polymer matrix composites were subjected to different environmental conditions during its service life. The main exposures are temperature, moisture, UV radiation and many more. In present work selected environmental conditions were used to evaluate the environmental durability and integrity of different FRP composites. Considering temperature, this was divided into various sections to cover a range of temperature environment as low and ultra-low temperatures, above and below-glass transition temperature (T_g), above and below ambient temperature, prior thermal conditions, post curing hardening and thermal cycle conditions.

Table 5: Temperatures Effect:

Environmental Condition (Temperature)			
Above and below Ambient	Above and below Glass transition temperature(T_g)	Thermal cycling	Low and ultra-low temperatures
+50,-50,+100 and -100	+60,+100,+150,+200,+250	Different durations of moisture ingress with 4hr ultra-low temperature	-20,-40,-60

Table 6:UV radiation treatment:

Environmental condition(UV radiation)	
Without treatment samples	30 days, 60 days treatment with moisture

Table 7-Fibre reinforced epoxy composites with nano-fillers

Fibre reinforced polymer matrix composites(addition of nanofillers)

Al₂O₃(nano particle)

3.2Experimental Methods

3.2.1Flexural Test(Short beam shear test)

Instron 5967 is a servo hydraulic-control and signal conditioning electronics instrument for material testing applications. It has fine position adjustment thumbwheel with 0.004mm resolution for precise positioning of crosshead while testing. Specimen protect also applied to the specimen outside a set threshold-protecting to overcome unwanted damage. Bluehill 3 software helps to get the data from the attached computer.

The test coupons of different sizes were cut from the laminates for physical and mechanical characterization. ILSS testing were conducted on an Instron 5967 test apparatus using three-point bend jig according to [ASTM: D2344-13](#).

The flexural methods are applicable to polymeric composite materials. A testing machine with controllable crosshead speed is used in conjunction with a loading fixture. It is a three point flexural test on a specimen with a small span, which promotes failure by inter-laminar shear. The shear stress induced in a beam subjected to a bending load, is directly proportional to the magnitude of the applied load and independent of the span length. Thus the support span of the short beam shear specimen is kept short so that an inter-laminar shear failure occurs before a bending failure.

This test method is defined by ASTM D 2344, which specifies a span length to specimen thickness ratio of five for low stiffness composites and four for higher stiffness composite. This test has an inherent problem associated with the stress concentration and the non-linear plastic deformation induced by the loading nose of small diameter.

With these variations the result signifies that the parabolic distribution of shear stress across the thickness of the specimen predicted by simple beam theory could be very well in the regions between the loading and support cylinder and the specimen fail in a shear mode. With

these modifications ASTM D 2344 may yet become a technically acceptable as well as popular shear test method.

3.2.2 Scanning Electron Microscope (SEM)

The scanning electron microscope (SEM) has been a well accepted tool for many years in the examination of fracture surfaces. For analysis of composite fractography, SEM by JEOL-JSM 6480 LV with the acceleration voltage of 15 kV was used. Cleaned, small in size and conductive samples are used during testing in SEM. The top surface of the specimens was coated with platinum using a sputter coater. The coating is used to make the surface conductive for scanning and prevents the accumulation of static electric charge for clear images during the microscopy. During the test samples are little tilt around 15-20° to drawn attractive and clear images of different failure modes.

The prominent imaging advantages are the great depth of field and high spatial resolution and the image is relatively easy to interpret visually.

Principle: A finely focused electron beam scanned across the surface of the sample generates secondary electrons, backscattered electrons, and characteristic X-rays. These signals are collected by detectors to form images of the sample displayed on a cathode ray tube screen. Features seen in the SEM image may then be immediately analyzed for elemental composition using EDS or WDS. The electrons that are emitted from the specimen surface have a spectrum of energies. Secondary and backscattered electrons are conventionally separated according to their energies. When the energy of the emitted electron is less than about 50eV, it is referred as a secondary electron and backscattered electrons are considered to be the electrons that exit the specimen with energy greater than 50eV. A critical point in understanding the formation of SEM images of fracture surfaces, and their interpretation, is an appreciation of the factors that affect this excited volume of electrons in the specimen. To understand the different failure mechanisms in FRP composites, photomicrographs were taken using a SEM. There is a dramatic change in the structure and properties of the composite when exposed to high and low temperatures.

3.2.3 Differential Scanning Calorimetry (DSC)

The DSC measurements were performed on a Mettler-Toledo 821 with intra cooler, using the STAR software with Temperature Modulated DSC (TMDSC) module. The temperature calibration and the determination of the time constant of the instrument were performed by standards of In and Zn, and the heat flow calibration by In. The underlying heating rate of

10°Cmin⁻¹ was used. In order to calibrate the heat flow signal, a blank run with an empty pan on the reference side and an empty pan plus a lid at the sample side was performed before the sample measurements. Standard aluminum pans were used. The experiments were performed in the temperature range from 25°C to 150°C.

Principle: Differential scanning calorimetry (DSC) is a thermoanalytical technique in which the amount of heat required to increase the temperature of a sample and reference is measured as a function of temperature and time. Both the sample and reference are maintained at nearly the same temperature throughout the experiment.

3.2.4 FTIR-ATR Spectroscopy analysis

FTIR analysis was performed in FTIR spectrophotometer interfaced with IR microscope operated in reflectance mode. The microscope is equipped with a video camera, a liquid nitrogen-cooled mercury cadmium telluride (MCT) detector and a computer controlled translation stage, programmable in the x and y directions. The spectra were collected in the 4000cm⁻¹ to 550 cm⁻¹ region with 8 cm⁻¹ resolution, 60 scans and beam spot size of 10µm-100µm. The spectral point-by-point mapping of the interface of the epoxy cured composites was performed in a grid pattern with the use of computer controlled microscope stage. Since the surface of the film was not perfectly smooth and its thickness was not uniform care should be taken to mount the sample such that a major portion of the plane was in the same focal plane. The FTIR imaging was performed in AIM-800 Automatic Infra red Microscope (SHIMADZU). There are certain limitations of refraction and reflection at the fibre surface in the spectroscopy that will finally affect the FTIR spectra of glass/epoxy composites. Due to this only a small percent of light reaches the detector. It is difficult to separate these optical effects from the samples.

Principle: In infrared spectroscopy, Infrared radiation is passed through a sample. Some of the infrared radiation is absorbed by the sample and some of it is passed through (transmitted). The resulting spectrum represents the molecular absorption and transmission, creating a molecular fingerprint of the sample. Like a fingerprint no two unique molecular structures produce the same infrared spectrum. This makes infrared spectroscopy useful for several types of analysis. Infrared spectroscopy is useful in the region to get structural information for organic compounds. This region is divided into two parts i.e. the functional group region 4000-1300 cm⁻¹ and 1300- 650 cm⁻¹ finger print region. Most of the functional groups give absorption bands in the high frequency part of the spectrum, which give small

number of bands. The FTIR image analysis suggests that there is a variation in the chemical structure of the matrix from the fiber to the bulk polymer.

3.2.5 Atomic force Microscopy (AFM)

The surface polished specimens of glass/epoxy and carbon/epoxy composites were exposed in a thermal conditioning environment at 50°C for different time period. After thermal conditioning the specimens were put in desiccators to protect them from moisture and dust. The specimens were taken out of the desiccators periodically and then scanned by VeecoDinnova atomic force microscope.

Principle: The AFM consists of a cantilever with a sharp tip (probe) at its end that is used to scan the specimen surface. The cantilever is typically silicon or silicon nitride with a tip radius of curvature on the order of nanometers. When the tip is brought into proximity of a sample surface, forces between the tip and the sample lead to a deflection of the cantilever according to Hooke's law. AFM has become a useful tool for characterizing the topography and properties of solid materials since its advent. Besides topography information, the phase lag of the cantilever oscillation, relative to the signal sent to the cantilever's piezo driver, is simultaneously monitored giving information about the local mechanical properties such as adhesion and viscoelasticity. Phase imaging is a powerful tool that provides nanometer-scale information often not revealed by other microscopy techniques.

Chapter- 4

Results and Discussion

4.1 Effect of high temperature on mechanical response of materials: Assisted with viscoelastic nature

Theories and thoughts

A judicious selection associated with fiber reinforcement, polymer resin matrix, and the interface/interphase offer unique physical and mechanical properties. However, a proper and uniform load transfer across the interface region between fiber and matrix is also an important concern in composite material. High temperature has the unwelcome effect on the valuable properties, leading to premature failure and fracture of the material. A number of potential solutions have been proposed to conquer these limitations. Polymer matrix composites behave in ductile manner at room temperature may become brittle at low temperature and show viscoelastic behavior at elevated temperature. The thermal aging behavior of epoxy resin is of unique importance due to their expanding use in structural application where elevated temperature is a common environmental condition. The location of failure and mode of failure dependent on the thermal and mechanical stresses present in the materials as well as the threshold load factor of the matrix to failure. It's a big challenge to give a conclusive statement on the effect of temperature on the fibre reinforced polymer composite material. The present investigation outlines the fabrications and characterization of glass fibre/epoxy, carbon fibre/epoxy and Kevlar fibre/epoxy composites subjected to above glass transition temperature (T_g) and below glass transition temperatures (T_g). Moreover, interlaminar shear strength, fractography, thermal and chemical analysis of the composite samples are determined. The loading rate sensitivity of fibre reinforced polymer composites at different temperatures has been also studied.

4.1.1 Introduction

With ever increasing advances in science and technology, FRP composite materials have shown great potential for various high performance structural applications. Their outstanding strength to weight ratio, fatigue resistance, corrosion resistance and lower manufacturing costs makes them superior than the conventional metals. Today aircraft, automotive, marine, chemical, construction and electrical industries are manufacturing most of their components with fibre composites [1-2]. Glass fibres and carbon fibres are primarily used as reinforcement in polymer matrix. There are previous investigations available about the degradation of FRP under high and low temperatures [3], high and low strain rates [4-6],

humidity [7], UV radiations [8], alkaline and high pH environments [9]. During the service period the combined effect of these harsh environmental conditionings is more deleterious on FRP composites. Most of the FRP components are subjected to different temperature and different rate of loading simultaneously. But there is a lack of literature in synergistic effect of temperature and loading rate on FRP composites. The impact response and mechanical properties of glass fibre/epoxy composite is significantly altered by temperature excursion. Differential thermal expansion of fibre and matrix at elevated temperature can degrade the interface which leads to the lower interlaminar shear strength of the composite [10]. At low temperature most polymer matrix behaves in brittle manner and do not allow the relaxation of residual stresses or stress concentration [11]. These residual stresses at cryogenic temperature may result in larger debonded interfaces. Interlaminar shear behaviour can be used to characterize FRP composite materials. Loading rate has a significant effect on the interlaminar shear strength of polymer composite and rate of loading can possibly change the failure mode [12]. Nardone et al [10] studied the effect of temperature on mechanical properties of GFRP and CFRP composite. The aim of the current investigation is to present the variation of mechanical properties of glass fiber/epoxy composite under the synergistic effect of temperature and rate of loading. GFRP composites were fabricated by compression molding press. The composite specimens were subjected to different temperatures. 3-Point bend test and 4-point bend test were conducted in order to characterize the mechanical behavior of laminated composite and to determine the influence of loading rate on interlaminar shear strength. To understand the interactions between various failure mechanisms in the fiber, matrix and fiber/matrix interface, microscopic analyses were conducted.

4.3.2 Experimental section

4.3.2.1 Material selection and fabrication technique

The required E-glass, carbon and Kevlar fibres and epoxy polymer matrix purchased from the following sources: Saint Gobin Limited Bangalore, India, Nikunj Bangalore India, Shah-Tools Industries, Mumbai, India and ATUL India Private Limited respectively.

Processing of the laminates

After curing, the laminate was cut into the required size for 3-point bend (Short- Beam Shear) test by diamond cutter. All the specimens were then dried in oven to remove moisture and other volatile entities. The specimens were then exposed to different

temperature. Conditioning temperatures are divided into 2 batches as above glass transition temperature and below glass transition temperatures. Testing temperatures are +60°C, +100°C, +150°C, +200°C and +250°C temperatures. Tests were performed in-situ inside the environmental chamber of INSTRON 5967. The samples are kept inside the furnace from room temperature to testing temperature with a holding time of 10 min. All the samples were tested at different loading rates ranging from low to high loading rates (1-103) mm/min. Six-seven samples are tested in each loading speed to obtain the consistency in the results. For comparison with the results one batch samples are tested at ambient +28°C temperature.

4.3.2.2 In-situ conditioning and characterization

Flexure strength: Universal testing machine with environmental chamber

Instron 5967 is a servo-control and signal conditioning electronics instrument for material testing applications. It has fine position adjustment thumbwheel, with 0.004mm resolution for precise positioning of crosshead while testing. Specimen protect also applied to the specimen outside a set threshold-protecting to overcome unwanted damage. Bluehill 3 software helps to get the data from the attached computer. The test coupons of different sizes were cut from the laminates for physical and mechanical behavior characterization. Interlaminar shear strength (ILSS) testing were conducted on an Instron 5967 test apparatus using three point bend jig according to ASTM 2344-10, shown in Fig 18. The dimension of the ILSS specimen was 45×6×4 mm³. The results were then compared with the data obtained from unconditioned specimens. The flexural methods are applicable to polymeric composite materials. The shear stress induced in a beam subjected to a bending load, is directly proportional to the magnitude of the applied load and independent of the span length. Thus the support span of the short beam shear specimen is kept short so that an inter-laminar shear failure occurs before a bending failure.

This test method is defined by ASTM D 2344, which specifies a span length to specimen thickness ratio of five for low stiffness composites and four for higher stiffness composite. The short beam shear (SBS) tests were performed on the composite samples at different temperature to evaluate the value of inter-laminar shear strength (ILSS). The loading arrangement is shown in a span length of 40 mm. The tests were performed with five increasing crosshead speed ranging from 1, 10, 100, 200, 500 and 1000 mm/min at different temperature. For each point of testing 4 to 5 specimen were tested and the average value was taken.

$$ILSS = 0.75 * P / bt$$

Where P=maximum load, b=width of specimen, t=thickness of specimen

Scanning electron microscope (SEM)

The scanning electron microscope (SEM) has been a well-accepted tool for many years in the examination of fracture surfaces. The prominent imaging advantages are the great depth of field and high spatial resolution and the image is relatively easy to interpret visually. To study the different failure mechanisms of the tested samples SEM analysis was carried out using a JEOL-JSM 6480 LV SEM. The samples were loaded onto the sample holder and placed inside the SEM, adjusting the working distance and hence the spot size the chamber was closed and vacuum was applied.

4.3.3 Results and Discussion

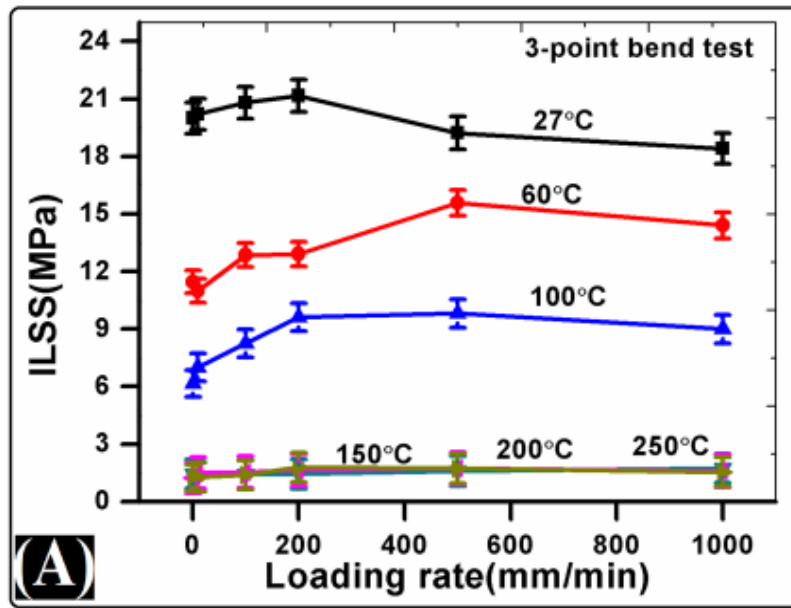
4.3.3.1 In-situ testing

3-point bend test (Glass fibre, Carbon fibre and Kevlar fibre)

Interlaminar Shear Strength Study (ILSS) with temperature variation

Glass fibre/epoxy composites

In-situ SBS tests were performed at five different temperatures (+27°C, +60°C, +100°C, +150°C, +200°C and +250°C). At each temperature the testings were carried out at varying cross head velocities (1,10,100,200,500 and 1000 mm/min). Fig. 16 Illustrates the interlaminar shear strength of 3-point bendtested specimens at various temperatures and loading rates and load-displacement curves. It is evident from the figure that the glass fibre/epoxy composite is loading rate sensitive at ambient temperature. Further as the testing temperature increases from ambient temperature to elevated temperature the loading rate dependency decreases and as the temperature approaches to glass transition temperature the composite becomes loading rate insensitive. So the temperature at which the composite is loaded decides its loading rate sensitivity.



(A)

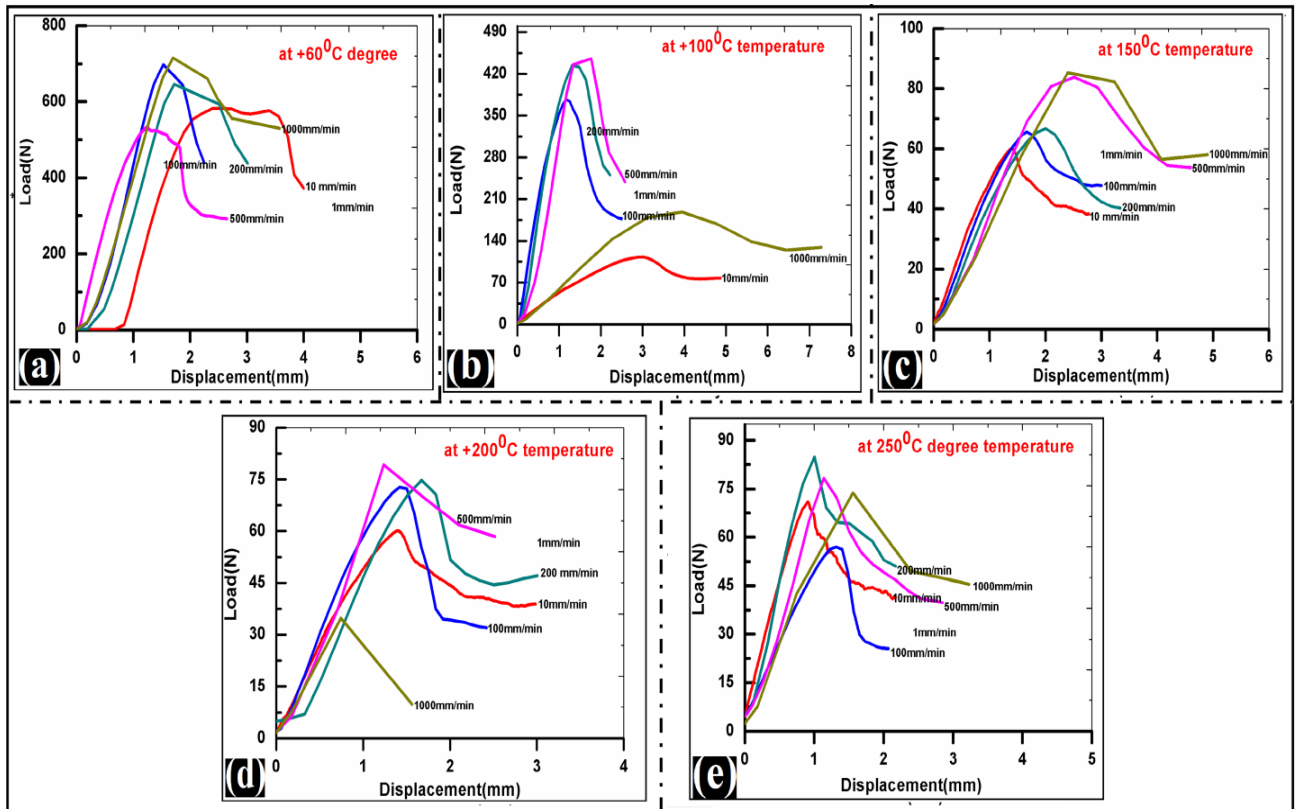


Fig.16. (A) Variation of ILSS with loading rates of glass fibre/epoxy composites with 3-point short beam shear test at different temperatures (a) Load-displacement curve of glass fibre/epoxy composites at +60°C temperature (b) load-displacement curve of glass fibre/epoxy composites at +100°C temperature (c) load-displacement curve of glass fibre/epoxy composites at +150°C temperature (d) load-displacement curve of glass fibre/epoxy composites at +200°C temperature (e) load-displacement curve of glass fibre/epoxy composites at +250°C temperature.

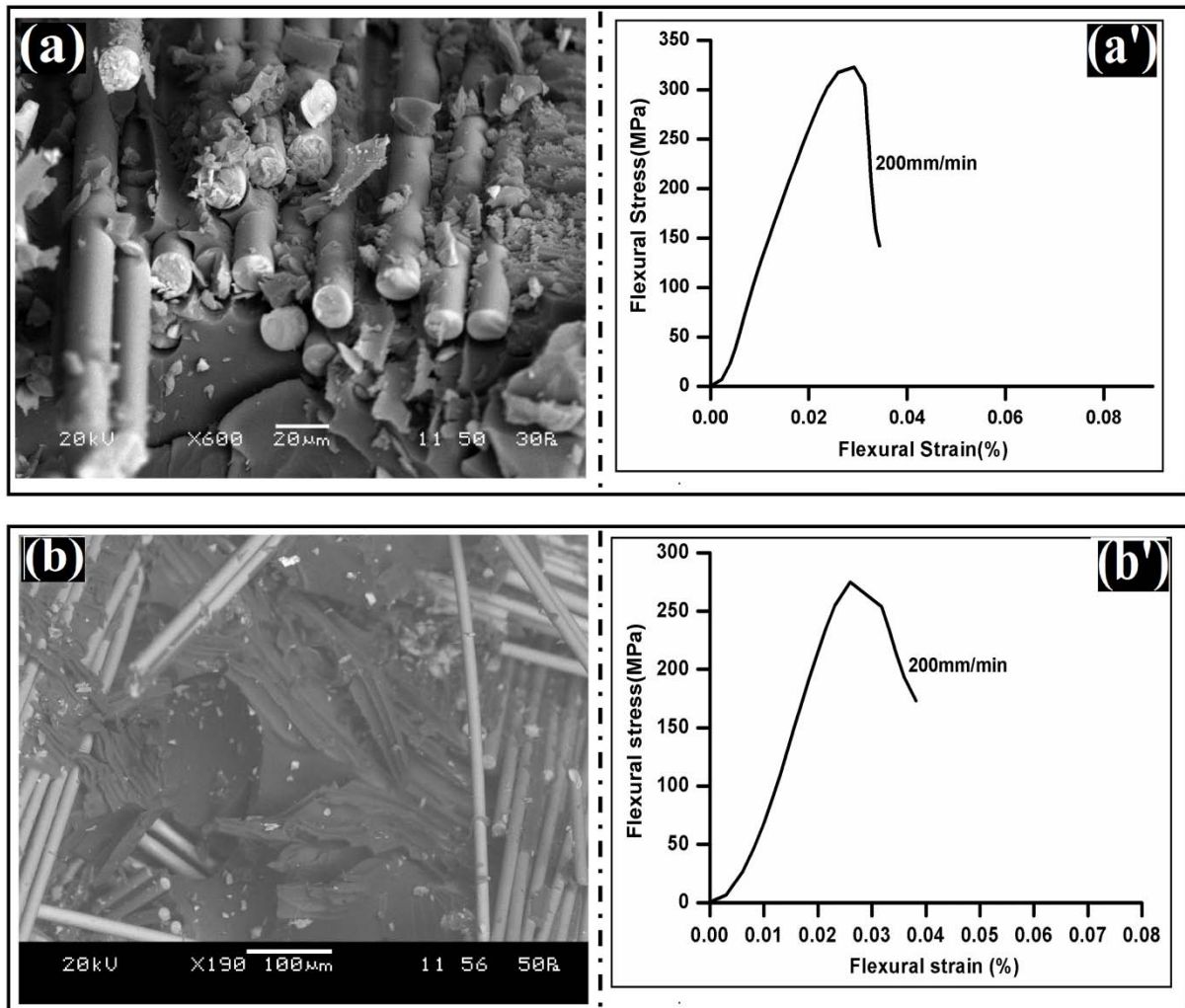
ILSS of glass fibre/epoxy composites at +60°C temperature increases with the increasing loading rate from 12 to 14 MPa with a transition at the 200mm / min and 500mm/min loading rate. In contrast to this, the ILSS values at ambient (+27°C) temperature decreases from 20 to 18 MPa with a transition at 200mm/min as shown in Fig.16. The ILSS values decrease with increasing temperatures. The decrease in the ILSS can be attributed to the formation of microcracks at interphase due to differential thermal expansion at the interface. Here the material state and properties of the epoxy matrix slightly unstable in nature. In this state large scale motion of main backbone chain is impossible. Above a glass transition temperature the ILSS values sharply decrease as compared to ambient temperatures. At this decomposition temperature, it starts decomposing with different phases as combustible gases, decomposing and smokes [17, 18]. This may be attributed as matrix behaves viscoelastic in nature. The main backbone chains possess much greater freedom of motion, thus the epoxy matrix is in rubbery state. Now the response to applied stress is much more pronounced and is effected on the fibre/matrix interface region [19-21]. It is also observed that glass fibre/epoxy at ambient and at +100°C temperature for 3-point bend test shows a decrease of ILSS values with a transition at 200 mm/min, but the ILSS values decrease from 20 to 5 MPa.

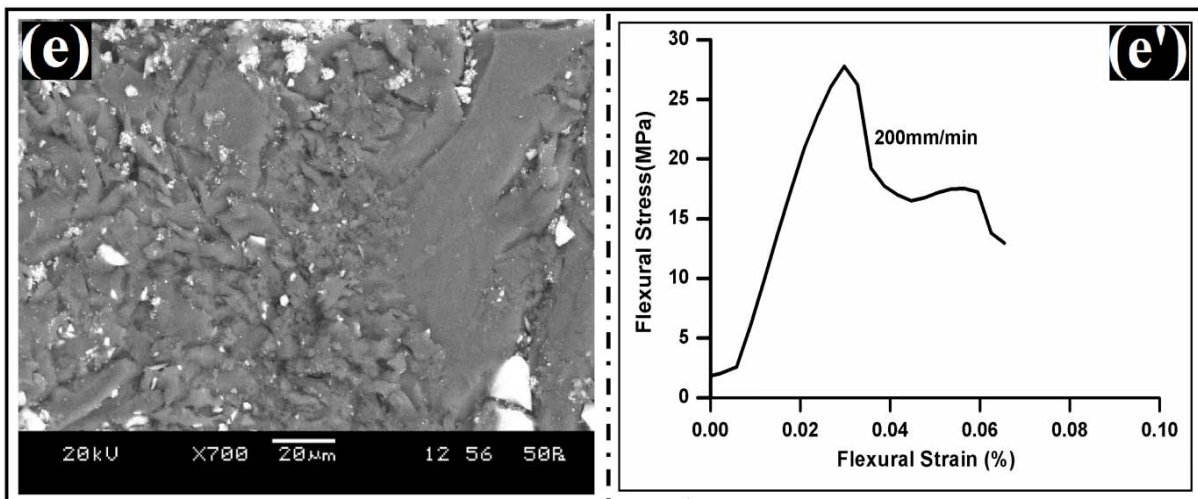
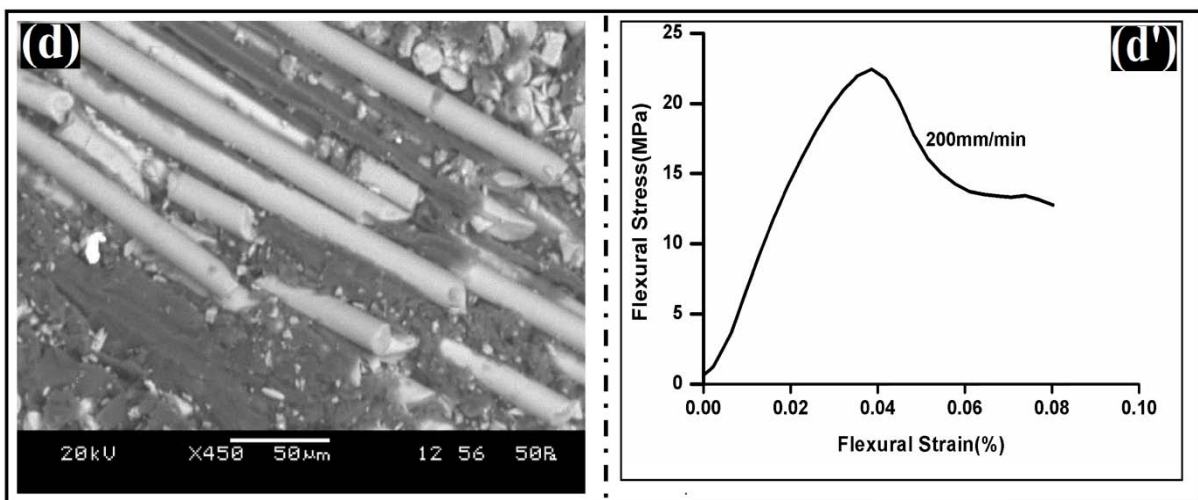
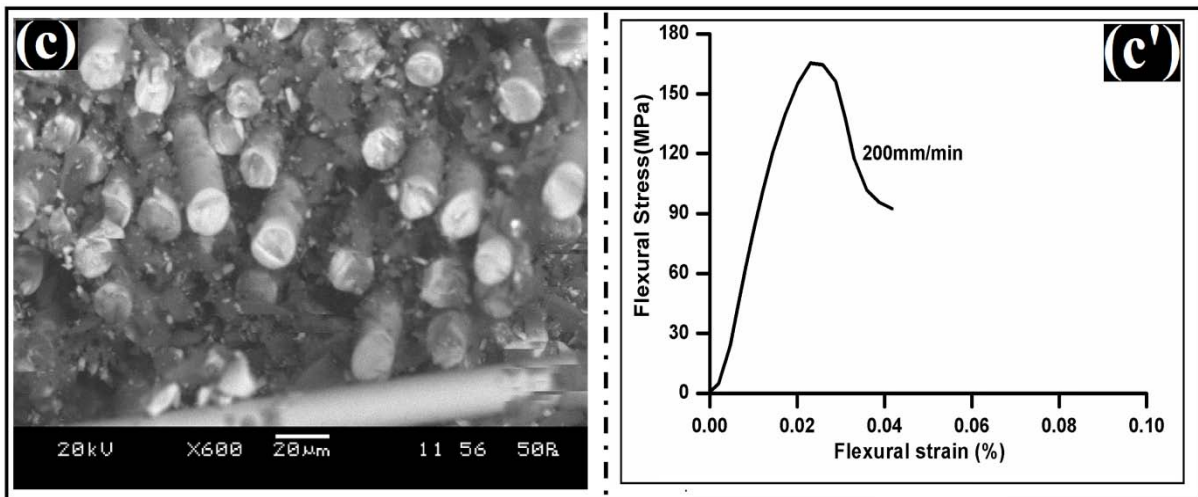
Fig.16 (a), (b) represents the load-displacement curve of the glass fibre/epoxy composites below T_g temperatures. As +60°C temperature (Fig. 16(a)) shows the load drops sharply after the peak load, to stable crack propagation. 1000mm/min curve carries the maximum load whereas the low loading rate as 1mm/min carries the minimum load. As +100°C temperature (Fig. 16 (b)) very close to glass transition temperature shows ductility in the high and low loading rates, i.e. at 1000mm/min and 10 mm/min whereas other loading rates follow the brittle to ductile transition. Fig. 16(c), (d) and (e) shows load-displacement curve of glass fibre/epoxy composites above glass transition temperatures. At +150°C temperature maximum load carried at high loading rates. At +200°C temperature shows the mixed transition of the material with the loading rates, but at +250°C temperature maximum curves shows the brittle behaviour of the materials as matrix faces the charring effects.

Fractography analysis

In order to establish a better comprehend interfacial study the broken samples of 3-point bend test at different temperatures and loading rates have been examined by scanning electron microscopy (SEM). Flexural stress with flexural strain curves of glass fibre/epoxy composites is plotted in Fig.20 at 200mm/min loading speed. With increase in temperature the strain to failure increases. At ambient temperature Fig.20 A shows interfacial debonding between fibre

and matrix resin. Because of this failure mode the ILSS values may decrease at 200mm/min and 500mm/min loading speed. The results show that loading rate has a significant effect on the response of failure modes. The maximum stress increases somehow with strain, but it falls sharply after yielding. This morphology associated with slow fracture, in which just need of enough energy to propagate the crack in the resin matrix [24, 25].





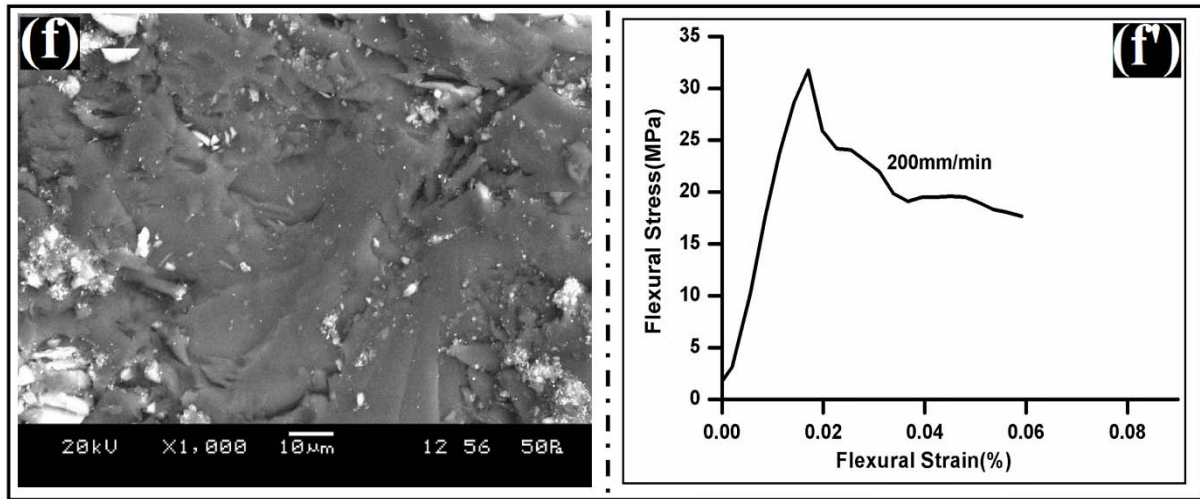


Fig.17: (a,a') Scanning electron microscopy images of 3-point bend tested glass fibre/epoxy composites at 200mm/min and flexural stress with flexural strain curve at ambient temperature, (b,b') at +60°C temperature, (c,c') at +100°C temperature, (d,d') at +150°C temperature, (e,e') at +200°C temperature, (f,f ') at +250°C temperature.

Fig.17 (b, b') shows the fibre imprint failure mode which plays dominant role at +60°C temperature. As fibre/matrix interface region was not strong enough to transfer the load to the fibre, the stress-strain curve shows very first yielding as compared to ambient temperature sample. Sliding of bunch of fibre in the matrix region was observed at +100°C temperature as shown in Fig.17 (c, c'). In case of above glass transition temperature matrix failure plays dominant roles for the variation of fibre/matrix interfacial bond strength. Fig.17 (d,d') shows toughened matrix near the fibre/matrix interface region at +150°C temperature. At +200°C and +250°C temperature resin rich area plays dominant role for the change in ILSS values. In all the cases the ILSS values were changing with increasing loading speed.

4.1.3.2 a Carbon fibre/epoxy composites

Interlaminar shear strength (ILSS) with temperature

In order to predict the short-term and long-term mechanical behavior of carbon fibre/epoxy composites at high temperatures, it is necessary to have a clear understanding of bahvior of ILSS with temperature at different loading rate.

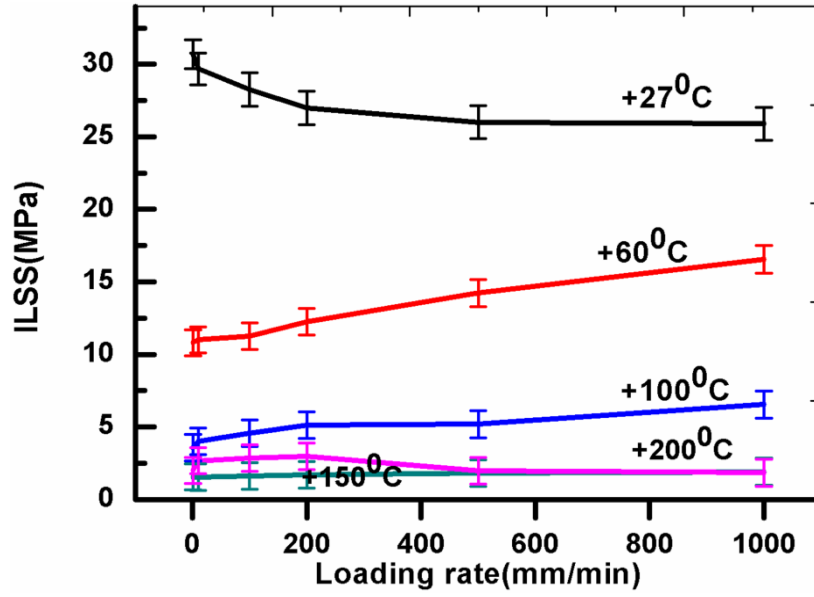


Fig 18: Interlaminar shear strength with loading rate of carbon fibre/epoxy composites at +27°C, +60°C, +100°C, +150°C and +200°C.

Fig.21 represents the interlaminar shear strength (ILSS) with loading rate curve at different temperatures. The ILSS values at ambient (+27°C) temperature decreases from 32 to 25 MPa with a transition at 200mm/min. The ILSS values decreases with increasing temperatures. But ILSS values increases with increase with loading rates. The reason may be due to weak bonding between fibre and matrix at high temperature. Without conditioning samples(at +27°C) carbon fibre have a proper bonding with matrix because presence of high bond strength carbon atom in the basal plane. This increases modulus values along the fibre axis. As the temperature increases, the basal plane layers get disturbed and low modulus values are obtained where weak Van der Waals forces are present. This may be the reason for low in ILSS as the temperature increases in case of carbon fibre/epoxy composites.

Fig.19 represents the load-displacement curve of the carbon fibre/epoxy composites above and below T_g temperatures. At ambient temperature (+27°C) carbon fibre/epoxy composites are failed by brittle in nature except at 500 and 1000mm/min. At +60°C temperature the load drops ductile manner after the peak load, showing little unstable crack propagation. 1000mm/min curve carry the maximum load whereas low loading rate as 1mm/min carry the minimum load. At +100°C temperature very close to glass transition temperature shows ductility in the high and low loading rates i.e. at 1000mm/min and 10 mm/min whereas other loading rates follow the ductile to brittle transition. At +150°C temperature maximum load carried at high loading rates. At +200°C temperature shows mixed transition of the material with the different loading rates.

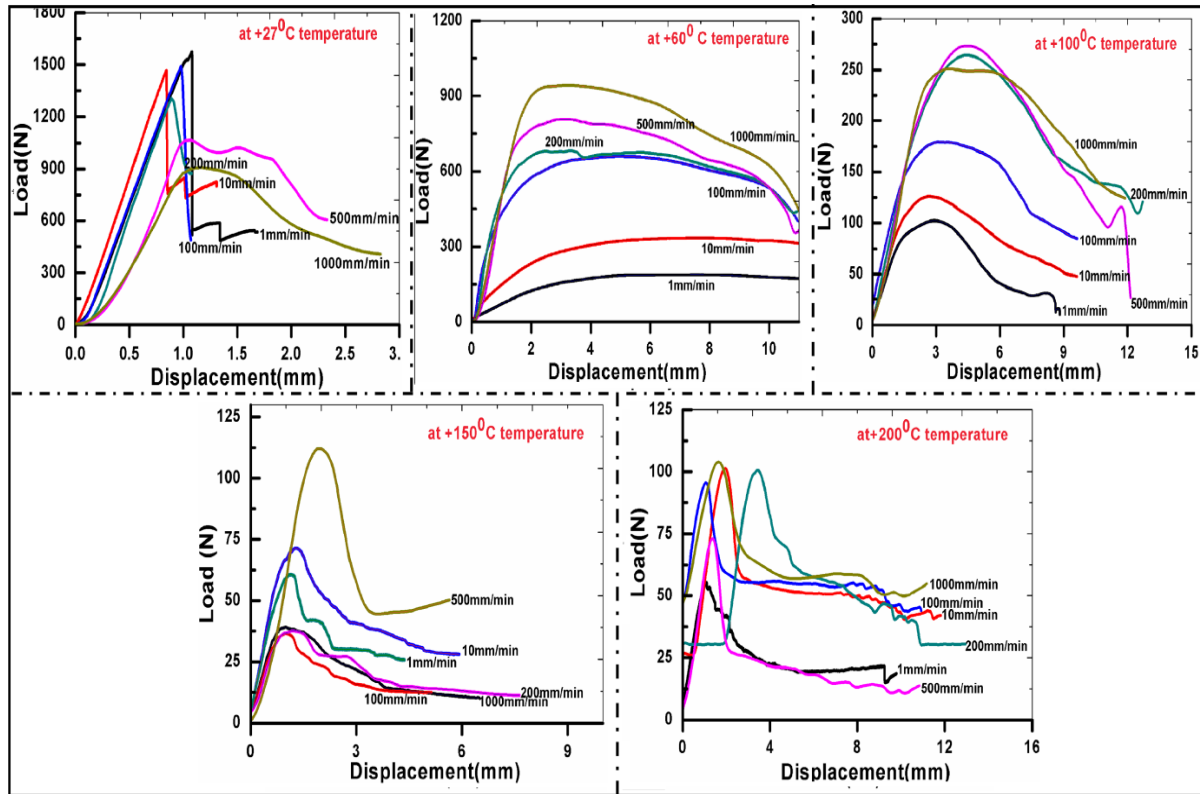
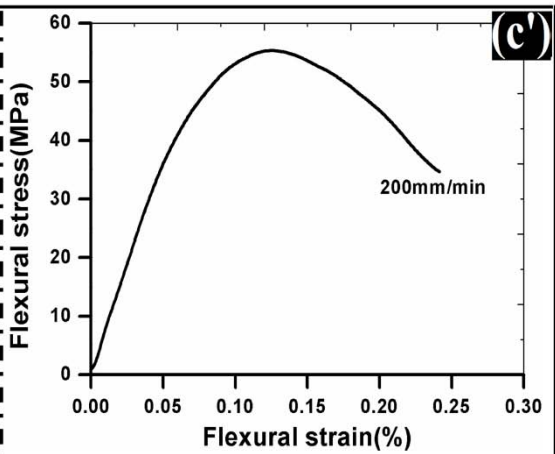
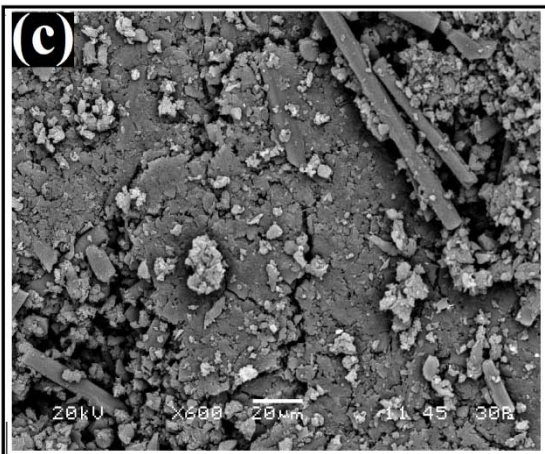
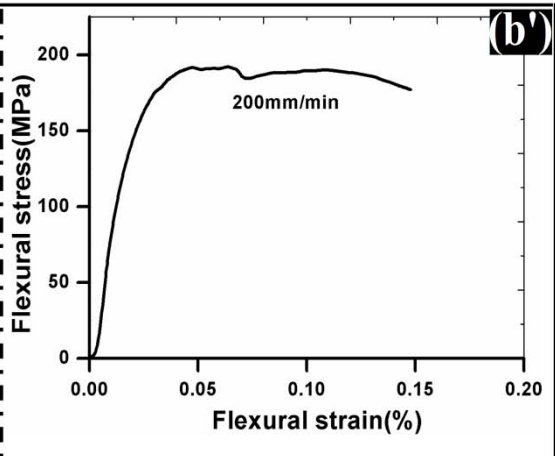
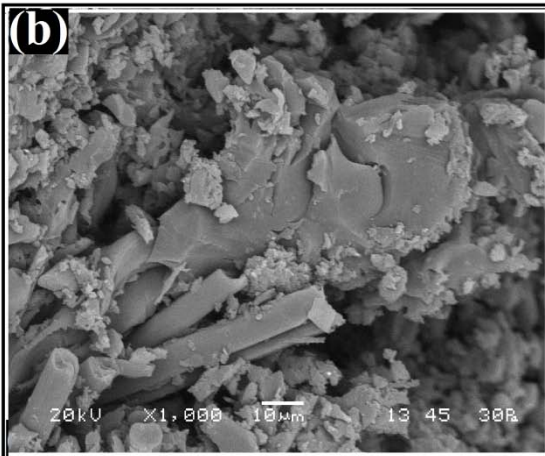
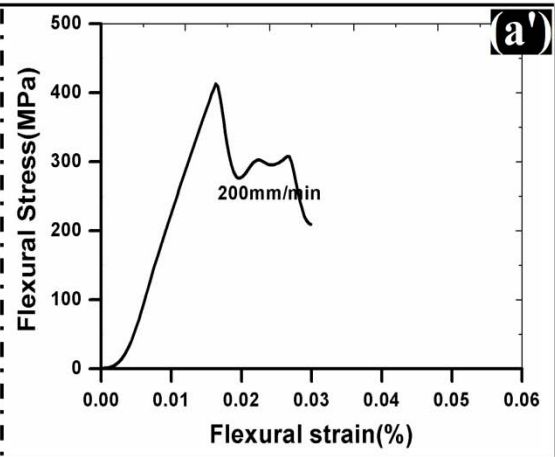
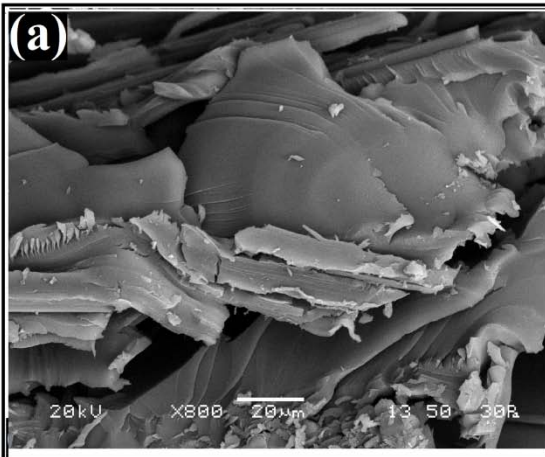


Fig. 19 Load-displacement curve of carbon fibre/epoxy composites above and below glass transition temperatures as +60°C temperature, +100°C temperature, +150°C temperature and +200°C temperature.

4.1.3.2b Fractography study

The fracture surfaces for the carbon fibre/epoxy composites at different temperature have been studied by the SEM and the results are shown in Fig.20. Riverline markings are observed on the broken matrix surface at without conditioning samples (at+27°C) temperature.



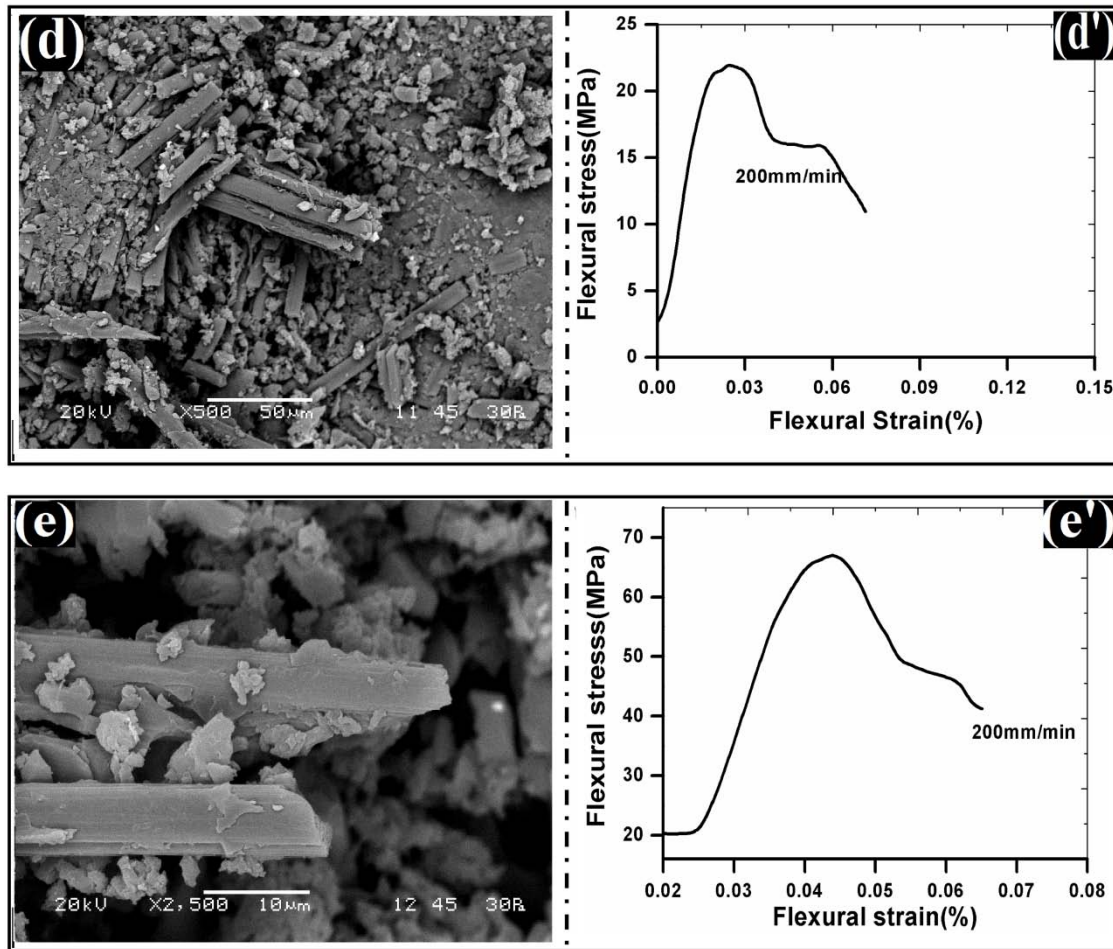


Fig. 20: represents the different failure modes observed at different temperatures and the stress-strain behavior of corresponding temperatures at 200mm/min loading speed (a) at ambient (+27°C) temperature (b) at +60°C temperature (c) +100°C temperature (d) +150°C temperature (e) +200°C temperature.

Matrix fracture failure mode obtained at +60°C temperature which may be the reason for weak bonding between carbon fibre and epoxy matrix. In this case the delaminations resistance of these materials may be low because of which specimens delaminate rather than translaminar failure. Stree-strain curve at this temperature shows high strain to failure values, although matrix fail but the fibres are intact with matrix which governs some load at this loading speed. As the temperature increases close to glass transition temperature at +100°C matrix shows small microcrack on the surface. Sometimes this microcracking referred to as ply splitting. At this failure mode carbon fibre have low strength transverse to the fibre axis. Thus material behaves ductile failue mode at this temperature. But at above glass transition temperature i.e +150°C and +200°C temperature fibre fracture plays dominant role in case of carbon fibre/epoxy composites. When matrix crack approaches to the broken fibre region the

shear stress leading to the fibre/matrix interface region which inducing weak adhesion. However, with increasing loading rate this mechanism will act to blunt the crack propagation. Microscopically carbon fibre shows crenulations and radial pattern appears on the fibre ends [28].

4.1.3.3a Kevlar fibre/epoxy composites

Interlaminar shear strength with loading rate study

At ambient temperature the shear strength value was more as compared to treated one. This may be attributed by failure of Kevlar fiber in fibrillation manner. FRP composites generally contains microvoids, microcracks with statically distributed sizes and damage sites. A weaker of interfacial bond may result in a low flexural strength of the laminate. But with increasing loading speed show higher shear strength for almost all loading speed. At lower cross head speed the polymer gets more time for relaxation due to which, there is less gross plastic deformation, thus resulting in enhancement of ILSS values [6]. The failure in tension brings into play the covalent bonding along the axis, which ultimately leads to chain scission and /or chain sliding or a combination thereof. However, they have poor properties under axial compression, torsion and in the transverse direction. Kevlar fiber have the distinction value of the highest tensile strength-to-weight ratio of any commercially available reinforcement fiber [22]. This fiber excel is in composite toughness or damage tolerance. The lower the stress concentration factor, the greater the resistance of the laminate to crack propagation. The structural integrity losses at higher cross head speed increases the crack density. Accordingly, the transverse, shear strength and stiffness are very low. The transverse stiffness of this fiber is similar to that of an isotropic polymer at low temperature. Damage tolerance includes both the ability to resist penetration during impact and the retention of properties after a given level of impact. Along with good impact resistance and damage tolerance, fiber has high fracture toughness or resistance to crack propagation.

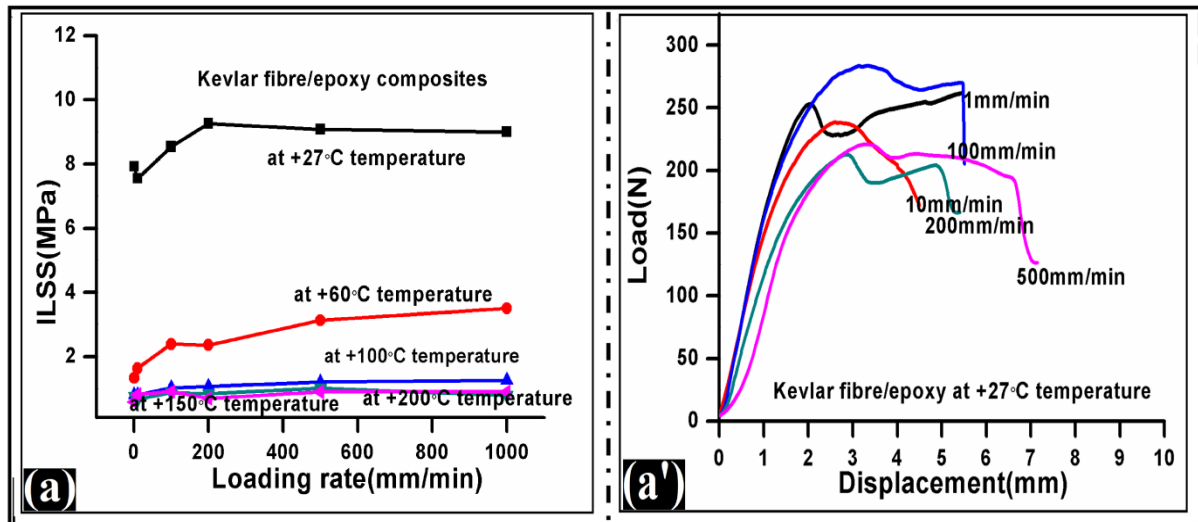


Fig 21: (a) Interlaminar shear strength (ILSS) values with loading rate curve at different temperature of Kevlar fibre/epoxy composites (a') load-displacement curve of without conditioning samples (+27°C) at different loading rates.

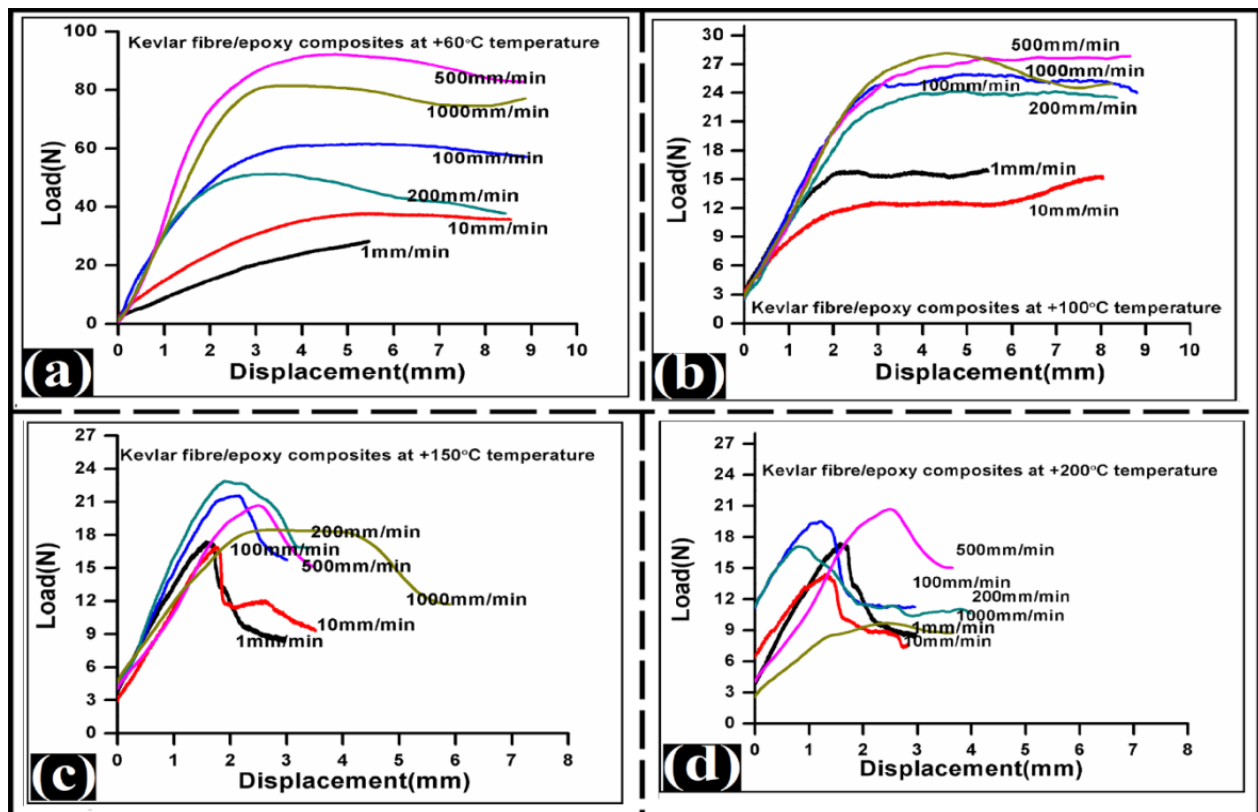


Fig.22 Load-displacement curves (a) at +60°C temperature (b) at +100°C temperature (c) at +150°C temperature (e) +200°C temperature

From the experimental results, it is found that ILSS values are more at ambient temperature. The research showed that the rising of the laminate strength at ambient temperature depended mainly on the fiber/matrix interface strength. There is a slight improvement in shear strength with each loading speed was observed. The more percentage of interfacial area here are strongly affected at these temperature. Kevlar fiber show high strength under axial tension. The specimens were first tested at ambient temperature at different loading rates. Thereafter, high temperature treatment was followed with the same loading rates. There is a slow drop in ILSS value at 200mm/min, may be due to less adhesion level at this loading speed. The variation of ILSS here is the net result of interfacial interaction shows in SEM. At temperature is likely to change the chemistry at the fiber/matrix interface region. At this temperature the polymeric matrix becomes stiffer and stronger but also less ductile. These phenomena may impart better adhesion at the interface.

4.1.3.3b Fractography Study(SEM)

Considering the influence of high temperature on the fracture micromechanisms in composites; the matrix and high radial expansion coefficient of fiber causes residual tensile stresses in the matrix. Regarding the fracture morphology of interlaminar (intralaminar) fracture at very each temperature, resin embrittlement doesnot play dominate role and thus decrease of ILSS value observed as compared to ambient temperature. Fig.23 represents fibril fracture of fibre end, thin riverline marking, toughened matrix, matrix roller and fibre imprints observed at ambient, +60°C,+100°C,+150°C,+200°C temperatures treatment of the samples. Local failure may initiate along a line defect, such as fiber and spread into the surrounding matrix. This phenomena leads to important fractographic features as riverlines. This is most valuable features for crack growth directions which observed sharply on SEM images. The convergences of pairs of planes from the tributaries of the rivers, ultimately converging into one crack therefore, the direction of riverlines markings is the direction of crack propagation of the matrix plane [23]. One of the most important phenomena of matrix fracture is the process by which multiple fractures initiates along the crack front, begin to propagate on several slightly different planes, and the subsequently converge onto one plane. The morphology of the matrix rollers is strongly dependent on the matrix type, interface strength which observed in SEM. As the matrix toughness increases the rollers become more elongated, exhibiting increasing plasticity. This may be the reason for increase of ILSS value in each loading speed. The stressing conditions and the environments that a composite is subjected play a key role in determining its loading failure process [24-27].

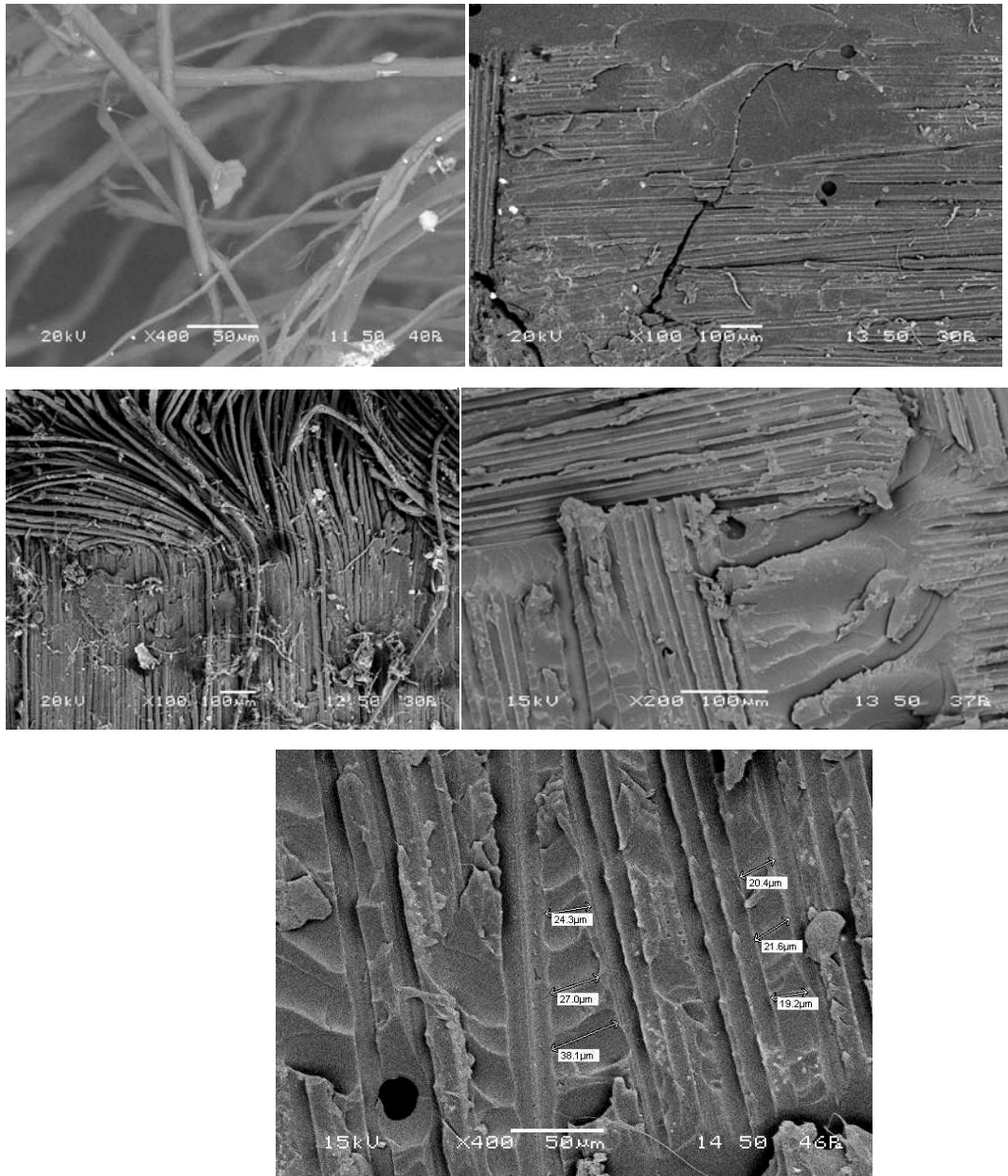


Fig. 23: Different failure modes observed at ambient temperature, +60°C, +100°C, +150°C, +200°C temperatures.

At +100°C micrograph represents the toughened matrix conditions of the woven fabric Kevlar/epoxy composites. Highly oriented aramid fiber fail in a fibrillar fashion. Fibrillar fracture also observed, signifies that the fracture surface is not transverse to the axis but runs along a number of planes of weakness parallel to the fiber axis, its axial tensile modulus increases but the shear modulus decreases. Examination of the fiber ends of a compression

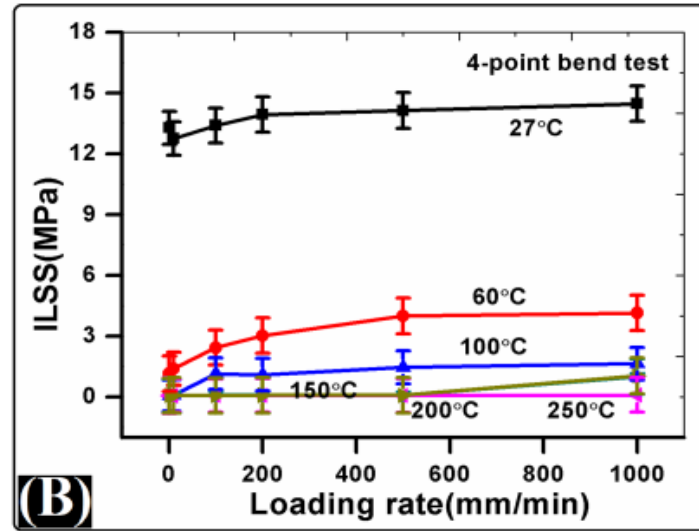
fracture shows further evidence of the microbucklingshown failure mechanisms. The fractographic features shown on the fiber ends exhibit the morphology particular to laminate compression failure. Across each individual fiber end is a line, which represents the neutral axis of the fiber as it undergoes bending. Microbuckling may occur on several planes giving rise to series of steps on the fracture surface, each step being a multiple of half the buckling wavelength. During failure involving compressive stresses, fibrillation occurs, which results in a large degree of new surface area. This fibrillation process results in high-energy absorption during the process of failure.

4.1.3.4a 4-point bend test(Glass fibre/epoxy composites)

Interlamianr shear strength with Loading rate study

Fig. 24 represents the glass fibre/epoxy composites at different temperatures with different loading rates subjected to 4-point fixture bend test. Fig. 24(A) illustrates ILSS verse loading rates at different temperatures compared with ambient samples. It can be seen that ILSS value changes significantly with temperatures and loading rates.

Curve shows for 4-point bend test very less percentage of change in ILSS values. However, the values obtained in above T_g shows significantly high percentage of change in ILSS values. The reason may be due to increase in crack density in the epoxy matrix. As increase in crack density more number of cracks overlaps into each other, forming larger cracks [22, 23]. In case of 4-point bend test, at $+60^\circ\text{C}$ temperature the ILSS values increases from 1 to 2 MPa with increasing loading speed and for ambient samples it follows a similar trend as ILSS increases from 13 to 14 MPa with increasing loading rates. When the specimen subjected to $+150^\circ\text{C}$ temperature, 200°C temperature and $+250^\circ\text{C}$ temperatures.



(A)

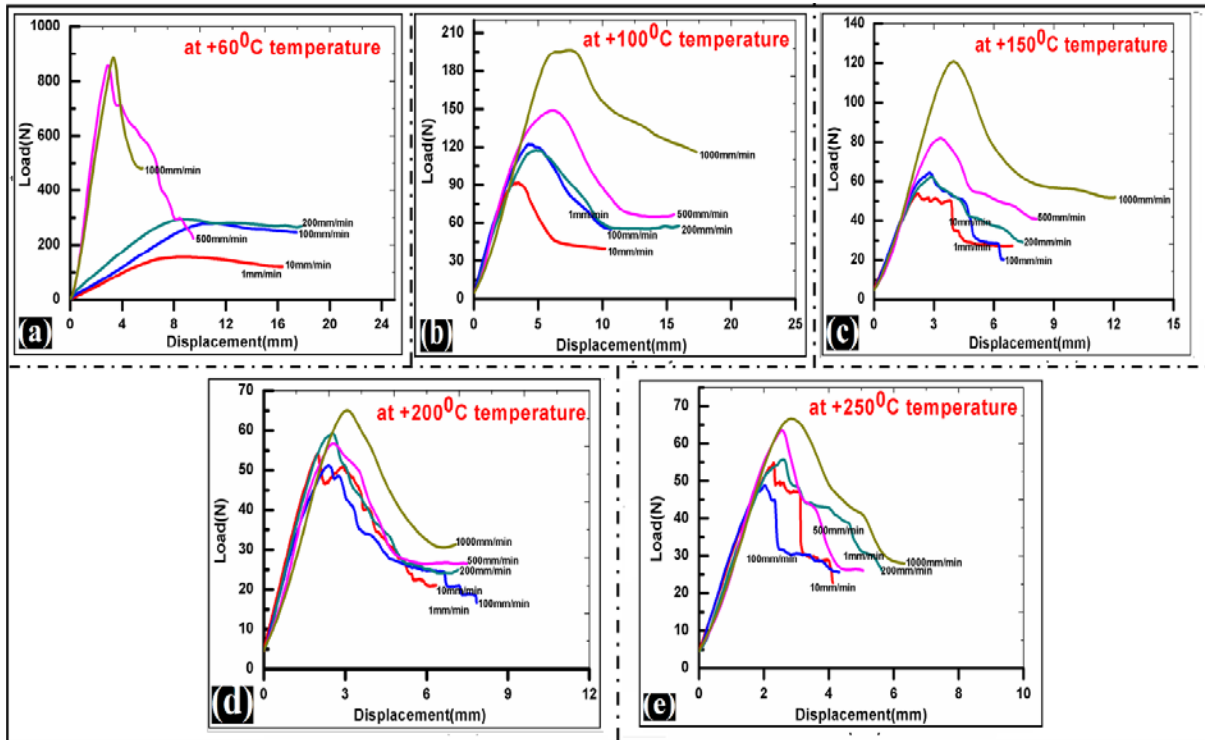


Fig.24(B) Variation of ILSS with loading rate of glass fibre/epoxy composites tested with 4-point bend test at different temperatures. (a) Load-displacement curve of glass fibre/epoxy composites at +60°C temperature (b) load-displacement curve of glass fibre/epoxy composites at +100°C temperature (c) load-displacement curve of glass fibre/epoxy composites at +150°C temperature (d) load-displacement curve of glass fibre/epoxy composites at +200°C temperature (e) load-displacement curve of glass fibre/epoxy composites at +250°C temperature.

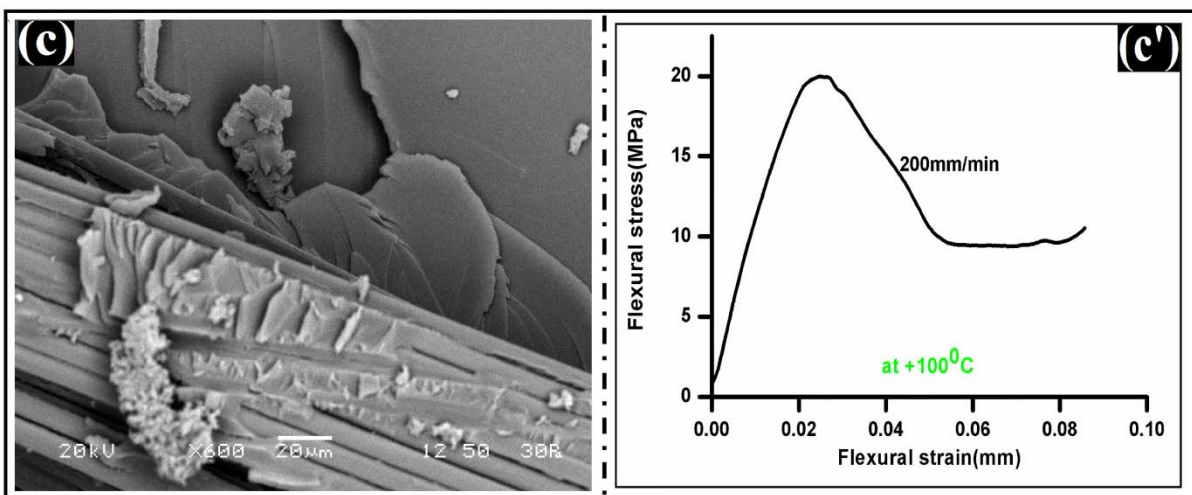
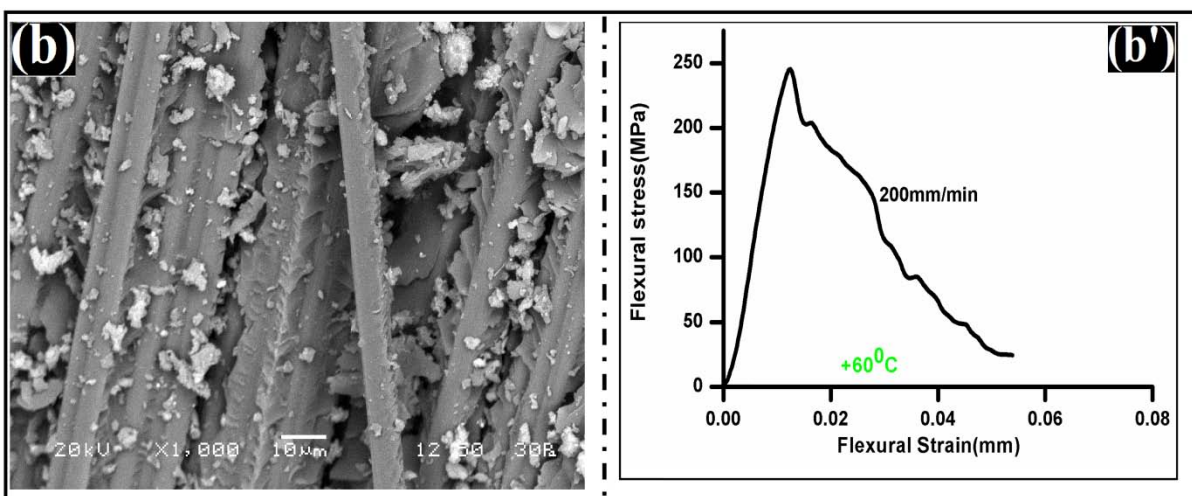
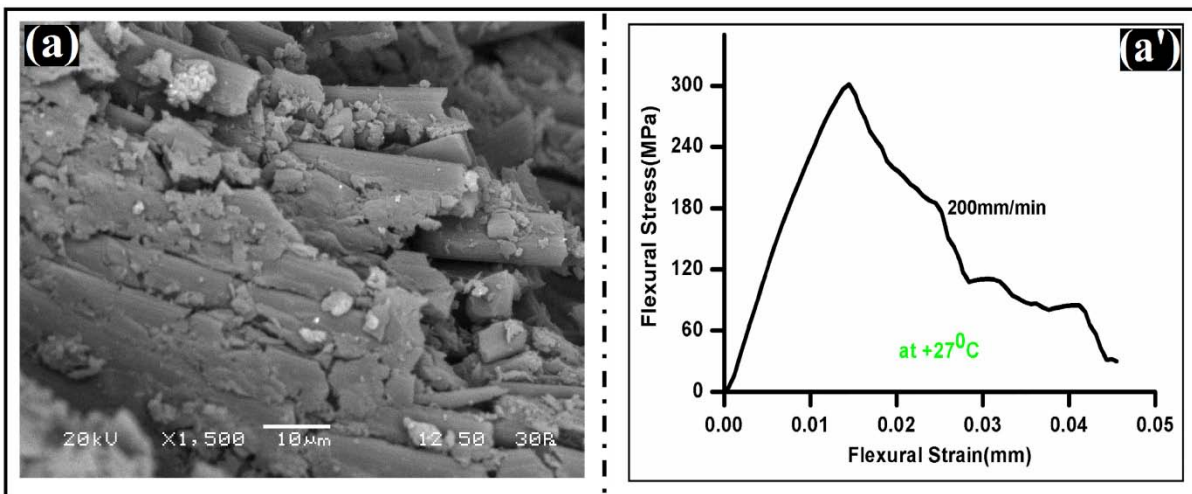
At 4-point bend test this follows the same trend. Fig.24(c), (d) and (e) displays the specimen subjected to +150°C temperatures, +200°C temperatures and +250°C temperatures respectively. It observed that ILSS values decreases with increasing temperature. As this temperature is above glass transition temperature (T_g), epoxy matrix behaves viscoelastic in nature. The specimen don't show any loading rate sensitivity during the 4-point bend test

It can be seen that nearly all values in 3-point bend test exhibit an important linear relationship with the values of 4-point bend test. In particular, the values obtained well below glass transition temperature (T_g),

The ILSS behaviour of the glass fibre/epoxy at 3-point bend test, significantly affected by temperatures and loading rates, while the 4-point bend test less remain largely unaffected with loading rates. To further understand the failure behaviour of composites, two more aspects will be investigated.

4.1.3.4b Fractography analysis

Fig. 25 (A) represents the scanning electron microscopy image at ambient temperature. (A') represents the stress-strain curve at 200mm/min. Here toughened matrix plays dominant role. It is at the interfacial region between fibre and matrix where stress concentration develop because of difference in the thermal expansion coefficient between the reinforcement and the matrix phase due to loads applied to the structure and the time of curing shrinkage. As stress concentration is very small in case of four points shear test toughened matrix plays the role of adhesion between fibre and matrix. Here stress-strain curve shows no significant change in load carrying capacity. The debonded interfacial regions appear to be nucleated by thermal stress is demonstrated in Fig 25(B) at +60°C temperature. The sharp fall in stress-strain curve shows small variation in failure to strain which shown in Fig. 25(B'). When temperature increases very close to the glass transition temperature matrix changes its behaviour. Cusps formation was observed at +150°C temperature which shown in Fig.25(C) and simultaneously Fig.25 (C') also represents the ductility in the curve.



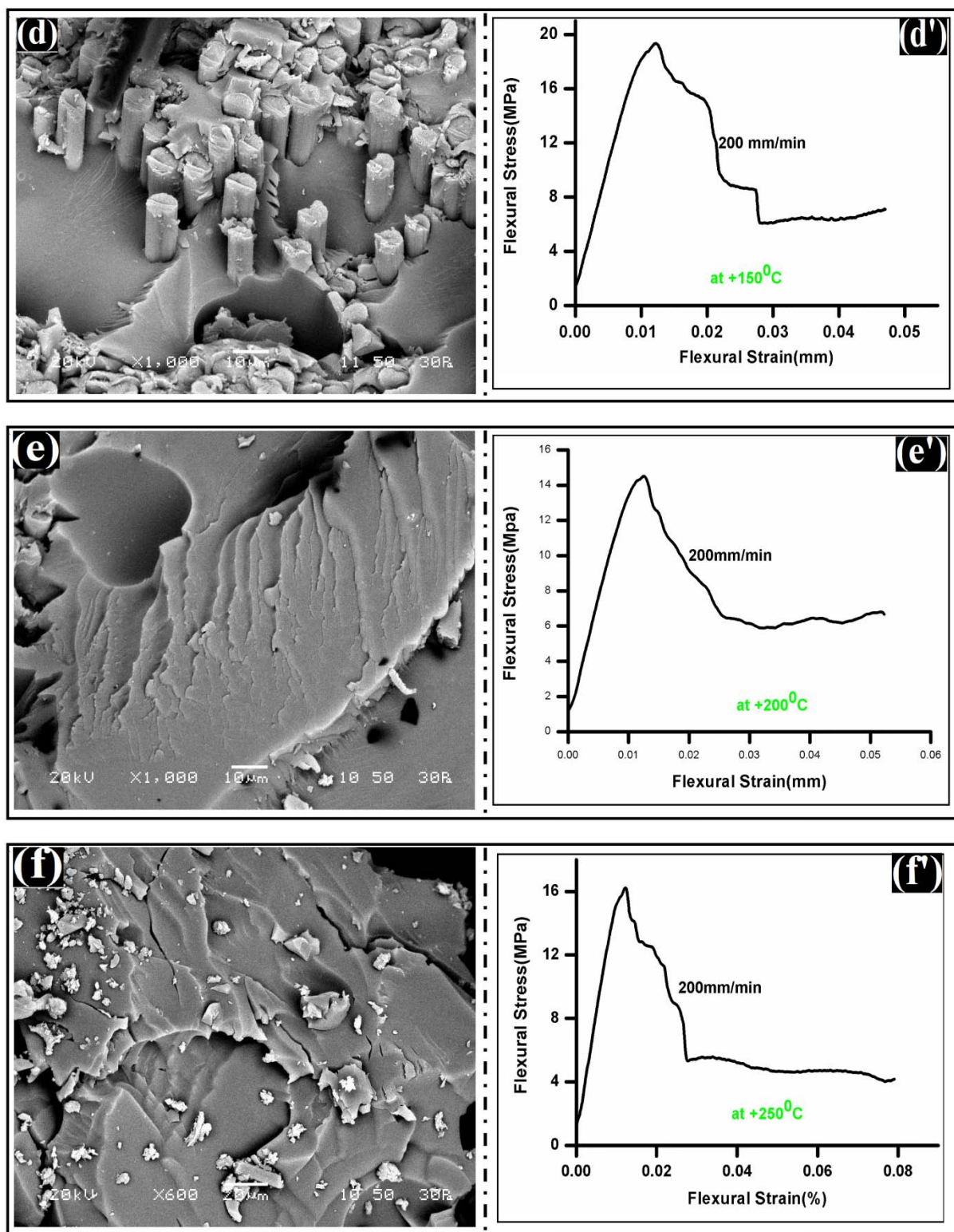


Fig.25: (A,A') Scanning electron microscopy images of glass fibre/epoxy composites tested at 4-point short beam shear test at 200mm/min and flexural stress with flexural strain curve at ambient temperature, (B,B') at +60°C temperature, (C,C') at +100°C temperature, (D,D') at +150°C temperature, (E,E') at +200°C temperature, (F,F') at +250°C temperature.

Fracture of fibers in Fig. 25(D) during processing / in service is generally an undesirable feature. Fracture in fibers, as in bulk materials, initiates at some flaw(s), internal /on the surface. In general, because of the high surface to volume ratio of fibers, the incidence of a fiber flaw leading to fracture is greater in fiber than in bulk material [26, 27]. Very frequently, a near surface flaw such as a microvoids/ or inclusions is responsible for the initiation of fracture of fibre. Above glass transition temperature at +200°C temperature small riverline marking was observed in epoxy matrix shown in Fig.25 (E). Riverline marking ultimately converging into one crack and shows to direction of failure. But as matrix behaves in viscoelastic in nature, these cracks got arrested and no significant change in ILSS values observed at this temperature. Stress-strain curve at +200°C temperature also signifies more strain to failure than the other testing temperature shown in Fig. 25(E').

Resin rich region was observed in Fig.25 (F) at +250°C temperature of glass fibre/epoxy composites. This failure mode will tend to be largest at ply interface region. Resin rich region can help to blunt stress concentrations and inhibit damage growth. Fig.25 (F') represents the stress-strain curve at +250°C temperature. This curve shows ductile to brittle failure mode. Ultimately, resin-rich region will imbue a site with locally low stiffness and strength, and at regions of high stress, it can act as an initiation site for failure.

One major problem in glass fiber is that of failure due to static fatigue. According to the chain-bundles model, if a fiber fractures, the matrix translates the load to the neighbouring fibres in the composite. The stress concentrations at the broken fiber ends, unless dissipated properly, may induce failure in adjacent fibers and precipitate catastrophic failure of the composite.

4.1.3.3 Spectroscopy Analysis (FTIR-ATR)

FTIR-ATR spectroscopy was used to verify the occurrence of surface oxidation of the samples through the investigation of a functional group change. In addition, structural changes in the matrix after high temperature conditioning were investigated by following ester group formation and chemistry changes of both epoxy polymer and fibre reinforced composite samples shown in Fig.29. In the carbonyl region ($1750\text{--}1700\text{ cm}^{-1}$), a sharp peak formed at 1715 cm^{-1} with a shoulder peak at 1735 cm^{-1} corresponding to carboxylic acid and ester groups, respectively [11].

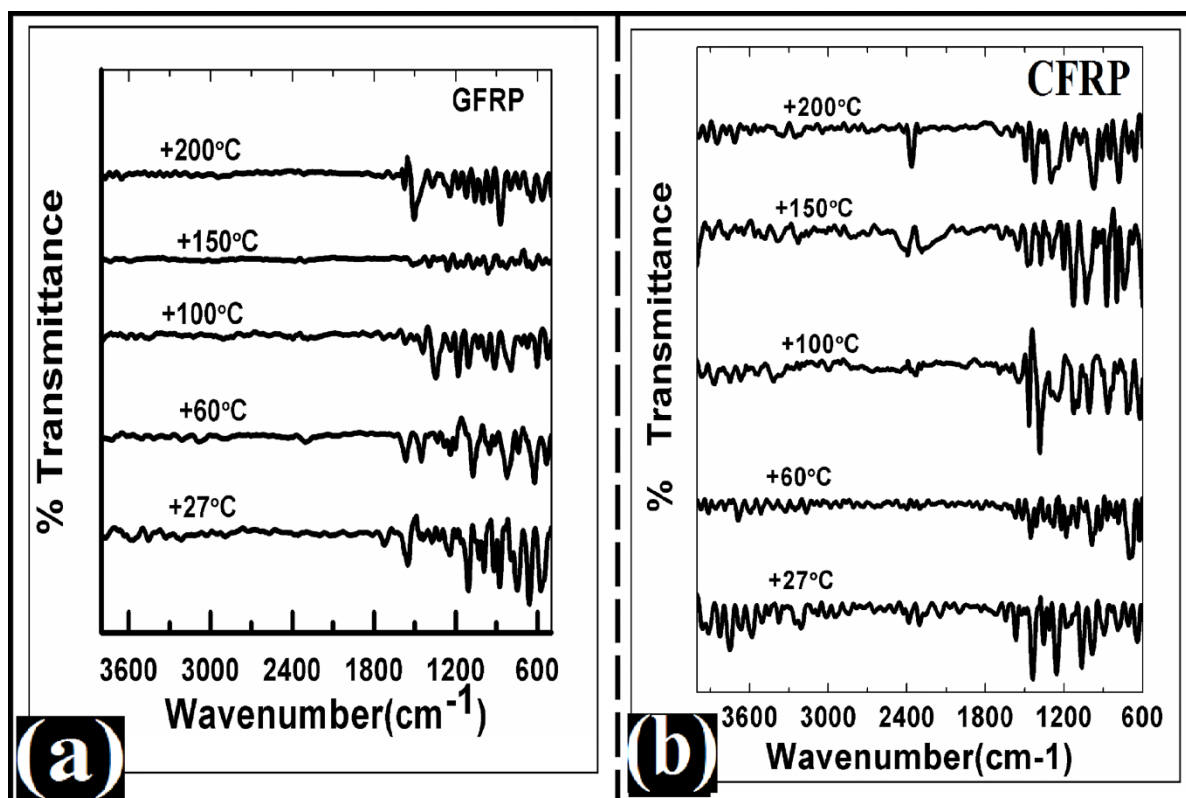


Fig 26: FTIR-ATR spectroscopy results of glass fibre/epoxy and carbon fibre/epoxy composites subjected to high temperatures.

The reactivity of some commercial epoxy resins has been increased by the presence of ether bonds that, even when separated from the epoxide ring by the methylene group, have a great activating effect on the epoxide group. Because of this reactivity, the epoxide groups can be opened not only by available ions and active hydrogens but also by tertiary amines. Each primary amine group is theoretically capable of reacting with two epoxide groups. In the case of bifunctional resins, it is expected that the epoxide group is opened by the primary amines. When the remaining secondary hydrogen combines with a new epoxy molecule, a branch point is formed. The rate at which the branching or the linear growth of the polymer occurs depends on the relative rate of the epoxide group with the hydrogens of the primary or secondary amines.

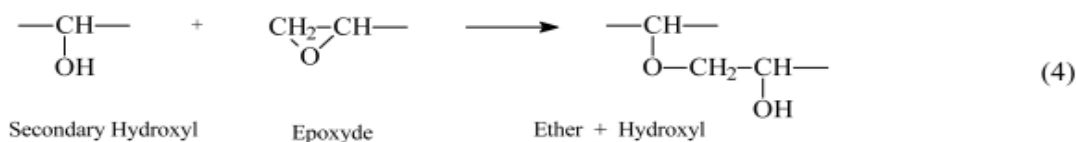
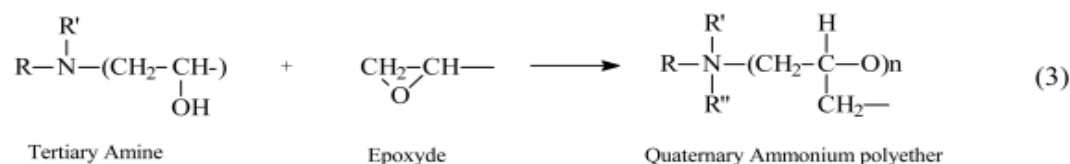
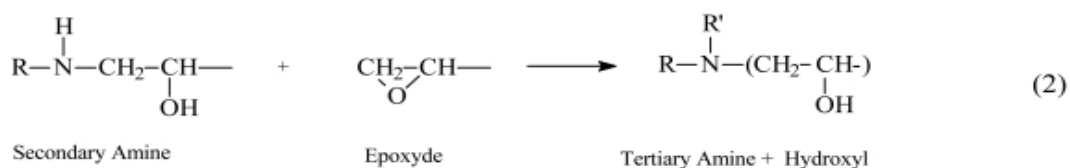
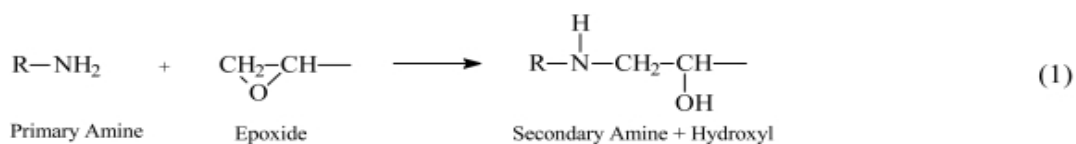


Fig. 27: Curing reaction of epoxy matrix resin.

4.1.3.4 Glass transition Study(TMDSC)

The glass transition temperature behavior at high temperature are illustrated in Fig.31

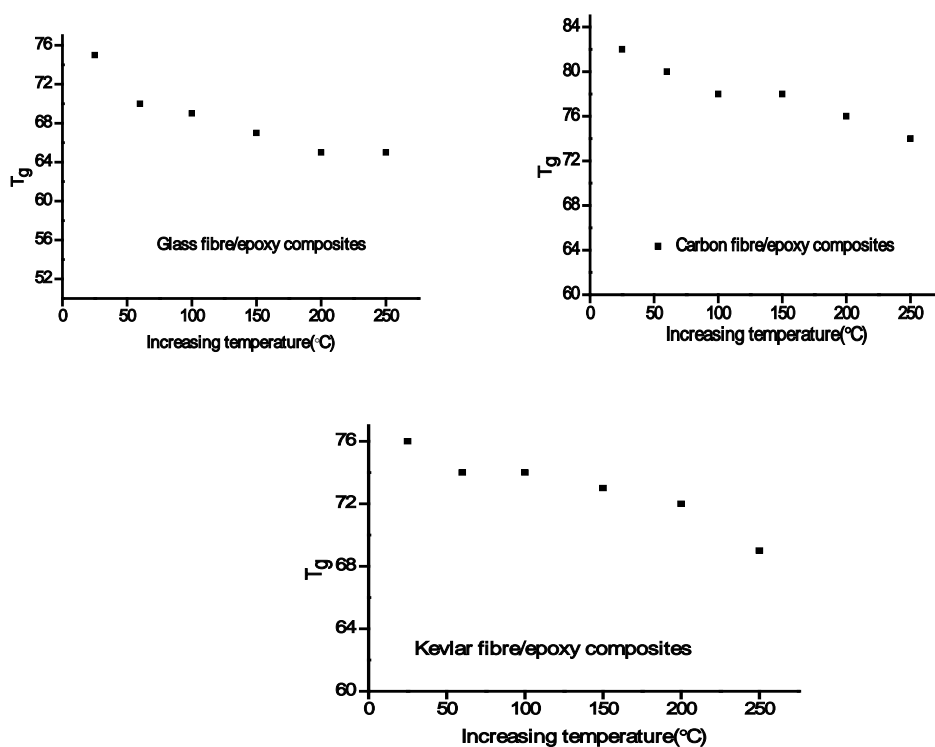


Fig.28 Glass transition temperatures values of glass fibre,carbon fibre and Kevlar fibre epoxy composite materials.

The physical cause of glass transitions of polymer are place change of molecular groups. Since the glass transition temperature (T_g) corresponds to a mobility change in a polymer and has a definite free volume associated with it, the jumping frequency of a segment is same magnitude for nearly all polymers. The T_g value usually decreases at high temperature. But the changes are not very significant. This is may be increase of cross-link density of matrix which decreases the molecular mobility of the polymer. Another reason behind this, it may be due to presence of thermal stresses in the epoxy resin matrix which going to degradae the bonding at the interface region. The covalent bond is going to replace by weakest bond. Glass fibre/epoxy composites are very weak in nature as compared to carbon fibre/epoxy composites. During the increase in T_g value matrix undergoes viscoelastic in behavior. Molecules are likely to unstable in nature at this stage. Because of this interfacial bond strength getting weak leads to change in T_g values. In the TMDSC measurement, the structure through the T_g region is nearly in the quasi-equilibrium state.

Summary and Conclusions

The loading rate sensitivity of glass fibre/epoxy composites at low and high temperatures at different fixture modes are reported here to deconvolute stress concentration and thermal factors. Four-point bend tests showed that the interlaminar shear strength is not affected by loading rate while epoxy matrix was affected by temperatures as it goes through its glass transition temperature. These observations are crucial for explaining the loading rate sensitivity of glass fibre/epoxy at high temperatures. Considering interlaminar shear strength and delamination behavior, the tested laminate characterized by SEM to reveal various failure modes. The present study may possibly reveal the following conclusions:

During 3-point short beam shear test the ILSS values at ambient ($+27^\circ\text{C}$) temperature decreases from 20 to 18 MPa with a transition at 200mm/min. The ILSS values decreases with increasing temperatures due to the presence of curing stress between the fibre/matrix interface regions. In case of 4-point short beam shear test ILSS value changes significantly with temperatures and loading rates.

Above glass transition temperature the ILSS values sharply decreases as compared to ambient temperatures. At this decomposition temperature, epoxy starts decomposing with different phases as combustible gases, decomposing and smokes. This may attributed as matrix

behaves viscoelastic in nature as the main backbone chains of polymer possess much greater freedom of motion.

From fractographic point of view various fibre failures plays dominant role in below glass transition temperatures whereas matrix failure plays above glass transition role. One general point observed from flexural stress- flexural strain curve was strain to failure in 3-point bend tested samples was smaller as compared to 4-point bend tested samples.

References

1. Gudes R.M.(2007).,Durability of polymer matrix composites:Viscoelastic effect on static and fatigue loading, Composite Science and Technology, Vol-**67**, 2574
2. Naik,N.K., Venkateswara.R.K., Ravikumar,G.,Vearraju,Ch.(2010).,Stress-strain behavior of composites under high strain rate compression along thickness direction: Effect of loading condition,, Materials and Design.,Vol-**31**, 396
3. Ray, B.C.(2006),Temperature effect during humid ageing on interfaces of glass and carbon Fibers reinforced epoxy compositesJ of Colloid and Interface Science. ,Vol-**298**, 111
4. Ray B.C. (2004), Effects of crosshead velocity and sub-zero temperature on mechanical behaviour of hygrothermally conditioned glass fibre reinforced epoxy composites. Material Science and Engineering, Vol- **379**:39.
5. S. Sethi, Ray B.C(2014), An assessment of mechanical behaviour and fractography studyof glass/epoxy composites at different temperatures and loading speeds, Materials and Design, Vol-**64**:160
6. S. Sethi, Rathore D, Ray B.C(2014), Effects of temperature and loading speed on interface-dominatedstrength in fibre/polymer composites: An evaluation for in-situenvironment, Materials and Design, Vol-**65**: 617
7. Tanoglu M.,Mcknight,S.H.,Palmese,G.R.,Gillespie,J.W.Jr,(2000),A new technique to characterize the fiber/matrix interphase properties under high strain rates, Composites Part A, Vol-**31**,1127
8. C, Dong, Ian J. Davies (2014), Flexural and tensile strengths of unidirectional hybrid epoxy composites reinforced by S-2 glass and T700Scarbon fibres. Materials Design., Vol-**54**: 955
9. Soutis,C.,Turkmen,D.(1997), Moisture and temperature effects on the compressive failure of CFRP unidirectional laminates, J. Composite. Material,Vol-**31**, 832
10. Rapnowski,P., Gentz, M.,Kumosa,M.,(2006). Mechanical response of a unidirectional graphite fiber/polyimide composite as a function of temperature, Composite. Science and. Technology., Vol-**66**, 1045
11. Ray, B.C. (2004),Loading Rate effects on Mechanical Properties of Polymer Composites at Ultralow TemperaturesJ of Applied. Polymer. Science,Vol-**100**, 2062
12. Fabio Nardone, Marco Di Ludovico, Francisco J. De Caso y Basalo, Andrea Prota , Antonio Nanni, Tensile behavior of epoxy based FRP composites under extreme service conditions, Composites: Part B 43 (2012) 1468–1474.

13. Piyush K. Dutta, David Hui, Low temperature and freeze thaw durability of thick composites, *Composites:Part B* 27B (1996) 371-379.
14. M.Z. Shah Khan, G. Simpson, E.P. Gellert, Resistance of glass-fibre reinforced polymer composites to increasing compressive strain rates and loading rates, *Composites: Part A* 31 (2000) 57–67.
15. Okenwa I. Okoli, The effects of strain rate and failure modes on the failure energy of fiber reinforced composites, *composite structures* 54 (2001) 299-303.
16. Ray B.C.,(2006).Effects of Thermal and Cryogenic Conditionings on Mechanical Behavior of Thermally Shocked Glass Fiber/Epoxy Composites,*J of Reinforced Plastic and Composite* ,Vol-**25**, 1227
17. Fereshteh-Saniee, F., Majzoobi,G.H., Bahrami,M.,(2005),An experimental study on the behavior of glass/epoxy composites at low strain rates,*J of Materials Processing Technology*,Vol-162, 39
18. Jang B Z., *Advanced Polymer Composites: Principle and Applications*. ASM International, Materials Park, OH, 1994
19. Hartwig,G.,*Polymer properties at room and cryogenic temperatures*. New York, Plenum Press, 1994
20. Ray B.C. (2006). Adhesion of glass/epoxy composites influenced by thermal and cryogenic environments. *J of Applied Polymer Science*, Vol-102:1943.
21. Kim K, Mai Y W., *Engineered Interfaces in Fiber Reinforced Composites*. Kidlington, Oxford ,U.K, Elsevier Publication, 1998
22. Greenhalgh E S. *Failure analysis and fractography of polymer composites*, Cambridge,UK ,CRC Publication, Woodhead Publishing, 2009
23. Ray B C.(2004).Thermal shock on interfacial adhesion of thermally conditioned glass fiber/epoxy composites rates, *Material. Letter.*,Vol- **58**, 2175
24. Parvatareddy H, Wang J.Z, Dillard D.A., Ward T.C.(1995), Environmental aging of high-performance polymeric composites: effects on durability, *Composites Science and Technology*, Vol-**53**,399
25. Sookay N.K., Klemperer,C.J, Verijenko,V.E., (2003) Environmental testing of advanced epoxy composites, *Composite Structures*, Vol-**62**;429
26. Karbhari V.M (2004), E-glass/vinyl ester composites in aqueous environments: effects on short-beam shear strength. *J Composite Construction*, Vol-**8**, 148
27. Myer M.W, Herakovich C.T, Milkovich SM, Short J.S, (1983), Temperature dependence of mechanical and thermal expansion properties of T-300/5208 graphite epoxy, *Composites*, Vol-**14**; 276.

4.1.1a AFM Study of thermally conditioned samples

Theories and Thoughts

The characterization of fractographic features associated with fibers, matrix and also interface/interphase has been emphasized here to analyze the surface topographical contours across the glass fiber and epoxy matrix. Atomic force microscope (AFM) and Scanning electron microscope (SEM) were performed to characterize the micro-failure features (like micro-voids, small matrix and interfacial cracks) and structural homogeneity/integrity of composites. AFM study showed that thermal conditioning has resulted non-homogeneous degree of cross-linking reflected by the height-scan images. The uneven post-curing may adversely affect the stress transmissibility integrity of interphase region, which may eventually lead to changes in thermophysical, mechanical and chemical characteristic of fibrous composite. Scanning micrograph indicates the increase in cusp thickness due to increase in plasticity of resin matrix.

4.1.1a.1 Introduction

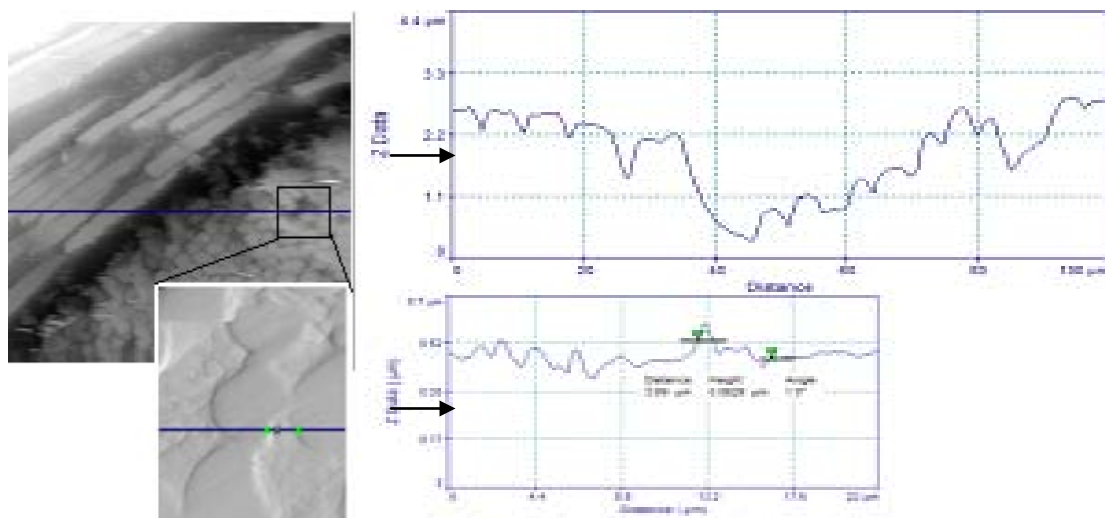
Polymer composite technology is based on taking advantage of the stiffness and strength of high performance fibers by dispersing them in a matrix, which acts as a binder and transfers forces to the fibers across the fiber/matrix interface. Severe environmental exposure affects physical and mechanical properties of polymer composite materials resulting in an undesirable degradation (1). An interfacial reaction may impart various morphological modifications to the matrix microstructural in proximity to the fiber surface (2). The interfacial adhesion and mechanical properties can be improved by increasing the fiber surface roughness particularly on the nanometer scale (3). As a result, extensive research has been devoted to the study of microstructural assessment of GFRP composite. The work represented here has identified both surface and interphase properties in terms of topography, fractography, adhesion and stiffness characterized by AFM, SEM the nanometer scale, which are essentially for the understanding of the macromechanical response to fracture. Special emphasis is placed on the local characterization of the fiber surface topography, interphase mechanical properties and adhesion features. The nanoscale crosslinking process of the epoxy resins near fiber surface influenced by the thermally conditioning treatment is analyzed by AFM and SEM.

4.1.1a.2 Experimental

The fracture surfaces of advanced polymer composites fibers were studied. The composites were treated to above glass transition temperature subjected to 3-point bend test until failure for a certain period of time. Then they were characterized with SEM and AFM techniques. E-glass reinforced epoxy polymer composite was fabricated by hand lay-up method. The composite panels were cut into small pieces which were made into a plug with the cross section exposed for polishing. Polishing steps covers all the grinding papers followed by cloth polishing and then 1 μ m alumina particles for micropolishing subjected to 30 min for each samples. Thermal conditioning was conducted by placing the specimen as prepared at +60°C for 1 hr in oven. After treatment the specimens were taken out and scanned by AFM. AFM demonstrates resolution of fraction of a nanometer by feeling the surface with a mechanical probe. These images in contact mode with a conducting P(n) doped silicon tip were obtained with a SPMLab programmed VeecoDilnnova multimode Scanning Probe Microscope. The scans were taken at scan rates of 1 Hz. Images are taken to analyze the surface topography in micro and sub-micron levels. However, 3D micrographs can be obtained from the analysis.SEM

4.1.1a.3 Results and Discussion

The AFM height-images scans of untreated glass fiber reinforced composite are shown in Fig 29 (a) and (b). Remarkable failure modes can be observed between the untreated and thermal conditioning GFRP composites. As shown in Fig 29(a) the failure of fibers seems to be occur.



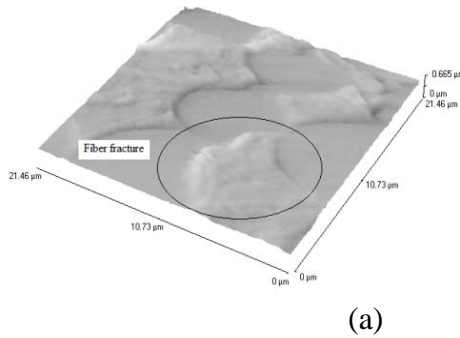
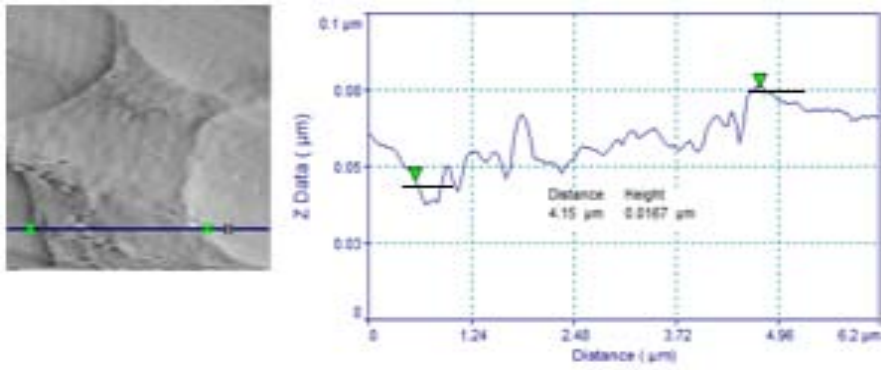


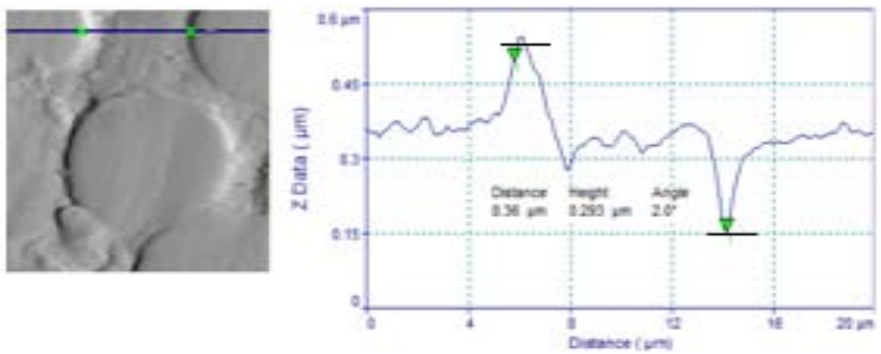
Fig 29: AFM topography images of untreated GFRP composites (a) line analysis of image (b) 3D image analysis

In untreated sample, the failure of fibers may be due to either by over loading or extensive strain. In PMC, the fibers have greater strain-to-failure. Stress concentrations from matrix cracks and fiber/matrix debonding can also promote fiber breakage which shown in Fig 29(a). If a fiber fracture occurs, the matrix translates the load to the neighboring fibers in the composite. The stress concentration at the broken fiber ends, unless dissipated properly, may induce failure in the adjacent fibers and tends to catastrophic failure. High stress concentration is expected to develop in the matrix near the fiber ends and the voids created by the broken fiber (4). Because of this the fiber/matrix interactions in the vicinity of fiber fracture also pompous. The three-dimensional morphological characteristics of fiber fracture are shown in fig 29(b).

After thermal conditioning at below glass transition temperature ($+60^{\circ}\text{C}$) for 1hr, the interface/interphase region is likely to affect which shown in height image analysis (Fig 30). The height distance between two peaks was $4.15\mu\text{m}$. The sharp fall of graph near the peak shows degradation of interface/interphase region. Between these two peaks the matrix plays dominate role for failure. As the non uniform degree of cross linking of matrix increases, the chain network as a whole becomes like to uneven. This should shift the tendency from a more localized shear banding mode to a more homogeneous diffuse shear yielding mode. The thermal misfit strain can also result in debonding effects at the interface region (5).



(a)



(b)

Fig 30: AFM topography image of treated GFRP interphase failure after treatment.

The SEM images of thermal conditioning of GFRP composite are shown in Fig 31. It is found that the cusps are formed with increasing manner. This may be due to, plasticity of the epoxy matrix at high temperature. The cusps resulting from the microcracks are thicker and have undergone greater deformation than the room temperature. The increase in cusp thickness implies fewer microcracks have formed because of increase plasticity (6).

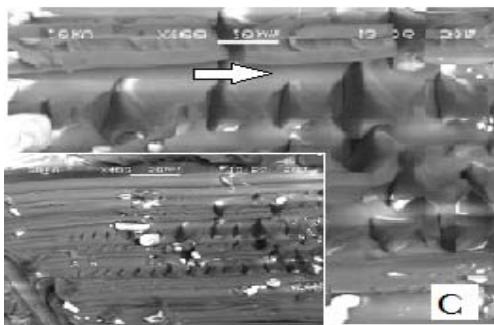


Fig 31: SEM micrograph matrix failure of GFRP composite after treatment.

In Fig 32: shows the adhesion level at the interface region. The sharp decrease of the graph at the 1st peak shows the presence of weak interface at one side of the fiber whereas, there is increase of the 2nd peak point gives strong interface region. The failure may initiate from a weak or defective fiber/matrix interface and consequently reduce ultimate performance. The anisotropic and heterogeneous character of composites naturally results in a large possibility of failure modes (7). It was found that the improved interfacial adhesion was strongly related to the hydroxyl, ether, or aromatic groups on the fiber surface, while surface structure had little influence on the interfacial adhesion, interlaminar shear strength and the failure behavior.

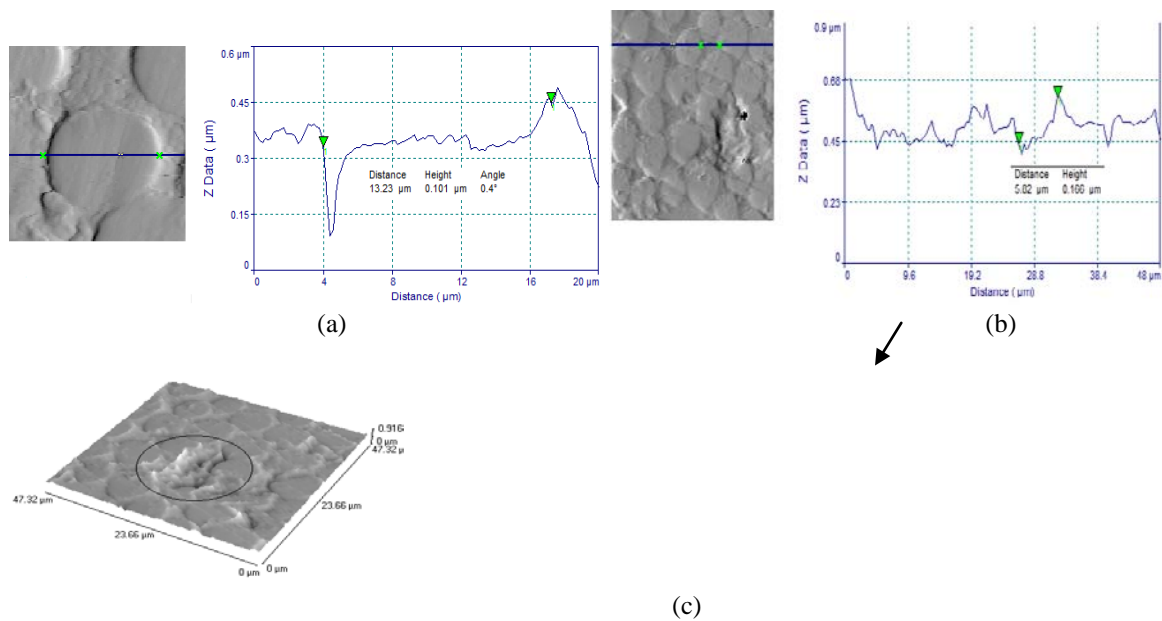


Fig 32: AFM topography image of treated GFRP adhesion failure after thermal conditioning treatment.

The delamination failure mode is known to be major life-limiting failure process in a composite laminate. Delamination can induce stiffness loss, local stress concentration and local stability that can cause buckling failure. There is some deviation also occur on the fiber surface. The frail in adhesion strength relative to fiber is attributed to weak covalent bonding between silane coating of the fiber and the polar group of the matrix (8).

It is more reasonable to consider that true contact area, in nanometer/atomic scale, played a dominant role in an efficient molecular interactions which is directly associated with interface adhesion and in true interphase fracture behavior.

4.1.1a.4 Conclusion

The study presented here has identified both surface and interphase properties in terms of topography, fractography and adhesion which are mostly characterized by AFM technique. Failure of fiber fracture due to extensive strain can be visualized by height image mode analysis. The increase in degree of cross-linking density by thermal conditioning resulted in reduction of the free volume of matrix. The resulted shrinkage of matrix because of greater cross-linking and loss of volatile matters has been indexed by the fall of height scan images of AFM. The increase in cusp thickness implies fewer microcracks have formed because of increased brittleness. The results reveal a unique view to the fractography study of GFRP composites. Potential work along this line will be able to achieve more information regarding failure and fracture of interface/interphase of polymer composite.

References

1. Hull D, Clyne T W. An Introduction to Composite Materials. Cambridge, U.K, Cambridge University Press, 1996
2. Zhao F, Huang Y. Improved interfacial properties of carbon fiber/epoxy composites through grafting polyhedral oligomeric silsesquioxane on carbon fiber surface. *J Mater. Lett.* 2010;64:2742-2744
3. Ray B. C. Thermal shock on interfacial adhesion of thermally conditioned glass fiber/epoxy composites. *J Mater. Lett.* 2004;58:2175-2177
4. Wang Y, Hahn T.H. AFM characterization of the interfacial properties of carbon fiber reinforced polymer composites subjected to hygrothermal treatments. *J Compos.Sci.Technol.* 2007; 67: 92-101
5. Kim K, Mai Y W., Engineered Interfaces in Fiber Reinforced Composites. Kidlington, Oxford U.K, Elsevier Publication, 1998
6. Jang B Z., Advanced Polymer Composites: Principle and Applications. ASM International, Materials Park, OH, 1994
7. Greenhalgh, E.S., Failure analysis and fractography of polymer composites, Cambridge, UK, CRC Publication, Woodhead Publishing, 2009
8. Gao S.L, Mader E, Zhandarov S.F. Carbon fibers and composites with epoxy resins: Topography, fractography and interphases. *J Carbon* 2004;42: 515-529

Please Note: The present results and discussions have already been published partly in Microscopy and Analysis, John Wiley and Sons Ltd. (published July 2014)

4.1.1b Effect of above ambient and below-ambient temperature on FRP composite materials with different loading rates.

Theories and Thoughts

The present investigation intends to study the influence of crosshead velocity and in-situ environmental conditioning i.e. high temperature and cryogenic temperature on micromechanical performance of glass fiber/epoxy, carbon fiber/epoxy and Kevlar fiber/epoxy polymer composites. 3-point short beam shear tests were conducted on the conditioned specimens to evaluate the interfacial properties and failure modes which are related to mechanical properties of the composites. The effect of crosshead velocity (within the range $1-10^3$ mm/min) on the interlaminar shear strength (ILSS) of all the three composite systems at different temperatures was studied. The glass transition temperature (T_g) of conditioned samples were measured by differential scanning calorimetry (DSC) in the temperature range of 25°C to 150°C temperature. At 1 mm/min loading rate, for both glass/epoxy and carbon/epoxy composites maximum increase in ILSS value was about 85.72% with respect to ambient, while for kevlar/epoxy composite 31.77% reduction in ILSS was observed at -100°C temperature.

4.1.1b.1 Introduction

In present century, fibre-polymer composites are the promising and reliable materials in different high performance and structural applications. Their superlative properties such as high specific strength and stiffness, high fatigue endurance, good corrosion and abrasion resistance, make them prime choice material in various industries such as aerospace, marine and automotive[1]. During their manufacturing and service periods the materials are exposed to various environments and loading conditions. The performance of these materials is governed by the response of their constituents i.e. fibre, matrix and the existing interface/interphase, in that particular environment. The sizing of fibres generally influences the chemistry and character of the interface/interphase and might generate structural gradient in the polymer matrix. Their susceptibilities to degradation are dependent on nature of environments and each of the constituent's responses differently and uniquely. Among the three constituents, the interface/interphase has very critical role to play on the performance and reliability of fibre reinforced polymer (FRP) composites [2]. Under low temperature environment or cycling from room temperature to low temperature with applying loads microcracks may generate and propagate in the polymer matrix and/or at the fibre/matrix interface [3]. Various structural damages such as fibre/matrix interfacial debonding and

potholing or delamination result in degradation of mechanical properties of FRP composites [4]. Cryogenic conditioning stimulates the formation of rows of cups due to coalesce of transverse microcracks that originate longitudinal cracks along the fibre. Potholing or localized surface degradation, micro cracking and delamination, are some of the more dramatic phenomena that can occur as a result of cryogenic cycling. At elevated temperature differential thermal expansion of fibre and matrix may leads to the formation of microcracks at the fibre/polymer interface [5].The fibre matrix interface also becomes susceptible to aggressive reactions under the exposure of high temperature environment, which can leads to degradation of both the fibres and the matrix.

Interlaminar shear strength is one of the most important mechanical properties of laminated composite which is also an indicative of fibre/matrix interfacial bond strength if all the other parameters are remains constant. Three point short beam shear test can be used to qualitatively evaluate apparent interlaminar shear strength of the laminated composites [6]. For short beam shear test, it is assumed that the specimen is subjected to pure shear loading but the effects of stress concentration cannot be eliminated completely. In a short-beam test, the low span-to-thickness ratio (typically, $L/h = 4$ or 5) minimizes bending stresses, allowing through-thickness shear stresses to dominate, and promoting interlaminar shear failure at the neutral plane [7].For a valid short beam shear test the specimen should fail under delamination mode through mid-plane, but due to the effects of stress concentration and material constraints, the origin of delamination may shift from the mid-plane to either upper or lower interlaminar planes. Further the variation of loading rate makes the stress distribution more complex and the failure of the composite includes various damage modes separately and/or interactively. Since the fibres are usually much stronger than the matrix, one may postulate fibre/matrix debonding and matrix failure as the two primary mechanisms of failure initiation [8]. Delamination and matrix cracks are intrinsically associated in the composite materials primarily under bending loads. Further, the interaction between these two damage modes constitutes a complex damage mechanism that has not been addressed at a realistic level [9]. One of the most frequent damage mechanisms is the delamination between the adjacent plies of the laminate. Many FRP composite components have tapered thickness, curved shapes, and plies with different orientations, which will also make the delamination grow with a mode mix that depends on the extent of the crack. Thus, delaminations generally grow in mixed-mode [10]. The toughest challenge faced by material scientists is to assess and ascertain its behavioural log in a range of loading rates. The

heterogeneity and responses of multiple distinct phases to varying loading conditions are most often complex and far away from comprehensive conclusion. The less substantial durability data related to the loading rate sensitivity of FRPs in conjunction with environmental exposures has created more confusion in using high factors of safety, and thus led to increased cost and weight of the composites [11, 12]. The endurance on durability and tailorability is most often underrated. Continuous crack growth usually occurs at low temperature and high strain rates, which promotes the brittle failure of the polymeric composite materials.

The rapid advancement of these fibre-polymer composites outstripped the understanding of appropriate failure analysis techniques. Researchers have investigated the interlaminar shear strength response of fibre-polymer composites at different environmental conditionings. Interlaminar shear strength of unidirectional graphite composites were decreased by 30 % under the exposure of elevated temperature [13]. Investigations on CFRP and GFRP sheets, which are exposed to 600 °C reported, that the residual tensile strength and stiffness severely degraded when the composite is exposed to a temperature, higher than the decomposition temperature of polymer resin and further increase in environmental temperature would not lead any further reduction in the aforesaid properties [14,15]. Effect of thermal environment on the residual mechanical performance of graphite-fabric epoxy composite was evaluated for constant 170°C temperature for 120, 240 and 626 h prior to flexural testing [16]. Unidirectional CFRP composite that had been aged at -196 °C for 555 h with half of the failure load undergone about 20% degradation in tensile strength compared to that at room temperature [17]. Some studies on strain rate sensitivity of glass/epoxy, carbon/epoxy, and kevlar/epoxy composite systems have been shown that the mechanical behaviour of these systems is strain rate sensitive [18-23]. Shokrieh et al. studied the in-plane shear failure properties of unidirectional glass/epoxy composites at various stroke rates from 0.0216 to 1270 mm/s [24]. The dynamic shear strength response showed an increase of approximately 37% over the measured quasi-static value. Al-Salehi et al. obtained the lamina in-plane shear properties at various rates of strain on glass/epoxy and Kevlar/epoxy filament wound tubes with winding angles $\pm 55^\circ$ and $\pm 65^\circ$, under internal hoop loading [25]. The results obtained from $\pm 55^\circ$ specimens indicated that with increasing strain rate from 1 to 400s⁻¹, the shear strength is increased by 70% for glass/epoxy, and 115% for Kevlar/epoxy materials. There is significant amount of literature available on the effects of temperature on mechanical properties of FRP composites but according to author's knowledge scarcely information

regarding the effects of temperatures on interfacial behavior (ILSS) in polymeric composites at different loading rates and temperature has been published to date.

The aim of the present study is to provide in-depth analysis of interlaminar shear test and failure mechanisms of glass fibre/epoxy, carbon fibre/epoxy and Kevlar fibre/epoxy composites under different temperatures and crosshead velocity. Different high and low temperature conditioning were performed using Instron with environmental chamber providing additional information regarding in-situ failure of laminate composites. Following the test, the fracture surfaces of the samples were scanned under SEM to understand the dominating failure modes. Microstructural assessments can also reveal the response of each constituent viz. fibre, matrix resin and the interface/interphase; under temperature and mechanical loading. This paper comprehensively presents the mechanical behaviour and structural changes in fibrous polymeric composite systems during the mechanical loading under high and low temperature service environment.

4.1.1b.2 Materials and Experimental Methods

4.1.1b.2.1 Materials

Present investigation includes three types of woven fabric reinforcement in epoxy resin i.e. glass fibres, carbon fibres and, kevlar fibres. The epoxy resin used is diglycidyl ether of Bisphenol A (DGEBA) and the hardener is Triethylene tetra amine (TETA) supplied by Atul Industries Ltd, Gujarat, India under the trade name Lapox, L-12 and K-6 respectively. Some properties of these reinforcements and epoxy resin used in the study are provided in the table-1. The volume fraction of fibres is 60%. The ratio of epoxy and hardener is taken as 10:1. The laminated composites has been prepared by hand lay-up method with 16 layers of woven fabric cloth of reinforcement and then placed in a hot press. Then the curing of the laminate has been carried out at 60°C temperature and 20 kg/cm² pressure for 20 minutes. The laminates were then removed from the press and kept at room temperature for 24 hours. The test specimens have been cut from the laminates using diamond tipped cutter as per standard.

4.1.1b.2.2 Experimental methods

3-point Short-beam shear test

The Short-beam shear tests are frequently applied to polymeric composite materials to evaluate the apparent interlaminar shear strength of the composite system. A testing machine with controllable crosshead speed is used in conjunction with a three-point loading fixture. The shear stress induced in a beam subjected to a bending load, is directly proportional to the

magnitude of the applied load and independent of the span length. Thus the support span of the short beam shear specimen is kept short so that an inter-laminar shear failure occurs before a bending failure. This test method is defined by [ASTM: D2344-13](#), which specifies a span length to specimen thickness ratio of five for low stiffness composites and four for higher stiffness composite. The SBS tests have been conducted as per [ASTM: D2344-13](#) with an Instron-5967 testing machine with span to thickness ratio 5 for glass fibre/epoxy and 4 for carbon fibre/epoxy and Kevlar fibre/epoxy composite systems.



Fig 33: (a) Schematic representation of 3-point short beam shear test. (b) Experimental set up for 3-point short beam shear test (c) Instron machine used for the test.

Fig 33 (a) represents the schematic view of 3-point short beam shear test (b) glass fibre/epoxy specimen failure during shear test and (c) represents the Instron testing machine with furnace and Dewar. 3-point short-beam shear tests were performed on a 30KN capacity Instron testing machine. The specimens were tested at room temperature, high temperature and low temperature. The shear testing at -50°C and -100°C temperature was conducted with specimens by spraying of liquid nitrogen in an environmental chamber where temperature was controlled by temperature controller, liquid nitrogen flow from dewar by controlling the pressure, whereas for high temperature ($+50^{\circ}\text{C}$ and $+100^{\circ}\text{C}$) specimen heated by environmental chamber by heating option. The in-situ tests have been performed on the samples at different temperatures viz; $+50^{\circ}\text{C}$, $+100^{\circ}\text{C}$, -50°C and, -100°C inside the environmental chamber of Instron-5967 with 10 minutes holding time to evaluate the inter-laminar shear strength (ILSS). The tests were performed with six crosshead speeds viz; 1, 100, 200, 500, 700 and 1000 mm/min. For each point of testing 5 to 6 specimens were tested and the average value was taken. The ILSS is calculated from the following expression of equation (1).

$$ILSS = 0.75 * F / bt \quad (1)$$

Where, F=maximum load, b=width of specimen and, t=thickness of specimen

4.1.1b.2.3 Scanning electron microscope (SEM)

The scanning electron microscope (SEM) has been a well-accepted tool for many years in evaluation of fracture surfaces. To study the different failure mechanisms of the tested samples micrographs of the failure samples was carried out using a JEOL-JSM 6480 LV SEM at 20 KV. For better identification of failure modes the fracture surfaces are tilt around 15°-20°. Prior to SEM, the top surface of the specimens were coated with platinum using a sputter coater. The coating is used to make the surface conductive for scanning and prevents the accumulation of static electric charge for clear images during the microscopy.

4.1.1b.2.4 Differential Scanning Calorimetry (DSC)

Differential scanning calorimetry measurements were made using a DSC 821 (Mettler-Toledo Instruments, India) with intra cooler, using STAR software. The temperature calibration and the determination of the time constant of the instrument were performed by standards of In and Zn, and the heat flow calibration by In. The underlying heating rate of 10°C/min-1 was used. The samples were referenced with an empty pan with a 50 mL/min nitrogen stream. The samples were heated to well above their bulk T_g for at least 5 min, cooled to well below the T_g and then heated (usually at 1°C/min) with a modulation rate of 1°C/min. The reported T_g was taken as the maximum of the derivative of the heat capacity curves.

4.1.1b.3 Results and Discussion

4.1.1b.3.1 Glass fibre /epoxy composites

Interlaminar behavior

The variation of ILSS for glass/epoxy composite system in-situ conditioned at +50° C, +100° C, -50° C and -100° C temperatures, and tested at 1, 100, 200, 500, 700, and 1000 mm/min loading rates, is shown in Fig 34. It is clearly evident from the figure that the above-ambient and sub-ambient temperature exposure alters the ILSS values and further at each temperature the ILSS is loading rate sensitive phenomenon, and the results are listed in Table 1. The ILSS values at -100° C temperatures are better as compared to other conditioning temperatures but

as the loading rate increased the ILSS decreased. The maximum ILSS for glass/epoxy composite is about 38.37 MPa, obtained at -100°C temperature and 1 mm/min loading speed, with an increase of 85.72% than the ILSS value (20.66 MPa) obtained at ambient temperature at 1 mm/min as shown in Fig.38. Greater value of shear strength at low loading speed can be attributed to longer relaxation time resulting in improved interfacial integrity of the composite material. Higher crosshead speed during testing minimizes the relaxation process at the crack tip. This could be the reason for reduced ILSS values at higher crosshead speed. At -50°C temperature, initially the ILSS decreases from 1 mm/min to 200 mm/min and then increased with further increase in loading rate. The slight fall in the value at 200 mm/min conditioning could be related to the lower degree of cryogenic compressive stresses at fibre/matrix interface.

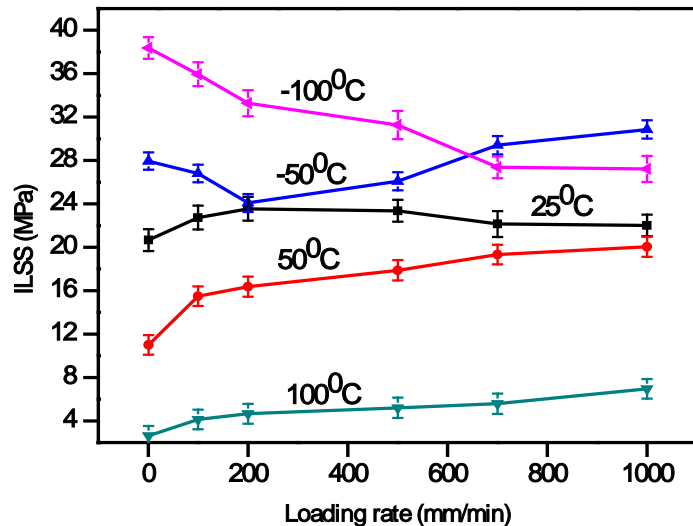


Fig.34: Variation of ILSS with loading rate for glass/epoxy composite system at different temperatures.

At $+50^{\circ}\text{C}$ and $+100^{\circ}\text{C}$ temperatures the ILSS increased with increasing loading rate. The reason may be the induced thermal stresses in the matrix region. Thermal stress induced micro-cracks in the polymer matrix and/or, at the fibre/matrix interface may possibly grow without blunting at a steady state. Some microcracks turn to potential cracks at low loading rates and cause significant reduction in interlaminar shear strength of the composite system

while as the loading rate increases the time available to propagate the microcracks is less. This can be attributed to higher ILSS at higher loading rates at these above-ambient temperatures. The effects of microcracks and fibre breakage can nucleate the other form of damage such as delamination hence degradation in the thermomechanical properties of the composite occurred [26]. This interfacial separation caused by the delamination may lead to premature buckling of the laminates at high temperature. The life-limiting failure process (delamination) induces stiffness loss, local stress concentration and local instability in the laminate. Further the effect of temperature on the ILSS is shown in Fig.35 at 1mm/min crosshead velocity; percentage change in the ILSS values under the exposure of different temperature is also shown in table-1.

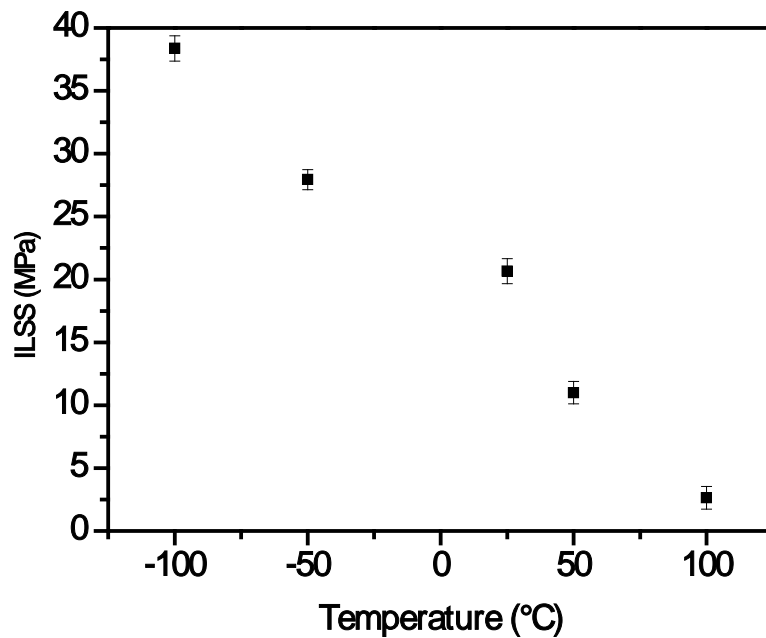


Fig.35: Interlaminar shear strength of glass/epoxy composite at 1 mm/min for different temperature.

Table-1: Percentage change in ILSS with temperatures at 1 mm/min.

Material	Loading speed	Testing temperature(°C)	ILSS (MPa)	Change in (%)
Glass fibre reinforced polymer composites (GFRP)	1mm/min	25	20.66	
		+50	11.0	46.75(↓)
		+100	2.63	87.27 (↓)
		-50	27.94	35.23 (↑)
		-100	38.37	85.72 (↑)

Failure fractography

To better comprehend the interfacial behavior and failure mechanisms of above ambient and sub ambient conditioned glass fibre/epoxy composites, the fracture surfaces after short beam shear tests have been examined by scanning electron microscopy (SEM). SEM micrographs of fracture surfaces are shown in Fig 36. The fracture surface of matrix at -100° C (Fig. 36 A, A') includes extensive riverline markings and fibre imprints. The convergence of pairs of planes from the tributaries of the rivers into one crack, form a trace markings known as river lines. Therefore the direction of crack growth is the direction in which riverlines converge. As multiple crack initiation and growth of riverlines shown in Fig 36 A. In Fig. 36A' fibre imprint refers to fibre matrix debonding. Here we also observed delamination failure modes on the laminate. At -50° C a significant difference in interfacial microstructure is observed which is shown in Fig. 36B, B'. The appearance of the cusps at relatively high magnification; cusps size is similar to that of the fibre spacing. However, the size of cusps is larger than particularly those which develop with in resin rich regions. These failures do not display a complete fibre matrix debonding from the fibre surface [27]. At high temperature, the resin exhibits greater plasticity, and cusps resulting from the microcracks are thicker and undergone greater deformation than at room temperature as shown in fig.36C, C' and Fig.36

D, D'. The increase in cusps thickness implies fewer microcracks formed because of the increased plasticity.

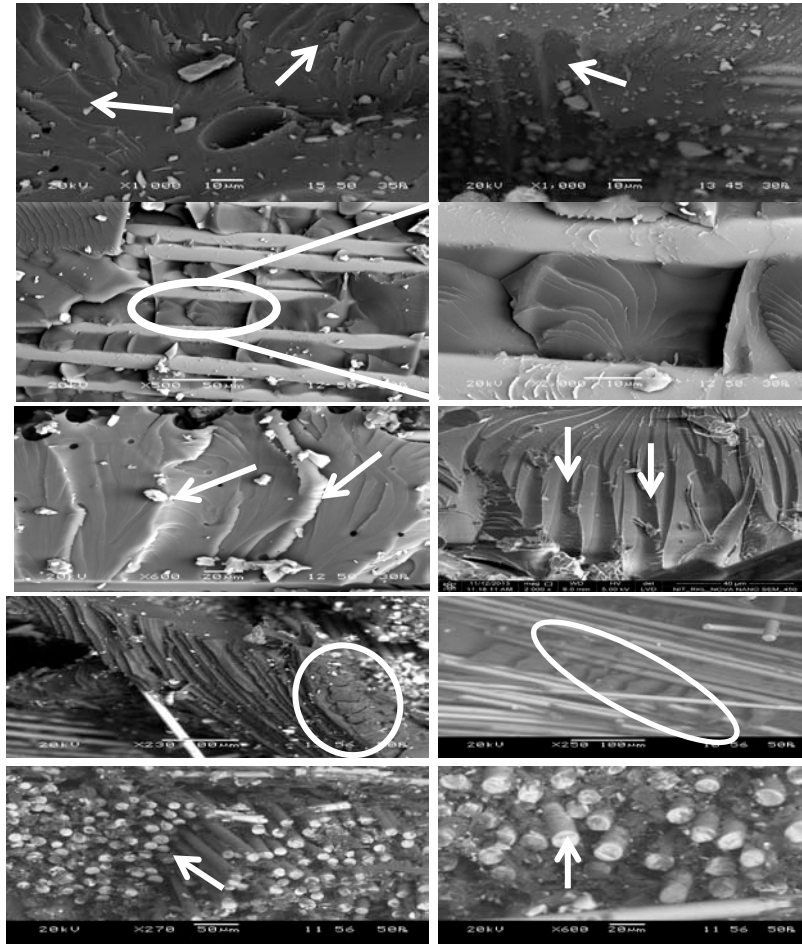


Fig 36: Scanning electron microscopy (SEM) images of the glass fibre/epoxy composites: (A, A') at -100°C temperature (B, B') at -50°C temperature (C,C') at ambient temperature (D,D') at $+50^{\circ}\text{C}$ temperature (E,E') at $+100^{\circ}\text{C}$ temperature

At $+50^{\circ}\text{C}$ temperature the matrix region consist few large cusps whilst the matrix between packed fibres consist a large amount of small cusps (Fig.39 D, D'). At $+100^{\circ}\text{C}$, the SEM micrographs show significant loss of polymer matrix between the fibres which affects the overall integrity of the composite system. These matrix dominated damages result in lower ILSS of glass/epoxy at $+100^{\circ}\text{C}$.

4.1.1b.3.2 Carbon fibre /epoxy composites

Interlaminar behavior

The interlaminar shear behaviour of woven fabric carbon fibre/epoxy composite with loading rate at different temperature is shown in Fig.40

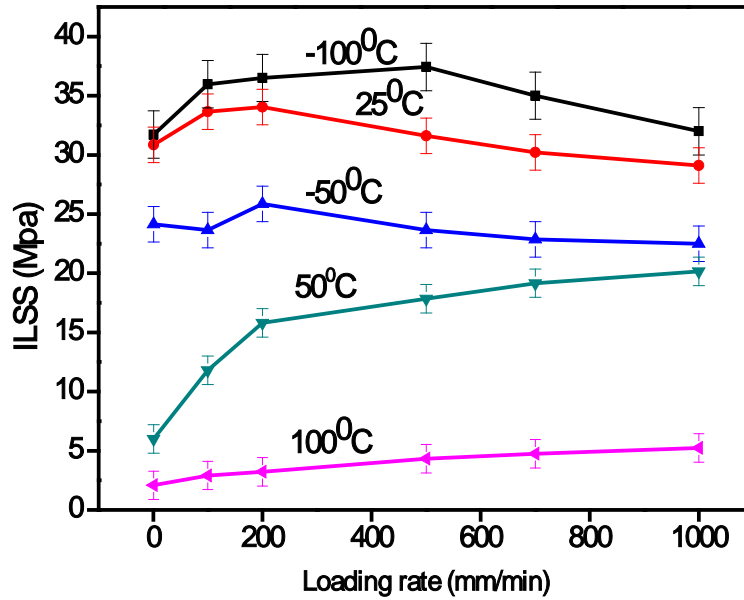


Fig.37: Variation of interlaminar shear strength with different loading rates at different temperatures for carbon fibre/epoxy composite system.

Interlaminar shear strength (ILSS) is one of the most important interfacial properties for composites. To better understand the interfacial strength between the carbon fibre/epoxy composites, three-point short beam shear test method was used to evaluate the interlaminar shear strength of the composites. It is readily observed that at -100°C temperature the carbon fibre/epoxy composites possess better ILSS compared to other testing temperatures. At -100°C temperature the variation of ILSS with loading rate is shown in fig.37. It can be seen from fig.6 that the as the rate of loading increases the ILSS of the composite also increases upto 500 mm/min but, after 500 mm/min shear values decreases because microcrack density has exceeded the critical crack density for delamination. The energy release rate monotonically decreases as the delamination failure grows [28]. Thus ILSS value decreases with increasing loading speed after 500mm/min. As shown in Fig.37 at -50°C temperature lower shear values were observed as compared to that of ambient temperature due to thermal prestress on the matrix resin. Here matrix behaves as brittle in nature which reduces the effective strain to failure and it is the source of matrix cracking [29]. But at 200mm/min the shear value decreases with loading rate. From the relaxation behavior the thermal prestress

would vanish after sufficient period of time. But with increasing loading speed the shear value shows no significant changes due to some microcracks behaves less dangerous since their stress concentrations are small. The laminates failed by very little delamination or no delamination because of low crack densities. However at high temperature $+100^{\circ}\text{C}$ there is a significant change in ILSS values with loading speed. These results are probably due to the shear band propagation in matrix resin at high temperature. Here crack propagation in matrix resin prone to by crack jumping (unstable or stick-slip) mode at slow loading rate. Yield stresses decreases with decreasing strain rates and increasing temperature, stick-slip crack growth may be attributed to plastic deformation at the crack tip prior to crack initiation [30]. Thus stress intensity factor is dependent on temperature and time. The size of the crack jump increases as the temperature approaches to glass transition temperature of the resin matrix. Thus shear value increases with increasing loading speed. But the ILSS value decreases with other testing conditions. At the vicinity of a glass transition temperature (T_g) viscoelastic processes decreases the modulus owing to unfreezing of molecular motion. At decreasing temperature due to thermal contraction a tighter packing and thus higher bond strength exist. As carbon fibre exhibit good interaction to matrix, they constitute good adhesion between fibre/matrix interface regions. When the force rises to a significant fraction of the force required to break a strong bond and threatens to break the backbone of the molecule, a domain unfolds. Thus, it could avoid the breaking of a strong bond in the backbone [31]. Hence ILSS value increases with increasing loading speed. Matrix ductility increases the critical loads for delamination onset and delamination resistance in the composite laminates. At this temperature it is very difficult to find the delamination failure mode. Further the effect of temperature on the ILSS is shown in fig.38. The results shown were obtained at 1 mm/min crosshead velocity. Percentage change in the ILSS values under the exposure of different temperature is also shown in table-3 for carbon/epoxy composite system.

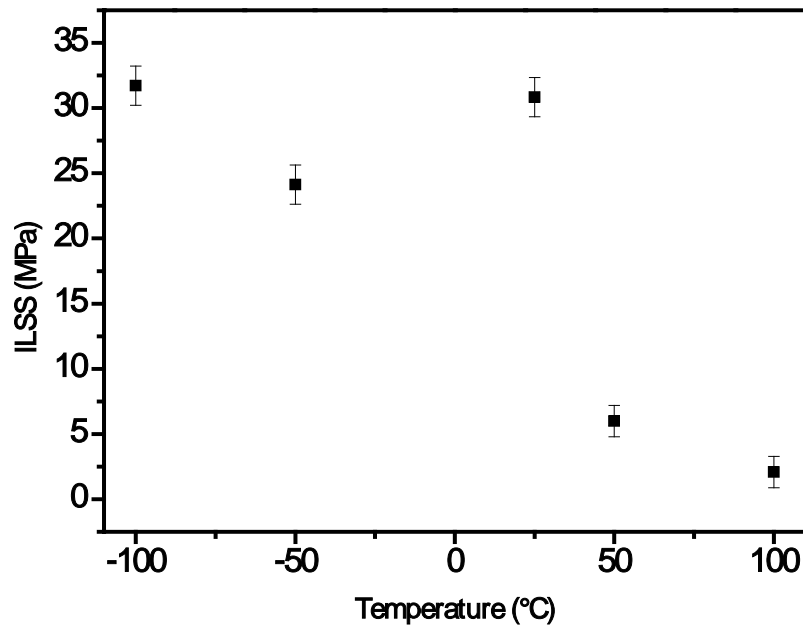


Fig.38: Interlaminar shear strength of Carbon/epoxy composite at 1 mm/min for different temperature.

Table-3: Percentage change in ILSS with temperatures at 1 mm/min loading speed

Material	Loading speed	Testing temperature(°C)	ILSS (MPa)	Change in (%)
Carbon fibre reinforced polymer composites (CFRP)	1mm/min	25	30.84	
		+50	5.99	80.57(↓)
		+100	2.08	93.25 (↓)
		-50	24.13	21.75 (↓)
		-100	31.72	85.72 (↑)

Failure fractography

The fracture surfaces for the carbon fibre/epoxy composites at different temperature have been studied by the SEM and the results are shown in Fig.39.

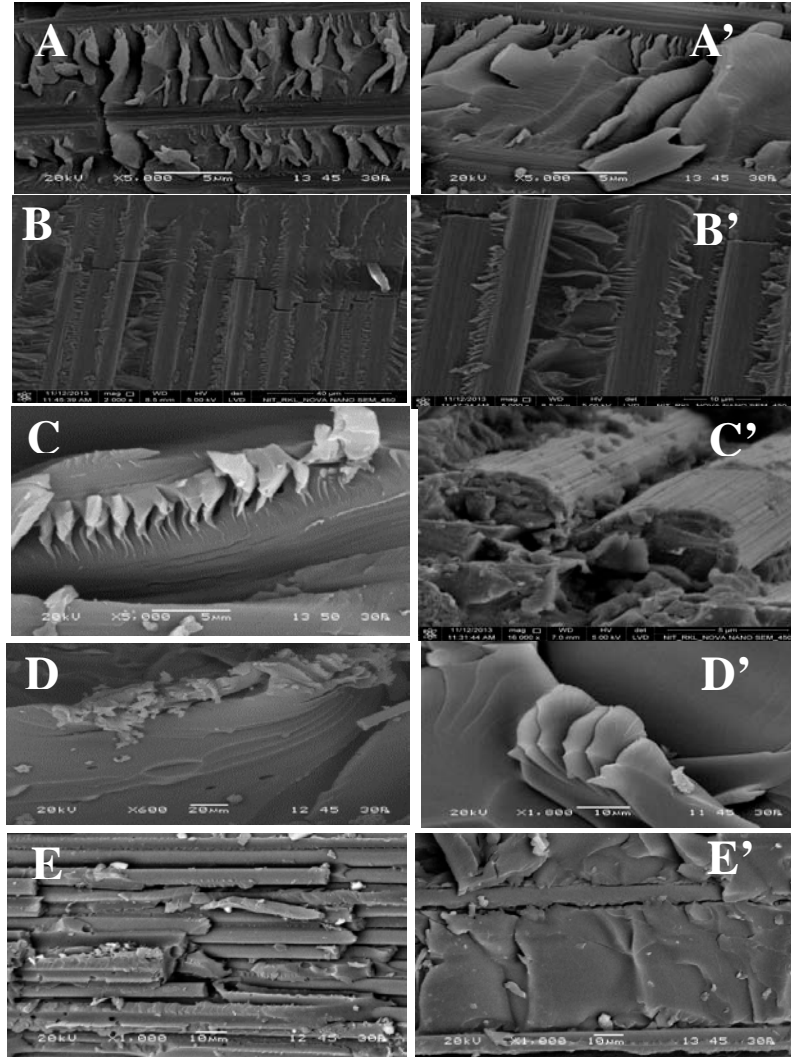


Fig 39: Scanning electron microscopy (SEM) images of the carbon fibre/epoxy composites: (A, A') at -100°C temperature; (B, B') at -50°C temperature; (C,C') at ambient temperature; (D,D') at $+50^{\circ}\text{C}$ temperature; (E,E') at $+100^{\circ}\text{C}$ temperature.

As the shear load increases the cusps steps become deeper following shallow cusps on the surface at -100°C temperature as shown in Fig.39 A, A'. This failure mode begins to dominant these cusps become more erect and closely spaced. At -50°C temperature fibre dominated fracture surface was observed in Fig.39 B, B'. Here the tilt cusps can be used to deduce the crack growth direction. A plastic deformation zone ahead of the crack tip may be formed by this matrix deformation and matrix microcracking. This deteriorates integrity of

the material and can result in low strength at high loading rate. Fig.39 C, C' shows the fracture surface of carbon fibre/epoxy composites at ambient temperature. These micrographs report good fibre/matrix strength and cohesive fracture in the matrix. Microscopically carbon fibre shows crenulations and radial pattern appears on the fibre ends [28]. At high temperatures matrix dominant failure modes were observed as shown in Fig.39. Matrix yielding in Fig.39 D, D' and extensive loss of matrix at +100° C can be observed in Fig.39 E, E'. Presence of these damage modes result in deterioration in the structural integrity of the composite system in high temperature environment.

4.1.1b.3.2 Kevlar fibre/epoxy composites

Interlaminar behavior

The effects of temperature on ILSS of Kevlar fibre/epoxy composites are shown in Fig.43. Here the specimens are subjected to insitu testing at high and low temperatures. It is readily observed that at ambient temperature the specimens possess better ILSS compared with other conditioning temperature.

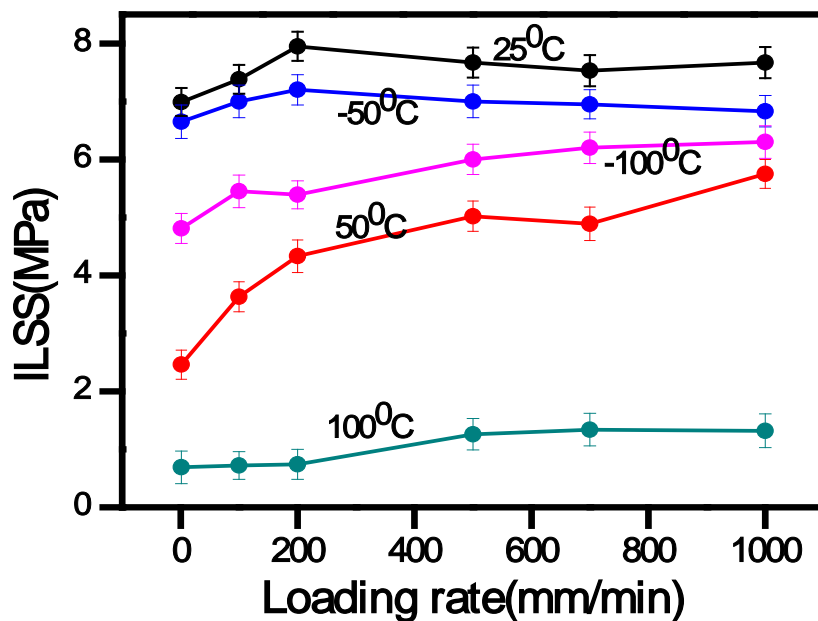


Fig.40: Variation of ILSS with loading rate for Kevlar/epoxy composite system at various temperatures and loading rates.

The variation of ILSS here is the net result of good adhesion at interface by physical and mechanical bonding at the interface. The ILSS value increases with increasing loading rate but reduction of ILSS value occurred may be due to less post curing effect. The thermal

conditioning is likely to change the chemistry at the fibre/matrix interface. The unique chemistry and morphology of Kevlar fibre is also manifested by the composite behaviour [32]. The bond between the fibre and the surrounding matrix can be weakened by exposure to active environments.

At high temperature residual stress effects are negligible, mechanisms such as fibre/matrix debonding and matrix ductility become important. As the temperature increases the substantial segments of polymer chains have enough energy to surmount local barriers which hinders molecular motions and begins to move. Here deformation refers to change in shape without change in volume. A ductile tearing mode of failure may result when large-scale shear yielding occurs at a crack tip. Still at high temperature (close to glass transition temperature) molecular motion is so extreme that even chain entanglements are no longer effective in restricting molecular segmental flow [33]. This change in flow behavior of polymer is due to decrease of the degree of chain interpenetration. In addition to the enhanced flow, confinement effects on the chain conformation can perturb the interfacial properties and ultimately the long term stability of the material [34]. So there is presence of weak interface at high temperature. The weak interface readily allows crack deflection. Here the composites can sustain a large deflection by permitting the absorption of more energy. At low temperature a noticeable improvement of shear value was observed compared to high temperature. The result may be attributed to the development of greater amount of shrinkage compressive stress. The fibre/matrix debonding is dominant for the low temperature conditioned Kevlar/epoxy composites. Further the effect of temperature on the ILSS is shown in Fig.41. The results shown were obtained at 1 mm/min crosshead velocity. Percentage change in the ILSS values under the exposure of different temperature is shown in table-4.

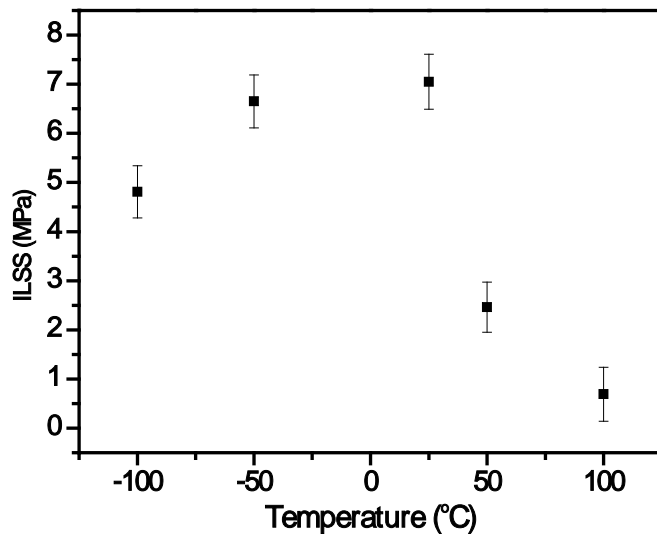


Fig.41: Interlaminar shear strength of Carbon/epoxy composite at 1 mm/min for different temperature.

Table-4: Percentage change in ILSS with temperatures at 1 mm/min.

Material	Loading speed	Testing temperature(°C)	Testing temperature(°K)	ILSS (MPa)	Change in (%)
Kevlar fibre reinforced polymer composites (KFRP)	1mm/min	25	298.0	7.05	
		+50	323.15	2.46	65.10 (↓)
		+100	373.15	0.69	90.21 (↓)
		-50	223.15	6.65	5.67 (↓)
		-100	173.15	4.81	31.77 (↓)

Fractography Study

The scanning photomicrograph Fig 42 A, A' shows the good adhesion between fibre and matrix in the unconditioned laminates. This strong interface may not permit a large deflection during fracture. The nature of this interface bond is not only significant for the strength and stiffness of the composites but it also controls the mechanism of damage and its propagation. In fig 42 B,B', the fibres show longitudinal splits which is known as fibrillation.

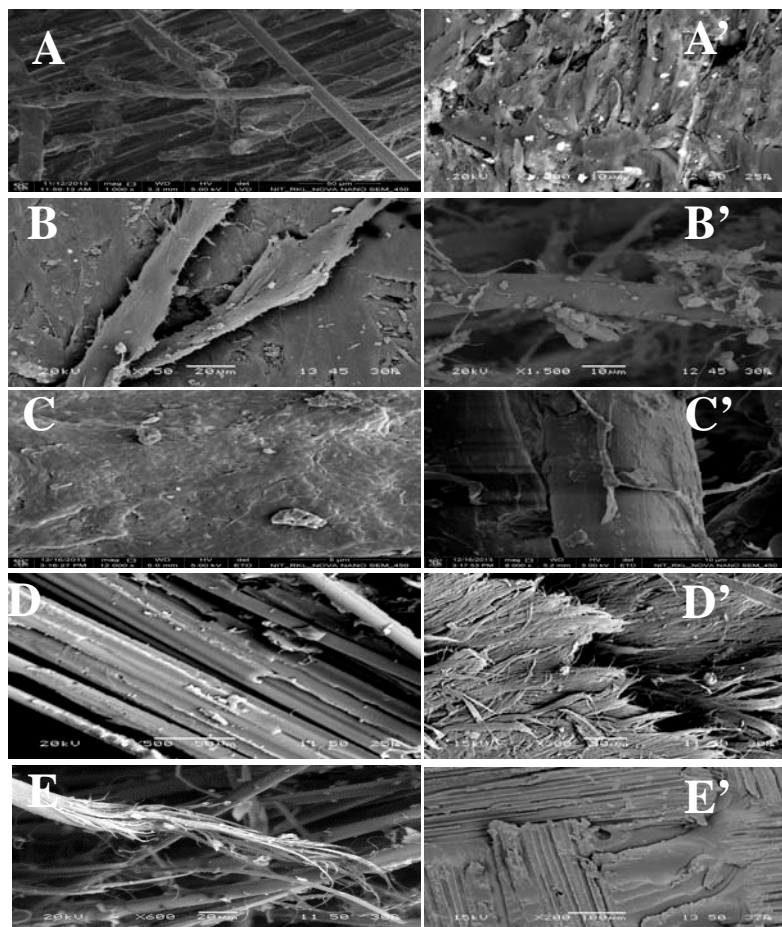


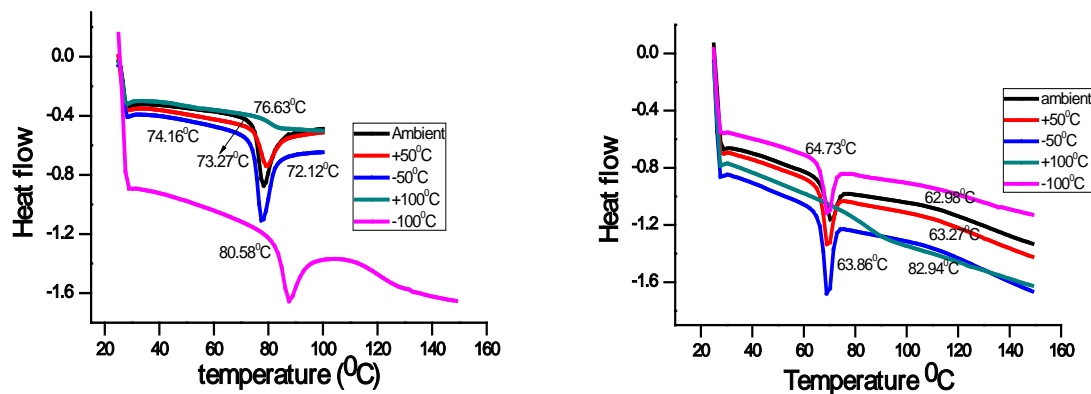
Fig 42: Scanning electron microscopy (SEM) images of the Kevlar fibre/epoxy composites: (A, A') at -100°C temperature (B, B') at -50°C temperature (C,C') at ambient temperature (D,D') at $+50^{\circ}\text{C}$ temperature (E,E') at $+100^{\circ}\text{C}$ temperature

Further, identification of local crack growth directions by examining these fibres is almost impossible. For the specimen tested at ambient temperature, a fibre/matrix debonding microstructure is shown on the Fig.42 C, C'. These composites display a complex matrix debonding from the fibre surface. A considerable amount of surface debris which has been

ground into the fracture surface is shown in Fig.42 D, D'. At +50 temperature the fractography shows fibre matrix debonding along with fibre fibrillation. A resin rich region associated with undulation and interstitial sites exhibit riverlines which provide information about the local crack growth direction and scale of plastic deformation. Kevlar fibre, themselves fail in shear, leading to the formation of kink banding within the fibre. Fig.42 E, E' represents the matrix ductility failure with fibre failure of Kevlar fibre/epoxy composites at high temperature.

Thermal analysis

Glass transition temperature (T_g) of all the samples is evaluated and summarised in Fig 46 . For glass/epoxy composite, the higher glass transition temperature is recorded for the samples exposed to -100°C temperature and the lower T_g value for +50°C temperature conditioned specimen (see Fig.46(a)). For carbon/epoxy composite specimens, exposure to +100°C temperature leads to significant increase in T_g as compared to ambient specimen (25°C temperature), while no significant change in T_g were observed for +50°C, -50°C, and -100°C temperature conditioned specimens (see Fig.46(b)). For Kevlar/epoxy composite, the higher glass transition temperature is observed for the samples exposed to +50°C temperature and the lower T_g value for the specimens tested at ambient temperature (see Fig.46(c)).



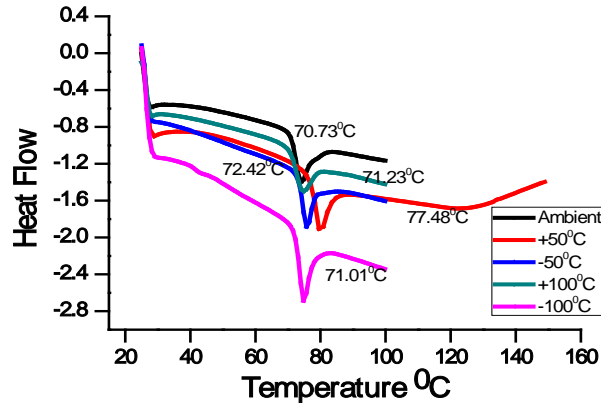


Fig 43: Comparison of glass transition temperatures of glass fibre/epoxy composites at different conditioning temperature. (a) Glass fibre/epoxy composites (b) Carbon fibre/epoxy composites (c) Kevlar fibre/epoxy composites

It is interesting to note that epoxy- based composites made with carbon fibre exhibit high glass transition temperature as compared to other epoxy based composites. The structure of the degraded material during conditioning of the carbon fibre is maintained by extensive inter-chain bonding between the polymer chain through C=O and N=H groups [35]. Within the low temperature conditioning range the glass transition temperature for the carbon fibre composites were found to be lower than that of glass fibre and Kevlar fibre epoxy composites. This might be attributed to unstable wetting of carbon fibre by epoxy resin at low temperature.

4. Conclusions

The influence of sub-ambient and above-ambient temperature and loading rate on the interlaminar shear strength of glass fibre/epoxy, carbon fibre/epoxy and Kevlar fibre/epoxy composite laminates has been studied. Considering interlaminar shear strength and delamination behavior, the tested laminate characterized by SEM to reveal various failure modes. The present study may possibly reveal the following conclusions:

Delamination is the life limiting failure process in a composite material. It induces great loss of stiffness, local stress concentration, and buckling failure of composite material. At -100°C temperature glass fibre/epoxy laminates shows better ILSS value but decreases with increasing loading speed. At +50° C and +100° C temperatures the ILSS increased with increasing loading rate. It is readily observed that at -100°C temperature the carbon fibre/epoxy composites possess better ILSS compared with that of the other testing

temperature. But after 500 mm/min shear values decreases because microcrack density has exceeded the critical crack density for delamination.

Furthermore, for Kevlar fibre/epoxy composites at ambient temperature the specimen possess better ILSS compared with other conditioning temperature. The variation of ILSS here is the net result of good adhesion at interface by physical and mechanical bonding at the interface. Different failure modes such as different types of cusps on the matrix region, riverline marking, fibre/matrix interfacial debonding, plastic deformation of matrix and fibre fracture were observed for the composite specimens failed after the exposure to different above-ambient and sub-ambient temperature.

It is found that the type of fibres and matrix present in the composites influences the amount of heat required and the glass transition temperature. This brings out that the microstructure of the fibre/matrix within the composites found to be influencing the amount of thermal energy absorbed by the materials and consequently affect the mechanical properties.

References

1. B.C. Ray, D. Rathore. Durability and integrity studies of environmentally conditioned interfaces in fibrous polymeric composites: Critical concepts and comments. *Adv. Colloid Interface Sci.* 2014; 209: 68
2. B.C. Ray. Temperature effect during humid ageing on interfaces of glass and carbon fibres reinforced epoxy composites. *J Colloid Interface Sci.* 2006; 298: 111.
3. B.C. Ray, S. Sethi. Mechanical Behavior of Polymer Composites at Cryogenic Temperatures. In: *Polymers at Cryogenic Temperature*, edited by Shusheel Kalia, Shao-Yun Fu, Springer Berlin Heidelberg, Germany 2013
4. B.C. Ray. Effects of crosshead velocity and sub-zero temperature on mechanical behavior of hygrothermally conditioned glass fibre reinforced epoxy composites. *Mater. Sci. Eng. A*, 2004; 379:39.
5. B.C. Ray. Thermal shock on interfacial adhesion of thermally conditioned glass fibre/epoxy composites. *Mater. Lett.* 2004; 58:2175.
6. D.F. Adams, L.A. Carlsson, R.B. Pipes, *Experimental Characterization of Advanced Composite Materials*, (third Ed.) CRC Press, Boca Raton 2003.
7. Y He, A. Makeev. Nonlinear shear behavior and interlaminar shear strength of unidirectional polymer matrix composites: A numerical study. *Int. J Solids Struct.* 2014; 51:1263.
8. L.E. Asp, L.A. Berglund, R. Talreja. Effects of fibre and interphase on matrix initiated transverse failure in polymer composites. *Compos Sci. Technol*, 1996; 56:651.

9. M F S F de Moura, Interaction of matrix cracking and delamination, In: Delamination of composites, edited by S. Sridharan, Woodhead publishing ltd 2008 341-342.
10. N. Blanco, E.K. Gamstedt, L.E. Asp, J. Costa. Mixed-mode delamination growth in carbon-fibre composite laminates under cyclic loading. *Int. J Solids Struct.*2004; 41:4219.
11. B.C. Ray, Effects of changing environment and loading speed on mechanical behavior of FRP composites. *J. Reinf. Plast. Comp.*, 2006; 25:1227.
12. C.E. Lundahl, J.H. Kreiner. Effect of composite properties on interlaminar shear strength. 31st International SAMPE Symposium, 1986: 1499.
13. S. Sethi., B.C Ray., An assessment of mechanical behaviour and fractography study of glass/epoxy composites at different temperatures and loading speeds. *Mater. Des.*,2014;64:160
14. S.K. Foster, L.A. Bisby. High Temperature Residual Properties of Externally Bonded FRP Systems, In: 7th International Symposium on Fibre-Reinforced (FRP) Polymer Reinforcement for Concrete Structures (FRPRCS-7), 2005, New Orleans, USA, 1235–1252.
15. C, Dong, Ian J. Davies, Flexural and tensile strengths of unidirectional hybrid epoxy composites reinforced by S-2 glass and T700Scarbon fibres. *Mater. Des.*, 2014;54: 955
16. S. Birger, A. Moshonov, S. Kenig. The effects of thermal and hygrothermal ageing on the failure mechanisms of graphite-fabric epoxy composites subjected to flexural loading. *Composites*, 1989; 20:341.
17. V.T. Bechel, J.D. Camping, R.Y. Kim. Cryogenic/elevated temperature cycling induced leakage paths in PMCs. *Compos Part B- Eng.*2005; 36:171.
18. M.Z. Shah Khan, G. Simpson, E.P. Gellert. Resistance of glass fibre reinforced polymer composites to increasing compressive strain rates and loading rates. *Compos: Part A-Appl.* 2000; 31:57.
19. A. Gilat, R.K. Goldberg, G.D. Roberts. Experimental study of strain-rate-dependent behavior of carbon/epoxy composites, *Compos Sci Technol* 2002; 62:1469.
20. N.K. Naik, V.R. Kavala. High strain rate behavior of woven fabric composites under compressive loading. *Mater Sci Eng A* 2008; 474:301.
21. M.M. Shokrieh, M.J. Omid. Compressive response of glass-fibre reinforced polymeric composites to increasing compressive strain rates. *Compos Struct* 2009; 89:517.
22. I.M. Daniel, B.T. Werner, J.S. Fenner Strain-rate-dependent failure criteria for composites. *Compos Sci Technol* 2011; 71:357.

23. Sung-Choong Woo, Tae-Won. Kim, High-strain-rate impact in Kevlar-woven composites and fracture analysis using acoustic emission. *Compos Part B-Eng.*2014;60:125
24. F.A.R. Al-Salehi, S.T.C. Al-Hassani, N.M. Bastaki, M.J. Hinton, Derived dynamic ply properties from test data on angle ply laminates. *Appl Compos Mater*, 1997;4:157
25. M.M. Shokrieh, M.J. Omid. Investigation of strain rate effects on in-plane shear properties of glass/epoxy composites. *Compos Struct* 2009; 91:95.
26. A. Kelly, C. Zweben: *Comprehensive Composite Materials*. Oxford U.K, Elsevier Science Publication, 2000.
27. E.S. Greenlagh: *Failure analysis and fractography of polymer composites*, Woodhead publishing, 2009.
28. J.A. Nairn, S. Hu. The initiation and growth of delamination induced by matrix microcracks in laminated composites. *Int. J Fracture*, 1992; 57:1.
29. G. Hartwig, *Polymer properties at room and cryogenic temperatures*. New York, Plenum Press, 1994.
30. S. Bandyopadhyay. Review of the microscopic and macroscopic aspects of fracture of unmodified and modified epoxy resins, *Mat Sci Eng A*, 1990;125:157.
31. B.L. Smith, T.E. Schaffer, M. Viani, J.B.Thompson, N.A. Frederrick, J Kindt, A. Belchers, G.D. Strucky, D.E. Morse, P.K. Hansma. Molecular mechanistic origin of the toughness of natural adhesives, fibres and composites. *Nature*, 1999; 399:761.
32. B.C. Ray. Adhesion of glass/epoxy composites influenced by thermal and cryogenic environments. *J Appl Polym Sci*, 2006; 102:1943.
33. J.J. Aklonis. Mechanical properties of polymer, *J Chem Educ*, 1981; 58:892.
34. K. Shin, S. Obukhov, J.T. Chen, J. Huh, Y. Hwang, S. Mok, P Dobriyal, P. Thiyagarajan, T.P. Russell. Enhanced mobility of confined polymers. *Nature Materials*, 2007; 6:961.
35. Jang B Z., *Advanced Polymer Composites: Principle and Applications*. ASM International, Materials Park, OH, 1994

Please Note: The present section has already been published partly in *Materials and Design*, 2015, 65,617-626.

4.2 Effect of low temperature on mechanical response of materials with different loading rates

Theories and Thoughts

At low temperatures, there is little thermal energy available and molecular motion is inhibited in the polymer matrix. Thus fibre/matrix interface degrades the interfacial bond strength, resulting in loss of microstructural integrity. Consequently, the relaxation and creep rates of polymers are highly sensitive to temperature. The interaction of a fibre with matrix materials depends strongly on the chemical/molecular features and atomic composition of the fibre surface layers as well as its topographical nature. The present study contains the low temperature effects on glass fibre/epoxy polymer composites at different loading rates.

4.2.1 Introduction

The cryogenic applications of polymer composites are recently drawing attention in various fields as new development in aerospace applications where storage and transportation of cryogenic liquids are required, transport vessels and components in spacecraft where low thermal contraction is necessary [1-3]. Glass fiber reinforced polymer (GF RP) woven laminates are usually used for the insulation of superconducting magnet coils operating at cryogenic temperatures [4,5]. Exposure to these cryogenic temperatures may cause delamination, microcracks and strain in matrix which may significantly reduce the stiffness and integrity of the material [6-8]. At cryogenic temperatures, due to difference in coefficient of thermal expansion between the fibre and the matrix phase, microcracks initiate and propagate through the laminates composites [9, 10]. Therefore, knowledge of the resistance to different failure modes of woven fabric composites laminates at cryogenic temperatures is essential to the materials scientist and designer analyst. To achieve the often-promise capabilities of polymer composites, the properties of the interfacial region between fibre and matrix must be controlled. The variation in interlaminar shear strength with loading rates is an important issue in the design of classes of polymer composite materials used in different structures subjected to suddenly applied loads at low temperatures. Interlaminar loading rate sensitivity is an importance concern, as it related to the loss of integrity of the material at low temperatures. The effect of varying loading rate on mechanical properties of fibre- reinforced polymer composites has been investigated and reported a variety of contradictory observations and conclusions [11-15]. Mechanical properties of polymers are strongly sensitiveto temperature and strain rate [16,17]. At low temperature the matrix material behaves as brittle in manner and do not allow relaxation of residual stresses or stress

concentration to take place [18, 19]. The generic behaviour of polymers must arise from the chainlike structure of the polymer molecules, but detailed insights into the underlying processes have been hard to come by [20]. Delamination failure mode is known to be the major life-limiting failure process in a composite laminate [21]. The fiber/matrix interface has always been considered as a crucial aspect of polymer composites as well as polymer nanocomposites [22]. The response of fiber/matrix interface within the composite plays an important role in determining the gross mechanical performance, because it transmits the load from the matrix to the fibres, which contribute the greater portion of the composite strength. Better the interfacial bond, better will be the ILSS, de-lamination resistance, fatigue and corrosion resistance.

The aim of this investigation was to study deformation and mechanical behaviour of glass fibre/epoxy composites subjected to 3-point short beam shear test at low and ultra-low temperature with different loading speeds. The laminates were tested at ambient (+27°C) temperature and at (-20°C, -40°C, -60°C) temperatures using liquid nitrogen gas in an environmental chamber installed on an Instron testing machine. Testing was carried out in different loading covering low to high medium speeds. Following the test the fracture surfaces were scanned under SEM microscope. A need probably exists for an assessment of mechanical performance of such potentially promising materials under the influence of changing environment and loading speed. Using fractography study to characterize the onset and growth of failure modes has become a generally accepted method.

4.2.2 Experimental Work

4.2.2.1 Materials

The material system selected for this work was E-glass fibre/epoxy polymer composites fabricated by hand lay-up method followed by compression moulding process. Diglycidyl ether of Bisphenol A (DGEBA) as epoxy and Triethylene tetra amine (TETA) as hardener supplied by Atul Industries Ltd, Gujarat, India under the trade name Lapox, L-12 and K-6 respectively. The volume fraction of fibres is 60%. The ratio of epoxy and hardener is taken as 10:1. The laminated composites have been prepared by hand lay-up method with 16 layers of woven fabric cloth of reinforcement and then placed in a compression moulding process. Then the curing of the laminate has been carried out at 60°C temperature and 15 kg/cm² pressure for 20 minutes. The laminates were then removed from the press and kept at room temperature for 24 hours. The test specimens have been cut from the laminates using diamond tipped cutter as per ASTM D2344-13 standard.

4.2.2.2 Low temperature conditioning and characterization techniques

3-point short-beam shear tests were performed on a 30KN capacity Instron testing machine. The shear testing at –low and ultra-low temperature was conducted with specimens by spraying of liquid nitrogen in an environmental chamber attached with Instron 5967 where temperature was controlled by temperature controller, liquid nitrogen flow from dewar by controlling the pressure. The in-situ tests have been performed on the samples at different temperatures viz; 25° C, -20° C, -40° C and, -60° C temperature inside the environmental chamber of Instron-5967 with 10 minutes holding time to evaluate the inter-laminar shear strength (ILSS). The tests were performed with six crosshead speeds viz; (1, 10, 100,300, 600, and 1000) mm/min. For each point of testing 5 to 6 specimens were tested and the average value was taken. The broken parts were observed under Scanning Electron Microscope (SEM) for the fractographic analysis.

For analysis of composite fractography, SEM by JEOL-JSM 6480 LV with the acceleration voltage of 15 kV was used. Cleaned, small in size and conductive samples are used during testing in SEM. the top surface of the specimens were coated with platinum using a sputter coater. The coating is used to make the surface conductive for scanning and prevents the accumulation of static electric charge for clear images during the microscopy. During the test samples are little tilt around 15-20° to drawn attractive and clear images of different failure modes.

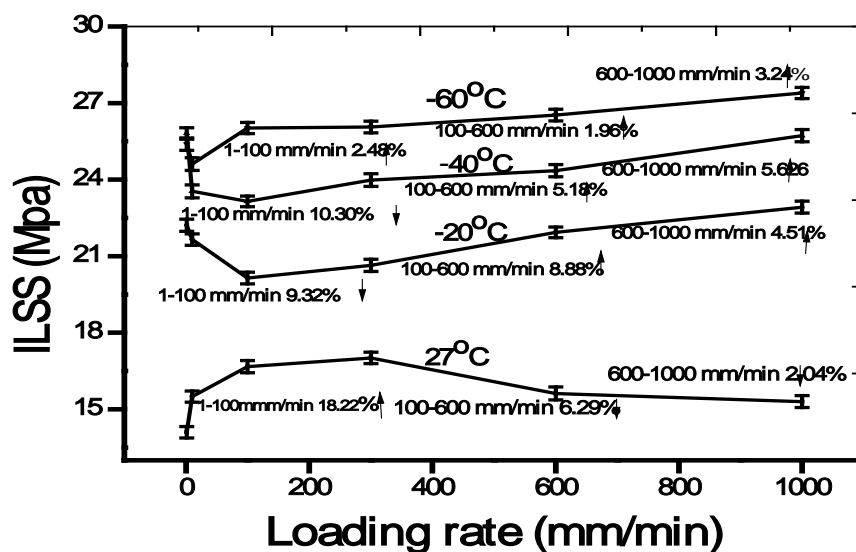
4.2.3 Results and discussion

4.2.3.1 Mechanical Study

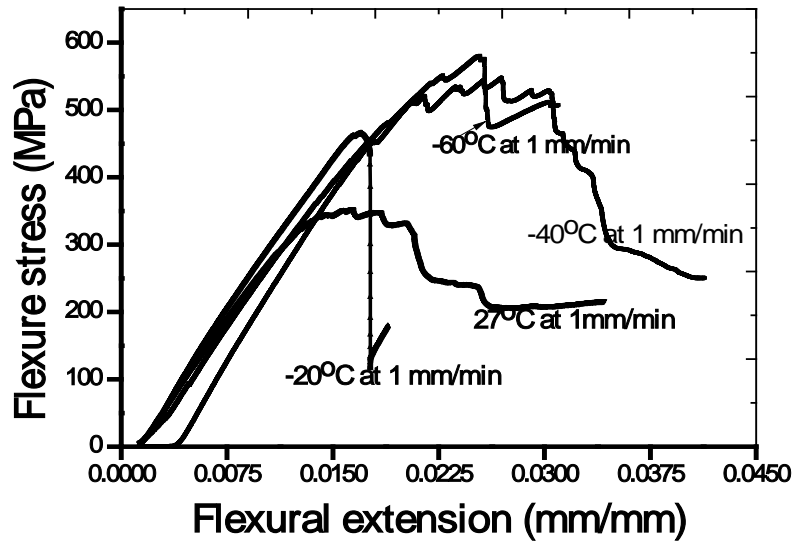
Interlaminar shear strength with temperatures

Variation of ILSS with different loading speeds at different temperatures of glass fibre/epoxy composites are shown in Fig 44(a). In the current study, glass fibre/epoxy composites subjected to low and ultra-low (27°C, -20°C,-40°C,-60°C) temperatures at different loading speeds. It can be illustrated that, at low temperature the glass fibre/epoxy composites shows loading rate sensitivity. At -60°C temperature maximum ILSS value was obtained and it increases with increasing loading speed with a transition 10mm/min. At low loading speed (1 to 100)mm/min it increases 2.48% (max), at medium loading speed (100-600)mm/min it increases 1.96% (max) whereas, at high loading speed (600-1000)mm/min it increases 3.24% (max). At -40°C temperatures low ILSS values obtained as compared to -60°C temperature but it increases with increasing loading speed with the transition at 100 mm/min. At low

loading speed (1-100) mm/min it decreases 10.30% (max), at medium loading speed (100-600) mm/min it increases 5.18%(max) and at high loading speed (600-1000) mm/min it increases 5.6% (max). Similarly at -20°C temperature glass fibre/epoxy composites also shows loading rate sensitivity. At low loading speed (1-100)mm/min it decreases 9.32% (max), at medium loading speed it increases 8.88% (max) whereas at high loading speed (600-1000) mm/min it increases 4.51% (max). In comparison to ambient temperature the ILSS value decreases 6.29% (max) with increases loading speed. This might be attributed to, at increased cross-head speeds or decreased temperatures crack propagation becomes unstable in the epoxy matrix resin [23,24]. Temperature and deformation rate control the process occurring at a crack tip. For unstable crack propagation, epoxy polymers matrix show crack arrest (slip-stick) behaviour which arises from adiabatic heating and plastic deformation at the crack tip, hence the ILSS value increases with increasing loading speed.



(a)



(b)

Fig 44: (a) Interlaminar shear strength with different loading rates of glass fibre/epoxy composites at 25°C, -20°C, -40°C and -60°C temperature (b) Flexural stress vs Flexural strain at 1mm/min loading speed.

Fig 44(b) represents the stress-strain curve of the glass fibre/epoxy composites at low and ultra-low temperature at 1mm/min loading speed. Here at -20°C temperature the composite fails in brittle manner whereas other conditioning temperature shows ductile failure mode. At ultra-low temperatures the fibre/matrix interface is very resistant, limited debonding will occur and local stress concentrations near the fibre ends will be quite high. Thus matrix cracks will thus be able to transverse to the fibre direction from this single flow. As a result, a tendency of brittle failure was observed.

4.2.3.2 Fractography study

Figs 45-48 shows SEM micrographs of broken mechanical tested samples of 25°C, -20°C, -40°C and -60°C temperatures at different loading rates. Different failure modes were observed during the insitu 3-point short beam shear test. Flexural stress-strain curve was plotted to analyse the failure behavior of material at different loading speeds. At ambient temperature different failure modes are observed with different loading speeds as shown in Fig. 45. Ply splitting region (A), fibre imprint (B) and fibre pull out (C) are plays dominant roles in 1000mm/min, 100mm/min and 1mm/min respectively. At high loading speed ply splitting develops because of excessive out-of-plane or interlaminar stresses generated at the

fibre/matrix interface. Here matrix failure occurred in some extent ductile manner. In contrast to this, at low and medium loading speed, matrix has sufficient time to transfer the stress to fibre and interface region and laminate fails in little brittle manner.

At ultra-low(-20°C) temperature the failure modes are delamination (A), debonding (B) and brittle fibre fracture (C) at 1mm/min, 100mm/min and 1000mm/min respectively shown in Fig. 46. Here the stress strain curve shows brittle to ductile transition with increasing loading speeds. Brittle failure or catastrophic crack growth in matrix starts when a critical stress field at the crack tip is exceeded. This is due to small specific heat at low temperatures, small deposition of inelastic deformation energy leads to an appreciable temperature rise. Under certain conditions adiabatic heating is high enough to reach a secondary dispersion region of a polymer where enhanced plastification occurs [25]. The fracture energy is increased by these processes.

Fig 47 represents SEM micrographs of glass fibre/epoxy composites subjected to -40°C temperature. Different failure modes are observed such as cusps (A), matrix tearing (B) and fibre/matrix interface failure (C) at 1mm/min, 100mm/min and 1000mm/min respectively. Here stress-strain curve shows ductile failure mode with increasing loading speeds. Cusps are usually generated from microcracks which are plays dominant role at low temperature. The occurrence of an adiabatic transition depends on the crack velocity and on the thermal diffusivity. In an adiabatic state, however, the heat transfer from the thermally active zone (i.e. plastification zone at a crack tip) to the passive zone (elastic bulk material) is negligible.

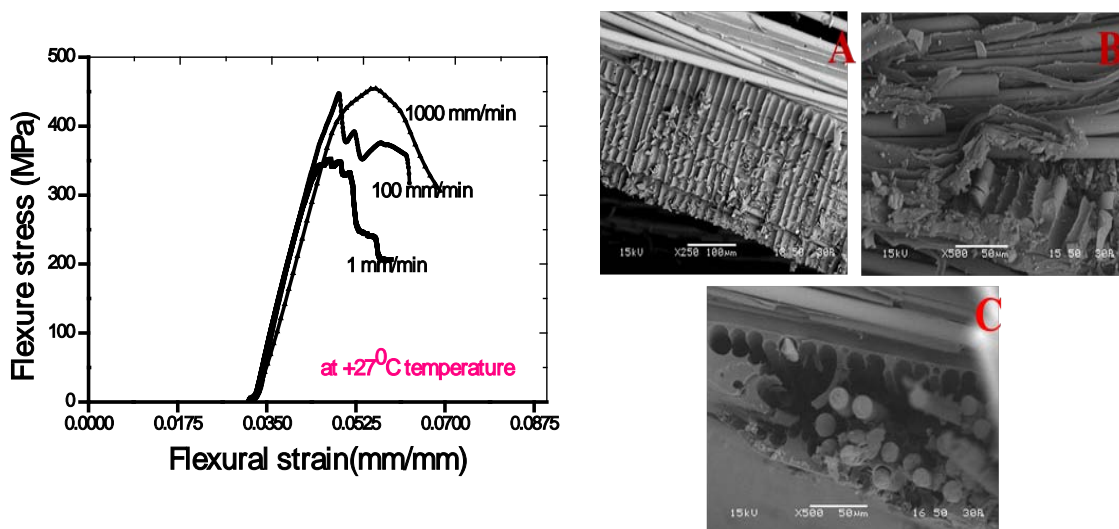


Fig 45: Fractography analysis of glass fibre/epoxy composites at ambient (27°C) temperature

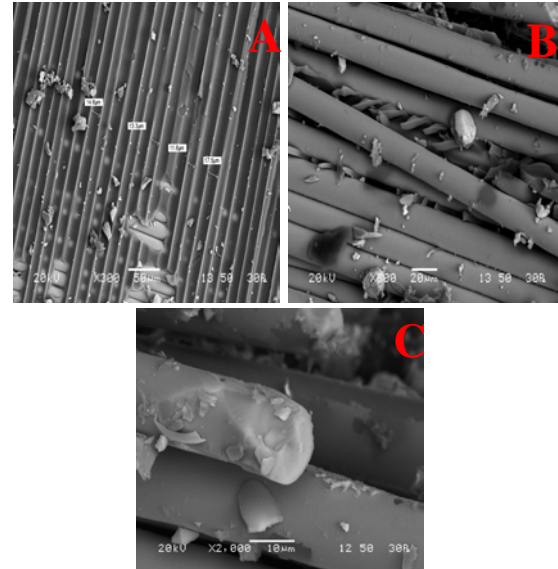
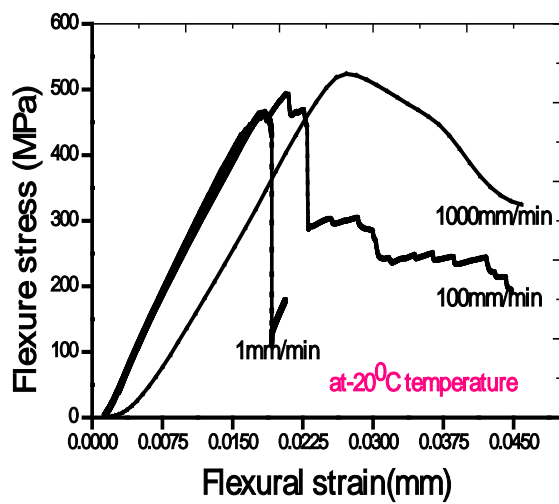


Fig 46: Fractography analysis of glass fibre/epoxy composites at ambient (-20°C) temperature

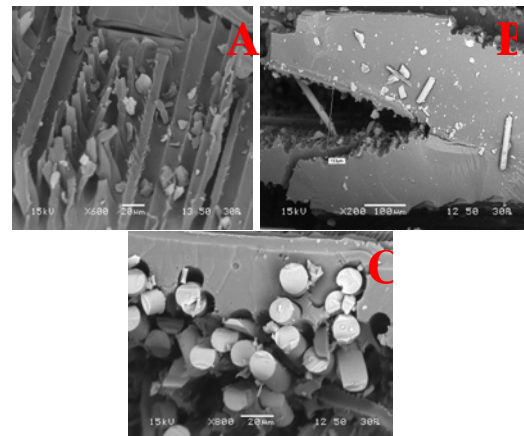
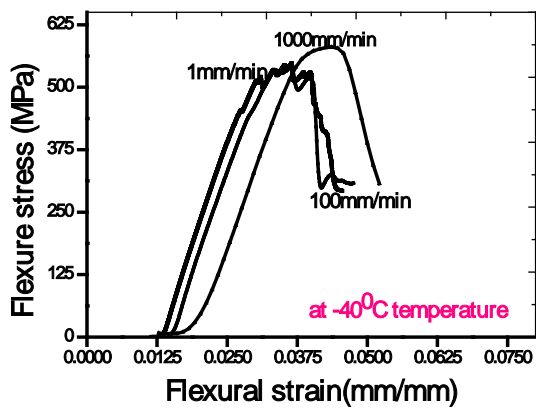


Fig 47: Fractography analysis of glass fibre/epoxy composites at -40°C temperature

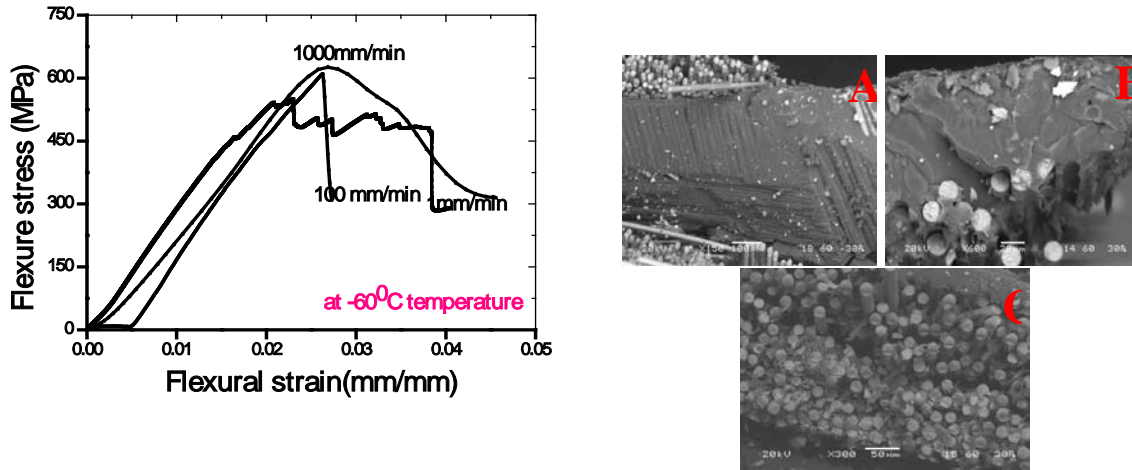


Fig 48: Fractography analysis of glass fibre/epoxy composites at -60° temperature

A further factor which influences the fracture processes is the fibre/matrix interfacial strength. Fig 48 shows different failure modes where fibre/matrix adhesion or interfacial strength plays dominant role. Scanning electron microscope shows toughened matrix (A), strong interfacial bonding (B) and fibre fracture (C) at 1000mm/min, 100mm/min and 1mm/min respectively. Stress-strain curve represents the mixed failure modes with different loading rates which solely depend upon the failure modes observed. This parameter dictates whether fibre/matrix debonding or fibre fracture controls the failure processes and material toughness.

Crack often initiates from delamination region or microcracks at the matrix ends and propagate in the matrix until they are arrested by some other failure modes present in the resin matrix. Failure can then propagate through a number of mechanisms, such as in-plane delamination, fibre fracture, riverline marking and toughened matrix. Which mechanisms plays dominate role is still under matter of discussion.

4.2.4 Conclusions

Based on the results from 3-point bend test, mechanical behavior of glass fibre/epoxy composites subjected to low and ultra-low temperature, is critically dependent upon the loading rate during the test. Maximum ILSS value was obtained at -60°C temperature; it was probably because of the unstable crack propagation occurred in the matrix with increasing loading speed. For unstable crack propagation, epoxy polymers matrix show crack arrest (slip-stick) behaviour which arises from adiabatic heating and plastic deformation at the crack tip, hence the ILSS value increases with increasing loading speed. Various failure modes were obtained at different temperatures which are responsible for the alternation of the mechanical

properties. Stress-strain curve and various failure modes observed during testing at different loading rates solely depend upon the temperatures. This parameter dictates whether fibre/matrix debonding or fibre fracture controls the failure processes and material toughness.

References

28. Gudes R.M.(2007).,Durability of polymer matrix composites:Viscoelastic effect on static and fatigue loading, Composite Science and Technology, Vol-**67**, 2574
29. Naik,N.K., Venkateswara.R.K., Ravikumar,G., Vearraju,Ch.(2010).,Stress-strain behavior of composites under high strain rate compression along thickness direction: Effect of loading condition,, Materials and Design.,Vol-**31**, 396
30. Ray, B.C.(2006),Temperature effect during humid ageing on interfaces of glass and carbon Fibers reinforced epoxy compositesJ of Colloid and Interface Science. ,Vol-**298**, 111
31. Ray B.C. (2004), Effects of crosshead velocity and sub-zero temperature on mechanical behaviour of hygrothermally conditioned glass fibre reinforced epoxy composites. Material Science and Engineering, Vol- **379**:39.
32. S. Sethi, Ray B.C(2014), An assessment of mechanical behaviour and fractography studyof glass/epoxy composites at different temperatures and loading speeds, Materials and Design, Vol-**64**:160
33. S. Sethi, Rathore D, Ray B.C(2014), Effects of temperature and loading speed on interface-dominatedstrength in fibre/polymer composites: An evaluation for in-situenvironment, Materials and Design, Vol-**65**: 617
34. Tanoglu M.,Mcknight,S.H.,Palmese,G.R.,Gillespie,J.W.Jr,(2000),A new technique to characterize the fiber/matrix interphase properties under high strain rates, Composites Part A, Vol-**31**,1127
35. C, Dong, Ian J. Davies (2014), Flexural and tensile strengths of unidirectional hybrid epoxy composites reinforced by S-2 glass and T700Scarbon fibres. Materials Design., Vol-**54**: 955
36. Soutis, C., Turkmen, D.(1997), Moisture and temperature effects on the compressive failure of CFRP unidirectional laminates, J. Composite. Material, Vol-**31**, 832
37. Rapnowski, P., Gentz, M., Kumosa, M.,(2006). Mechanical response of a unidirectional graphite fiber/polyimide composite as a function of temperature, Composite. Science and. Technology., Vol-**66**, 1045
38. Ray, B.C. (2004),Loading Rate effects on Mechanical Properties of Polymer Composites at Ultralow TemperaturesJ of Applied. Polymer. Science,Vol-**100**, 2062
39. Fabio Nardone, Marco Di Ludovico, Francisco J. De Caso y Basalo, Andrea Prota , Antonio Nanni, Tensile behavior of epoxy based FRP composites under extreme service conditions, Composites: Part B 43 (2012) 1468–1474.
40. Piyush K. Dutta, David Hui, Low temperature and freeze thaw durability of thick composoites, Composites:Part B 27B (1996) 371-379.

41. M.Z. Shah Khan, G. Simpson, E.P. Gellert, Resistance of glass-fibre reinforced polymer composites to increasing compressive strain rates and loading rates, *Composites: Part A* 31 (2000) 57–67.
42. Okenwa I. Okoli, The effects of strain rate and failure modes on the failure energy of fiber reinforced composites, *composite structures* 54 (2001) 299-303.

4.3 An assessment of high and low temperature on prepreg glass fibre/epoxy composite materials

Theories and Thoughts

As with any engineering materials, polymer composites can be exposed to diverse range of environmental conditionings. Weather and radiation factors that contribute to degradation in plastics include temperature variations, moisture ingress, sunlight exposure, oxidation, microbiologic attack, and other environmental elements. At high temperatures, there is sufficient thermal energy available to the molecules of polymer to allow easy rotation, movement, and disentanglements. Aim of this present investigation related to study the effects of high and low temperature on prepreg glass fibre/epoxy composites.

4.3.1 Introduction

Over the past years, prepreg glass/epoxy composites have been successfully used as precursors in the manufacture of high-performance composites such as airplane components, fishing rods, motor vehicles, sporting goods and water skis [1-3]. The epithet prepreg refers to a preimpregnated lamina (viscoelastic material) comprised of aligned fibers embedded in an uncured or partially cured resin. The development and experimental characterization of these marvelous materials, held together primarily through Vander Walls interactions and entanglements, have been the focus of significant research over the past decades. Despite the challenges and expenses inherent in polymer composite processing, applications remains a major topic of interest due to their potential for high strength to weight ratio, specific strength and structural integrity. These properties are translatable to the macroscale through the incorporation of glass fibre reinforcement into epoxy matrix resin and composites. However, these materials while subjected to certain environmental conditions that may prove damaging to installed wraps. These include moisture, UV radiation, thermal effects, alkalinity, humidity and underwater [4, 5]. At high and low temperature exposure plays a dominant role during its

short term and long term service life. The interface between the fibre reinforcement and matrix resins can increase resistance to fracture, join materials of different character, make them deform more easily and provide motility. While they represent only a tiny fraction of the overall volume, interfaces are essential for the integrity and durability of the overall composite material [6].

During their service period it comes across many type of loading rates as static to dynamic with wide range of loading rates (striking rates). Few literatures have addressed the mechanical behavior and fractography at different temperatures [7, 8, 9]. Regarding chemistry of this composite material Huang et al [10] present the degree of impregnation of prepreg through NIR spectra, describing the flow of resin matrix through fiber tows. Grunenfelder et al [11] addressed the effect of voids on both autoclave and VOB pre-cured laminates they observed that the high pressures during autoclave processing were sufficient to restrain the void formation. Boey et al [12] studied use of high pressure of up to 7000 KPa by means of isostatic press without vacuum application the reduction of void levels as 3%. Considering all the research works we followed autoclave curing cycle for the fabrication of composites materials which was discussed in experimental part. On the other hand we know severe environmental exposure affects physical and mechanical properties of polymeric composite materials resulting in an undesirable degradation. As the material is heterogeneous and anisotropic in nature, damage and degradation of material often be strongly influenced by local processes. The anisotropy contributes to more complexity in the assessment of the damage mechanisms and in their impact on the composite responses. An aggressive progress is needed, specifically in the aerospace industry to tailor thermal expansion together with the low material density. Optimization of structural component through improving the prepreg composite material the resin and the fiber is a challenge for the material scientist as well as the process engineer. Therefore, scaling concepts need to be applied in the development of new products to aid the formulation and processing of these heterogeneous, anisotropic and viscoelastic material. Okoli [13] studied the 3-point bend test of glass/epoxy laminates with increasing strain rates to find a relationship between energy to failure and strain rate. They reported a change in failure modes observed as strain rate increased. Shah Khan [14] studied the resistance of glass fiber reinforced polymer composites with increasing loading rates (2 to 1000 KN/sec) and compressive strain rates (10⁻³/sec to 10²/sec). They found that in-plane elastic modulus and strength increases with strain rate and then decreased at higher strain rates. In the present study 3-point bend tests were conducted on glass/epoxy laminates at

increasing loading rates to ascertain the relationship between ILSS and loading rate. Very limited work has been devoted related to ILSS with loading rate, which is the fundamental knowledge to understand the reliability and structural applications of GFRP composites. To meet this challenge, researchers and designers must give way to new paradigms, guided by microstructural characterization of complex phenomena that are discovered and then reported in a timely way.

4.3.2 Experimental procedure and processing

4.3.2.1 Experimental details

Glass/epoxy (GFRP) prepreg composites which contain the reinforcement as E-glass fiber and matrix as epoxy were prepared. After synthesis of GFRP prepreg composites it was planned to cure with autoclave following the cure cycle shown in Figure 1. GFRP prepreg consists of 60 wt% E-glass fiber and 40 wt% matrix epoxy with a 0/90° weave. The prepreg material used in the testing was the epoxy prepreg made by HEXCEL, supplied by Hindustan Aeronautics Limited (HAL) having specification Hexply 913-37%-7781-1270, containing a proprietary curative and glass cloth filter with a 0/90° weave. This prepreg is unique as it can be stored at room temperature for 24 days.

4.3.2.2 Processing of the laminates

Glass/epoxy composite laminates were cured by autoclave method following 5 steps of the cure cycle which shown in Fig 49. Here first dwell time at 75°C for 45 minutes. Whereas second time at 135°C for 65 minutes. Here pressure is 2.5 bar and vacuum is 0.8 bar. After curing, the laminate was cut into the required size for 3-point bend (Short- Beam Shear) test by diamond cutter. Then stability test was done for the composite laminates. Here the laminates were weighed. One batch of sample was treated with +50 °C temperature for thermal conditioning whereas another batch for -50°C for cryogenic treatment tests. For comparison one batch for ambient +28 °C temperature testes sample. The samples were kept inside the furnace at +50°C temperature and allowed to stay at that temperature for 10 min as soaking period. Similarly for cryogenic temperature the samples were kept at -50° C temperatures and allowed to stay at that temperature for 10 min as soaking period with help of blowing liquid nitrogen gas.

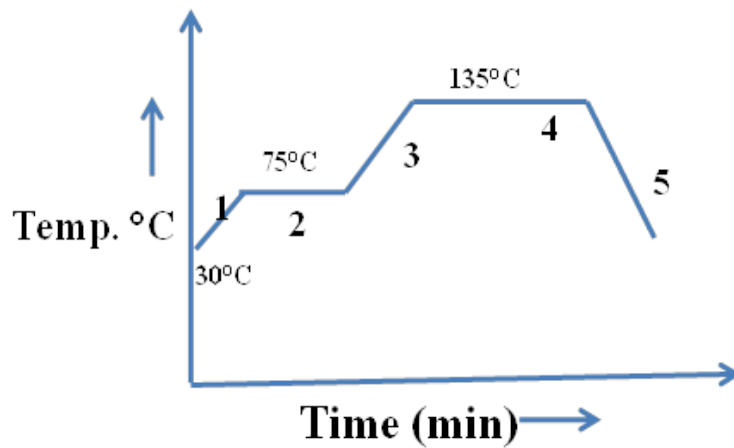


Fig 49: Curing cycle for glass/epoxy composite followed within autoclave

The GFRP prepreg laminates were then cured by autoclave. The material manufacturer's recommended cure cycle was employed for autoclave processing which is shown below.

1. Heat from room temperature to 30°C at 1-2°C/MIN
2. 1st Dwell at 75°C±5°C for 45 MIN
3. Heating rate 1-2°C/MIN
4. 2nd Dwell at 135°C±5°C for 65 MIN
5. Cooling rate 2-5°C/MIN

The cured panels fabricated from cure cycle outlined above were subjected to conditioning.

4.3.2.3 Characterization equipment and procedures

Flexure strength: Instron 5967 with environmental chamber (insitu testing)

Instron 5967 is a servo-control and signal conditioning electronics instrument for material testing applications. It has fine position adjustment thumbwheel with 0.004mm resolution for precise positioning of crosshead while testing. Specimen protect also applied to the specimen outside a set threshold-protecting to overcome unwanted damage. Bluehill 3 software helps to get the data from the attached computer.

The test coupons of different sizes were cut from the laminates for physical and mechanical characterization. ILSS testing were conducted on an Instron 5967 test apparatus using three-point bend jig according to [ASTM: D2344-13](#) shown in Fig 50



Fig 50: Instron 5967 with environmental chamber used during the in-situ testing of sample.

The dimension of the ILSS specimen was $60 \times 40 \times 4 \text{ mm}^3$. Thirty six specimens were tested from two conditions panels with six loading speed (3 specimens each) for each test. The results were then compared with the data obtained from unconditioned specimens. The flexural methods are applicable to polymeric composite materials. A testing machine with controllable crosshead speed with environmental chamber is used in conjunction with a loading fixture. The shear stress induced in a beam subjected to a bending load is directly proportional to the magnitude of the applied load and independent of the span length. Thus the support span of the short beam shear specimen is kept short so that an inter-laminar shear failure occurs before a bending failure.

This test method is defined, which specifies a span length to specimen thickness ratio of 5 for low stiffness composites and 4 for higher stiffness composite. The loading arrangement is shown in a span length of 40 mm. The tests were performed with 6 increasing crosshead speed ranging from 0.1, 1, 100, 300, 800 and 1000 mm/min at different temperatures. For each point of test 3 specimens were tested and the average value was taken. ILSS was calculated by equation (1)

$$ILSS = 0.75 * P/bt \quad (1)$$

Where, P = maximum load, b = width of specimen, t = thickness of specimen

Scanning electron microscope (SEM)

The scanning electron microscope (SEM) has been a well accepted tool for many years in the examination of fracture surfaces. The prominent imaging advantages are the great depth of field and high spatial resolution and the image is relatively easy to interpret visually. To study the different failure mechanisms of the tested samples micrographs of the failure samples was carried out using a JEOL-JSM 6480 LV SEM. The samples were loaded onto the sample holder and placed inside the SEM, adjusting the working distance and hence the spot size the chamber was closed and vacuum was applied.

4.3.3 Results and discussions

4.3.3.1 Mechanical properties (3-point bend test)

Fig 51(a) represents the short beam shear test curves based on different loading rates. The ILSS vs. crosshead speed curves gives different ILSS values at different speed of loading. It was found that ILSS values depend on working temperature of the material. Here we considered 3 modes of loading phase while correlating with interlaminar shear strength, Mode A (1 to 500) mm/min, Mode B (500 to 1000) mm/min and Mode C (0.01 to 1000) mm/min.

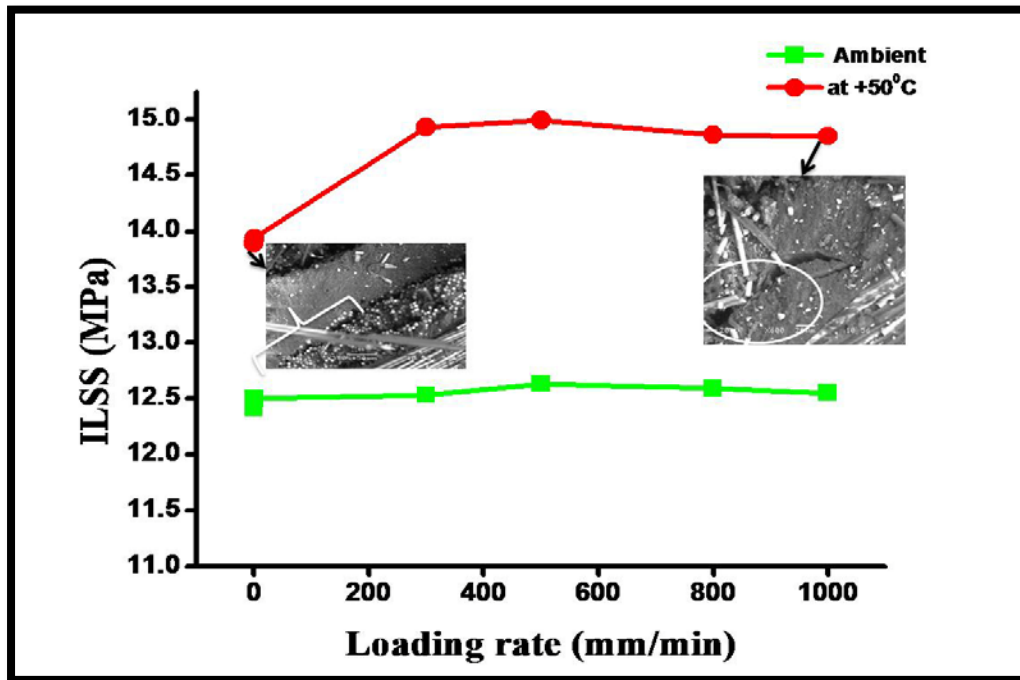


Fig 51(a) Loading rate with ILSS of GFRP samples at different temperature.

When the specimen at ambient subjected to 3-point bend test the ILSS values increases with increasing with loading rate in each loading phase. In contrast to this, when the specimen treated with +50°C temperature, the strength had decreases in each modes of loading speed but the ILSS value is more than ambient temperature. In Mode A, it decreases by 16.14% (Max.), Mode B 9.75% (Max) and Mode C 6.05%(Max) was observed. This may be due to spreading of process zone (PZ) in large depth (softer resin) in epoxy resin matrix resin which leads to increase in degree of fiber bridging. In this condition, fiber/matrix debonding is critical and also exhibit increased deformation which shown in Fig 51 at low and high loading rates. When sample is loaded there is widespread microscopic damage arises throughout the laminate. Large damage can be sustained to a critical value at which failure occurs by the propagation of cracks. These cracks are much more complex in nature than cracks in homogeneous materials. The failure of a composite involves the fractures of the load-bearing fibers and the matrix as well as a complex combination of cracks propagated along the interfaces [15]. Thus ILSS values decreases in every mode of loading.

While at -50°C temperature, the ILSS values increases by 51.09% (max.) in Mode A, in Mode B it decreases by 18.12% (max) again in Mode C it decreases by 3.72% (max). There is a noticeable decrease of ILSS values in higher cross head speed. In contrast to above, at ambient temperature ILSS value is increased by 27.07% (Max.) in Mode A, in Mode B it decreases by 16.42% again in Mode C it is increased by 8.37%.

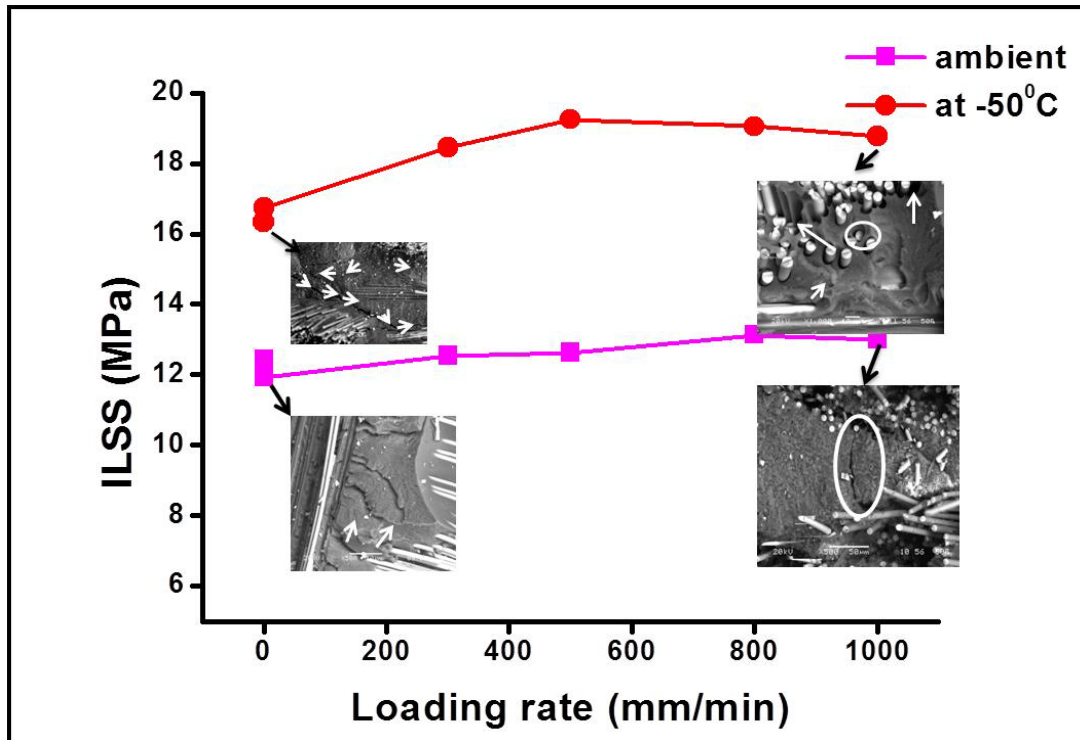


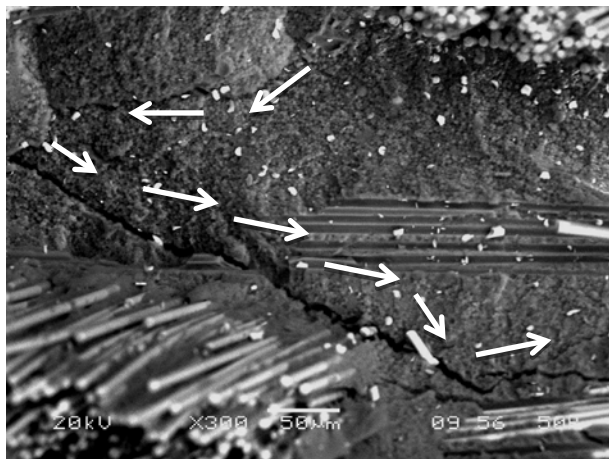
Fig 51(b) Loading speed with ILSS curves of glass/epoxy composite at different temperature

The reason behind the reduced values of ILSS at low temperature after Mode A loading duration (medium cross head speed), loading time is less than the mechanical relaxation time i.e. time is not sufficient for plastic deformation to take place at the crack tip thus matrix becomes brittle and fracture strain decreases. Thus fiber/matrix bond strength is well tailored and it is unusual for bare fibers to be exposed. From fractographic prospective of sample reveals that failures manifest from matrix microcracking to fiber fracture and fibers pull-out which shown in Fig 51(b). However, increased high cross head speed (Mode B) the fracture stress and strain increases and matrix become more tough and ductile. Here fracture starts to preferentially occur at fiber/matrix interface region. Heat capacity at matrix is less, thus an appreciable temperature rise occurred in front of the crack tip even small value of inelastic energy at low temperature. It is anticipated as by existing of adiabatic heating i.e. unstable crack propagation [16]. In this state, rate of heat generation is lower than for its removal (thermally active zone to passive zone). Thus ILSS value decreases at higher cross head speed which shown in Fig 51(b). This may also be hypothesized of preexisting microcracks, notches, debris i.e. with a stable element (low-energy crack growth). This fracture may be arrested and then reinitiated, or may lead to initiation and growth of secondary mode of failure.

4.3.3.2 SEM fractographic analysis

The failed specimen surfaces were viewed under SEM to study how changing failure modes affect the ILSS value as loading rate increased. Identification of the cause of fracture through fractography has become a standard investigation technique. The large depth of focus and the fact that the actual surface can be examined make the SEM, an important tool for research and for failure analysis. Microscopic material failure is defined in terms of crack propagation and initiation. Such methodologies are useful for gaining insight in the cracking of specimens and sample structures under well-defined global load distributions [17]. Microscopic failure considers the initiation and propagation of a crack. Fig (52, 53, 54, and 55) shows impact fracture surfaces of the prepreg composites from which progressive changes in the locus of failure can be clearly identified as a result of change in test temperature for a given loading condition.

-50 degree 1mm/min



800mm/min

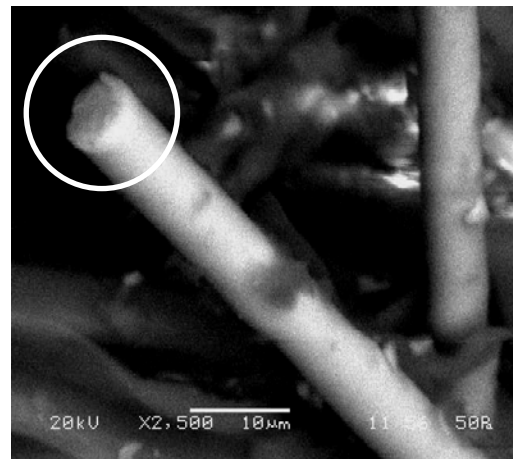


Fig 52: Matrix micro cracking and brittle fracture of fiber at -50 degree at 1mm/min and 800mm/min

-50 degree 1000 mm/min

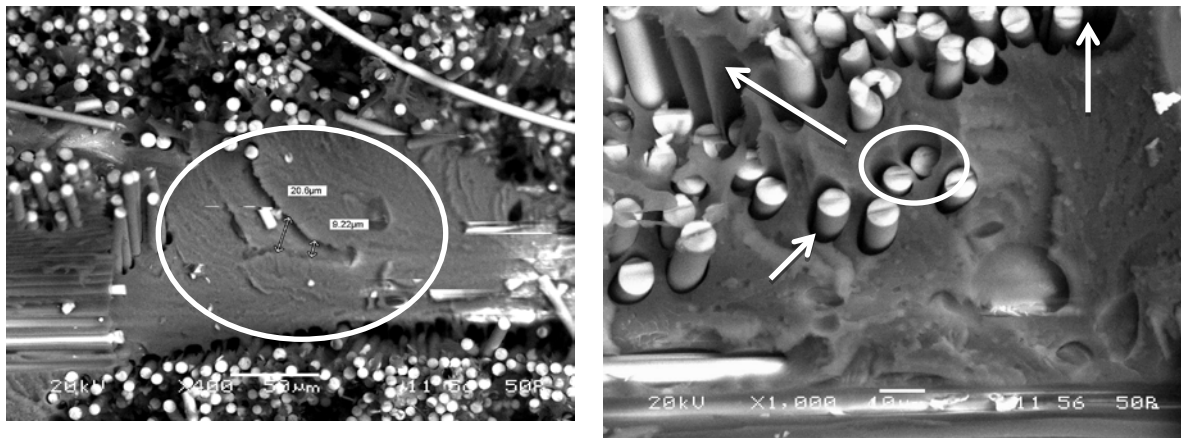


Fig 53: Cleavage marking and fiber/matrix debonding at -50 degree 1000mm/min

Fig(53) shows uniform propagation of matrix microcracking at -50°C temperature. The locus of failure is not exactly at the interface region but is significantly above it. However, there is some fiber imprint are visible on the surface. This is because of development of internal residual tensile stresses in the matrix resin at low temperature. As matrix behaves as brittle manner at low temperature the molecular motion will be abysmal; molecular motion will be small and re-orientation modes will be relatively simple [18]. Similarly the deportment of interface region of glass/epoxy at low temperature doesn't undergo any significant change which tends to high adhesion bond strength. Thus very tiny interfacial failure observed at low loading speed (Mode A). Here cohesive failure of the bulk matrix plays the dominant role. At higher crosshead speed 800mm/min brittle failure of fiber observed. Brittle fibers have low fracture strain and low energy absorbing capability [19].Fibers can fracture early at the weak cross section point, which is not necessarily the direction of crack propagation.

At low temperature (-50°C temperature) when specimen subjected to 1000mm/min cleavage marking on the matrix surface and fiber pull-out observed. As the applied loading rate increases 1000mm/min the fracture proceeds, the broken fibers will likely pullout from the matrix which observed in SEM micrograph. When the matrix behaves as brittle, the energy of fracture is fairly low and there is little step marking formed during failure, which is refereed to cleavage marking [20]. The characteristic feature of cleavage fracture is flat facets which generally are about the increasing size of 9.22µm to 20.6µm. Cleavage fracture represents brittle fracture occurring in the matrix region, which shown in Fig 54. These are indications of

the absorption of energy by local deformation. The direction of the river pattern represents the direction of crack propagation. Quasi-cleavage fracture is related but distinct to cleavage fracture. It is observed chiefly low temperature. The term quasi cleavage is used because the facets on the fracture surface are not true cleavage planes. Quasi-cleavage fractures often exhibit dimples and tear ridges around the periphery of the facets [21].

Ambient 1mm/min

Ambient 800mm/min

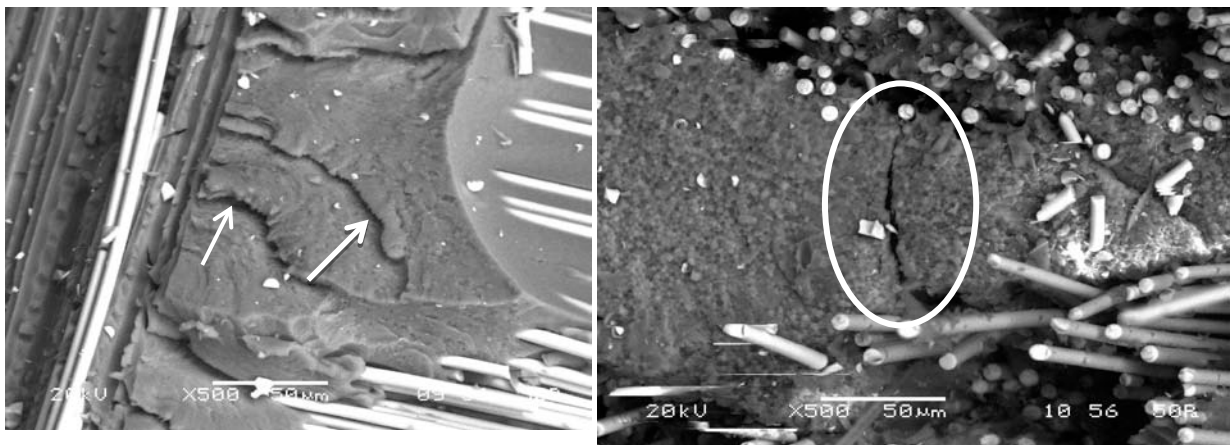


Fig 54: Scanning electron micrograph at ambient 1mm/min and 800mm/min shows steps and welts as well as matrix cracking respectively.

+50 1mm/min

800mm/min

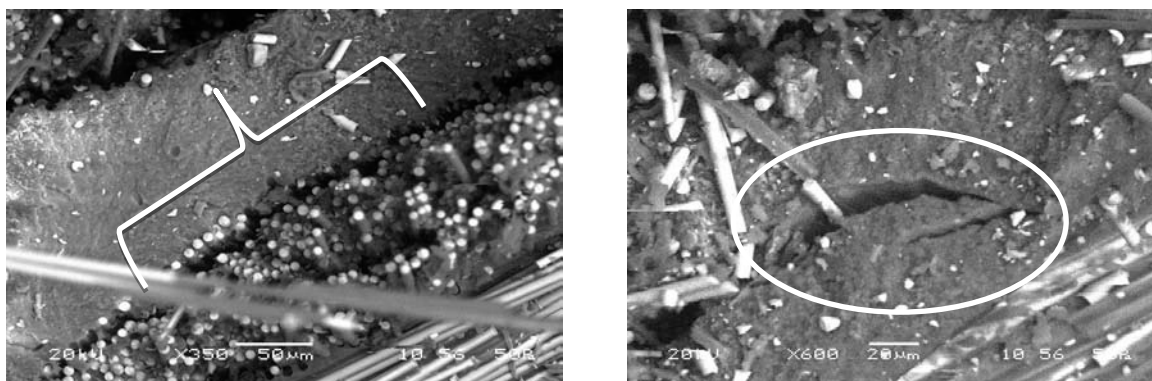


Fig 55: Thermal conditioning sample at 1mm/min and 800mm/min showing fiber/matrix debonding and macromatrix cracking.

In contrast to the foregoing phenomena, fracture surface of ambient samples subjected to 1mm/min, 800mm/min and 1000mm/min was shown in Fig (54) display fiber pull-out, steps and welts, tiny nodules on the matrix surface, matrix cracking, and progressive interfacial debonding. In addition, there are significant changes in the morphology of the matrix fracture. Besides that, other important matrix fracture is scraps and ribbons. When multiple microcracks are formed and begin to propagate in several planes, and they subsequently converge onto one plane. Ambient temperature signifies the beginning of the steps and welts as well as macromatrix cracking. Both the things are parallel to the fracture propagation direction. This failure mode was observed at low loading speed. The steps are identified by toughened matrix or smooth region, while welts are identified by ribbons. If the crack planes overlap before they coalesce to form scarp [22]. When the loading rate increases 800 mm/min density of crack plane increases and macomatrix cracking plays the dominant role.

Above discussions associated with matrix failure modes at high as well as low temperature, which are responsible for integrity and durability of polymer matrix composites.

Fig (55) shows fiber/matrix debonding as well as cohesive failure of matrix at low and high loading rate respectively at +50° C temperatures. Damage initiation for cohesive failure observed at the matrix resin where severity of stress state occurred.

4.3.4 Conclusions

In this investigation, an experimental study was carried out on the failure of GFRP composites in thermal and cryogenic environment. Parameters such as temperature and loading rate were considered to assess and evaluate mechanical behavior. The present study may possibly reveal the following conclusions:

The percentage of ILSS value decreases during above-ambient temperature testing in every mode of loading rate ranges because of thermal conditioning effect which leads to spreading of process zone in the matrix resin which impart high fiber/matrix debonding.

In contrast to, at sub-ambient temperature the percentage of ILSS value increases in Mode A, phase and decreases in Mode B and C due to unstable crack propagation (adiabatic heating) at the crack tip. This yield matrix microcracking to fiber fracture and then fiber pull-out.

In comparison when a virginal sample is tested the percentage of ILSS value increases in each mode of loading speed which may be due to preexisting stable element (low-energy crack) which divulge steps and welts along with matrix cracking in the matrix region.

The load carrying capacity and the strain at yield increases with increasing the loading rate in each environmental conditioning treatment.

References

1. Saponara V.L. Environmental and chemical degradation of carbon/epoxy and structural adhesive for aerospace applications: Fickian and anomalous diffusion, Arrhenius kinetics; *Compos. Struct.* 2001; 93: 2180-2195
2. Collings T.A., Mead D.L. Effect of high temperature spikes on a carbon fibre-reinforced epoxy laminate, *Composites*; 1988;19: 61-66
3. Takeda T., Takano S., Shindo Y., Narita F. Deformation and progressive failure behavior of woven-fabric-reinforced glass/epoxy composite laminates under tensile loading at cryogenic temperatures, *Compos. Sci. Technol.*; 2005;65: 1691-1702
4. Haddad H., Kobaisi M.A, Influence of moisture content on the thermal and mechanical properties and curing behavior of polymeric matrix and polymer concrete composite, *Mater. Des.*;2013;49:850–856
5. Moyeenuddin Ahmad S., Abdullah A. M., Holdsworth P.G., Long term durability of pultruded polymer composite rebar in concrete environment, *Mater. Des.*;2014; 57:616–624
6. Sjogren B.A., Berglund L.A., The effects of matrix and interface on damage in GRP cross-ply laminates, *Compos. Sci. Technol*, 2000; 60: 9-21
7. Kim R.Y, Steve L. D. Experimental and analytical studies on the damage initiation in composite laminates at cryogenic temperatures. *Compos. Struct.* 2006;76:62-66
8. Choi S, Sankar B V; Fracture toughness of transverse cracks in graphite/epoxy laminates at cryogenic conditions; *Compos part B- ENG* 2007;38;193-200
9. Fiedler B, Hojo M., Ochiai S., Schulte K., Ando M., Failure behavior of an epoxy matrix under different kinds of static loading, *Compos. Sci Tech* 2001;61; 1615-1624
10. Jiang B, Huang YD; Investigation of the impregnation degree of the prepreg by near infrared spectroscopy; *Composites Part B*; 2011;41:946-948
11. Grunenfelder L K, Nutt S R; Void formation in composite prepreps – Effect of dissolved moisture *Compos. Sci. Technol.* 2010;70:2304-230
12. Boey F Y C, Lye S.W; Void reduction in autoclave processing of thermoset composites Part 1: High pressure on void reduction. *Composites*; 1992;23:261-265

13. Okoli, O.I, Smith, G.F. The Effect of Strain Rate and Fiber Content on the Poisson's ratio of Glass/epoxy Composites, *Compos. Struct.* 2000; 48:157-161.
14. M.Z. Shah Khan, G. Simpson, E.P. Gellert, Resistance of glass-fibre reinforced polymer composites to increasing compressive strain rates and loading rates, *Composite Part A* ; 2000;31:57–67
15. Shim S B, Seferis J.C, Eom S Y, Shim Y.T; Thermal characterization and comparison of structural prepregs with different cure temperature. *Thermochim. Acta* 1997; 291:73-79
16. Ray B. C.; Temperature effect during humid ageing on interfaces of glass and carbon Fibers reinforced epoxy composites. *J. Colloid Interf.Sci.* 2006; 298:111-117
17. Sethi S. Panda P., Nayak R., Ray B.C., Experimental studies on mechanical behavior and microstructural assessment of glass/epoxy composites at low temperature, *J. Reinf. Plast. Compos.* 2011;31:77-84
18. Gilat, A., Goldberg, R.K., Roberts, G.D; Experimental Study of Strain-rate-dependent Behavior of Carbon/epoxy Composite. *Compos. Sci. Technol.* 2002; 62: 1469-1476.
19. Saatkamp T., Hartwig G.; Fracture energy of polymer at low temperatures. *Cryogenics* 1991; 31: 234-237.
20. Hartwig G., Polymer properties at room and cryogenic temperatures. New York, Plenum Press.1994
21. Kim K, Mai Y W, Engineered Interfaces in Fiber Reinforced Composites. Kidlington Oxford U.K, Elsevier Publication. 1998
22. Greenhalgh E S. Failure analysis and fractography of polymer composites Cambridge,UK CRC Publication, Woodhead Publishing, 2009

Please Note: The present results and discussions have already been published partly in *Materials and Design*, 2014, 64,160-165

4.4 Thermal cycle on interlaminar shear strength of FRP composites.

Theories and Thoughts

Polymer composite materials are ultra-light anisotropic and heterogeneous infrastructural materials, a popularly introduced in the last few years in wide range of applications. However, their exceptional durability and integrity of mechanical performances, they are vulnerable to aggressive natural environmental conditioning factors such as harsh temperature variations, moisture, UV radiation and some cyclic exposure. It is widely accepted that special caution needs to be observed when using these materials to manufacture mechanically critical airframe components inside a full-scale structure. Carbonfibre reinforced plastics (CFRP) are currently the most used composites in the aeronautical industry (for example in the Boeing 787 and the currently in development Airbus 350 XWB).

4.4.1 Introduction

Widespread application spectrum of FRP's covers almost every type of advanced engineering structures. Their usage includes various components in aircraft, helicopters, spacecraft, boats, ships, offshore platforms and also in automobiles, chemical processing equipment, sports goods, and civil infrastructure such as buildings and bridges [1]. The behaviour and performance of advanced structural FRP composites cannot be explained only in terms of specific properties of its constituent fibre and matrix but the existing interface/interphase between fibre and matrix has great significance as well [2, 3]. The presence of moisture at the interface can modify the interfacial adhesion thereby affecting the mechanical performance of the FRP composites. During thermal cycling differential coefficient of thermal expansions and residual stresses is a main cause in FRP composite material. The behavior of the interfacial contact between fibre and matrix is strongly influenced by the presence and nature of residual stresses[4]. A very large thermal expansion mismatch may result in debonding at the fiber/matrix interface and/or a possible matrix cracking due to thermal stress [5-7]. The fiber/matrix interface is likely to affect the overall mechanical behavior of fiber-reinforced composites. The present investigation related to study the thermal cycle effects on glass fibre and carbon fibre/epoxy composites laminates.

4.4.2 Materials and Methods

4.4.2.1 Materials

The material system selected for this work was E-glass fibre/epoxy and carbon fibre/epoxy polymer composites fabricated by hand lay-up method followed by compression moulding process. Diglycidyl ether of Bisphenol A (DGEBA) as epoxy and Triethylene tetra amine (TETA) as hardener supplied by Atul Industries Ltd, Gujarat, India under the trade name Lapox, L-12 and K-6 respectively. The volume fraction of fibres is 60%. The ratio of epoxy and hardener is taken as 10:1. The laminated composites has been prepared by hand lay-up method with 16 layers of woven fabric cloth of reinforcement and then placed in a compression moulding process. Then the curing of the laminate has been carried out at 60°C temperature and 15 kg/cm² pressure for 20 minutes. The laminates were then removed from the press and kept at room temperature for 24 hours. The test specimens have been cut from the laminates using diamond tipped cutter as per ASTM D2344-13 standard.

4.4.2.2 Methods and characterization techniques

Universal Testing machine

3-point short-beam shear tests were performed on a 30KN capacity Instron testing machine. The thermal cycling testing in presence of moisture and low temperature was conducted with specimens with an ultra-low environmental chamber. Moisture absorption was conducted in a multifunctional chamber of humidity. The thermal cycle divided into 3 cycle as half-cycle, full-cycle and one and half-cycle. In half cycle we only consider samples exposed to moisture for 24 hr and then suddenly transferred to ultra-low chamber at -20°C for 4 hr. In case of full-cycle specimens again exposed to moisture for 48 hr and then immediate transfer to at -20°C temperature. Again in one and half cycle again the half cycle treatment was repeated for the test. The tests were performed with six crosshead speeds viz; (1, 10, 100, 200, 500, and 1000) mm/min. For each point of testing 5 to 6 specimens were tested and the average value was taken. The broken parts were observed under Scanning Electron Microscope (SEM) for the fractographic analysis.

Scanning electron microscope (SEM)

For analysis of composite fractography, SEM by JEOL-JSM 6480 LV with the acceleration voltage of 15 kV was used. Cleaned, small in size and conductive samples are used during testing in SEM. the top surface of the specimens were coated with platinum using a sputter coater. The coating is used to make the surface conductive for scanning and prevents the

accumulation of static electric charge for clear images during the microscopy. During the test samples are little tilt around 15-20° to drawn attractive and clear images of different failure modes.

4.4.3 Results and Discussion

4.4.3.1 Interlaminar shear strength study (ILSS)

Fig 56. shows the interlaminar shear strength study with loading rate of glass fibre/epoxy composites. There is a sign of decrease of ILSS value was observed at each increasing loading speed. The reason may be due to presence of high residual stress in composite material. Due to poor adhesion between glass fibre and epoxy matrix during these thermal cycle testing, debonding plays dominant role for the deadhesion. The misfit strain between fibre and matrix also result in debonding at interface region [4].

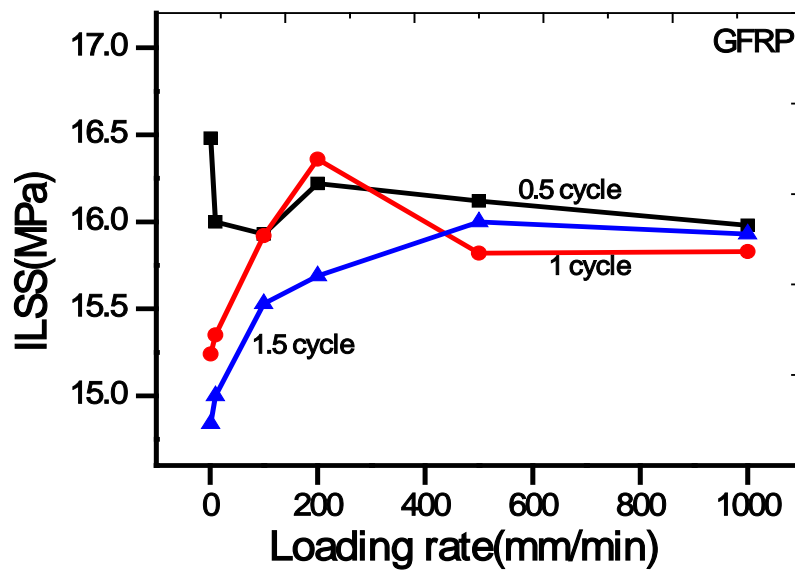


Fig.56 Interlaminar shear strength with loading rate at different thermal cycle of glass fibre/epoxy composites.

The ultra-low temperature conditioning cause differential contraction and increases resistance to debonding by mechanical debonding. Because of this the ILSS values increases with increasing loading speed.

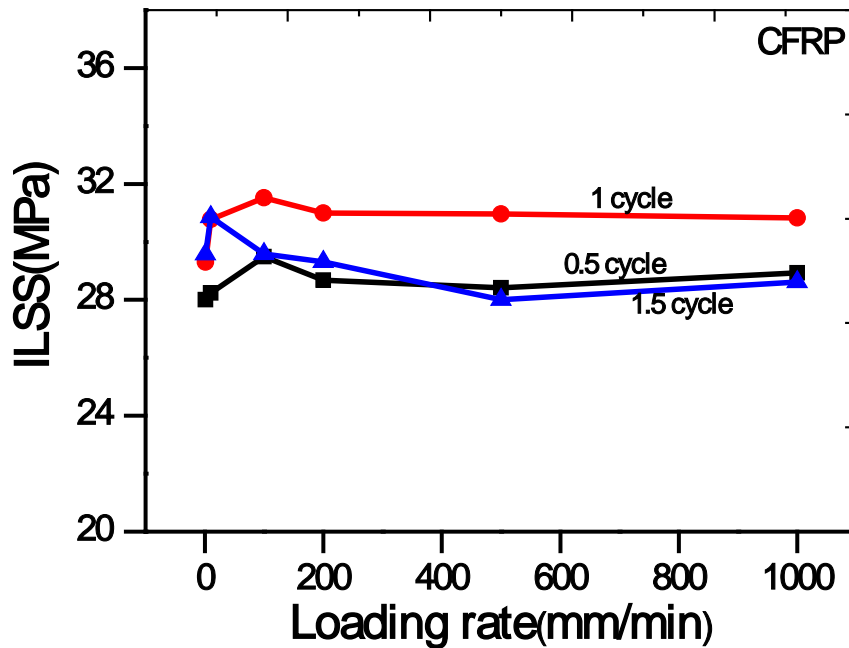
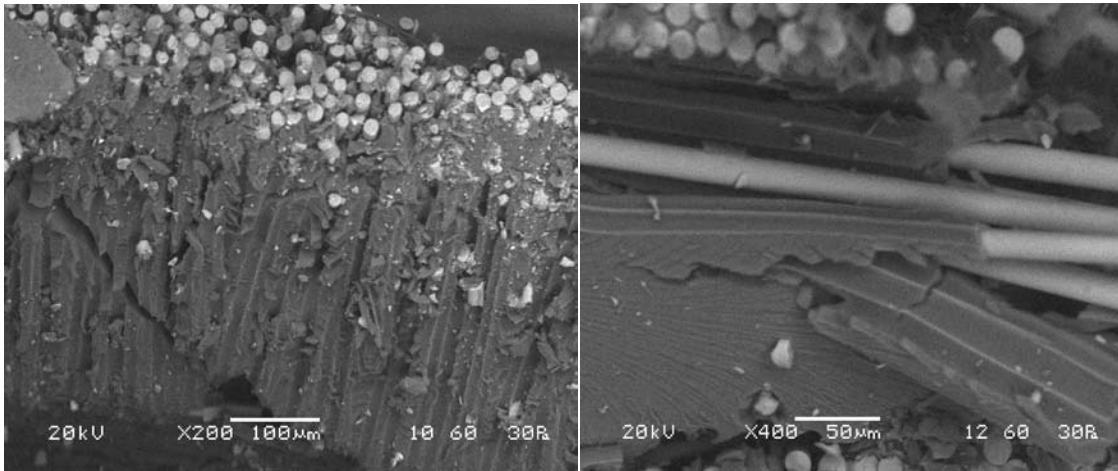


Fig.57 Interlaminar shear strength with loading rate at different thermal cycle of carbon fibre/epoxy composites.

In case of carbon fibre/epoxy composites there is a sign of increase of ILSS values with increase in thermal cycle treatment but after one cycle it decreases which shown in Fig.57. The reason may be due to presence of less residual stress in the interface region.

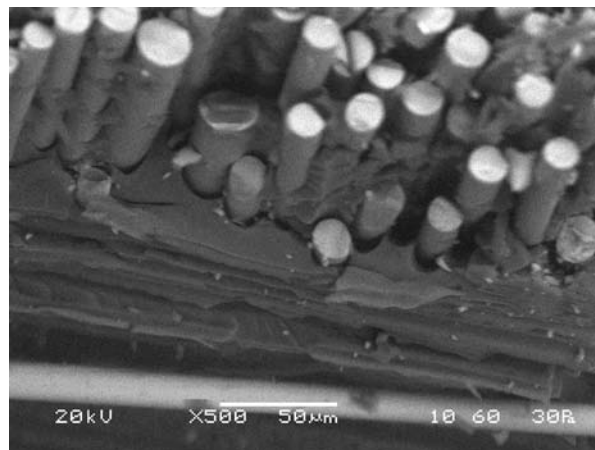
4.4.3.2 Fractography study(SEM)

Fig.58 represents fibre imprints, riverline markings and fibre/matrix debonding failure modes. However, there is some fiber imprint are visible on the surface. This is because of development of internal residual tensile stresses in the matrix resin at 0.5 cycle treatment. As matrix behaves as brittle manner after moisture ingress the molecular motion will be abysmal; molecular motion will be small and re-orientation modes will be relatively simple [18]. Similarly the deportment of interface region of glass/epoxy at low temperature treatment doesn't undergo any significant change which tends to high adhesion bond strength. Here cohesive failure of the bulk matrix plays the dominant role. At higher crosshead speed 800mm/min brittle failure of fiber observed. Brittle fibers have low fracture strain and low energy absorbing capability [19]. Fibers can fracture early at the weak cross section point, which is not necessarily the direction of crack propagation.



(a)

(b)



(c)

Fig. 58 Different failure modes were observed in glass fibre/epoxy composites (a) fibre imprint at 0.5 cycle treatment (b) riverline marking at 1 cycle treatment (c) fibre/matrix debonding at 1.5 cycle

Carbon fibre/epoxy composites

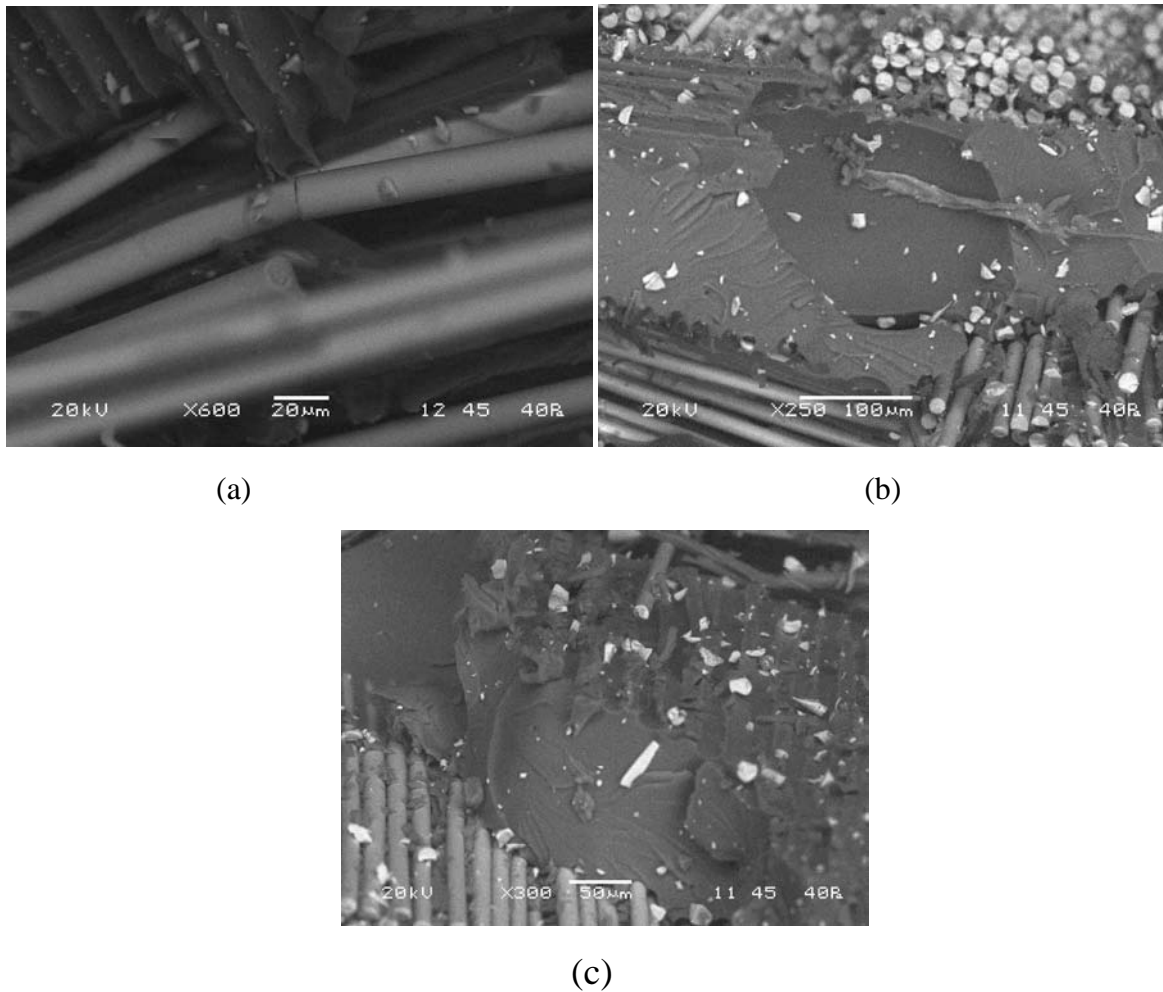


Fig.59. Different failure modes are observed in carbon fibre/epoxy composites (a) fibre fracture at 0.5 cycle treatment (b) toughened matrix at 1 cycle treatment (c) fibre/matrix debonding at 1.5 cycle treatment.

In case of carbon fibre/epoxy composites fibre fracture, toughened matrix and matrix failure modes were observed. As the applied loading rate increases 1000mm/min the fracture proceeds, the broken fibers will likely pullout from the matrix which observed in SEM micrograph. When the matrix behaves as brittle, the energy of fracture is fairly low and there is little step marking formed during failure, which is refereed to toughened matrix [20]. The characteristic feature of toughened matrix is flat facets. This fracture represents brittle fracture occurring in the matrix region, which shown in Fig 59. These are indications of the absorption of energy by local deformation. Quasi-cleavage fracture is related but distinct to cleavage fracture. It is observed chiefly low temperature. The term quasi cleavage is used because the facets on the fracture surface are not true cleavage planes.

4.4.4 Conclusion

The percentage of ILSS value decreases during above-ambient temperature testing in every mode of loading rate ranges because of thermal conditioning effect which leads to spreading of process zone in the matrix resin which impart high fiber/matrix debonding.

In contrast to, at sub-ambient temperature the percentage of ILSS value increases in Mode A, phase and decreases in Mode B and C due to unstable crack propagation (adiabatic heating) at the crack tip. This yield matrix microcracking to fiber fracture and then fiber pull-out.

In comparison when a virginal sample is tested the percentage of ILSS value increases in each mode of loading speed which may be due to preexisting stable element (low-energy crack) which divulge steps and welts along with matrix cracking in the matrix region.

References

1. Saponara V.L. Environmental and chemical degradation of carbon/epoxy and structural adhesive for aerospace applications: Fickian and anomalous diffusion, Arrhenius kinetics; *Compos. Struct.* 2001; 93: 2180-2195
2. Collings T.A., Mead D.L. Effect of high temperature spikes on a carbon fibre-reinforced epoxy laminate, *Composites*; 1988;19: 61-66
3. Takeda T., Takano S., Shindo Y., Narita F. Deformation and progressive failure behavior of woven-fabric-reinforced glass/epoxy composite laminates under tensile loading at cryogenic temperatures, *Compos. Sci. Technol.*; 2005;65: 1691-1702
4. Haddad H., Kobaisi M.A, Influence of moisture content on the thermal and mechanical properties and curing behavior of polymeric matrix and polymer concrete composite, *Mater. Des.*;2013;49:850–856
5. Moyeenuddin Ahmad S., Abdullah A. M., Holdsworth P.G., Long term durability of pultruded polymer composite rebar in concrete environment, *Mater. Des.*;2014; 57:616–624
6. Sjogren B.A., Berglund L.A., The effects of matrix and interface on damage in GRP cross-ply laminates, *Compos. Sci. Technol*, 2000; 60: 9-21
7. Kim R.Y, Steve L. D. Experimental and analytical studies on the damage initiation in composite laminates at cryogenic temperatures. *Compos. Struct.* 2006;76:62-66
8. Choi S, Sankar B V; Fracture toughness of transverse cracks in graphite/epoxy laminates at cryogenic conditions; *Compos part B- ENG* 2007;38;193-200

9. Fiedler B, Hojo M., Ochiai S., Schulte K., Ando M., Failure behavior of an epoxy matrix under different kinds of static loading, *Compos. Sci Tech* 2001;61; 1615-1624
10. Jiang B, Huang YD; Investigation of the impregnation degree of the prepreg by near infrared spectroscopy; *Composites Part B*; 2011;41:946-948
11. Grunenfelder L K, Nutt S R; Void formation in composite preregs – Effect of dissolved moisture *Compos. Sci. Technol.* 2010;70:2304-230
12. Boey F Y C, Lye S.W; Void reduction in autoclave processing of thermoset composites Part 1: High pressure on void reduction. *Composites*; 1992;23:261-265
13. Okoli, O.I, Smith, G.F. The Effect of Strain Rate and Fiber Content on the Poisson's ration of Glass/epoxy Composites, *Compos. Struct.* 2000; 48:157-161.

4.5 Effect of UV treatment on loading rate sensitivity

Theories and Thoughts

The many concurrent chemical processes taking place in polymers exposed to UV radiation result in several different modes of damage, each progressing at a different rate. It is usually the critical first-observed damage process that determines the useful service life of the Fibre reinforced polymer composite material. The basic mechanism for photo-initiated degradation is the same for all polymer materials. Damage occurs when lightphotons interact with the molecular chains that make up the polymer structures. The shorter wavelengths possessing higher photon energies are more strongly absorbed inmost polymeric materials, and have a greater potential to break chemical bonds in thatmaterial. The objective of this study is toinvestigate the above properties of glass fibre/epoxy laminated composites, subjected to UVradiation attacks.

4.5.1 Introduction

Glass and carbofibre -reinforced epoxy resin composites have received considerable attention and are widely used as structural materials in the construction, automotive, and aerospace industries [1–3]. These composites offer a variety of distinct advantages, including high specific strength and stiffness, corrosion and fatigue resistance and ease of handling and fabrication. However, there are concerns with their long-term durability and performance during their service life under harsh and changing environmental conditions. Ultraviolet (UV) light from the solar spectrum combined with atmospheric oxygen is potentially amongst the most damaging weathering conditions which affect polymers deleteriously, re

ferred to as photo-oxidation [4–6]. UV light can be absorbed by the chromophoric groups present in the polymers and the energy absorbed can cause the dissociation of the polymer covalent bonds (mostly C–C and C–H) to produce free radicals, followed by molecular chain scission and/or cross-linking. Chain cross-linking during photo-oxidation reactions reduces molecular mobility and in turn results in excessive embrittlement of the polymer matrix, which is mainly responsible for the formation of microcracks [7,8]. Photo-oxidation also induces the formation of the UV-absorbing chromophores which impart discoloration to the polymer if they absorb visible wavelengths. Furthermore, they can decompose to new free radicals, activating the auto-oxidative degradation process [8]. At an elevated temperature, the oxidative reactions are accelerated, which in turn results in rapid degradation. The aim of this investigation related to study the loading rate sensitivity of glass fibre/epoxy and carbon fibre/epoxy composites when subjected to UV radiation effects.

4.5.2 Materials and Methods

4.5.2.1 Materials

The material system selected for this work was E-glass fibre/epoxy and carbon fibre/epoxy polymer composites fabricated by hand lay-up method followed by compression moulding process. Diglycidyl ether of Bisphenol A (DGEBA) as epoxy and Triethylene tetra amine (TETA) as hardener supplied by Atul Industries Ltd, Gujarat, India under the trade name Lapox, L-12 and K-6 respectively. The volume fraction of fibres is 60%. The ratio of epoxy and hardener is taken as 10:1. The laminated composites has been prepared by hand lay-up method with 16 layers of woven fabric cloth of reinforcement and then placed in a compression moulding process. Then the curing of the laminate has been carried out at 60°C temperature and 15 kg/cm² pressure for 20 minutes. The laminates were then removed from the press and kept at room temperature for 24 hours. The test specimens have been cut from the laminates using diamond tipped cutter as per ASTM D2344-13 standard.

4.5.2.2 Methods and characterization techniques

Universal Testing machine

3-point short-beam shear tests were performed on a 30KN capacity Instron testing machine. The thermal cycling testing in presence of moisture and low temperature was conducted with specimens with an ultra-low environmental chamber. Moisture absorption was conducted in a multifunctional chamber of humidity. The thermal cycle divided into 3 cycle as half-cycle, full-cycle and one and half-cycle. In half cycle we only consider samples exposed to moisture

for 24 hr and then suddenly transferred to ultra-low chamber at -20°C for 4 hr. In case of full-cycle specimens again exposed to moisture for 48 hr and then immediate transfer to at -20°C temperature. Again in one and half cycle again the half cycle treatment was repeated for the test. The tests were performed with six crosshead speeds viz; (1, 10, 100, 200, 500, and 1000) mm/min. For each point of testing 5 to 6 specimens were tested and the average value was taken. The broken parts were observed under Scanning Electron Microscope (SEM) for the fractographic analysis.

Scanning electron microscope (SEM)

For analysis of composite fractography, SEM by JEOL-JSM 6480 LV with the acceleration voltage of 15 kV was used. Cleaned, small in size and conductive samples are used during testing in SEM. the top surface of the specimens were coated with platinum using a sputter coater. The coating is used to make the surface conductive for scanning and prevents the accumulation of static electric charge for clear images during the microscopy. During the test samples are little tilt around $15\text{-}20^{\circ}$ to drawn attractive and clear images of different failure modes.

4.5.3 Results and Discussion

Interlaminar shear strength with loading rate study

Fig.60 represents the variation of interlaminar shear strength with loading rate of glass fibre/epoxy and carbon fibre/epoxy composites subjected to UV treatment in different time duration.

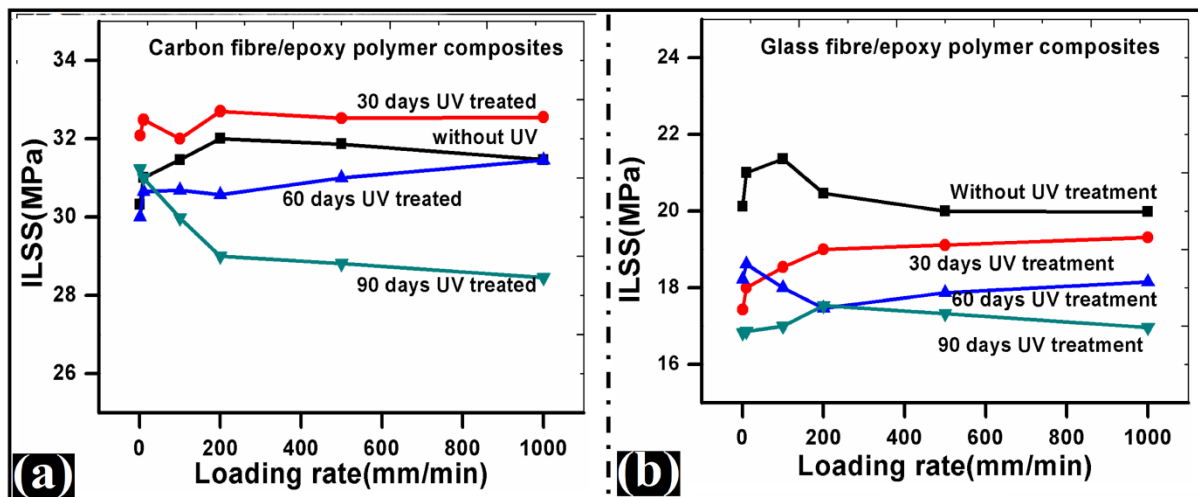


Fig.60 Interlaminar shear strength with loading rate at different time exposure of UV treatment (a) carbon fibre/epoxy composites (b) glass fibre/epoxy composites.

From the above graph we found that in case of carbon fibre the ILSS value decreases with the UV treated samples except 30 days of exposure. In case of glass fibre the ILSS value decreases with increasing days of exposure for UV treatment. The untreated samples are compared with treated samples. Carbon fibre/epoxy sample surfaces are less degraded as compared to glass fibre/epoxy composite samples. The decrease of ILSS may be due to surface outgassing of the volatile materials which are responsible for shrinkage of the epoxy matrix[9]. This shrinkage effect has a great impact on interfacial bond strength of the composite materials. The shrinkage effect was less in carbon fibre/epoxy composites due to high interfacial bond strength between carbon fibre/epoxy as compared to that of glass fibre/epoxy.

Fractography Study

Glass fibre/epoxy composites

Glass fibre/epoxy shows different failure modes shown in Fig.61

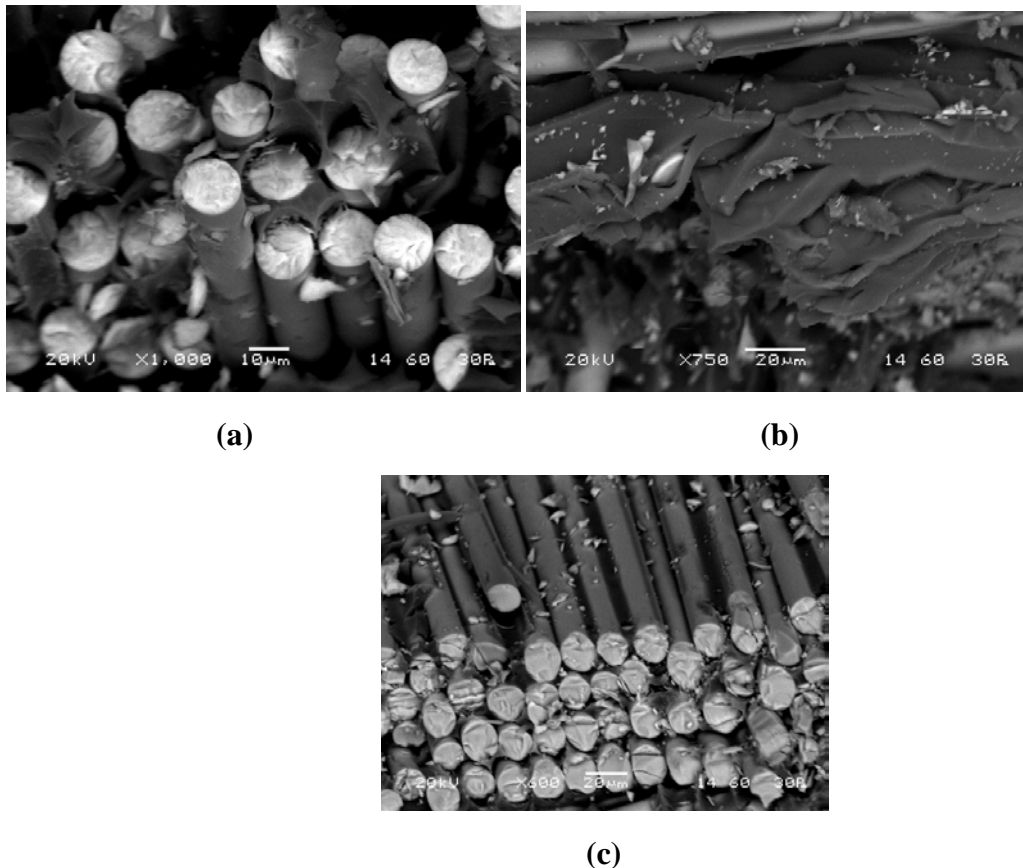


Fig.61 (a) Bunch of fibre fracture (b) resin tearing (c) fibre fracture sliding failure modes observed in glass fibre/epoxy composites at 30 days, 60 days and 90 days UV treatment of samples.

Fig.61 represents the various failure modes observed on glass fibre/epoxy composites. As surface degradation occurred during this treatment, matrix failure dominant role for the degradation of mechanical properties. UV light can be absorbed by the chromophoric groups present in the epoxy matrix and the energy absorbed can cause the dissociation of the matrix covalent bonds (mostly C–C and C–H) to produce free radicals, followed by molecular chain scission and/or cross-linking. Chain cross-linking during photo-oxidation reactions reduces molecular mobility and in turn results in excessive embrittlement of the polymer matrix, which is mainly responsible for the formation of microcracks

Carbon fibre/epoxy composites

Carbon fibre/epoxy shows various failure modes during UV treatment at different interval of time shown in Fig.62

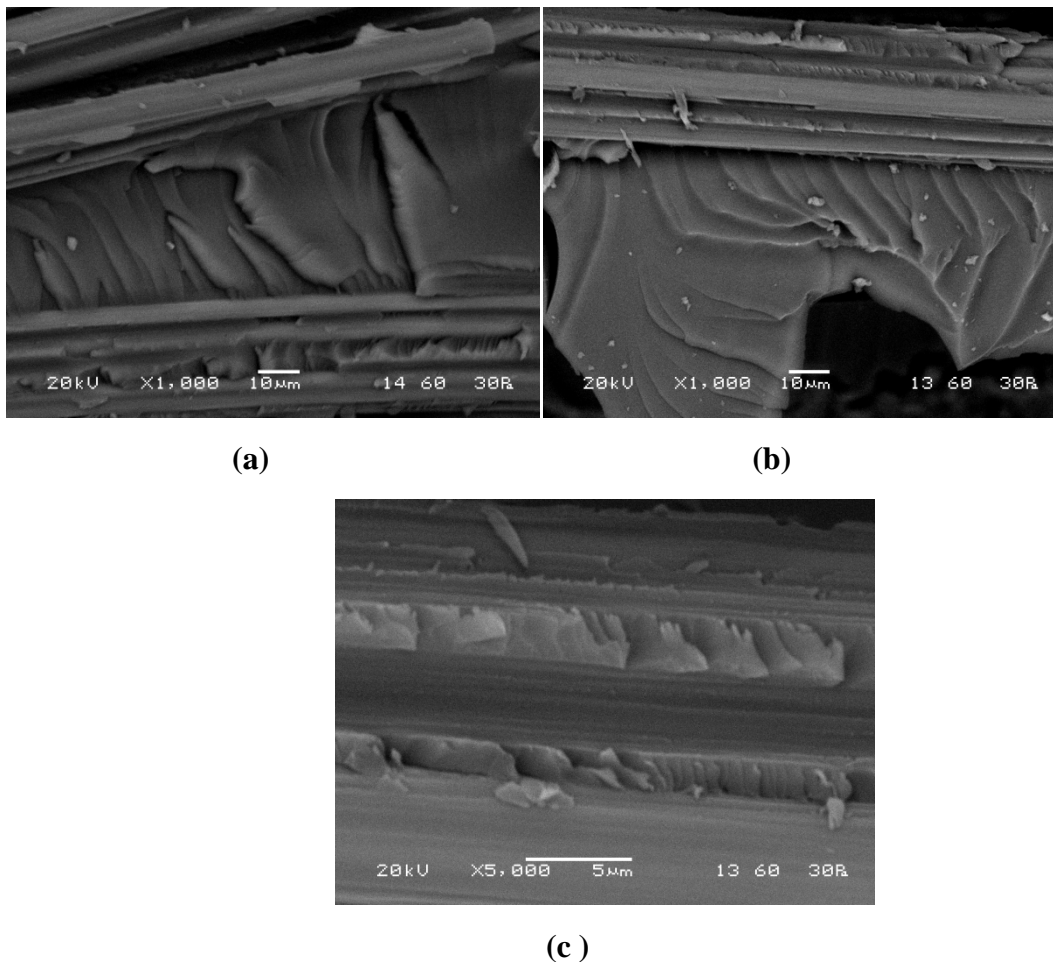


Fig: 62 (a) steps formation on the matrix resin (b) deep riverline marking (c) small cusps formation failure modes are observed in carbon fibre/epoxy composites at 30 days, 60 days and 90 days UV treatment of the samples.

Cusps failure modes are clearly visible for the carbon fibre/epoxy composites under different duration of treatments which shown in Fig.65. The appearance of the cusps at relatively high magnification; cusps size is similar to that of the fibre spacing. However, the size of cusps is larger than particularly those which develop with in resin rich regions. These failures do not display a complete fibre matrix debonding from the fibre surface [27]. At high temperature, the resin exhibits greater plasticity, and cusps resulting from the microcracks are thicker.

4.5.4 Conclusions

Interlaminar shear strength (ILSS) is one of the most important interfacial properties for composites. To better understand the interfacial strength between the carbon fibre/epoxy composites, three-point short beam shear test method was used to evaluate the interlaminar shear strength of the composites. It is readily observed that at -100°C temperature the carbon fibre/epoxy composites possess better ILSS compared to other testing temperatures. Different failure modes were observed which plays potential role during the failure of the samples.

References

1. A. Kelly, C. Zweben: Comprehensive Composite Materials. Oxford U.K, Elsevier Science Publication, 2000.
2. E.S. Greenlagh: Failure analysis and fractography of polymer composites, Woodhead publishing, 2009.
3. J.A. Nairn, S. Hu. The initiation and growth of delamination induced by matrix microcracks in laminated composites. Int. J Fracture, 1992; 57:1.
4. G. Hartwig, Polymer properties at room and cryogenic temperatures. New Work, Plenum Press, 1994.
5. S. Bandyopadhyay. Review of the microscopic and macroscopic aspects of fracture of unmodified and modified epoxy resins, Mat Sci Eng A, 1990;125:157.
6. B.L. Smith, T.E. Schaffer, M. Viani, J.B.Thompson, N.A. Frederrick, J Kindt, A. Belchers, G.D. Strucky, D.E. Morse, P.K. Hansma. Molecular mechanistic origin of the toughness of natural adhesives, fibres and composites. Nature, 1999; 399:761.
7. B.C. Ray. Adhesion of glass/epoxy composites influenced by thermal and cryogenic environments. J Appl Polym Sci, 2006; 102:1943.
8. J.J. Aklonis. Mechanical properties of polymer, J Chem Educ, 1981; 58:892.

9. K. Shin, S. Obukhov, J.T. Chen, J. Huh, Y. Hwang, S. Mok, P. Dobriyal, P. Thiagarajan, T.P. Russell. Enhanced mobility of confined polymers. *Nature Materials*, 2007; 6:961.

4.6 Effect of nanoparticles addition to evaluate FRP composites under different environmental conditioning

Theories and Thoughts

The chain relaxation dynamics and glass transition of polymer nanocomposites (PNCs) are profoundly influenced by the relative strength of the chain-particle interactions and the morphology, particularly the particle dispersion and the interparticle spacing, l_D . Sufficiently strong particle-chain enthalpic interactions lead to permanent attachment of chain segments to the nanoparticles. However, the performance of fibre-reinforced composites, to a large extent, is controlled by the properties of fibre-matrix interface. Good interfacial properties are essential to ensure efficient load transfer from matrix to fillers, which helps to reduce stress concentrations and improves overall mechanical properties. Consequently, there is great interest in developing new concepts for improving the strength of carbon fibre-matrix interface. Aim of this present investigation related to study the effect of nanoparticles on the mechanical behavior of composites and its variation with loading rates.

4.6.1 Introduction

Functionlization of nanoparticles with polymer chains opens new avenues in nanostructure materials and composites by tailoring the interactions of the nanoparticles with its constituents. Polymer nanocomposites incorporating alumina nanoparticles are a novel class of composite materials that are unique mechanical properties, while maintaining if not enhancing, the neat polymer properties. When designing polymer nanocomposites as structural materials for use, undergo different loading conditions such as static/quasi-static, creep, impact and fatigue [1]. Alumina/epoxy based polymer nanocomposites are widely used in aerospace applications, trigger to meet high durability conditions that conventional composite materials compete to meet [2]. Nanostructures constitute a bridge between molecules and infinite bulk systems. The physical and chemical properties of nanomaterial can differ significantly from those of the atomic-molecular or the bulk materials of the same composition. Jacob and co-workers [3, 4] explored the assessment of loading rate on the mechanical behavior of polymer composites. This is a summarization of the published work related to the effect of strain rate on tensile, shear, flexural properties of composite

materials. The strain-rate sensitivity is less pronounced at higher conditioning time. It may be assumed that the failure mechanisms are loading rate sensitivity phenomenon [5]. Hence, in recent years introducing rigid nanofillers as alumina into epoxy resin to form polymer-matrix nanocomposites has become a popular method for improving mechanical properties of epoxy-based composites materials [6-10]. Zhao.Su. et al reported APTES- Al_2O_3 /epoxy nanocomposites exhibits increase in fracture energy at 10-15 phr due because of good adhesion level. Debonding, plastic void growth and plastic deformation of matrix are the key reason of increase of fracture energy [11].

Current interest in alumina/epoxy nanocomposites has been generated and maintained because nanoparticles filled polymers exhibit unique combinations of properties not achievable with conventional composites. In the present study, glass fiber reinforced composites filled with alumina nanoparticle have been prepared. Alumina nanoparticle was well dispersed in epoxy polymer matrix to achieved high mechanical performance. The results show that it is possible to improve the interlaminar shear strength with the loading rate variations. Clearly, no follow-up work in this area will be commendation for better understanding of effect of nanoparticle in FRP composites in assessment of loading rate sensitivity.

4.6.2 Methods and experiments

Experiments were performed using alumina nanoparticles-epoxy based glass reinforced polymer nanocomposites. Alumina particles with an average size of $10\mu\text{m}$ and $< 50\text{ nm}$ were purchased from Sigma Aldrich of was selected as the reinforcement materials. Experiments were performed using samples that had fabricated as per ASTM standard 2344-10 having dimensions $60 \times 40 \times 4\text{ mm}^3$. Epoxy-alumina nanocomposites were prepared via magnetic stirrer and sonicator methods. 1hpr of alumina nanoparticles was added to epoxy at 70°C to reduce resin viscosity and then thoroughly stirred on a magnetic stirrer for 10 min followed by sonicating with sonicator to break any aggregates. The directionality of woven roving in GFRP composites was $0^\circ/90^\circ$, and the fabric had plain weave architecture. After curing, the laminate was cut into the required size for 3-point bend (Short- Beam Shear) test by diamond cutter. Specimens were tested from two conditions panels with six loading speed (3 specimens each) for each test in INSTRON (Model 5967). The results were then compared with the data obtained from unconditioned specimens. The shear stress induced in a beam subjected to a bending load, is directly proportional to the magnitude of the applied load and independent of the span length. Flexure strain expression in BLUE-Hill software for 3-point bend test is

$$\frac{Ex \times t \times 6}{(SP)^2} \text{Ex- Extension, t-thickness}$$

Whereas Flexure stress expression is $\frac{P \times 1.5 \times SP}{w \times t^2}$ SP- Support span, P-load, w-width

Thus the support span of the short beam shear specimen is kept short so that an inter-laminar shear failure occurs before a bending failure. The shear stress induced in a beam subjected to a bending load, is directly proportional to the magnitude of the applied load and independent of the span length. Thus the support span of the short beam shear specimen is kept short so that an inter-laminar shear failure occurs before a bending failure. The specimens were focused in JEOL scanning electron microscope. At the best compromise between the tendency for the specimen to charge and to obtain optimum resolution, an accelerating voltage of 15KV was used for all micrographs. To enhance the contrast, which was particularly important for the relatively shallow topography of the basic longitudinal texture, the specimen normal had to be tilted away from the incident electron beam toward the collector by 20 to 25°. During experiments, various loading (striking) speed were performed i.e. (1, 10, 100, 200, 500) mm/min.

4.6.3 Results and Discussion

The alumina nanoparticles size has an effect on the loading rate sensitivity of the composites when this is dispersed around epoxy polymer matrix. The relationship between the interlaminar shear strength and loading rate of glass epoxy/alumina fiber reinforced composites at room temperature is shown in Fig 63(a) and (b), where the change in stress-strain curve during both the experiments are plotted in Fig 64(a) and (b). The increase of ILSS value with loading speed observed in 1% alumina/epoxy glass fiber reinforced composites at room temperature. Indeed, the stress-strain curve of alumina/epoxy nanocomposites shows ductile behavior which increases with increase in loading speed. Nevertheless, the most striking result is that mirror, mist and hackle region observed in fractography analysis shown in Fig 65. The increase of percentage value of ILSS with loading rate of alumina epoxy nanocomposites in compared to epoxy glass fiber reinforced composites shown in Fig 63.

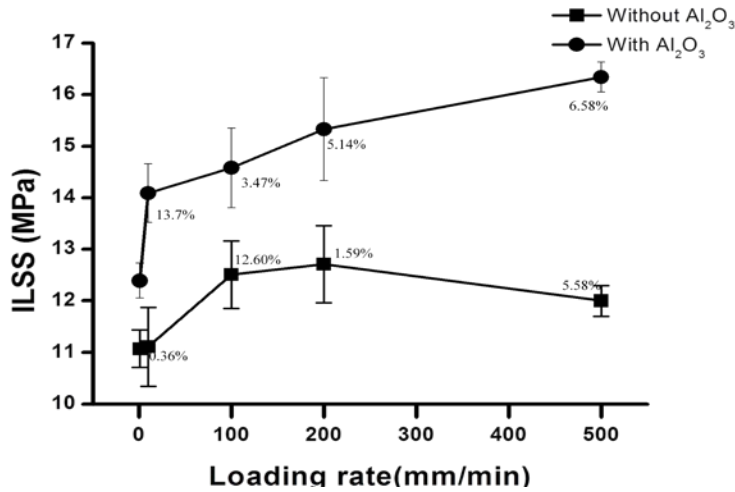


Fig 63(a): 3-Point bend test data for (●) alumina/epoxy glass fiber reinforced nanocomposites (■) without alumina/epoxy glass fiber reinforced composites

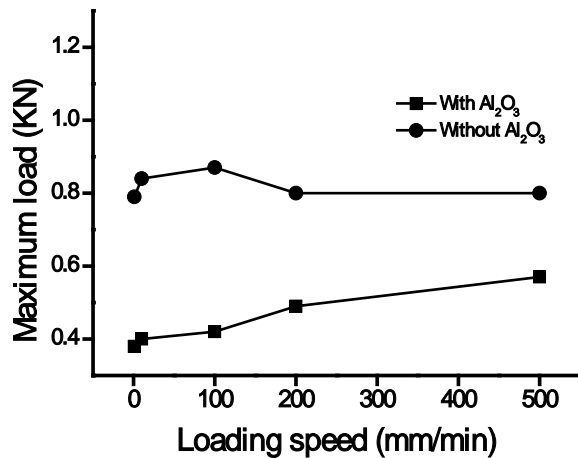


Fig.66(b): Load-displacement curve for glass fibre/epoxy composites was plotted with and without nano-filler.

The improved in interlaminar shear strength (ILSS), which the nanocomposites exhibit, are due to the behavior of the interfacial interaction zone (IZ) which surrounds the nanoparticle [12, 13]. This is a region in which the structure and properties have been altered because of presence of filler material. Formation of double layer at the interface region because of a common surface, which is created by molecular mobility (physic-chemical bond) of matrix affect the interfacial interaction zone. Thus with the low volume fraction of filler, which may then affect the entire matrix due to their large surface to volume ratio, through an interaction zone. The dispersed nanofillers are able to improve the ILSS value with the loading rate to maintain or even improve ductility because they are much smaller than the critical crack size of polymer matrix and need not initiate failure with no decrease of strain-to-failure value. The

loading rate sensitivity of the polymer composites was appeared to be nonlinear and contradictory value at some point shown in Fig 63(b). This phenomenon may be attributed by, weak adhesion, fiber/matrix debonding and matrix cracking visualise in fractography result. It seems that greater the strain rate and the loading velocity, the greater the mechanical properties [14]. This mechanical behavior of composites depends on the ability to interface (region of stress concentration develops) to transfer stress from the matrix to the reinforcement fiber [15]. The mechanical behavior displayed by these nanocomposites is seen in the stress-strain curves presented in Fig 64 (a),(b). In this graph GFRP laminates at various loading rate at room temperature is compared with 1% alumina/epoxy nanocomposites that displays ductile behavior increases with loading rate. When sample loading with nanoparticles, there is a transition from brittle to ductile behavior is observed. And at other loading speeds that don't behave ductile manner, because of pre-existing flaws or, inclusions which is the cause of damage and degradation of composite laminates [16]. First form of damage in composite laminate is usually matrix microcracks which are transverse to the loading direction [17,18]. Mechanical and fracture behavior of laminates strongly influenced by loading rate, material microstructure and environmental conditions [19,20,21].

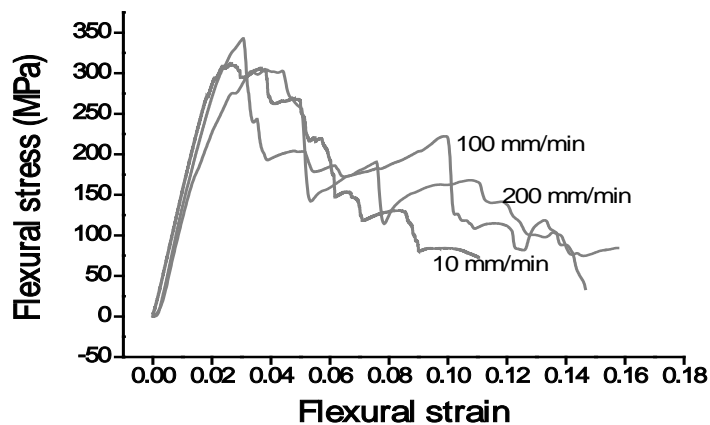


Fig 64 (a): Average stress-strain curves for the woven GFRP composite with nanoparticles

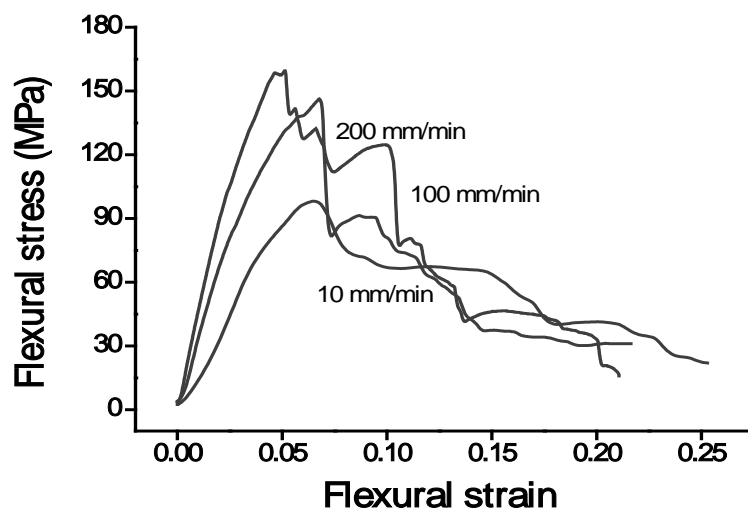


Fig 64 (b) Average stress-strain curves for the woven GFRP composite without nanoparticles

The much rougher fracture surface with fine mirror, mist and hackle marking appear in the nanocomposites [22, 23]. This is an example of morphology of brittle tensile failure at a microscopic level as shown in Fig 65 (a),(b). This shows nanoparticles dispersed glass/epoxy composites which has been loaded in short beam shear test (flexural loading). Failure initiated at the central region near upper face of glass fiber. At the marked “O” point where small pin-head sized defect was located on the laminate surface. At the area immediately adjacent to this becomes flat means fracture behavior is flat. A slow movement of fracture surface observed in this region, it means enough energy for propagation of crack. As the crack extends the propagation of crack speed increases producing rugged fracture topography. This leads to formation of radial lines. These radial lines used to infer the crack growth direction. The movement from featureless region to rugged region is referred as mirror, mist and hackle development in the brittle matrix. This failure mode was observed at 1mm/min loading speed during the test. The relative proportions of this region are dependent on loading condition, environmental parameters and toughness of the matrix. The interfacial debonding observed in the mirror zone was not seen in the hackle zone. Figure 65 (c),(d) represents scanning micrograph of without alumina nanoparticles glass fiber/epoxy polymer composites. Matrix cracking and fiber imprint plays adverse effect on the interfacial shear strength of the glass fiber/epoxy reinforced polymer composites.

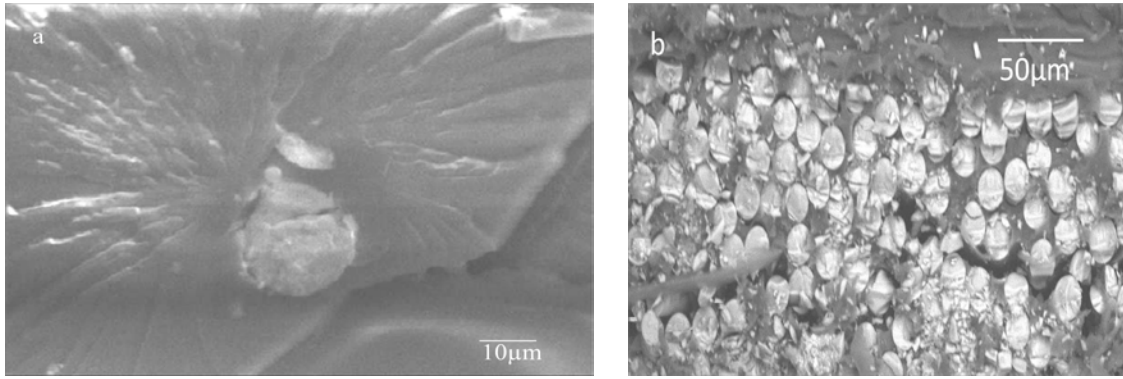


Fig 65:(a),(b) Scanning electron micrograph of epoxy resin and fiber of alumina/epoxy glass fiber reinforced composites. Tilted 20°.

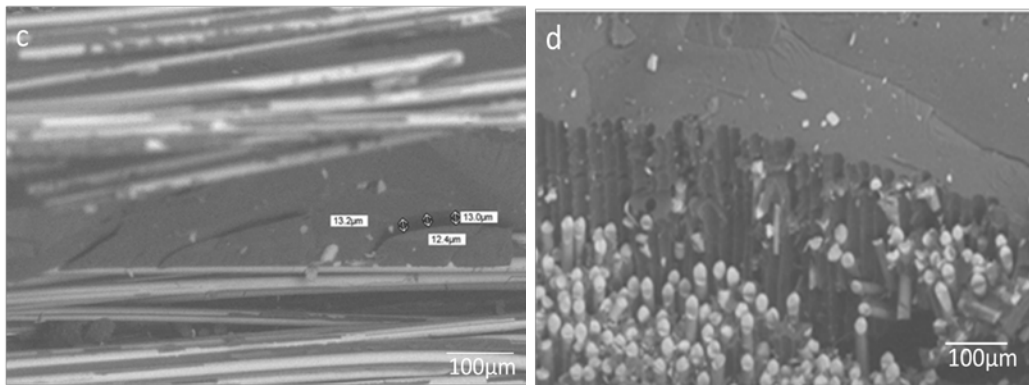


Fig 65 (c),(d): Scanning electron micrograph of epoxy glass fiber reinforced composites. Tilted 20°.

4.6.4 Conclusions

Polymer nanocomposites were synthesized, fabricated and tested with different loading speed. When an interfacial interaction zone (IZ) exists between nanoparticles and polymer matrix at room temperature, the percentage increase of ILSS value with loading rate was obtained. Here the mode of yielding changing from brittle-to-ductile transition. Presence of mirror, mist and hackle region in the polymer matrix around the edge of glass fiber require both the understanding and integrity of composite material.

References

1. Naik N.K.: Mater Design, 2010, Vol.31, pp. 396-401.
2. Njuguna.J. and Pielichowski. K: Adv Eng Mater, 2003, Vol.5, pp. 769-778.
3. Jacob G.C., Starbuck J.M. Fellers. J.F., Simunovic. S., Boeman. R.G.: J.Appl. Polym.Sci, 2005, Vol.96, pp. 899-904
4. Jacob G.C., Starbuck J.M. Fellers. J.F., Simunovic. S., Boeman. R.G., J.Appl. Polym.Sci., 2004, Vol.94, pp. 296-301
5. Ray B.C.: Mater.Sci.Eng.A., 2004, Vol.379, pp. 39-44
6. Omrani. A., Simon. L.C., Rostami. A.A.:Mater.Chem.Phys, 2009, Vol.114, pp145-150.
7. Zeng.K.Y, Lim.S.H, He.C.B: Mater.Sci. Eng.A, 2010, Vol.527, pp. 5670-5676
8. Wetzel. B., Rosso.P, Friedrich.K: Eng. Fract. Mech., 2006,Vol.73,pp.2375-2398
9. Wetzel.B., Hauptert. F., Zhang.Q.M: Compos. Sci.Technol., 2003,Vol.63,pp.2055-2067
10. Quaresimin.M.,Salviato., M.,Zappalorto.M.: Composites Part B.,2012,Vol.43,pp.2290-2297
11. Van Vliet.K.J., Schmidt. D.J.,Cebeci.,F.C.,Kalcioğlu.L.,Wyman.S.G.,Ortiz.C., ACSNano, 2009, Vol.3 ,pp.2207-2216
12. Gamby.D. Nguyen.T.H.: Compos. Sci. Technol.,2007,Vol.67,pp.438-452
13. Khan.M.Z.S.,Simpson.G.,Gellert.E.P.:Composites Part A.,2000,Vol.31,pp.57-67
14. Wong.C.P., Sun.Y., Zhang.Z.,Moon.K.S.:J. Polym. Sci.Part B:Polym.Phys. 2004.Vol.42.,pp.3849-3858
15. Tjong.S.C.: Mater. Sci. Eng. R, 2006, Vol.53, pp.73-197
16. Singh.R.P.:Material letters,2004. Vol.58,pp.408-412
17. Ray. B.C.: J. Reinf.Plast. Compos.,2005, Vol.24, pp.1771-1776
18. Ray.B.C.: J. Reinf. Plast. Compos., 2006, Vol.25, pp.1227-1240
19. Ray.B.C.: J. Colloid Interface. Sci, 2006., Vol.298, pp.111-117
20. Ray.B.C.:J. Reinf. Plast. Compos., 2006, Vol.25, pp.329-333
21. Ray.B.C.: J.Appl.Polym. Sci., 2006,Vol.100,pp.2289-2292
22. Vaia.R.A.,Maguire.J.F.: Chem. Mater., 2007. Vol.19, pp.2736-2751
23. Pitsa.D. and Danikas. M.G: Nano: Brief report and reviews. 2011,vol.6, pp. 497-508

4.7 Effect of strain rate and environment on the dynamic flexural behavior of GFRP and CFRP composites

Theories and Thoughts

Large number of structural applications fibre reinforced composite materials are subjected to low velocity static loading to high velocity dynamic loadings during its service period producing different dynamic states of stress. Damage and degradation in composite structures is a critical phenomenon starting from micro to macro failure by changing its mechanical behavior. Focusing on dynamic failure behavior of these materials in terms of its mechanical testing and interfacial characterization at different environmental conditions will be helpful for the designer analyst. Material characterization is needed to determine composites mechanical properties, stiffnesses and strengths as a function of strain rate. Therefore, it is utmost important to characterize these materials under relevant dynamic loading conditions and to identify the appropriate failure criteria to apply in the design of dynamically loaded structures.

4.7.1 Introduction

FRP composite materials have shown great potential for various high performance structural applications. Their outstanding strength to weight ratio, fatigue resistance, corrosion resistance and lower manufacturing costs makes them superior than the conventional metals. Today aircraft, automotive, marine, chemical, construction and electrical industries are manufacturing most of their components with fiber composites [1-2]. Fabio Nardone et al [23] studied the effect of temperature on mechanical properties of GFRP and CFRP composite. They have reported that for GFRP specimen the loss in mechanical properties for the temperature range (-15°C to +36°C) was not significant but for CFRP specimen (temperature range +20°C to +70°C) a decrease of 28.8 and 27.7% of ultimate tensile strength and computed ultimate FRP tensile strain respectively were reported. P.K. Dutta et al [24] studied the durability of FRP composites under low temperature and freeze thaw cycling. They reported that increase in young's modulus (E) and shear modulus (G) values controls the flexural properties of composite at low temperature. Thermal cycling resulted in crack growth which can be the obstacle in the applicability of FRP composite in such harsh environment. M.Z. Shah Khan et al [25] studied the effect of compressive strain rate and loading rate on mechanical properties of GFRP composite. Strength and modulus of woven GFRP composite for compressive loading in in-plane orientation were investigated. They found that initially from 0.005/s strain rate both strength and modulus increased upto 1.0/s

and then decreased with further increase in strain rate. For normal loading the modulus and strain at maximum stress found unaffected with the variation of strain rate while the strength were increased by approximately 20 % between the strain rates 0.1/s to 11.0/s. O.I.Okoli [26] studied the effect of strain rate and failure modes on the failure energy of glass/epoxy composites. Their experimental results suggest an increase in tensile, shear, and flexural energy of 17%, 5.9%, and 8.5%, respectively, per decade increase in log of strain rate. At quasistatic crosshead rates the failure includes the brittle failure with fiber pullout, while brittle failure with substantial matrix damage is dominating failure mode as the crosshead speed increases. The latter failure mode is more energy consuming suggesting an increase in the energy absorption with the increasing crosshead rates. Ray B.C. et al. [27] found that the ultra-low temperature (77K) conditioning results in substantial degradation in interlaminar shear strength of glass/polyester composites while the same cryogenic conditioning investigation [28] on glass/epoxy composite shown improvement in Interlaminar shear strength. C. Kanchanomai et al. [29] studied the effect of loading rate on fracture behaviour and mechanism of thermoset epoxy polymer. From the analysis of the load-displacement curves at different loading rates they suggested that the displacement to fracture is decreases with increasing loading rate and become stable after a rate of 100 mm/min. Dominating failure mechanisms at low loading rates includes formation of shear lips, a stretched zone and crack blunting while brittle fracture were observed for specimen tested at 10 mm/min or higher. Delamination is also one of the most frequent life limiting failure mode in laminated composites.

Aim of the current investigation is to present the variation of mechanical properties of glass fiber/epoxy composite under the synergetic effect of temperature and rate of loading. GFRP and CFRP composites were fabricated by compression moulding press. The composite specimens were subjected to thermal spike at different temperature. 3-point bend test and 4-point bend test were conducted in order to characterize the mechanical behavior of laminated composite and to determine the influence of loading rate on interlaminar shear strength. To understand the interactions between various failure mechanisms in the fiber, matrix and fiber/matrix interface, microscopic analyses were conducted.

4.7.2 Experimental

4.7.2.1 Material and Methods

Woven fabric E-glass fiber and carbon fiber reinforced composite laminates were prepared by hand lay-up technique. The polymer matrix used for the present investigation was DGEBA epoxy resin with hardener (HY 951). The weight fraction of fiber and matrix were 60:40. GFRP laminate include 16 layers of the glass fiber cloth while the desired thickness of CFRP laminates were achieved in 12 layers. The laminates were cured and 3-point bend test specimens for the evaluation of interlaminar shear strength were extracted.

Rectangular specimens, 50mm x 6mm, were extracted from the prepared sheets of GFRP composite material. In the case of the material exposed only to ambient temperatures, a Flow CNC waterjet was utilized to extract the specimens. Specimen thickness was approximately 3mm, and was observed to vary slightly with each sheet of prepared material. As any exposure to moisture may have disturbed existing properties in the sheets GFRP material that were exposed to elevated temperatures, a conventional vertical bandsaw was used to extract such specimens. Four unique specimen types of GFRP material resulted. In all cases, were extracted such that the reinforcing fibers remained oriented along the length and width of the rectangular specimen.

4.7.2.2 Temperature conditioning

Present investigation includes two types of woven fabric reinforcement in epoxy resin i.e. glass fibres and carbon fibres. The epoxy resin used is diglycidyl ether of Bisphenol A (DGEBA) and the hardener is Triethylene tetra amine (TETA) supplied by Atul Industries Ltd, Gujarat, India under the trade name Lapox, L-12 and K-6 respectively. Some properties of these reinforcements and epoxy resin used in the study are provided in the table-1. The volume fraction of fibres is 60%. The ratio of epoxy and hardener is taken as 10:1. The laminated composites has been prepared by hand lay-up method with 16 layers of woven fabric cloth of reinforcement and then placed in a hot press. Then the curing of the laminate has been carried out at 60°C temperature and 20 kg/cm² pressure for 20 minutes. The laminates were then removed from the press and kept at room temperature for 24 hours. The test specimens have been cut from the laminates using diamond tipped cutter as per standard.

4.7.2.3 Experimental Setup

A Hopkinson bar experimental apparatus was utilized to provide dynamic loading to the three point bend specimens. In this case only an incident bar and striker bar were employed, as compared to the traditional split Hopkinson bar which also utilizes a transmission bar. Alloy 7075 aluminum, 13mm in diameter, was used to construct both the 2m long incident bar and the 150mm long striker bar. The configuration of the modified Hopkinson bar experimental apparatus is depicted below in Figure (66) and figure (67), with the oscilloscope and load cell amplifier also visible in figure.

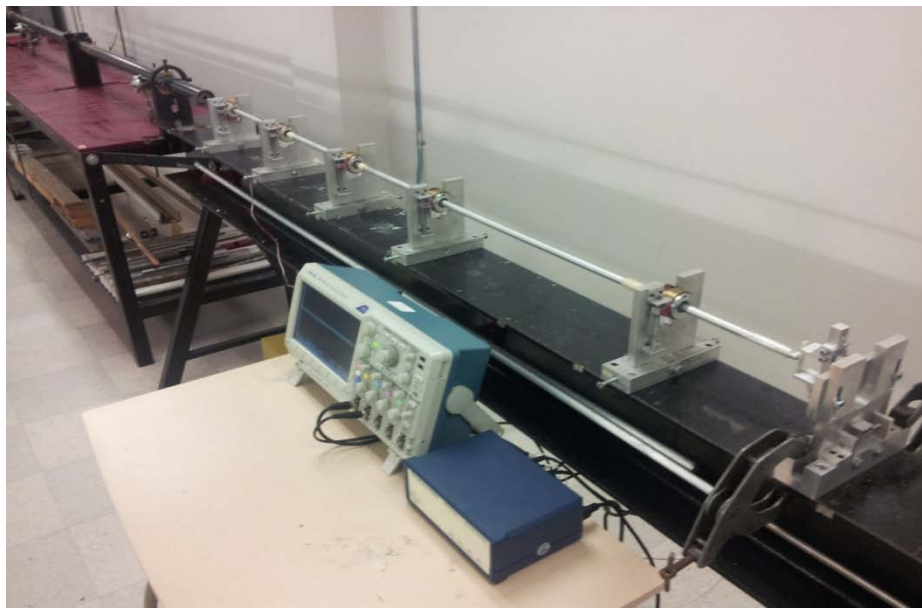


Fig.66 Configuration of Experimental Apparatus.

The incident bar was machined such that the end contacting the specimen exhibited a 3mm radius. A special 3 point bend loading fixture was designed and constructed to facilitate the tests. This fixture incorporated a pair of moveable supports, each of which exhibited a 3mm radius in contact with the specimen. A span length of 40mm between the two supports was chosen for the current work. Furthermore, to acquire data relating to the force applied to the specimen, a pair of PCB piezoelectronic load cells was integrated into the structure of the loading fixture. This assembled fixture can be seen below in figure (70) and (71).

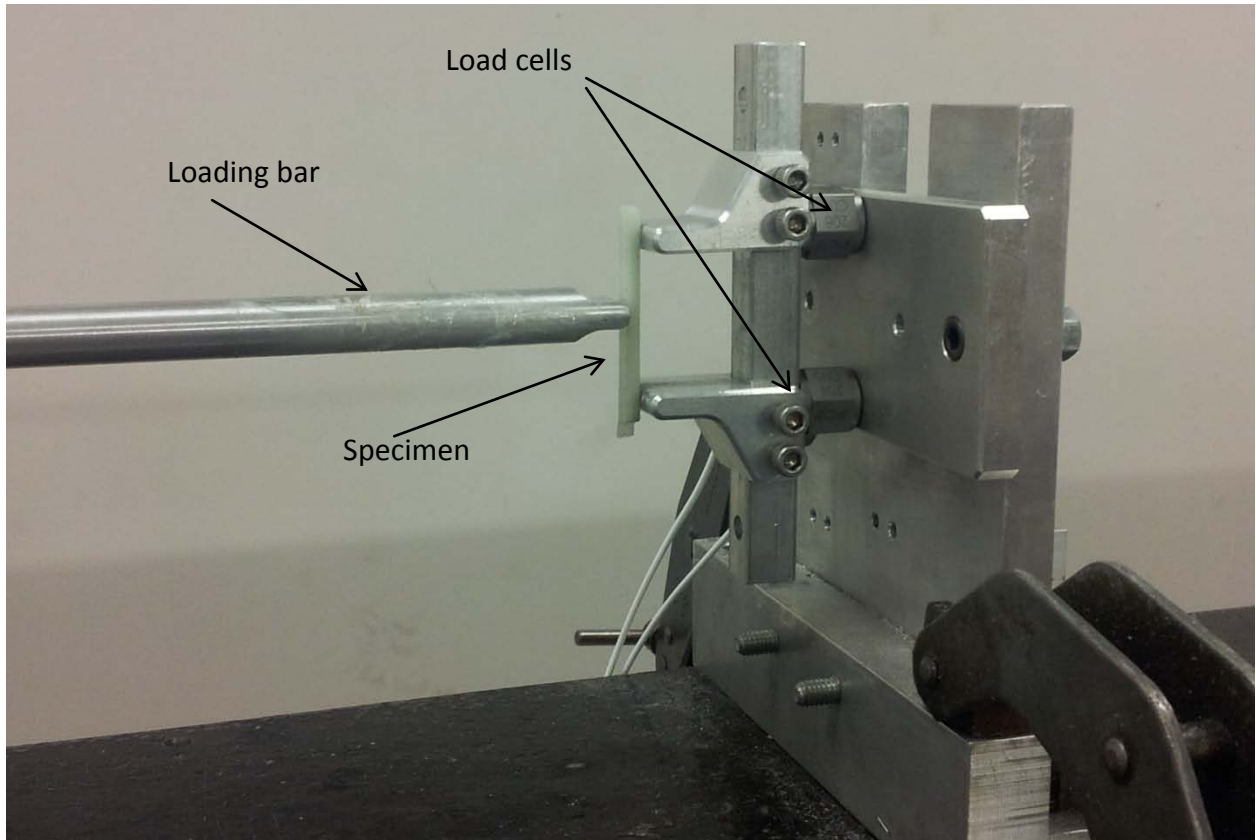


Fig.67: Loading Fixture, Specimen, and Incident Bar

In order to capture specimen displacement, 2D digital image correlation (DIC) was used in conjunction with a Photron SA-X2 high speed camera, operating at a frame rate of 400k fps. In this experiment only the midpoint displacement was required and hence only a small portion of the specimen shown in figure 67 is considered which allow us to get a 128X8 pixel at a framing rate of 400k fps. The field of view of the specimen along with the loading bar considered in this experiment is shown in figure 68. The images were analyzed, correlating displacement of a selected point near the center of thickness of each specimen. An oscilloscope was used to collect load cell data, and also to trigger image acquisition of the high speed camera.

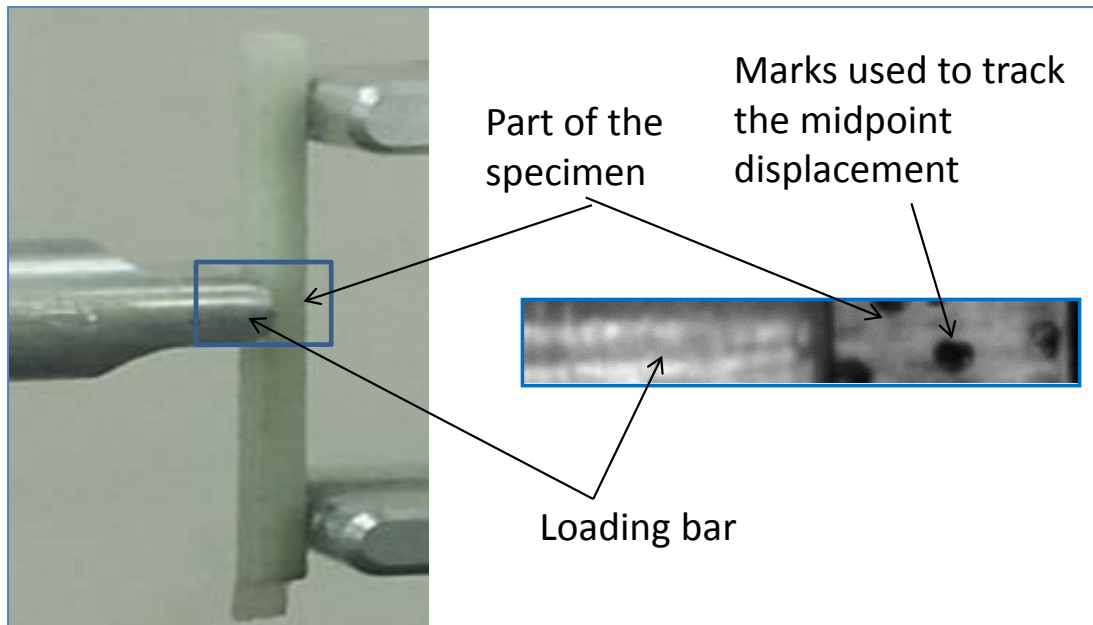


Fig.6.8 Loading arrangement and field of the camera system

Experimental Procedure

It should be noted that the use of strain gages, as typical in most Hopkinson bar experiments, was omitted in the current testing. Strain gage data proved inappropriate for the current work, as the impedance of the specimen was far too dissimilar from that of the specimen impedance, preventing collection of useable data. As the specimen impedance was very low as compared to that of the incident bar, the great majority of the incident wave was reflected from the specimen. The sum difference between the incident and reflected waveforms, interpreted as the strain wave transmitted through the specimen, did not exceed levels of the expected noise present in the strain gage data. Otherwise, experiments using the modified Hopkinson pressure bar apparatus were carried out in a typical fashion. For each test, the striker bar is fully seated into the barrel of the gas gun. Some specified pressure was then added to the tank of the gas gun. By rapidly opening a ball valve placed between the tank and the barrel of the gas gun, this pressure was introduced to the backside of the striker bar, thus propelling it to some initial velocity at impact with the incident bar. Loading rates were varied by altering the tank pressure of the Hopkinson bar apparatus; pressure of 5psi, 10psi, and 15psi were observed in the testing. Exhaustive interlaminar shear strength (ILSS) tests were conducted, acquiring data only from load cells. Each specimen type was exposed to all three loading rates, and to ensure consistency each unique test was repeated three times. Subsequently, more concise tests were conducted utilizing 2D DIC to capture specimen

displacement. Using load data acquired from the load cells in conjunction with displacement observed using DIC, stress-strain relationships could be plotted. Such testing was done for each specimen type, exposed to each of the three loading rates described.

Data analysis

Maximum flexural stress

The stress for three-point bend specimens can be calculated for any point on the load-deflection curve by the following equation.

$$\sigma = \frac{3PL}{2bh^2} \quad (1)$$

Where;

- σ = stress at the outer surface at mid-span (MPa)
- p = applied force (N)
- L = support span (mm)
- b = width of beam (mm)
- h = thickness of beam (mm)

According to the ASTM standard D7264, the maximum flexural stress for the specimen can be obtained from load data and should be valid up to 2% strain. In our experiment the strain before fracture are lower than 2 %, hence calculating the maximum flexural stress using the ASTM standard D7264 is valid.

Similarly the maximum strain at the outer surface also occurs at mid-span, and it may be calculated as follows,

$$\varepsilon = \frac{6\delta h}{L^2} \quad (2)$$

Where:

- ε = maximum strain at the outer surface (mm/mm)
- δ = mid-span deflection (mm)
- L = support span (mm)
- h = thickness of beam (mm)

Finally, the interlaminar shear strength is calculated from the maximum shear stress. Using elementary beam theory the maximum shear stress can be given as

$$\tau = \frac{3}{4} \frac{P}{Wt} \quad (3)$$

Where p is the maximum load, W and t are width and thickness of the specimen respectively.

4.7.3 Results and Discussion

4.7.3.1 Stress-strain

The flexural strain of the composites has been extracted from the midpoint point displacement of the sample captured by DIC. To make visualization easy, images were arranged in such a way that the midpoint displacement of the specimen are arranged in ascending order from top to bottom. A typical sequence of midpoint displacement for both CFRP and GFRP is given in figure 69. But mainly we focused on GFRP composite material. It is clearly visible that, the loading bar stays in-contact with the specimen until the fracture initiated, after which visibly separated. Note that the framing rate of the experiment was 400,000 frame per-second, which results in $2.5 \mu s$ between each images. The midpoint displacement as a function of time extracted from the image is used to calculate the flexural strain. A typical flexural strain as function of time plot is shown in fig 69.

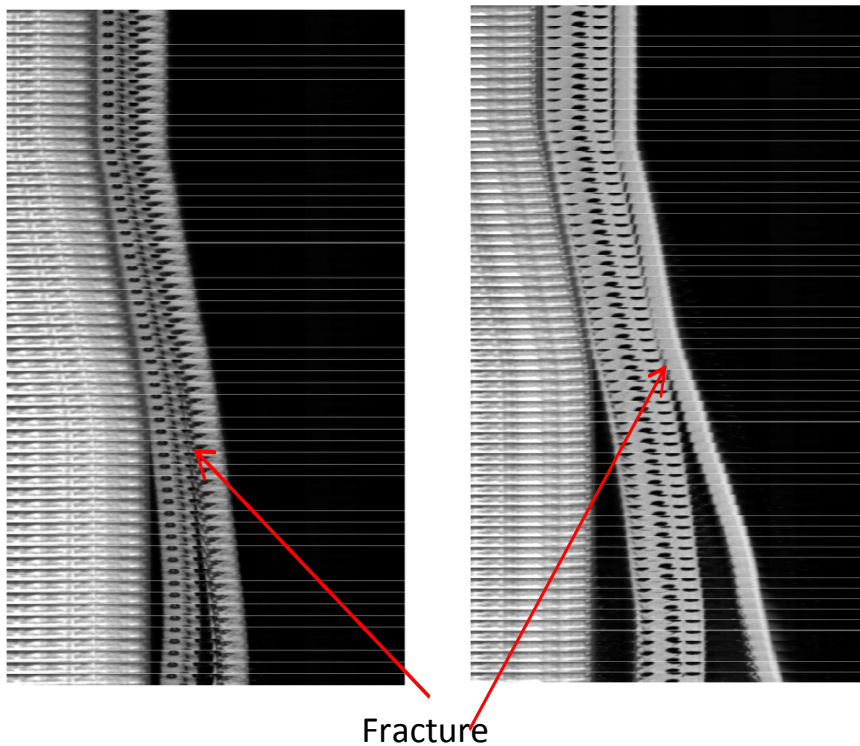


Fig 69 Typical mid-point deflection a) CFRPAMB at 300/s b) GFRP5_250 at 500 /s

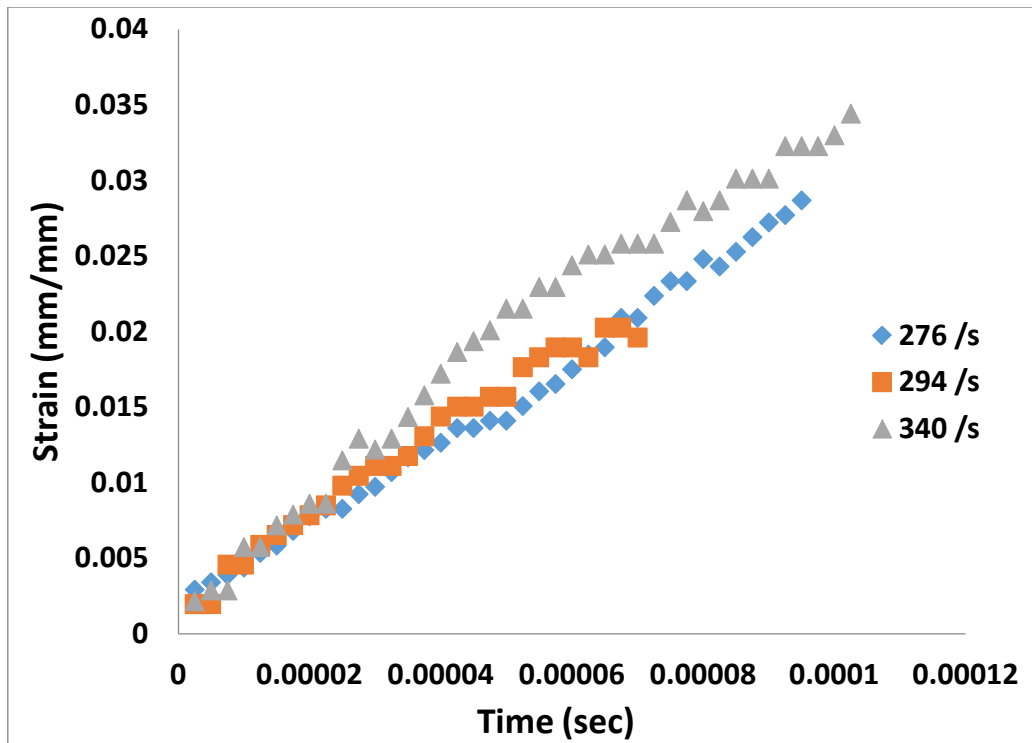


Fig70. Typical Strain-time plot for GFRP_AMB at different strain rate
 GFRP and CFRP sample at ambient temperature subjected to 5 psi load is shown in figure 70,71.

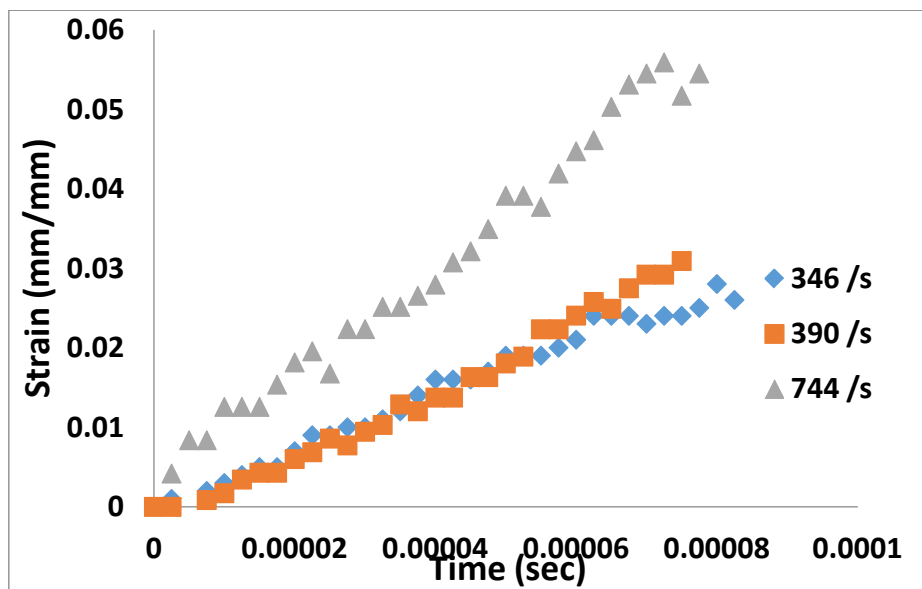


Fig 71: Typical Strain-time plot for CFRP_60s at different strain rate

On the other hand, load data measured by the load cells are used to calculate the flexural stress. A typical load time plot measured by the load cells are shown in figure 74.

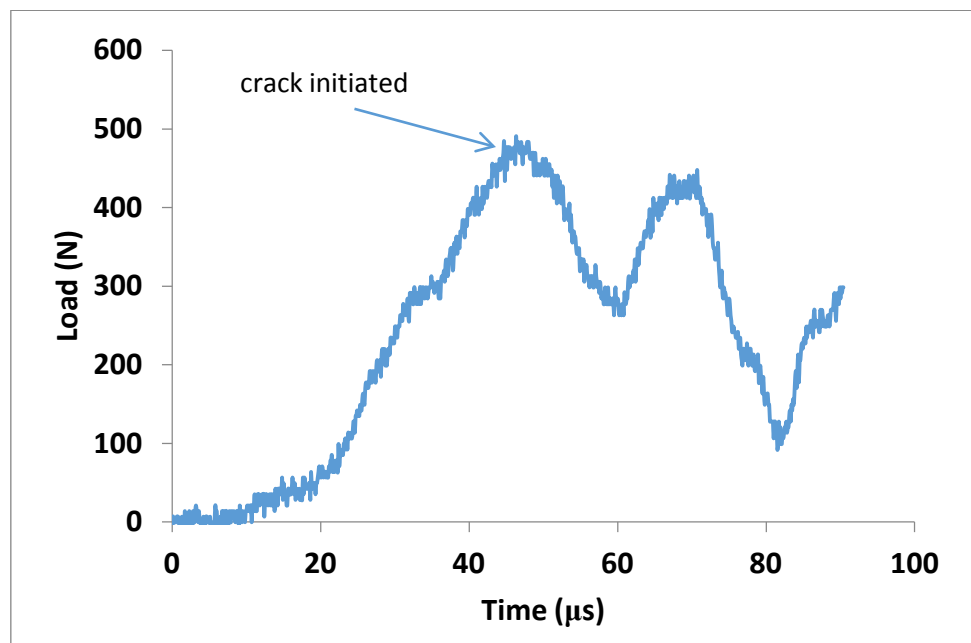


Fig.72 Typical load- time plot for CFRP_AMB at 276 /s

From the figure it is easy to find where the fracture happened and consistently the strain-time plot also showed the same time at which the crack initiated. Finally the load time plot along Eq. 2 is used to calculate the flexural stress of the sample.

4.7.3.2 Fractography Study

Matrix dominated failure properties

Fig. shows different matrix dominated failure mode at different testing pressures as 5 psi, 10psi and 15psi of glass fibre/epoxy composites.

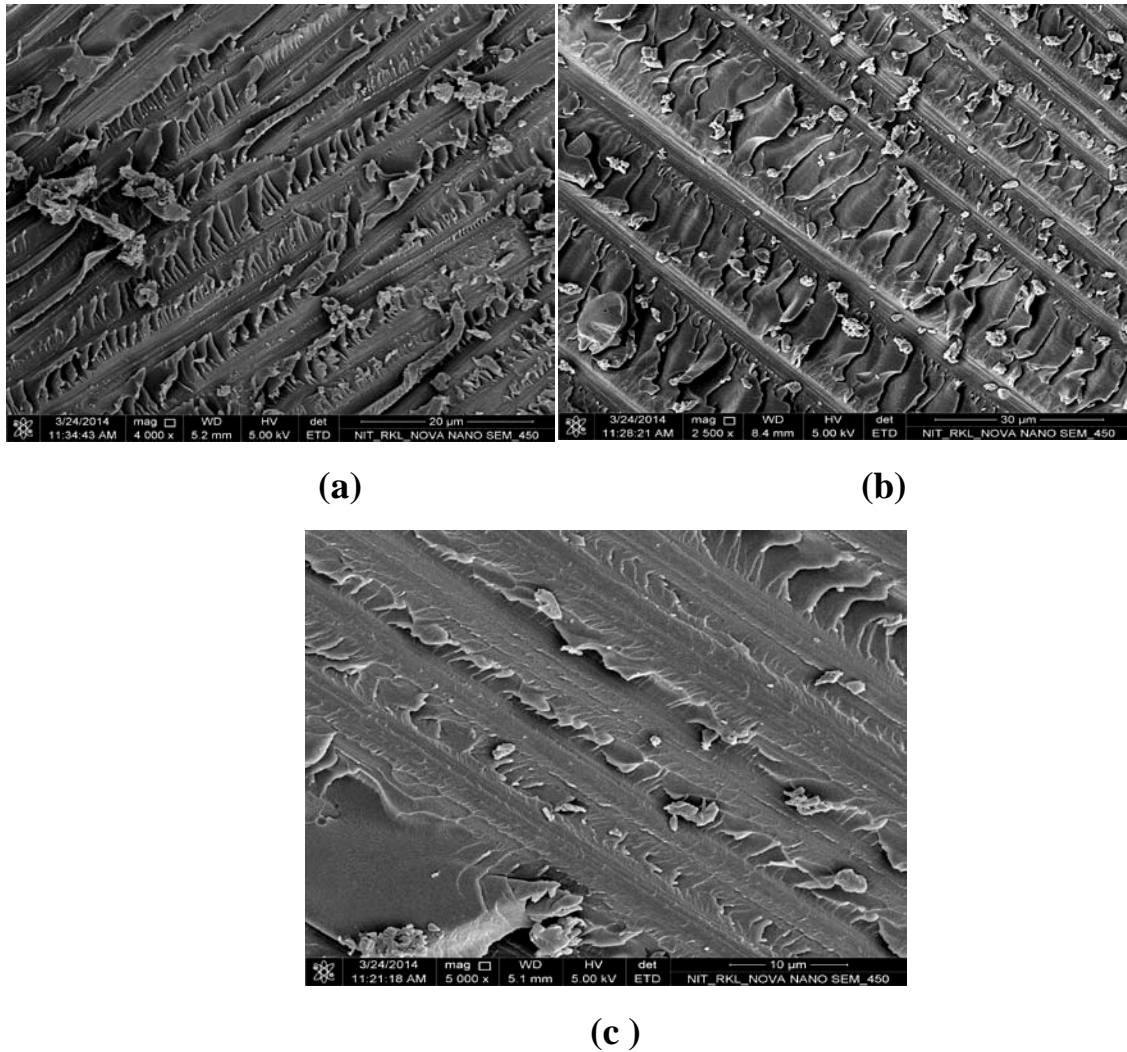


Fig:73 (a) Angles cusps formation on the matrix surface at 5 psi (b) Cusps formation between the fibres spacing at 10 psi (c) Cusps in very small size at 15 psi.

From the above micrographs shows Fig.73. different failure modes which are responsible for the initiation and propagation of crack. As delaminations failure modes are always driven by fibre directions and interfiber spacing, cusps are usually generated between the fibres. We can observed that the size of the cusps are the size of the spacing between the fibres. In case of 5psi, the cusps are formed only on the matrix region and not have any uniform size. However at 10psi cusps orientation becomes more alignment with the fibre axis as compared to 5 and 15psi which leads to more local failure of the glass fibre/epoxy composite material. During thermal spike treatment the samples are leads to development of thermal stresses. Thus the presence of these thermal stresses could be the reason for the formation of cusps in the matrix resin. This induces the addition of extra stresses between fibre and matrix interface which weakening the interfacial region.

Fibre dominated failure properties

However, we also observed the fibre failure modes which are responsible for the failure of the components during dynamic testing shown in Fig.74

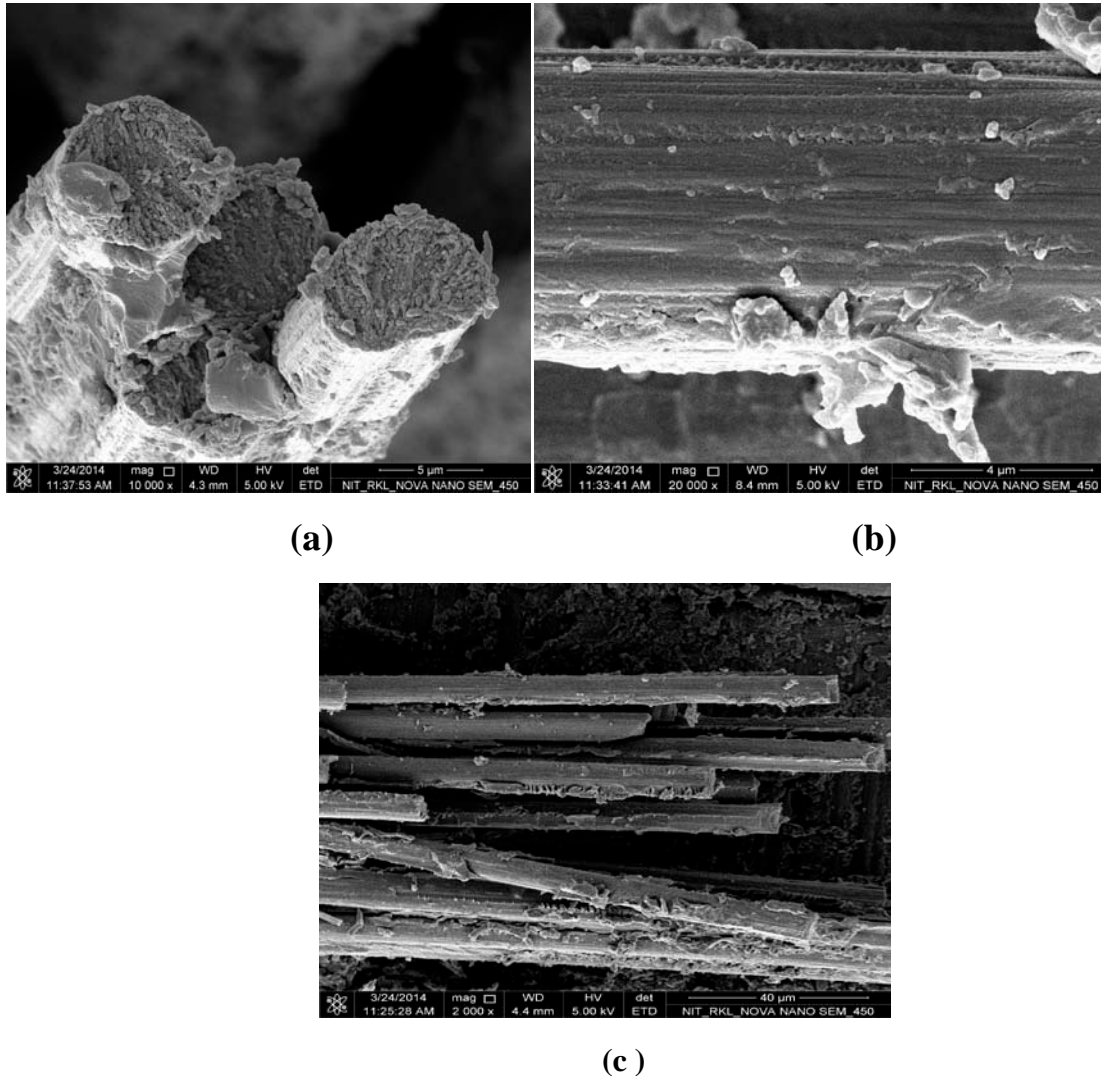


Fig:74 (a) Tension failure of glass fibre/epoxy at 5psi (b) deahesion between fibre and matrix at 10psi (c) bunch of fibre failure at 15psi

The interfacial strength between glass fibre/epoxy matrix is usually quite poor. In this case the fibres are tends to fracture individually at different points along their length which observed in 5psi tested samples. Thus the failure surface are less flat and seems to be tension failure on the fibre surface. In otherwords we can say tension failure of fibre leads to degree of fibre brooming, tends to ply splitting. However in case of 10psi deahesion between fibre and matrix we observed. Here fibre/matrix interface strength plays prime role. When thermal stresses generated on the matrix surfaces matrix cracks are formed due to coefficient of thermal expansion etween fibre and matrix. In this condition shear stresses generated on the

matrix surface which then parallel to the fibre axis and ultimately shear stress generated at the interface region. This could be the reason for the deadhesion between fibre and matrix at 10psi. The bunch of fibre failure observed in 15psi tested samples.

4.7.4 Conclusions

A glass fibre/epoxy composite material was characterized over a wide range of strain rates, from 104 to over 400 s⁻¹, at dynamic testing machine. Stress–strain curves to failure, mid-point deflection were observed. It was found that, for the range of strain rates investigated, time was linearly varies with strain rate. In case of load-time curve we can observed the crack initiation time with the strain rate. Various failure modes were also observed which are responsible for the failure of these materials. Different types of cusps are formed in the matrix region with different strain rate whereas different fibre fracture also observed in the conditioned samples.

References

1. White, S. R.; Sottos, N.; Geubelle, P.; Moore, J.; Kessler, M. R.; Sriram, S.; Brown, E.; Viswanathan, S., Autonomic Healing of Polymer Composites. *Nature***2001**, 409, 794-797.
2. Katerelos, D.; Kashtalyan, M.; Soutis, C.; Galiotis, C., Matrix Cracking in Polymeric Composites Laminates: Modelling and Experiments. *Composites Science and Technology***2008**, 68, 2310-2317.
3. Gamstedt, E.; Talreja, R., Fatigue Damage Mechanisms in Unidirectional Carbon-Fibre-Reinforced Plastics. *Journal of Materials Science***1999**, 34, 2535-2546.
4. Ray, B.C., Temperature Effect During Humid Ageing on Interfaces of Glass and Carbon Fibers Reinforced Epoxy Composites. *Journal of Colloid and Interface Science***2006**, 298, 111-117.
5. Ray, B.C., Thermal Shock on Interfacial Adhesion of Thermally Conditioned Glass Fiber/Epoxy Composites. *Materials Letters***2004**, 58, 2175-2177.
6. Bandyopadhyay, A.; Valavala, P. K.; Clancy, T. C.; Wise, K. E.; Odegard, G. M., Molecular Modeling of Crosslinked Epoxy Polymers: The Effect of Crosslink Density on Thermomechanical Properties. *Polymer***2011**, 52, 2445-2452.
7. Polanský, R.; Mentlík, V.; Prosr, P.; Sušír, J., Influence of Thermal Treatment on the Glass Transition Temperature of Thermosetting Epoxy Laminate. *Polymer Testing***2009**, 28, 428-436.
8. Sun, P.; Zhao, Y.; Luo, Y.; Sun, L., Effect of Temperature and Cyclic Hygrothermal Aging on the Interlaminar Shear Strength of Carbon Fiber/Bismaleimide (Bmi) Composite. *Materials & Design***2011**, 32, 4341-4347.

9. Takeda, T.; Miura, M.; Shindo, Y.; Narita, F., Fatigue Delamination Growth in Woven Glass/Epoxy Composite Laminates under Mixed-Mode Ii/Iii Loading Conditions at Cryogenic Temperatures. *Cryogenics***2013**, 58, 55-61.
10. Jakobsen, J.; Jensen, M.; Andreasen, J. H., Thermo-Mechanical Characterisation of in-Plane Properties for Csm E-Glass Epoxy Polymer Composite Materials–Part 2: Young's Modulus. *Polymer Testing***2013**, 32, 1417-1422.
11. Sethi, S.; Ray, B. C., An Assessment of Mechanical Behavior and Fractography Study of Glass/Epoxy Composites at Different Temperatures and Loading Speeds. *Materials & Design***2014**, 64, 160-165.
12. Shah Khan, M.; Simpson, G.; Gellert, E., Resistance of Glass-Fibre Reinforced Polymer Composites to Increasing Compressive Strain Rates and Loading Rates. *Composites Part A: Applied Science and Manufacturing***2000**, 31, 57-67.
13. Birger, S.; Moshonov, A.; Kenig, S., The Effects of Thermal and Hygrothermal Ageing on the Failure Mechanisms of Graphite-Fabric Epoxy Composites Subjected to Flexural Loading. *Composites***1989**, 20, 341-348.

Chapter 5

Summary and Conclusions

Concerns are expressed critically here regarding the environmental and experimental variants on mechanical performance of FRP composites. During their service life, these materials face many challenging environmental conditions which affect the durability and integrity of these materials. In recent years, a concerted effort has been made by researchers and structural designers to improve the environmental resistance and damage tolerance characteristics of the polymer composites. The small changes nucleated at the fibre/polymer interface by environmental exposures may quite often outcrop the possibility of weakest zone to challenge the integrity of the composites. Different micro-characterization techniques and precise modelling are to be ascertained time to time to predict the durability of the materials in the long-term applications. In this research, some of the fundamental knowledge governing the mechanical behavior response and subsequent load-bearing properties of these materials has been identified. An explicit scientific explanation to better comprehend the theories of environmental degradation is the need of the hour to utilize the promises and prospects of fibrous polymeric composites to the fullest potential with minimum risk factors and maximum environmental durability. The unprecedented failures of these materials during service conditions necessitate a holistic approach to be more comprehensively conclusive on environmental damage and degradation of polymeric composites. The influence of sub-ambient and above-ambient temperature and loading rate on the interlaminar shear strength of glass fibre/epoxy, carbon fibre/epoxy and Kevlar fibre/epoxy composite laminates has been studied. Considering interlaminar shear strength and delamination behavior, the tested laminate characterized by SEM to reveal various failure modes. The present study may possibly reveal the following conclusions: Delaminations is the life limiting failure process in a composite material. It induces great loss of stiffness, local stress concentration, and buckling failure of composite material. At -100°C temperature glass fibre/epoxy laminates shows better ILSS value but decreases with increasing loading speed. At $+50^{\circ}\text{C}$ and $+100^{\circ}\text{C}$ temperatures the ILSS increased with increasing loading rate. It is readily observed that at -100°C temperature the carbon fibre/epoxy composites possess better ILSS compared with that of the other testing temperature. But after 500 mm/min shear values decreases because microcrack density has exceeded the critical crack density for delaminations. Furthermore, for Kevlar fibre/epoxy composites at ambient temperature the specimen possess better ILSS compared with other conditioning temperature. The variation of ILSS here is the net result of

good adhesion at interface by physical and mechanical bonding at the interface. Different failure modes such as different types of cusps on the matrix region, riverline marking, fibre/matrix interfacial debonding, plastic deformation of matrix and fibre fracture were observed for the composite specimens failed after the exposure to different above-ambient and sub-ambient temperature. It is found that the type of fibres and matrix present in the composites influences the amount of heat required and the glass transition temperature. This brings out that the microstructure of the fibre/matrix within the composites found to be influencing the amount of thermal energy absorbed by the materials and consequently affect the mechanical properties. Based on the results from 3-point bend test, mechanical behavior of glass fibre/epoxy composites subjected to low and ultra-low temperature, is critically dependent upon the loading rate during the test. Maximum ILSS value was obtained at -60°C temperature; it was probably because of the unstable crack propagation occurred in the matrix with increasing loading speed. For unstable crack propagation, epoxy polymers matrix show crack arrest (slip-stick) behaviour which arises from adiabatic heating and plastic deformation at the crack tip, hence the ILSS value increases with increasing loading speed. Various failure modes were obtained at different temperatures which are responsible for the alternation of the mechanical properties. Stress-strain curve and various failure modes observed during testing at different loading rates solely depend upon the temperatures. This parameter dictates whether fibre/matrix debonding or fibre fracture controls the failure processes and material toughness. An attempt has been initiated here to compile and comprehend scattered literature in focusing the importance of understanding the interfaces with micro-techniques and advanced tools. Emphasis has also been given to interfacial susceptibility to environmental variants and their deleterious effects on interfacial strength and stability. The micro changes in the interfacial health may manifest a substantial variation in properties and performances of FRPs.

Critical Comments and Future scope of work

The interface of composite materials plays an important role to sustain the structural integrity of the system. Thereby, its function is critical and decisive in stress transmissibility under loading. The health of interphase/interface determines the reliability and durability of the composite systems in the service life. The changes occurring at the interface are highly sensitive and susceptible to degradations under different environmental conditionings. Since the interphase is a region of chemical inhomogeneity, thus it provides an easy path of the system for becoming more susceptible to thermal, chemical, thermochemical and mechanochemical degradations. Sometimes migration and or attraction of polar adherents of low molecular weight impurities from the bulk thermoset polymers onto adherents manifest a weak boundary layer of high cross-link density. However, a high performance composite functions because a weaker interface or matrix stops a crack running continuously between the strong brittle reinforcements. There are still scientific arguments about whether the interface should be weak in shear or in tension. Whichever is correct, the situation is not quantitative and we do not know how weak we can make the interface. Improved interfacial properties reduce the effects of fatigue; however, failure is inevitable. If reversible covalent bonds can form between the polymer network and the reinforcement material, then interphase will be capable of healing, resulting in improved durability of the composite.

Critical experimental investigation for an interface assessment

The fibrous composite is full of holes and channels. Liquids and gases percolate down these and attack the fibres during service period causes premature failure. Their effects perhaps mitigated if we know the exact location, size distribution and how many numbers they were by the help of non-destructive testing. To obtain a clear picture of micro characterization of interface, various techniques have been employed, as attenuated transform infrared spectroscopy (ATR-FTIR), positron annihilation lifetime spectroscopy (EIS), and solid-state nuclear magnetic resonance (NMR), Raman Spectroscopy. Concerning the micromechanical analysis of fibre-matrix interfaces in composites, various linear relationships has been proposed as interlaminar shear strength (ILSS), interfacial shear strength (IFSS) or the capacity of the interface to transfer the stress from the matrix to the fibre. Fibre/matrix adhesion involves very complex physical and chemical mechanisms. One of the most important physical aspects is the geometry of reinforcing fibres, which influences adhesion between fibre and matrix, stress transfer and local mechanisms of failure. In addition to

chemical bonding, the fibre/matrix bond strength in shear is largely dependent on the roughness of the fibre surface and the fibre/matrix contact area can be analyzed by AFM which shown in Fig.75.

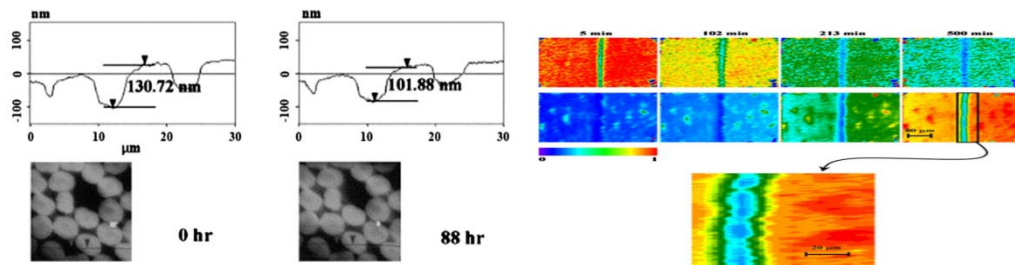


Fig: 75 Topography change of AS4/VRM34 exposed to 100% RH for different periods of time. The vertical distance between the two selected points decreased from 130.7 nm before treatment to 83.7 nm after 1495 h of hygroscopic treatment at 100% RH.

Chemically specific images (IR absorption) of the amine groups, H–N–H (top), and hydroxyl groups, OH (middle), as a function of the curing time. The bar range from 1 to 0, indicating a relative absorbance scale. Theoretical explanation by an interface modeling concept

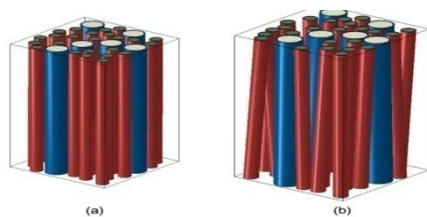


Fig: 76 Unit cell FE model of glass fibre hybrid composites(a)aligned (b)misaligned fibres

The coated interlayer should improve compatibility between the fibre and the matrix by forming a strong but tough link between both phases. The interphase thickness has been evaluated as the thickness of the transition zone, where the matrix hardness increased and the friction coefficient decreases close to the fibre surface. Various models were reported shown in Fig. 76 for the easy evaluation of interfacial integrity of the materials. Optimisation of the stress transfer capability of the fibre –matrix interface region is critical to achieving the required composite performance level. During curing stage compressive radial stresses are build-up at the interface region. Assuming that the coefficient of static friction at the interface is non-zero, these compressive stresses will contribute a frictional component to the apparent shear strength of the interface. Enormous efforts have been conducted for a comprehensive understanding of the interphase properties so as to produce advantageous interactions and maximize potential performances of the polymer matrix composites.

List of Publications based on the thesis

- **S.Sethi, B.C.Ray**, Environmental effects on fibre reinforced polymeric composites: Evolving reasons and remarks on interfacial strength and stability, *Advances in Colloid and Interface Science*, DOI No- 10.1016/j.cis.2014.12.005, Impact Factor-9.4
- **S.Sethi, D.K Rathore, B.C.Ray**, Effects of temperature and loading speed on interface dominated strength in fibre/polymer composites: An evaluation for in-situ environment. *Materials and Design*, 2015,65 ,617-626, Impact Factor-3.2
- **S.Sethi, B.C.Ray**, An assessment of mechanical behavior and Fractography study of Glass/Epoxy prepreg composites at different temperatures and loading speeds. *Material and Design*. 2014, 64,160-165, Impact Factor-3.2
- **S.Sethi, B.C.Ray**, Experimental study on mechanical behavior and microstructural assessment of Kevlar/epoxy composites at low temperature., *Journal of Mechanical Behavior of Materials*, DE Gruyter Publication, 2014, Vol-23/3-4, 2014
- **S.Sethi, B.C.Ray**, A study on fibre/matrix contour and interface/interphase integrity by SEM and AFM techniques. *Microscopy and Analysis*, John Wiley and Sons Ltd. (published July 2014)
- **S.Sethi, B.C.Ray**, An assessment of interfacial chemistry and character of fiber/polymer micro-composites., *Journal of Polymer and Composites*, 2013,1, 1-5
- **S.Sethi, B.C.Ray**, Effects of nanoparticle in FRP composites on evaluation of loading rate sensitivity. *International Journal of Composite Materials*,2013,3,1-6
- **S.Sethi, B.C.Ray, P.K.Panda, R.K.Nayak** , Experimental studies on mechanical behavior and microstructural assessment of glass/epoxy composites at low temperatures., *Journal of Reinforced Plastics and Composites* January 2012, 31, 77-84, Impact Factor-1.1
- **S.Sethi, B.C.Ray**, Evaluation of structural integrity and mechanical behavior of advanced FRP composites. *International Journal of Structural Integrity*.2011,2, 214-222.

BOOKS& BOOKS CHAPTERS

- **Sanghamitra Sethi** and Bankim Chandra Ray, Assessment of interfacial and mechanical behavior of FRP composites: Progress and degradation of Polymer composites. LAP LAMBERT Academic Publishing (August 10, 2012) ISBN-13: 978-3659170409.
- **Sanghamitra Sethi** and Bankim Chandra Ray, Mechanical behavior of polymer composites at cryogenic temperatures (Chapter 4), Edited by SusheelKalia and Shao-yun Fu. *Polymers at Cryogenic Temperature*, Springer-Verlag, Germany. ISBN – 978-3-642-35334-5, April- 2013

CONFERENCE PROCEEDINGS

- **Interface assessment in composite materials** - International conference on Recent Trends in materials and characterization (RETMAC-2010), NIT Surathkal, Karnataka, INDIA from 14th FEB – 15th FEB' 2010.
- **Assessment of interfacial chemistry and integrity in advanced FRP composites by FTIR-Imaging and Temperature modulated DSC techniques. 3rd National Symposium for Materials Research Scholars - MR - 10**, at IIT Bombay, Mumbai (Maharashtra), INDIA from 7th May – 8th May 2010.
- **Evaluation of environmental damage and degradation study of fiber/polymer composites** -The international congress of environmental research ICER-10, MAURITIUS from 16th Sep -18th Sep 2010.
- **A microscopic study of failure in fibrous composite material** - National metallurgical day-Annual Technical Meeting(NMD-ATM) IISC - Bangalore, INDIA from 14th Nov-16th Nov 2010.
- **Failure and fracture studies of fibrous composites: Thermal conditioning effects**- National metallurgical day-Annual Technical Meeting (NMD-ATM) Hyderabad, INDIA from 13th Nov-16th Nov 2011.
- **Loading rate sensitivity of FRP composites; an overview**- International symposium for research scholars on Metallurgy, Materials science and Engineering(ISRS), IIT Madras from 20th Dec-22nd Dec 2012.
- **Environmental and Experimental stability of FRP composites**. International Conference on Composite materials, International Centre of Goa, 13th -16th February, 2013
- **An evaluation of the failure behavior with changing loading rate in E-glass fiber/epoxy composites at low temperatures**. Designing composite materials: Avoiding large structural failures, An International Conference: DFC12/SI6, Queen's College, Cambridge, England from 8th-11th April 2013